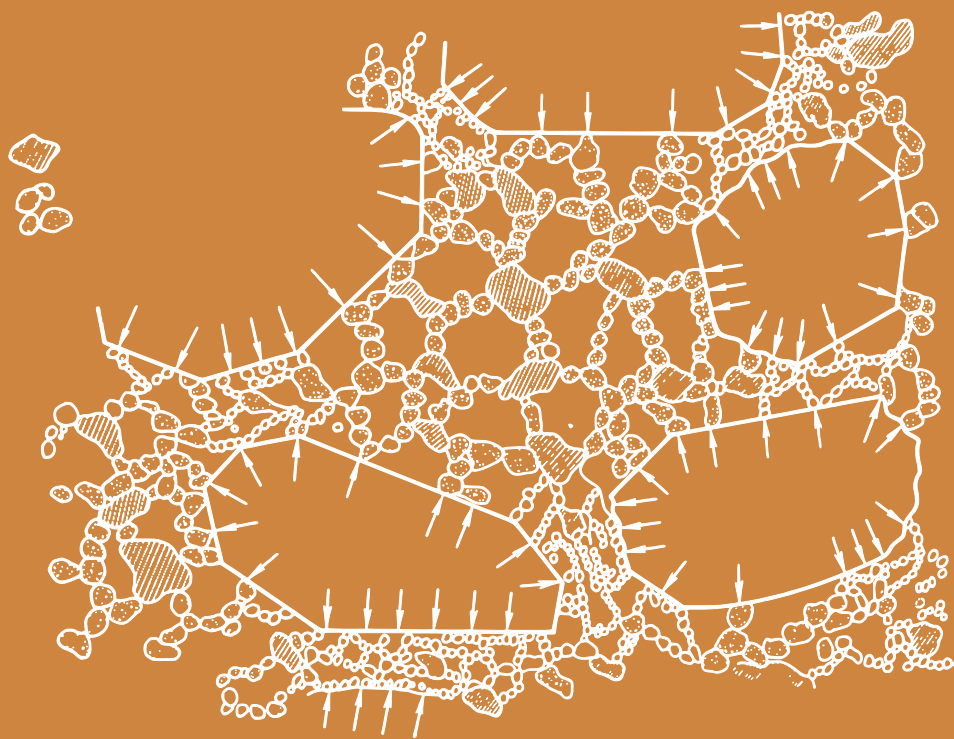


N. Tsytoich

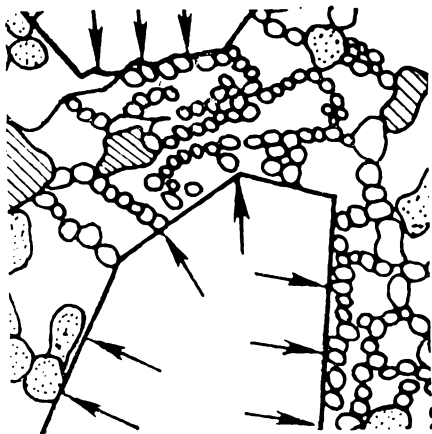
# SOIL MECHANICS



Mir Publishers Moscow







И. А. Цытович

МЕХАНИКА  
ГРУНТОВ

Издательство «Высшая школа»  
Москва

N.Tsytovich

# SOIL MECHANICS

(Concise Course)

*Translated from the Russian*

*by*

V. Afanasyev

Mir

Publishers

Moscow

*First published 1976*  
*Revised from the 1973 Russian (second) edition*

### **The Greek Alphabet**

Αα	Alpha	Ιι	Iota	Ρρ	Rho
Ββ	Beta	Κκ	Kappa	Σσ	Sigma
Γγ	Gamma	Λλ	Lambda	Ττ	Tau
Δδ	Delta	Μμ	Mu	Υυ	Upsilon
Εε	Epsilon	Νν	Nu	Φφ	Phi
Ζζ	Zeta	Ξξ	Xi	Χχ	Chi
Ηη	Eta	Οο	Omicron	Ψψ	Psi
Θθ(θ)	Theta	Ππ	Pi	Ωω	Omega

*На английском языке*

© *English translation, Mir Publishers, 1976*

# CONTENTS

Preface . . . . .	7
Introduction . . . . .	8
<b>CHAPTER ONE. THE NATURE AND PHYSICAL PROPERTIES OF SOILS . . . . .</b>	<b>12</b>
1.1. Geological Conditions of Soil Formation . . . . .	12
1.2. Components of Soils . . . . .	13
1.3. Structural Bonds and Structure of Soils . . . . .	17
1.4. Physical Properties and Classification Indices of Soils . . . . .	20
<b>CHAPTER TWO. BASIC LAWS OF SOIL MECHANICS . . . . .</b>	<b>31</b>
2.1. Compressibility of Soils. The Law of Compaction . . . . .	32
2.2. Water Perviousness of Soils. The Law of Laminar Filtration . . . . .	44
2.3. Ultimate Contact Shear Resistance of Soils. Strength Conditions . . . . .	49
2.4. Structural-Phase Deformability of Soils . . . . .	70
2.5. Features of the Physical Properties of Structurally Unstable Subsidence Soils . . . . .	77
<b>CHAPTER THREE. DETERMINATION OF STRESSES IN SOIL . . . . .</b>	<b>85</b>
3.1. Stress Distribution in the Case of a Three-Dimensional Problem . . . . .	86
3.2. Stress Distribution in the Case of a Planar Problem . . . . .	103
3.3. Pressure Distribution over the Base of the Foundation of Structures (Contact Problem) . . . . .	112
<b>CHAPTER FOUR. THE THEORY OF ULTIMATE STRESSED STATE OF SOILS AND ITS APPLICATION . . . . .</b>	<b>123</b>
4.1. Stressed State Phases of Soils with an Increase in Load . . . . .	123
4.2. Equations of Ultimate Equilibrium for Loose and Cohesive Soils . . . . .	128
4.3. Critical Loads on Soil . . . . .	133
4.4. Stability of Soils in Landslides . . . . .	148
4.5. Some Problems of the Theory of Soil Pressure on Retaining Walls . . . . .	161
4.6. Soil Pressure on Underground Pipelines . . . . .	167
<b>CHAPTER FIVE. SOIL DEFORMATIONS AND SETTLEMENT OF FOUNDATIONS . . . . .</b>	<b>174</b>
5.1. Kinds and Causes of Deformations . . . . .	174
5.2. Elastic Deformations of Soils and Methods for Their Determination . . . . .	175
5.3. One-Dimensional Problem of the Theory of Soil Consolidation . . . . .	185
5.4. Planar and Three-Dimensional Problems in the Theory of Filtration Consolidation of Soils . . . . .	202

5.5. Prediction of Foundation Settlements by the Layerwise Summation Method . . . . .	207
5.6. Prediction of Foundation Settlements by Equivalent Soil Layer Method . . . . .	219
<b>CHAPTER SIX. RHEOLOGICAL PROCESSES IN SOILS AND THEIR SIGNIFICANCE . . . . .</b>	<b>238</b>
6.1. Stress Relaxation and Long-Term Strength of Cohesive Soils	241
6.2. Creep Deformations in Soils and Methods for Their Description	246
6.3. Account of Soil Creep in Predictions of Foundation Settlements	253
<b>CHAPTER SEVEN. DYNAMICS OF DISPERSE SOILS . . . . .</b>	<b>264</b>
7.1. Dynamic Effects on Soils . . . . .	264
7.2. Wave Processes in Soils under Dynamic Loads . . . . .	267
7.3. Changes in the Properties of Soils Subject to Dynamic Effects	275
7.4. The Principal Prerequisites for Taking the Dynamic Properties of Soils into Account in Vibrational Calculations of Foundations . . . . .	281
List of Books Recommended . . . . .	288
Index . . . . .	289

## PREFACE

This is a textbook in the course of Soil Mechanics for higher-school students of civil engineering and hydrotechnical engineering, and also for students of other specialities associated with construction of engineering structures, such as road constructors, ameliorators, geologists, soil scientists.

The Author has made an attempt to write a concise course on the basis of a wide synthesis of natural sciences and to present the theoretical data in the most simple and comprehensive form, without depreciating, however, the general scientific aspect of the problem; his other aim was to present a number of engineering solutions of problems in the theory of soil mechanics (calculations of strength, stability and deformability), which might be widely used in engineering.

The book is based on the course of lectures given by the Author at the Moscow Civil Engineering Institute, his earlier book (*Soil Mechanics*, 4th ed., Moscow, Stroiizdat, 1963), and the newest research works in soil mechanics, both Soviet and foreign, and their practical applications.

Some problems in the book are discussed from new standpoints which take into account the principal properties of soils: contact shear resistance, structure-phase deformability (including creep of skeleton), compressibility of gas-containing porous water, and the effect of natural compaction of soils.

The book shows some new methods used for determination of characteristics of soils and gives some new solutions of the theory of consolidation and creep of soils, which can be used for predictions of settlement rates of foundations of structures and their time variations; a separate chapter discusses rheological processes in soils and their significance.

All letter designations in the book are given in accordance with recommendations of the International Society of Soil Mechanics and Foundation Engineering (ISSMFE).

The Author

## INTRODUCTION

*Soil mechanics* is the mechanics of natural disperse (finely divided) bodies and constitutes a branch of the general *geomechanics* which also includes global and regional geodynamics, mechanics of massive rocks, mechanics of natural soils, and mechanics of organic and mineral-organic masses (silts, peats, etc.).

On the other hand, soil mechanics is one of the divisions of *structural mechanics* based on the laws of theoretical mechanics (i.e., mechanics of absolutely incompressible rigid bodies) and the relationships of deformable bodies (the laws of elasticity, plasticity, and creep), which, however, are only indispensable but not sufficient conditions for the development of the science of soil mechanics. If the laws and relationships of theoretical mechanics and structural mechanics of continuous deformable bodies are supplemented with the relationships describing the state and properties of soils caused by their dispersity (compressibility, water permeability, contact shear resistance, and structural-phase deformability) and if soils are regarded as natural disperse bodies intimately associated with the conditions of their formation and the surrounding physico-geological medium, only then can the soil mechanics be developed as a branch of science.

By *soils* will be understood all "loose deposits" (a geological term) of the weathered crust of the Earth's rock mantle (lithosphere), both cohesionless (loose) and cohesive, in which the strength of bonds is only a small fraction of the strength of mineral particles. A very characteristic feature of soils as natural bodies is their dispersity, in which they differ radically from mineral rocks (massive-crystalline, metamorphic, sedimentary, etc.) possessing a rather high strength. Mineral aggregates and grains in rocks are bonded together and possess rigid (crystallizational, cementational, etc.) internal bonds whose strength is of the same order as that of mineral grains proper.

In estimations of soils as bases of future structures, of essential importance is the thickness of a soil layer above the *bed rock*. Naturally, rocks, if considered in large volumes, may be regarded to consist of separate components less strongly bonded together than themselves, so that the relationships of soil mechanics may be applicable

to such rocks to a definite extent, but with appropriate additional conditions.

The upper layer of natural earth, which has been altered under the combined action of climate, water, gases, plants, and animals and enriched in humus, is a specific structural mineral-organic formation called the *humus soil*.

Soil mechanics studies only mineral soils, i.e., natural disperse materials, and only rarely has to deal with rocks and mineral-organic formations.

**Formation of soil mechanics and the role of Soviet scientists.** The first fundamental work on soil mechanics was the study made by C. Coulomb in France in 1773 on the theory of loose bodies, which for many years was almost the sole engineering theory successfully employed in practical calculations of soil pressure on retaining walls.

In 1885, Prof. J. Boussinesq, also of France, published his work *Application des potentiels a l'étude de l'équilibre et du mouvement des solides élastiques*; the results of his study were first applied to soil mechanics by Soviet scientists (N. N. Ivanov, 1926) and further were laid as the basis for determination of stresses in soils under various loads.

It should be noted that as far back as 1915, Prof. P. A. Minyaev applied the theory of elasticity to calculations of stresses in loose soils, and in 1923, Prof. N. P. Puzyrevsky proposed *The General Theory of Stressed State in Earthen Soils*, having applied the theory of elasticity to calculations of bases; the same year, Acad. N. N. Pavlovsky published a fundamental work on the theory of motion of ground waters, which laid the basis for modern methods of calculations of filtration.

An important stage in the development of soil mechanics was the studies of Prof. K. Terzaghi published in his books *Erdbau-mechanik auf bodenphysikalische Grundlage* (1925) and especially in *Theoretical Soil Mechanics* (1943) (Russian translation published in 1961).

A very large contribution to modern soil mechanics was made by Prof. N. M. Gersevanov in *Fundamentals of Dynamics of Soil Masses* (1931-33), in which the author refined the equation of one-dimensional consolidation of fully saturated soil masses proposed by Terzaghi, formulated the differential equations of planar and three-dimensional problems in the theory of filtration consolidation of soils, developed some particular solutions, and discussed a wide circle of other problems in soil mechanics.

Of especial importance for the theory of deformation of water-saturated soils are the works of Prof. V. A. Florin, generalized in his monograph *Fundamentals of Soil Mechanics* (1959-1961), where he formulated, in a convenient form, the differential equations of the

planar and three-dimensional problems of filtration consolidation and developed general methods for their solution in finite differences. V. A. Florin has made a substantial contribution to the theory of consolidation and solved some problems with a special account of compressibility of porous water, creep of the soil skeleton, variability of the parameters, etc.

It should be noted that Coulomb's engineering theory of loose bodies, which was used almost without alterations for about 170 years, found a new more rigorous development in the works of Soviet researchers (first in the work of V. V. Sokolovsky *Statics of Loose Bodies*, 1942, and then in the works of S. S. Golushkevich and V. G. Berezantsev, 1948), who also developed efficient methods for solving problems involved in this theory.

Much attention was paid by Soviet scientists to investigations of combined action of structures and compressible soils in their bases (the works of Acad. A. N. Krylov, Profs. N. P. Puzrevsky, G. E. Proktor, M. I. Gorbunov-Posadov, B. N. Zhemochkin, A. P. Sinitsyn, S. S. Davydov, I. A. Simvulidi et al.).

A great role in the application of soil mechanics to the practice of hydrotechnical construction was played by the works of Profs. N. N. Ivanov and N. N. Maslov et al. at the Svir hydraulic power station; they predicted settlements and inclinations of hydrotechnical structures and ensured their stability on powerful layers of clayey soils.

A wide development of studies in the theory of soil consolidation and the results of unique experiments and observations made in the USSR enabled the Soviet researchers (N. M. Gersevanov, D. E. Polshin, N. N. Maslov, M. I. Gorbunov-Posadov, S. A. Roza, A. A. Nichiporovich, K. E. Egorov, N. A. Tsytoich, Yu. K. Zaretsky et al.) to develop methods for predicting settlements of structures and, on their basis, a new progressive method for designing foundations by ultimate deformations of bases.

Soviet scientists have also made an appreciable contribution to the mechanics of various regional kinds of soils: non-saturated subsiding, loess soils (N. Ya. Denisov, Yu. M. Abelev, V. G. Bulychev, A. K. Larionov et al.), frozen soils and permafrost (N. A. Tsytoich, M. N. Goldstein, S. S. Vyalov et al.), and nonuniformly compressed weak clayey soils (B. D. Vasilyev, B. I. Dalmatov, N. A. Tsytoich, M. Yu. Abelev et al.).

Finally, it should be mentioned that fundamentals of soil mechanics as a new branch of science were first formulated and the first course of lectures on the subject was published in the USSR (N. A. Tsytoich, *Fundamentals of Soil Mechanics*, 1934).

The role of Soviet scientists and their achievements in the theory of soil mechanics cannot, naturally, be exhaustively described by this brief list; their names will be encountered more than once in the book.

---

**Significance of soil mechanics.** Soil mechanics is the theory of natural soil bases. The role of soil mechanics as an engineering science is enormous and can only be compared with that of the Strength of Materials. Without knowledge of the fundamentals of soil mechanics, it is impossible to design correctly modern engineering structures, residential buildings (especially high ones), ameliorating structures, roads, earthen and hydrotechnical structures (embankments, dams, hydraulic power station buildings, etc.).

The application of soil mechanics makes it possible to utilize more fully the load-bearing capacity of soils and to precisely account for deformations of soil bases under the action of loads from structures, which provides most safe and also economic engineering solutions.

The role of soil mechanics in engineering will continue to grow, which will enable wider and better utilization of scientific achievements in building practice.

## Chapter One

### THE NATURE AND PHYSICAL PROPERTIES OF SOILS

#### 1.1. GEOLOGICAL CONDITIONS OF SOIL FORMATION

Natural soils are the product of physical and chemical weathering of rocks. Their properties were formed in the course of their formation and subsequent existence depending on the surrounding conditions. The age of natural soils in most cases (except for new deposits) is rather great, measuring thousands, millions, or hundreds of millions of years (for instance, the age of Cambrian clays is about 500 mln years).

During the long period of existence of soils, natural conditions varied many times, and soils were repeatedly redeposited, compacted under the weight of new surface deposits, decompacted through erosion of these deposits, sometimes flooded with water and again deflooded through tectonic lifts, etc. Some soils were subjected to the pressure of thick layers of continental ice, displaced by ice, water, air flows, etc. All this provided conditions for the formation of natural soils, that determine the specific features of individual kinds of soils and cannot be reproduced artificially. Because of the very long time of existence of soils, even very slow physico-chemical processes occurring in them with negligibly slow rate may be of importance.

In view of what has been said above, natural soils should be considered in close interaction with the surrounding physico-geological medium and with account of continuous variations of their properties which occur sometimes slowly, but sometimes very rapidly.

According to their origin and the conditions of formation, all soils may be divided into (1) *continental deposits: eluvial* (located at the place of their original formation); *deluvial* (located at the slopes of the same upland where they have been formed and transferred only by the action of the force of gravity and through washing-off by atmospheric waters); *alluvial* (transferred by water flows over substantial distances and forming thick stratified deposits); *glacial* (formed through the action of glaciers) — boulder clays and sand clays; *water-glacial*—sand and pebble soils; *sea-glacial* soils—bandy clays, loams, and sandy loams; *eolian* (the products of physical weathering of rocks of desert regions, transferred by air flows)—loess soils and dune sands; (2) *marine deposits: layers of disperse*

clays, organogenous shelly soils, etc.; mineral-organic formations—silt, peaty soils, etc.; various sands and pebble soils.

It can be seen from this brief list of kinds of soil that the composition of natural soils may be very diverse and their physical nature, very complicated.

## 1.2. COMPONENTS OF SOILS

The composition of natural soils may include very diverse components which can be classed into three large groups as follows: (1) solid mineral particles; (2) water in various forms and states; and (3) gaseous inclusions. In addition, some soils may contain organic and mineral-organic compounds which can also affect the physical properties of these soils (this problem will be discussed in a separate section).

*Solid mineral particles in soils.* These represent a system of solid mineral grains which may vary in their shape, composition, and size (from a few centimetres—pebbles to tiniest colloidal particles less than 1 micron—disperse clays).

A factor of importance in the evaluation of the properties of solid soil particles is their *mineral composition*. Thus, some minerals, such as quartz and feldspar, interact only slightly with the surrounding water, whereas other minerals, for instance, montmorillonite, can interact substantially more actively and in a different way. The smaller the particles of a soil, the greater their unit surface area (per  $\text{cm}^3$  or per gram) and the larger the number of centres of interaction with the surrounding water and in contacts between solid particles proper. For instance, particles of kaolin (a clay mineral) have a unit surface area of  $10 \text{ m}^2/\text{g}$ , whereas those of montmorillonite have a very large unit surface area of  $800 \text{ m}^2/\text{g}$ , which inevitably affects the properties of natural soils containing particles of montmorillonite. The presence of particles of mica (which are very slippery and have only a negligible shear resistance) has an essential effect on the physical properties of the soils containing such particles; this circumstance must always be taken into account.

According to BC&R\*, all soils are classed by the size of their mineral particles into three types as follows:

1. *Coarse-grain soils* (pebbles, if particles are rounded off and rubbles, if particles are sharp-edged) containing more than 50 per cent by weight of particles larger than 2 mm in size.

2. *Sandy soils* are divided into the following groups: coarse-grained (with more than 50 per cent by weight of particles larger than 0.5 mm); medium-grained (with more than 50 per cent by weight of particles larger than 0.25 mm); fine-grained (with more than 75 per cent by weight of particles larger than 0.10 mm); and dusty sands (with less than 75 per cent by weight of particles larger than

\* BC&R—Building Code and Regulations adopted in the USSR.

0.10 mm). (All particles larger than 0.05 mm are regarded as sand particles, and those of a size from 0.005 mm to 0.05 mm, as dusty particles.)

3. *Clayey soils* are not divided into groups in view of the large diversity of the size, shape and mineral composition of their particles. It should only be noted that all soil particles from 0.01 micron to 0.005 mm in size are considered as clay particles.

Because of their extreme dispersity, clay particles can envelop all solid sand grains and inclusions in clayey soils, so that the weight content of clay particles in a clayey soil can appreciably affect the

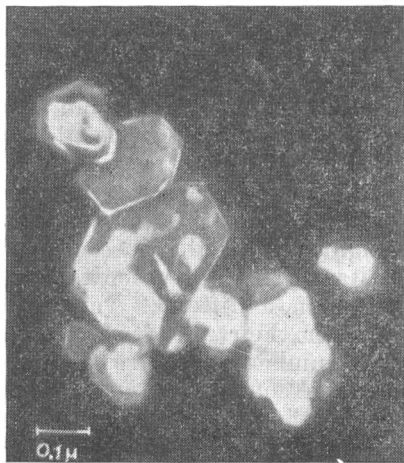


Fig. 1. Polygonal flaky particles of kaolinite

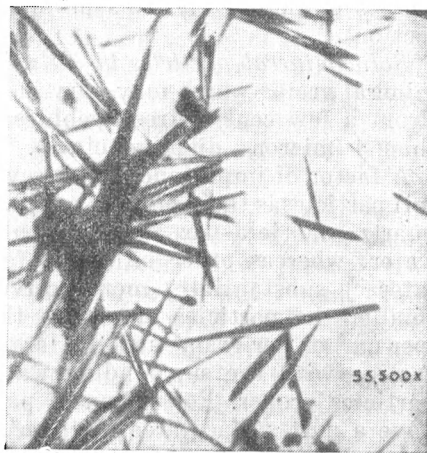


Fig. 2. Needle-shaped particles of attapulgite

physical properties of the latter. For that reason, clayey soils are named (see Sec. 1.4) according to the total content of clay particles (of a size less than 0.005 mm) in them.

As distinct from sand particles which have a compact shape (i.e., their size is approximately the same in all directions), clay particles may be very diverse in shape and in most cases have the form of thin flakes with the major size 10-50 times their thickness; the shape of clay particles may be either polygonal (kaolinites, Fig. 1) or needle-like (attapulgites, Fig. 2).

The mineral composition of clay particles is also of large importance. Thus, crystals of montmorillonite (of which montmorillonite clays are composed) possess a *movable crystal lattice* which under proper conditions is capable of entraining molecules of water, so that the crystals can swell appreciably and increase in their volume,

whereas particles of kaolinite, attapulgite and hydromica possess such properties only to a substantially lower extent.

All what has been said above has an appreciable effect on the properties of natural clayey soils.

*Water in soils.* The kinds and properties of water in soils may vary depending on the content of water and the forces of its interaction with mineral particles, which are mainly determined by hydrophilicity of these particles.

Mineral particles in soils have a negative charge, whereas molecules of water are dipoles charged positively at one end (an atom of oxygen) and negatively (two atoms of hydrogen) at the other. On contact of solid mineral particles with water, electromolecular forces of interaction are formed that strongly attract dipoles of water to the surface of mineral particles (especially in the upper layers) and the greater the unit surface area of the particles, the larger the number of water molecules in a *bonded* state. According to the modern views, electromolecular forces of interaction are very strong and attain several thousands of kilograms per square centimetre at the surface of mineral particles (for the first row of bonded molecules of water). As solid particles move away from the surface, these forces attenuate rapidly and become close to zero at a distance of approximately 0.5 micron from the surface. The layers of 1-3 rows of water molecules that are the closest to mineral particles and contact the solid surface are so firmly bonded with the surface by the forces of electromolecular interaction that they can be removed neither by an external pressure of a few atmospheres nor by the action of water pressure; these layers form films of what is called *firmly bonded adsorbed water*.

With an increase of the distance from the solid surface of soil particles, the layers of water molecules, enveloping the mineral particles, will be bonded and orientated by the boundary phase with ever weaker forces; they form layers of *loosely bonded* (lyosorbed) water, which can be squeezed from soil voids by an external pressure of a few  $\text{kgf/cm}^2$  (sometimes up to a few tens of  $\text{kgf/cm}^2$ ).

Finally, the molecules of water located beyond the sphere of interaction of electromolecular forces with the surface of mineral particles will form the so-called *free* (according to Prof. A. F. Lebedev), or *gravitational water*, whose motion occurs under the action of a pressure gradient and the *capillary water* which is drawn up to a definite height above the ground water level by the forces of capillary tension (the capillary menisci formed under the action of superficial adsorption forces in narrow voids of soil are responsible for capillary forces in soils).

Electromolecular interaction of water with the surface of mineral particles is shown schematically in Fig. 3.

*Gaseous inclusions* (vapours and gases). These are always present in some or other amount in soils. The gaseous inclusions may be in

the following states: (a) *closed state*, i.e., located in vacuoles (voids) between solid mineral particles, the latter being enveloped with films of bonded water; (b) *free state*, when gases (air) communicate

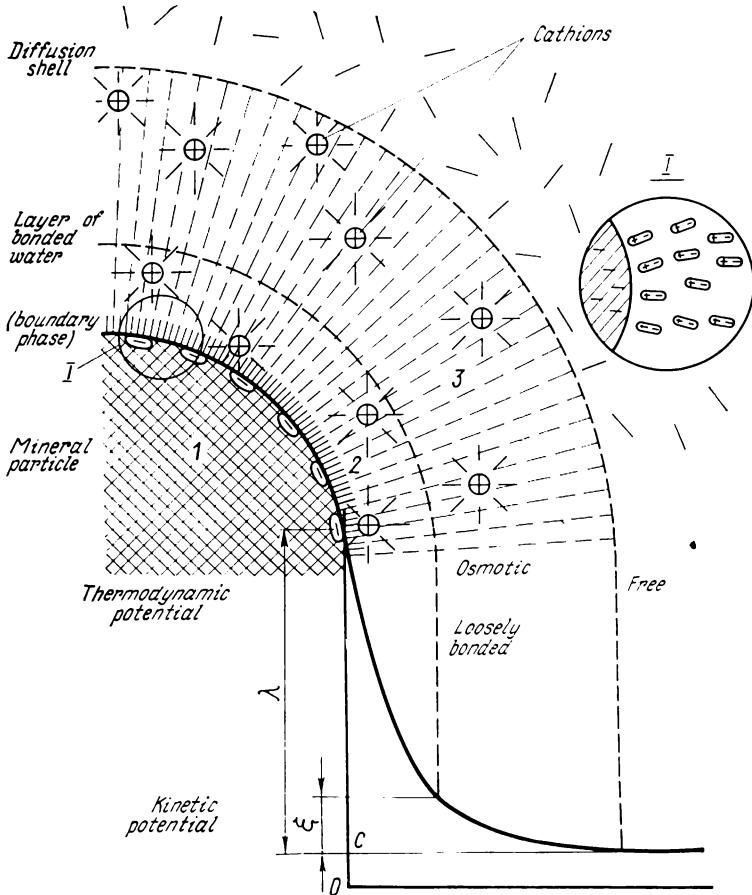


Fig. 3. Electromolecular interaction between the surface of mineral particle and water

1—mineral particle; 2—bonded water; 3—loosely bonded (osmotic) water

with the atmosphere; and (c) *dissolved state*, i.e., dissolved in the pore water.

Gas bubbles, either present in closed state or contained in the pore water, may have an appreciable effect on the deformability of soils, because they are responsible for the compressibility of the pore water and increase soil elasticity.

The content of free gases (air) communicating with the atmosphere has, however, no special significance in soil mechanics, since these gases practically do not participate in the distribution of pressures between soil particles.

### 1.3. STRUCTURAL BONDS AND STRUCTURE OF SOILS

The structural properties of disperse materials (including clayey soils which are very complex disperse mineral formations) depend not so much on the strength of individual mineral grains (which may be very large), as on the specific structural features, among which the most important are the structural bonds between individual mineral particles and aggregates.

These bonds are of a very complicated nature and are defined by the combination of the external and internal energy fields acting in the soil, these fields being caused by *molecular forces* of electromagnetic nature. The character of their action depends on the interface area, the chemical nature of solid mineral particles, and the structure and properties of substances filling the voids between particles.

Molecular forces that act directly between solid particles (Van der Waals forces) can appear only with a very close contact between solid particles and the distances of the order of several rows of molecules (but not more than a few tens) between them. Such distances can be observed in soils composed of solid particles and subjected to the action of a substantial external pressure which is transformed at the points of contact into enormous forces, or in very dense moist soils, where the films of bonded water and colloidal shells around particles are destroyed by an external pressure. Van der Waals forces are enormous, but their total action depends on the number of points of direct contact, which, generally speaking, are not numerous in soils.

According to the physico-chemical classification of disperse solids proposed by Acad. P. A. Rebinder, the structural bonds in water-saturated soils can be *coagulation* (usually the original ones, appearing through the fall-out of particles in water and coagulation of colloids in the presence of electrolytes), *condensation* (appearing through the compaction of coagulation structures up to the direct contact of mineral particles with each other or by way of polymerization of gels) or, finally, *crystallization* (appearing through the formation of nuclei of solid crystals, which then grow and combine through the action of interatomic chemical forces). Crystallizational bonds (bonds between crystals of silicon, iron oxides, etc.) are *brittle*, the strongest and irrestorable after destruction; coagulation and condensation bonds are *soft* and can be restored to some or other extent after being destroyed.

Structural bonds in soils may be very diverse depending on the

properties of mineral particles and water solutions that fill the voids in soils, and also on the conditions of the original accumulation of mineral sediments and their subsequent lithogenesis (transformation into a rock) by passing through a sedimentation stage (formation of sediments), diagenesis (transformation of sediments into solid rocks), and metamorphism (transformation of rocks).

It follows from what has been said above (and also from the works of Acad. P. A. Rebinder, Profs. N. N. Maslov, N. Ya. Denisov, A. K. Larionov, T. W. Lambe et al.) that the following main kinds of structural bonds may be distinguished in soils:

(1) *water-colloidal* (coagulation and condensational) — viscoplastic, soft, and restorable;

(2) *crystallizational*—brittle (hard), irresterable, which may be either water-stable or water-unstable.

Soils with water-unstable crystallizational bonds possess the properties that are intermediate between those of soils with colloidal bonds and those of soils with crystallizational bonds. These bonds are formed irrespective of the magnitude of the surface area of mineral particles through the formation of *cleavages of amorphous substances*, natural cements, humic compounds and glues, whose strength depends on the content of water in them.

*Water-colloidal bonds* are caused by the electromolecular forces of interaction between mineral particles, on the one hand, and water films and colloidal shells, on the other. The strength of these forces depends on the thickness of films and shells. The thinner the water-colloidal shells, i.e., the lower the moisture content of water-saturated soils, the stronger the water-colloidal bonds, since thinner shells provide for a higher molecular attraction of bonded water dipoles and a higher gluing action of the substances, which, according to V. S. Sharov, is due to partial dissolution of clay particles in water. Water-colloidal bonds are plastic and restorable; with an increase in the moisture content they quickly reduce almost to zero.

*Crystallization bonds* appear under the action of the forces of chemical affinity, thus combining with mineral particles (at points of contact) into new polycrystalline substances that are very strong but brittle and irresterable after destruction. The strength of these bonds depends on the composition of minerals. Thus, the bonds formed by gypsum or calcite are less strong and water-stable, while opal, iron and silicon oxides can form more strong and water-stable crystallizational bonds.

As has been shown by T. W. Lambe, the structure of soils, i.e., a regular location of mineral particles and aggregates of various size and shape, depends not only on the nature of their structural bonds, but also on the magnitude and nature of contacts between clay particles proper: "edge-to-face" (with a loose constitution) or "face-to-face" (with a more compact constitution).

According to A. K. Larionov\*, the structure of soils may be very diverse and is defined by the quantitative and morphological relationships between the solid, liquid and gaseous phases forming a soil. For the formation of the strength of clayey soils, of large importance are the nature of aggregations of particles and the *development of microstructural defects*.

As seen from the above, the structure of natural soils is rather complicated; the structure of marine clay deposits which has been

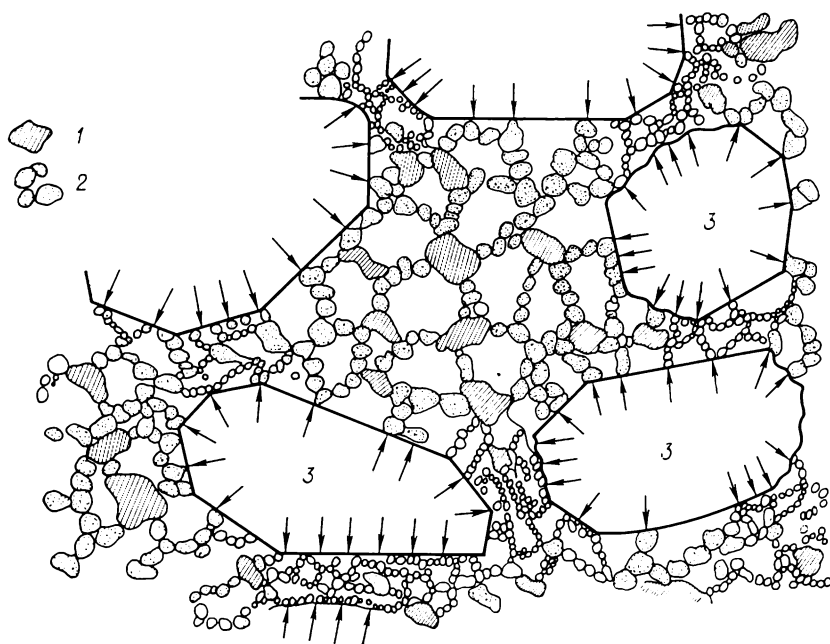


Fig. 4. Structure of clay

1—clay particles; 2—compacted colloids; 3—sand grains

studied in detail by Prof. A. Casagrande (Fig. 4) may be taken as an example.

The natural structure, composition and state of soils determine, in the main, the deformation and strength properties of soils and their work in foundation bases, with the *structural strength of soils and the stability of their structural bonds* under external actions being characteristics of prime importance.

\* Larionov A. K. Inzhenerno-geologicheskoe izuchenie strukturnykh ryklykh osadochnykh porod (Engineering-Geological Studies of Structural Loose Sedimental Rocks), Moscow, Nedra Publishers, 1966.

For the estimation of constructional properties of disperse soils, a rather important characteristic is also the *constitution* (structure) of natural soils, i.e., the spacial location and mutual position of particles and aggregates, which characterize *non-homogeneity* of the soil in a layer.

The following main kinds of constitution of natural clayey soils are distinguished:

(1) *lamellar* (fine- and coarse-bedded, bandy, obliquely lamellar, shaly, etc.);

(2) *compact* (massive and latent-lamellar);

(3) *composite* (porphyrous, cellular, macro-porous, etc.).

#### 1.4. PHYSICAL PROPERTIES AND CLASSIFICATION INDICES OF SOILS

The complicated structure of natural soils and the effect of physico-geological processes (sometimes very long) require that in estimation of soils their properties be determined either under conditions of the natural state or by samples of natural undisturbed structure.

Natural soils differ from rocks (massive crystalline formations) mainly in that they have *no cleavage* (i.e., the number of crystallization bonds is relatively low) and possess an appreciable *porosity* caused by their discreteness.

In order to determine the *physical properties of soils* (porosity, water saturation, etc.), we have to know three simplest characteristics: unit weight  $\gamma$  of the soil of natural structure; specific weight  $\gamma_s$  of solid particles of the soil; and natural moisture content  $W$  of the soil.

**The unit weight  $\gamma$**  of the soil is determined on samples of the soil taken from boreholes by a sampling tube, with the minimum disturbance of the soil structure, or from trial pits, by a cutting ring. It must be calculated with a sufficient accuracy (up to 0.01 gf/cm<sup>3</sup>), since it is the most important initial characteristic of soils, which is indispensable for determination of a number of characteristics entering the equations of soil mechanics. The soil unit weight is conditioned by the geological history of the formation and subsequent existence of the soil and must be determined on samples of undisturbed structure with a high accuracy.

**The specific weight  $\gamma_s$**  of the soil is a characteristic, mainly, of its mineral composition and is determined by means of a pycnometer. For most soils, it varies within the narrow limits, from 2.50 to 2.80, and is equal, on the average, to 2.65 for sands and 2.70 for clays.

**The moisture content  $W$**  of the soil is determined by the results of weighing a natural sample of the soil before and after complete drying (at 105°C).

In order to explain certain terms used in the subsequent discussion, let us introduce the following designations for a definite volume of soil:  $V_1$  = volume of solid particles;  $V_2$  = volume of voids (pores);  $g_1$  = weight of solid particles;  $g_2$  = weight of water in soil voids (the weight of air in voids may be neglected).

Let us agree that the soil *unit weight* is the ratio of the weight of the whole soil (with all its inclusions) to its volume, i.e.,

$$\gamma = \frac{g_1 + g_2}{V_1 + V_2}$$

that the *specific weight* is the ratio of the weight of solid particles of soil to their volume only, i. e.,

$$\gamma_s = \frac{g_1}{V_1}$$

and that the *moisture content* of the soil is the ratio of the weight of water to the weight of dried soil (or to the weight of solid particles), i.e.,

$$W = \frac{g_2}{g_1}$$

Let us also introduce some additional concepts: the *unit weight of soil skeleton* (or of dry soil)  $\gamma_d$ , i.e., the ratio of the weight of solid particles to the total volume of the soil

$$\gamma_d = \frac{g_1}{V_1 + V_2}$$

and the *unit weight of water*  $\gamma_w$ , i.e., the ratio of the weight of water in a certain volume to the magnitude of that volume

$$\gamma_w = 1 \text{ gf/cm}^3 = 0.001 \text{ kgf/cm}^3$$

**The void ratio and water-saturation ratio or index of saturation.** The *porosity*, or *void ratio of the soil*  $e$  is the ratio of the volume of voids to the volume of soil skeleton, i.e.,

$$e = \frac{n}{m} \tag{1.1}$$

where  $n$  = volume of voids in unit volume of soil

$m$  = volume of solid particles in the same unit volume of soil

It is natural that  $n + m = 1$ .

The volume of solid particles  $m$  in the soil is equal to the ratio of the weight of solid particles in a unit volume (which is numerically equal to  $\gamma_d$ ) to their specific weight  $\gamma_s$ , i.e.,

$$m = \frac{\gamma_d}{\gamma_s}$$

Then, taking into account that  $n = 1 - m$ , we get

$$e = \frac{\gamma_s - \gamma_d}{\gamma_d} \quad (1.2)$$

As regards the unit weight of soil skeleton  $\gamma_d$ , it can be easily found if we note that the soil moisture content  $W$  is equal to the ratio of the weight of water  $\gamma - \gamma_d$  to the weight of soil skeleton  $\gamma_d$ , i.e.,

$$W = \frac{\gamma - \gamma_d}{\gamma_d}$$

whence the unit weight of soil skeleton is

$$\gamma_d = \frac{\gamma}{1 + W} \quad (1.3)$$

Here and further, the soil weight moisture content  $W$  is taken in fractions of unity (for instance,  $W = 0.20$ , etc.).

Formulae (1.2) and (1.3) make it possible to determine the porosity of natural soils, which is the most important characteristic of their natural compaction and plays an important part in soil mechanics (in predictions of settlements of foundation bases, etc.).

The void ratio  $e$  of soils may vary within a rather wide range (approximately from  $e = 0.20$  to  $e = 1.5$  for mineral soils and from  $e = 2$  to  $e = 12$  for mineral-organic soils). For sufficiently compacted soils,  $e < 1$ ; when  $e > 1$ , this means that the soil is rather loose, unconsolidated; so that erection of residential buildings or industrial structures on it will require special measures on artificial strengthening.

It will be noted that an important relationship follows from the definition of void ratio. We have

$$\left. \begin{aligned} e &= \frac{n}{m} \quad \text{or} \quad e = \frac{n}{1-n} \\ n + m &= 1 \end{aligned} \right\} \quad (a)$$

Solving the set of equations (a) relative to  $n$  and  $m$ , we get: the volume of voids in a unit volume of soil

$$n = \frac{e}{1 + e} \quad (1.4)$$

and the volume of solid particles

$$m = \frac{1}{1 + e} \quad (1.5)$$

The *index of saturation*  $I_w$  of soils (or, according to BC&R, the degree of moisture content  $G$ ) is the ratio of the soil natural moisture

content  $W$  to its total water content at full saturation  $W_{f.s}$  which corresponds to the full filling-in of soil voids with water, i.e.,

$$I_w = \frac{W}{W_{f.s}} \tag{1.6}$$

With full filling-in of voids with water, the moisture content will be equal to the ratio of the weight of water in the volume of voids ( $\frac{e}{1+e} \gamma_w$ ) to the weight of solid particles ( $\frac{1}{1+e} \gamma_s$ ), i.e.,

$$W_{f.s} = \frac{\frac{e}{1+e} \gamma_w}{\frac{1}{1+e} \gamma_s} = \frac{e \gamma_w}{\gamma_s} \tag{b}$$

Substituting this expression for  $W_{f.s}$  into (1.6), we obtain the following expression for the index of saturation:

$$I_w = \frac{W \gamma_s}{e \gamma_w} \tag{1.6'}$$

Assuming the unit weight of water to be  $\gamma_w = 1 \text{ gf/cm}^3$ , we obtain from expression (b) a new expression for the porosity of fully saturated soils:

$$e = W_{f.s} \gamma_s \tag{1.7}$$

i.e., the *void ratio of a fully saturated soil is the product of the moisture content by specific weight.*

The index of saturation of natural clayey soils is close to unity. In many cases, however, it is slightly less than unity because of the presence of gas bubbles in the water, which has an appreciable effect on the compressibility of the pore water. In order to take into account the compressibility of pore water, the index of saturation must be determined to a high accuracy (to 0.1 per cent).

According to the BC&R classification, cohesionless (loose) soils are divided into the following groups:

Low-moist . . . . .	at $I_w \leq 0.5$
Moist . . . . .	at $0.5 < I_w \leq 0.8$
Saturated . . . . .	at $I_w > 0.8$

An incompletely saturated soil (at  $I_w < 1$ ) is a *three-phase particulate system* composed of solid mineral particles, water, and gases; at full saturation ( $I_w = 1$ ), unconsolidated soils (in most cases located below the ground-water table): sands, sand loams, silts, weak loams and clays, with the presence of *free, hydraulically continuous water* in their voids, represent a special class of two-phase soils, or what is called the *soil mass*, to which the special theory of filtration consolidation (compaction) of soils is fully applicable.

It will be noted that in soils located below the ground-water table *in the state of soil mass*, the soil skeleton is subjected to uplifting action of water.

Noting the weight of solid particles in water ( $\gamma_s - \gamma_w$ ) and their volume ( $\frac{1}{1+e}$ ) in a soil unit volume, we get the following expression for the soil unit weight lightened by the weight of the water it has displaced:

$$\gamma' = \frac{\gamma_s - \gamma_w}{1+e} \quad (1.8)$$

and noting that  $\frac{1}{1+e} = 1 - n$ , we have another expression for ( $\gamma'$ )

$$\gamma' = (\gamma_s - \gamma_w) (1 - n) \quad (1.8')$$

**Classification indices of soils.** These are employed for classing the soils into categories, so as to be able to predict in outline the behaviour of the soils when building structures are being erected thereon, and to choose the standard pressures on soil bases (for specifying the preliminary dimensions of foundations), and in some cases, in order to determine the applicability of some or other theoretical solutions of soil mechanics (the theory of loose bodies, the theory of filtration consolidation, the theory of creep, etc.) in practical calculations.

The classification indices of soils include the *substance composition* of soils (grain-size distribution and mineral composition, moisture content, and gas content) and the *characteristics of their physical state* (density for sandy soils and consistency for clayey soils). These last characteristics are conditional in a definite sense and provide an indirect method for an approximate determination of some calculation indices of the mechanical properties of soils, by using some standard data and other materials (for instance, BC&R).

**The grain-size distribution** of sandy and stony soils, according to which these soils are classed into groups, has been indicated in Sec. 1.2.

For clayey soils, however, of prime importance is not the total grain-size distribution, but the content of small and tiniest particles (of flat flaky or thin needle-like monomineral particles of at least 0.005 mm in size) and, what is most important, the range of moisture content within which the soil remains plastic.

The content of clay particles in soil is determined from special laboratory analyses by methods usually discussed in the courses on soil science. The range of moisture content within which the soil remains plastic can be determined by a simple test. This range is characterized by the plasticity index  $I_p$ , which is equal to the difference between two weight moisture contents, expressed as a percen-

tage, that are characteristic of clayey soils: the *liquid limit*  $W_L$  and the *plastic* (rolling-out) *limit*  $W_p$

$$I_p = W_L - W_p \quad (1.9)$$

The liquid limit  $W_L$  corresponds to moisture content at which the soil is transformed into a *liquid state*. This moisture content is found by a standard test, by determining the moisture content of a soil paste (the soil artificially mixed with water) of such a thickness at which a standard balancing cone (according to the USSR Standards, of a weight of 76 gf and the apex angle of 30 degrees) penetrates the soil paste under its own weight to a depth of 10 mm.

The plastic (rolling-out) limit  $W_p$  corresponds to a moisture content at which the soil loses its plasticity. It is approximately equal to the moisture content of a thread made from that soil and rolled out on paper until the soil loses its plasticity, i.e., until a thread 3 mm in diameter, being dried during rolling-out, begins to crumble; pieces of the soil that lost their plasticity are then gathered, weighed, dried up, weighed again, and the moisture content  $W_p$  is calculated.

By continuing the test further, the minimum diameter to which the soil can be rolled out into a thread is determined. As has been shown by special experiments, this diameter is different for various soils and corresponds to a definite weight content of physical clay in the soil.

Notwithstanding a rather elementary and conditional determination of the liquid and plastic limits (the initial concept of these limits was proposed by Prof. Atterberg of Sweden in 1911), these limits, when compared with the natural moisture content of soils, may well characterize the *physical state of clayey soils* and are recommended by BC&R.

On the basis of numerous research studies, and taking into account what has been said above on the characteristic moisture limits of clayey soils, the following simplified grain-size classification of soils may be recommended for building purposes (Table 1.1).

Table 1.1

Simplified Classification of Soils

Type of soil	Plasticity characteristics		Content of clay particles, weight, %
	plasticity index, % $I_p = W_L - W_p$	diameter of soil thread, mm	
Clay	$> 17$	$< 1$	$> 30$
Loamy soil	17-7	1-3	30-10
Sandy loam	$< 7$	$> 3$	10-3
Sand	Not plastic	Cannot be rolled out	$< 3$

Each of the indices given in Table 1.1 can fully characterize the clay content in soils.

**The density of loose soils**, which is of prime importance for the estimation of their work as bases of structures, cannot be evaluated visually, and therefore special tests are to be made, either laboratory tests (by determining the void ratio and the density index on samples of soil taken from boreholes or trial pits) or field tests (by dynamic or static *sounding* directly at the place of location of the soils).

For pure (not micaceous) sands, it is sufficient to determine their natural void ratio [on samples of natural structure by determining  $\gamma$ ,  $W$ , and  $\gamma_s$  and using formulae (1.2) and (1.3)] and compare it with the standard data (such as given in Table 1.2) in order to class the soil to some or other category of density.

Table 1.2

Standard Data on Density of Sands

Kinds of sand	Dense	Medium-dense	Loose
	with the void ratio of		
Gravelly, coarse-grain, and medium-grain sands	$< 0.55$	0.55-0.70	$> 0.70$
Fine-grain sands	$< 0.60$	0.60-0.75	$> 0.75$
Dusty sands	$< 0.60$	0.60-0.80	$> 0.80$

A more general characteristic of the density of sandy soils of any mineral composition is their density index  $I_D$ , determined by the formula

$$I_D = \frac{e_{\max} - e}{e_{\max} - e_{\min}} \quad (1.10)$$

where  $e_{\max}$  = void ratio of sand soil in the most loose state, determined for the most loosened sample of the soil (which is achieved, for instance, by pouring dry sand carefully into a measuring vessel)

$e$  = void ratio of the soil in natural state [to be calculated by formulae (1.2) and (1.3) and the data on the unit weight  $\gamma$ , moisture content  $W$ , and specific weight  $\gamma_s$ ]

$e_{\min}$  = void ratio of the soil in the most compacted state (determined for a soil sample compacted to the constant minimum volume in a vessel by vibration or multiple tapping)

With  $I_D \leq \frac{1}{3}$ , loose soil  
 $I_D = \frac{1}{3} - \frac{2}{3}$ , medium-dense soil  
 $I_D = \frac{2}{3} - 1$ , dense soil

The design resistances of soils for preliminary calculations of sand bases are specified according to BC&R depending on the density, water saturation, and composition of sands.

For some sands located below the ground-water table, determination of the density characteristics (void ratio and density index  $I_D$ ) by

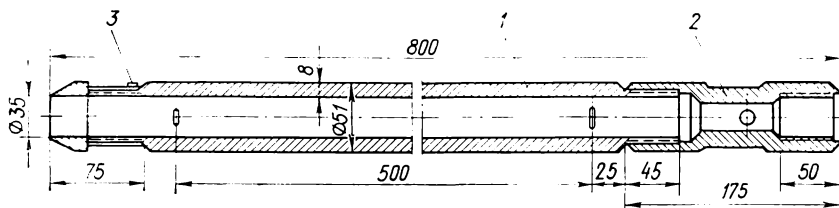


Fig. 5. Sampling tube for dynamic sounding of soils (designed at Fundament-proekt Institute)

1—steel sleeve consisting of two halves; 2—connecting tube; 3—shoe

samples of natural structure is connected with certain difficulties and sometimes is even impossible because of the impossibility of taking samples of undisturbed natural structure. In the last case, and especially when characteristics of relative compaction of various soil strata are to be determined, methods of field *sounding* of natural soils have found application.

At present, two methods of soil sounding are used: a dynamic method and a static one.

For *dynamic sounding*, tests with a standard sampling tube, 51 mm in outside diameter (Fig. 5), have found wide use. The tube is driven vertically to a depth of 30 cm into the soil (in the interval of depths from 15 to 45 cm below the upper level of a borehole) by strokes of a free-falling hammer weighing 63.5 kgf from a height of 71 cm. During the test, the number of strokes required to drive the sampling tube to a given depth is fixed. The denser the soil, the larger the number of strokes required.

Table 1.3 gives some generalized data on relationship between the number of strokes  $N$  required to drive a sampling tube to a depth of 30 cm and the density index  $I_D$  of sand soils.

The second method of sounding, which is more effective and more corresponds to the work of soils under structures in conditions of natural compaction, is the method of *static sounding* by pressing a standard cone (36 mm in diameter, with a base area of 10 cm<sup>2</sup>,

Table 1.3

## Data on Dynamic Sounding with Sampling Tube

Number of strokes $N$	Density index $I_D$	Category of sand soils
1-4	0.2	Very loose
5-9	0.2-0.33	Loose
10-29	0.33-0.66	Medium-dense
30-50	0.66-1.00	Dense
> 50	1	Very dense

and apex angle of 60 degrees) into the soil. Pressing is effected by a special apparatus, with a dynamometer measuring the ultimate resistance of the soil to pressing, the data obtained being used for estimation of the density index of sands and the consistency of clays.

Generalized data on static sounding of sand soils are given in Table 1.4.

Table 1.4

Ultimate Resistance of Soils to Pressing,  $\text{kgf}/\text{cm}^2$ , in Static Sounding

Sounding depth, m	Coarse-grain		Medium-grain		Fine-grain	
	dense	medium-dense	dense	medium-dense	dense	medium-dense
5	150	150-100	100	100-60	60	60-30
10	220	220-150	150	150-90	90	90-40

It will be noted that the data given in Table 1.4 are only relative indices, since the resistance to pressing depends not only on density, but also on structural properties of soils.

The density of sand soils can also be determined by the method of gamma-logging with a radioactive probe, which, however, is beyond the scope of this book.

**Consistency of clayey soils.** Compaction of clayey soils is determined through their *consistency* which is understood as the thickness and, to a certain extent, viscosity of the soil, that make the latter capable of withstanding plastic deformation and depend both on the ratio between solid particles and water in the soil and the forces of interaction between soil particles.

Consistency may be characterized by the relative consistency  $B$  (according to BC&R) or the liquid index  $I_L$  (according to the inter-

national classification), the latter being determined by the expression

$$I_L = \frac{W - W_p}{W_L - W_p} \quad (1.11)$$

According to BC&R, the following *kinds of consistency* of clays are distinguished depending on the magnitude of  $I_L$ :

Hard . . . . .	$I_L \leq 0$ , i.e., when $W \leq W_p$
Semi-hard . . . . .	$I_L = 0-0.25$
Stiff plastic . . . . .	$I_L = 0.25-0.50$
Soft plastic . . . . .	$I_L = 0.50-0.75$
Liquid plastic . . . . .	$I_L = 0.75-1.0$
Liquid . . . . .	$I_L \geq 1$

The consistency of clayey soils can also be estimated by the data of *static sounding* (by their resistance to pressing), which sometimes gives more reliable results than those found by the liquid and plastic limits,  $W_L$  and  $W_p$ .

Some approximate data on the resistance of clayey soils to static sounding (penetration of a 36-mm standard cone, with the base area of 10 cm<sup>2</sup> and apex angle of 60 degrees) are given in Table 1.5.

Table 1.5

Determination of Consistency of Clayey Soils by Results of Static Sounding

Resistance of soil to cone, kgf/cm <sup>2</sup>	Consistency
> 100	Hard
100-50	Semi-hard
50-20	Stiff plastic
20-10	Soft plastic
< 10	Liquid plastic

The characteristics of consistency of clayey soils are of no less importance for their general estimation as the density indices for sand soils, since their values are used for specifying the design resistances of building bases (for preliminary determination of the dimensions of foundations, and for buildings of the 3rd and 4th classes, for final determination). Thus, for instance, for fine-grain dense sands with a low moisture content the design resistance (standard pressure) is 3 kgf/cm<sup>2</sup>; for medium-dense sands, 2 kgf/cm<sup>2</sup>,

and at full saturation, 1.5 kgf/cm<sup>2</sup>. Similarly, for clays of *hard consistency*, with the void ratio  $e \leq 0.5$ , the standard pressure is 6 kgf/cm<sup>2</sup>, whereas for the same clays, but with  $e \geq 1.1$  and an almost liquid consistency, only 1 kgf/cm<sup>2</sup>.

In addition, as will be shown in later chapters, the consistency of clayey soils is of importance for determining the applicability of some or other design theories: the theory of continuous (single-component) deformable masses (elasticity, plasticity, viscous flow), the theory of filtration consolidation, the theory of inherent creep, etc.

## Chapter Two

### BASIC LAWS OF SOIL MECHANICS

We shall discuss in this chapter the basic laws of soil mechanics as the mechanics of disperse bodies. These laws, together with the equations of theoretical mechanics and mechanics of deformable continuous bodies, give a system of equations which is sufficient to solve the problems in soil mechanics. These basic laws, the main characteristics of soils required in their application, and their principal practical applications are given in Table 2.1. These laws are

Table 2.1

Basic Laws of Soil Mechanics

Property	Regularity	Parameter	Practical application in soil mechanics
Compressibility	Compaction law	Coefficient of relative compressibility	Determination of settlements of foundations
Water permeability	Law of laminar filtration	Coefficient of filtration	Predictions of the rate of settlement of water-saturated soil bases
Contact shear resistance	Condition of strength	Coefficient of internal friction and cohesion	Calculations of ultimate strength, stability and pressure upon retaining structures
Structural-phase deformability	Principle of linear deformability	Deformability moduli	Determination of stresses and deformations of soils

the most important relationships describing the mechanical properties of disperse (finely divided) bodies, such as soils.

Thus, the *compressibility* of soils, which is caused by variation of their porosity, and therefore, of their total volume, under the action of external forces owing to repacking of particles (i.e., variation of the content of solid particles in a unit volume of soil) is a property

inherent only in disperse materials and not considered in the structural mechanics of continuous bodies. One has, however, to distinguish between the compressibility of soils as their very characteristic property caused by variation of their porosity, and the total deformability of soils which is inherent in all physical bodies but has certain peculiarities in soils.

The *water permeability*, being a property common for all porous bodies including soils, is variable in the latter and changes in the process of compaction of soils under load.

The *contact shear resistance* is caused only by internal friction in loose soils and both by friction and cohesion in cohesive soils.

Finally, the *deformability* of soils depends both on resistivity and yieldability of their structural bonds [i.e., whether the bonds are continuous or act only at points of contact between mineral particles; whether they are plastic (water-colloidal) or brittle (crystallizational), etc.] and on the deformability of individual components forming the soils. Then, with a single loading and a pressure exceeding the strength of rigid structural bonds, the soils will always have (along with a recoverable deformation) a *residual deformation* exceeding many times the recoverable deformation.

## 2.1. COMPRESSIBILITY OF SOILS. THE LAW OF COMPACTION

The *compressibility of soils* is one of their most characteristic properties, which distinguishes them from massive rocks and other solid bodies. It consists in their capability of varying (sometimes substantially) their structure (the packing of solid particles) under the action of external factors (compressive loads, drying, coagulation of colloids, etc.) to a more compact one owing to a reduction of their porosity.

A *reduction of porosity* of soils with a more compact packing of their particles can occur owing to the development of certain local shears of particles which is accompanied with slippage of finer particles into the voids of the soil and (especially for water-saturated disperse clayey soils) owing to a variation of the thickness of water-colloidal shells of mineral particles under the action of an increased pressure, drying, coagulation, etc.

In addition, repacking of particles is affected by the *creep of the soil skeleton* and shells of firmly bonded water (which also can be related to the soil skeleton), which is caused by distortion of the shape of crystalline lattices of mineral particles and a slow viscous flow of molecular layers of firmly bonded water.

It should also be noted here that a variation of porosity of soils that are completely saturated with water is only possible with a change in their moisture content (i.e., with squeezing-out or

sucking-in of water) and a certain internal compression of gaseous inclusions; for non-saturated soils, however, porosity can be changed without changing the moisture content.

Variations in the volume of voids of disperse soils at drying (in the process of dewatering of diffuse shells and an increase of capillary compression), and also as a result of slow physico-chemical processes (for instance, ageing of colloids) are taken into account only in exceptional cases, so that the main process of variation of volume of soils is their *compaction under load*.

We have to distinguish between the *compactibility* of soils under short action of dynamic loads (mechanical) and *compaction* under a long action of a constant static load (compression, consolidation, etc.).

*Mechanical compaction* by means of vibrational, tamping and like mechanisms gives good results only for low-moisture loose sandy and non-saturated soils in which mineral particles are in rigid contact; this contact is then easily disturbed, which ensures recombination of particles and their denser packing. In water-saturated sands, however, dynamic loads cause substantial water heads, the soil becomes suspended in a certain region, undergoes liquefaction under definite conditions, and spreads over a large area. However, the greater the external pressure onto the soil surface under dynamic action (for instance, vibrational), the less effective this action, since the forces at points of contact of particles are more difficult to overcome.

In clayey soils, which are only slightly liable to compaction under dynamic loads, the heads arising in the water attenuate at very short distances because of the low permeability of these soils, so that no liquefaction occurs.

With *compaction of soils under a continuous constant load* (compression of soils), at least two different ranges of pressures must be considered: (1) when the external pressure is less than the strength of structural bonds and (2) when these bonds have been destroyed.

In the first case, as has been shown by the experiments carried out at the Moscow Civil Engineering Institute and at other research centres, no compaction of the soil occurs, since the deformations arising under the action of the external load are elastic deformations of structural bonds, so that the soil deforms as a continuous quasi-solid body.

In the second case, i.e., when rigid structural bonds have been disturbed (at pressures exceeding the structural strength), soil compaction will be substantial. For soils with water-colloidal bonds, this compaction will occur owing to compression of water-colloidal shells of mineral particles and squeezing-out of a certain amount of water and, to a certain extent, owing to the creep of the soil skeleton. For clayey soils considered, squeezing-out of water is only

possible when the head formed by the action of an external load exceeds a certain initial value.

For soils possessing both soft water-colloidal bonds and rigid crystallizational bonds, the process of compaction is much more complicated.

**Relationship between moisture content, pressure and void ratio.**

In order to determine the compressibility of soils, these are subjected to compaction tests under load in conditions of the one-dimensional problem, i.e., when deformations of the soil can proceed only in one direction and all other forces except the external load are ineffective.

Tests of water-saturated soils are carried out with the soil surface covered with water, so as to prevent drying of the soil during the tests (which may last from several hours to a few days), and therefore, to prevent the formation of forces of capillary pressure in the soil.

Compressibility tests of soils are carried out in devices with rigid walls (odometers) in order to ensure that the soil be compacted in one direction only (to prevent from lateral expansion, Fig. 6). Such

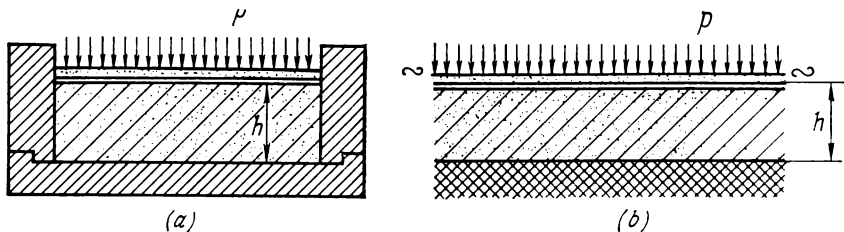


Fig. 6. Schemes of soil compression  
(a) in rigid ring; (b) under continuous load

boundary conditions correspond in nature to compression of an individual layer of soil under the action of a continuous uniformly distributed load (for instance, the weight of the upper layers of the soil, see Fig. 6b). The soil surface is loaded in separate increasing steps (for instance 0.05, 0.10, 0.25, 0.5, 1.0, 2.0, and 4.0 kgf/cm<sup>2</sup>), since the more the soil is compacted by the previous step of load, the less its deformation, and therefore, the higher accuracy of measurements is required.

Prof. K. Terzaghi et al. have found by experiments that for water-saturated but low-permeable clayey soils each increment of external pressure causes a corresponding definite variation in moisture content. The relationship between moisture content and pressure can be represented in the form of a diagram (Fig. 7a) which is called the compression curve. Since for fully saturated soils there is a definite relationship between moisture content and void ratio [relationship

1(.7)], their compression curve (Fig. 7a) can be easily reconstructed into the coordinates "void ratio—pressure" (Fig. 7b).

It has been shown by later research that compression curves are applicable for estimation of compressibility of any disperse materials (either cohesive or loose), but for water-permeable materials

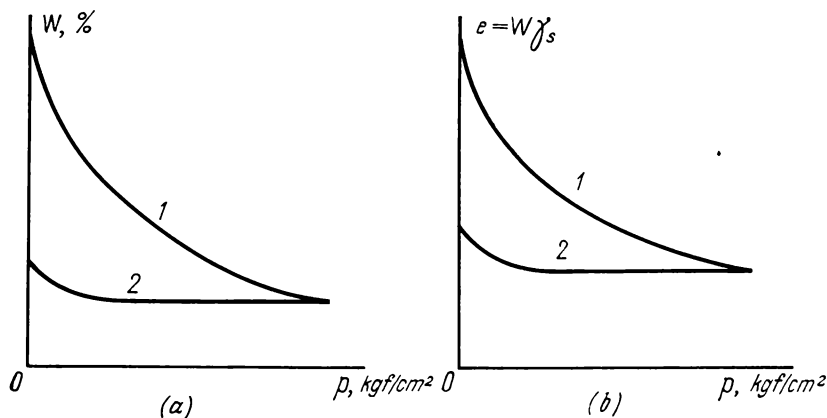


Fig. 7. Compression curves for clayey soils  
1—compression curves; 2—decompression (swelling) curves

(sands) they cannot be constructed by variations of moisture content, since the moisture content is restored almost instantaneously while unloading these materials.

A more general method for constructing compression curves is the method of determining the void ratio from settlements of soil samples when they are compacted in a compression apparatus.

Let us denote:

$e_0$  = initial void ratio of the soil [which can be calculated by formulae (1.2) and (1.3) and the data on unit weight, moisture content, and specific weight of the soil]

$e_i$  = void ratio of the soil with any step of loading

$s_i$  = total settlement of the sample under the given load ( $p_i$ ) measured from the beginning of loading

$\Delta n_i$  = variation in soil porosity (volume of voids) from the beginning of loading

$h$  = initial height of the soil sample

Then, noting that the void ratio  $e$  is the ratio of the volume of voids to that of solid particles, we have

$$e_i = e_0 - \frac{\Delta n_i}{m} \quad (c_1)$$

Since for the soil sample being tested without the possibility of lateral expansion the variation in the volume of voids  $\Delta n_i$  is numerically equal to the product of the settlement  $s_i$  by the sample area  $F$ , i.e.,

$$\Delta n_i = s_i F \quad (c_2)$$

and the volume of solid particles in the whole volume of the soil, noting expression (1.5), is

$$m = \frac{1}{1+e_0} Fh \quad (c_3)$$

then, substituting (c<sub>2</sub>) and (c<sub>3</sub>) into (c<sub>1</sub>), we get

$$e_i = e_0 - (1 + e_0) \frac{s_i}{h} \quad (2.1)$$

Formula (2.1) is used for calculations of the void ratio corresponding to the given steps of load, from which the whole compression curve can be constructed.

In a number of cases (for instance, in estimations of deformability of subsidence soils and when accounting for the non-linearity of compression with a wide range of pressures) the compressibility of

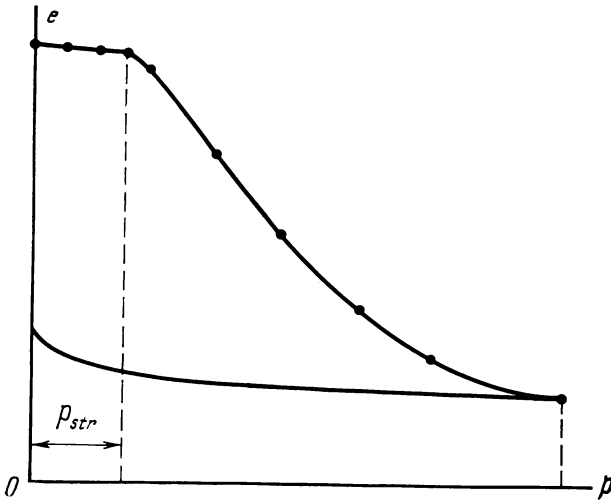


Fig. 8. Compression curves for undisturbed samples of soil

soils is characterized by what is called the *modulus of settlement* (introduced by Prof. N. N. Maslov in 1941)  $\epsilon_p = s_i/h$ , which is the relative deformation of the soil at the given pressure, expressed in parts per mille (mm/m).

For soils of natural undisturbed structure, the compression curve has two portions (Fig. 8): (1) up to pressures not exceeding the structural strength  $p_{str}$  of soil, an almost straight portion with very small variations of void ratio and (2) a curvilinear portion with substantial variations of void ratio, which indicates that the soil has been compacted under a load exceeding its structural strength. Under lower loads, no compression of the soil occurs.

Further we shall discuss only compression curves at pressures exceeding the structural strength of soils.

As regards the structural strength  $p_{str}$ , it is a rather important characteristic of soils, as will be shown in later chapters. Its magnitude can be found from the compression curve of an undisturbed structure by testing the soil (until its structural strength is attained) with very small steps of loading (approximately 0.02-0.10 kgf/cm<sup>2</sup>); the sharp bend of the compression curve then corresponds to attainment of the structural strength of the soil (see Fig. 8).

Another method for determining the structural strength of soils, proposed by Prof. E. I. Medkov, is based on the results of tests of the soil lateral pressure at triaxial compression and corresponds to the pressure at which the lateral pressure of the soil is practically absent.

Special testing techniques are required for determination of these pressures. At present the structural strength of soils can be determined with a certain degree of approximation which mainly depends on the accuracy of measurements.

If we plot a compression curve in semi-logarithmic coordinates (Fig. 9), then variations in the soil void ratio (for pressures exceeding the structural strength) will depend *linearly* on the logarithm of variation of the external pressure. The equation of the compression curve for a wide range of pressures can then be written in the form

$$e_i = e_0 - C_c \ln \left( \frac{p_i}{p_0} \right) \quad (2.2)$$

where  $e_0$  and  $p_0$  = initial void ratio and initial pressure (in excess of the structural strength)

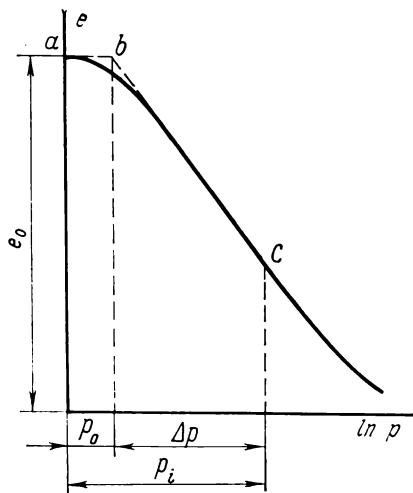


Fig. 9. Compression curve in semi-logarithmic coordinates

$e_i$  and  $p_i =$  void ratio and pressure corresponding to the  $i$ -th step of loading

$C_c =$  coefficient of compression

The coefficient of compression  $C_c$  is the tangent of the semi-logarithmic curve with the axis of pressures and is numerically equal to the difference between the void ratio when  $p_i = e = 2.72$  kgf/cm<sup>2</sup> (Napierian number) and  $p_0 = 1$  kgf/cm<sup>2</sup>, since  $p_i = 1$  when  $p_i = e \ln$ .

This coefficient (which is a dimensionless number) characterizes the compressibility of soils within a wide range of pressures.

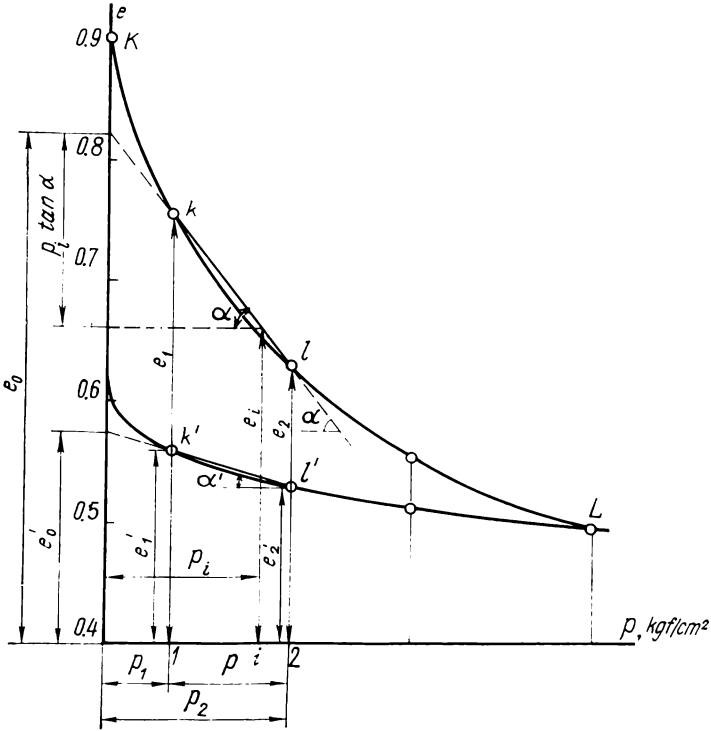


Fig. 10. Determination of parameters of a compression curve section

If we limit ourselves to a small variation of pressures (of the order of 1 to 3 kgf/cm<sup>2</sup>, which is common for bases of structures), then the section  $kl$  of the compression curve in Fig. 10 can be assumed to be a straight line with an accuracy sufficient for practical purposes. Then, according to designations of Fig. 10, we have

$$e_i = e_0 - \tan \alpha p_i \quad (2.3)$$

The tangent of the section of the compression curve with the axis of pressures,  $\tan \alpha$ , characterizes the compressibility of the soil in the range of pressures considered (between  $p_1$  and  $p_2$ ), since the greater the angle of slope  $\alpha$ , the greater the soil compressibility. This parameter has been termed the *coefficient of compressibility* of soils and is denoted by  $m_0$ , i.e.,

$$m_0 = \tan \alpha \quad (2.4)$$

The coefficient of compressibility can be expressed through the values of  $p$  and  $e$  for the extreme points  $k$  and  $l$  of the straight section  $kl$  (see Fig. 10)

$$m_0 = \frac{e_1 - e_2}{p_2 - p_1} \quad (2.4')$$

or, denoting  $p_2 - p_1 = p$  (where  $p$  is the increment of pressures or what is called the *acting pressure*), we have

$$m_0 = \frac{e_1 - e_2}{p} \quad (2.4'')$$

or, in words, the *coefficient of compressibility is the ratio of variation of the void ratio to the acting pressure*.

Substituting  $m_0$  for  $\tan \alpha$  in equation (2.3), we get the equation of the straight section of a compression curve in the form

$$e_i = e_0 - m_0 p_i \quad (2.3')$$

For the section  $k'l'$  of the curve of swelling (unloading) (see Fig. 10), we can find in a similar way that

$$e'_i = e'_0 - m'_s p_i \quad (2.3'')$$

where  $m'_s = \tan \alpha'$  is the *coefficient of swelling* (unloading).

In calculations of compaction settlements of soils, use is often made of the so-called *coefficient of relative compressibility*  $m_v$ , which is expressed as follows:

$$m_v = \frac{m_0}{1 + e_0} \quad (2.5)$$

Its physical meaning can be found from the following relationships. From equation (2.3'), we have

$$e_0 - e_i = m_0 p_i \quad (d_1)$$

On the other hand, it follows from expression (2.1) that

$$e_0 - e_i = (1 + e_0) \frac{s_i}{h} \quad (d_2)$$

Equating the right-hand parts of (d<sub>1</sub>) and (d<sub>2</sub>) and noting expression (2.5), we get

$$m_v = \frac{s_i}{hp_i} \quad (2.5')$$

i.e., the coefficient of relative compressibility is equal to the relative settlement  $s_i/h$  per unit acting pressure  $p_i$ .

Thus, we have established the following characteristics of compressibility of soils:  $C_c$ ,  $m_0$ , and  $m_v$ , the first coefficient being an abstract number, and the coefficients  $m_0$  and  $m_v$  having the dimension inverse to the unit pressure (cm<sup>2</sup>/kgf).

**The law of compaction.** Equation (2.3') describes variations of void ratio only for a straightened section of the compression curve and therefore is an approximate equation. If variations of pressures are infinitely small, then variations of void ratio will be *strictly* (exactly) proportional to the variations in pressure. Differentiating equation (2.3'), we then have

$$de = -m_0 dp \quad (2.6)$$

This relationship is of especial importance in soil mechanics and is used as a basis for a number of its principal laws: the principle of linear deformability, the principle of hydrocapacity, the differential equation of consolidation, etc., and is termed the *law of compaction of soils*.

This law is expressed as follows: *an infinitesimal variation of the relative volume of soil voids is directly proportional to an infinitesimal variation of pressure.*

At small variations of pressures, equation (2.6) can be applied to finite variations of  $e$  and  $p$ . According to Fig. 10,

$$e_1 - e_2 = m_0(p_2 - p_1) \quad (2.7)$$

The law of compaction can then be formulated as follows: *with small variations of compacting pressures the variation of void ratio is directly proportional to the variation of pressure.*

**General case of compression relationship.** In the general case, variations of soil void ratio  $e$  at compression are dependent not only on the magnitude of vertical normal stresses  $\sigma_z$ , but also on horizontal stresses  $\sigma_y$  and  $\sigma_x$ .

According to Prof. N. M. Gersevanov, we make the simplest assumption that the void ratio in any point of the soil mass is dependent only on the sum of all normal stresses  $\theta$  acting in that point. This is a widely used assumption, since for very viscous and dense clayey soils the variations of void ratio are affected to a certain extent by the shear stresses which are responsible for creep of the soil skeleton. For a "soil mass" in our definition, to which we relate all fully saturated *non-compacted* soils (fine sands and sand loams,

weak loams and clays) with a non-compressible mineral skeleton and the *presence of free* (non-bonded) *water*, this assumption is very close to the actual conditions.

Let us determine the sum of principal stresses in the case of a soil layer being compressed without lateral expansion. For this, we

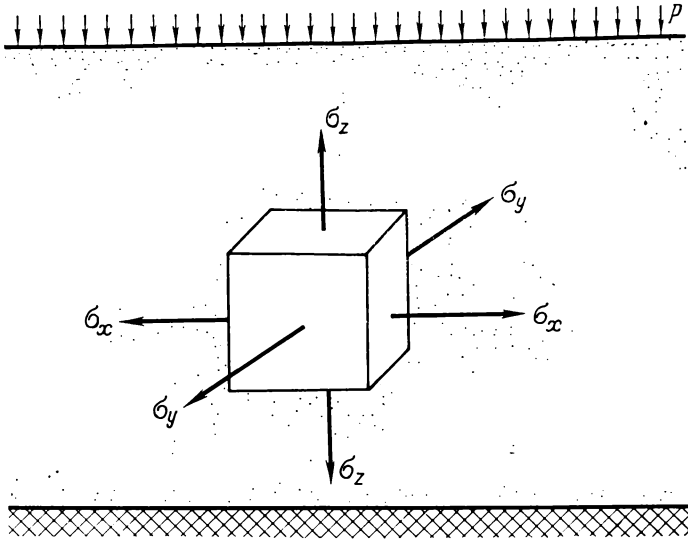


Fig. 11. Stresses in soil element under the action of continuous uniformly distributed load

separate an elementary parallelepiped (Fig. 11) which will be subjected only to the action of normal (principal) stresses  $\sigma_x$ ,  $\sigma_y$ , and  $\sigma_z$  under conditions of the problem considered.

Since horizontal deformations (lateral expansion) of the soil are unfeasible, then the horizontal relative deformations are equal to zero, i.e.,  $\epsilon_x = \epsilon_y = 0$ , whence it follows that  $\sigma_x = \sigma_y$ . In addition, we have  $\sigma_z = p$  from the condition of equilibrium.

Let us write the well-known expression for the horizontal relative deformation  $\epsilon_x$  under the action of stresses along three mutually perpendicular directions

$$\epsilon_x = \frac{\sigma_x}{E_o} - \frac{\mu_o}{E_o} (\sigma_y + \sigma_z) \quad (e_1)$$

where  $E_o$  and  $\mu_o$  are moduli of deformability of the soil, which are similar to the modulus of elasticity and Poisson's ratio for elastic bodies, but relate to the total deformation of the soil, which is designated by letter "o".

Substitution of  $\sigma_x = \sigma_y$ ,  $\sigma_z = p$ , and  $\epsilon_x = 0$  into (e<sub>1</sub>) gives

$$\sigma_x = \sigma_y = \frac{\mu_o}{1 - \mu_o} p \quad (e_2)$$

or

$$\sigma_x = \sigma_y = \xi_0 p \quad (e_3)$$

where

$$\xi_0 = \frac{\mu_o}{1 - \mu_o} \quad (2.8)$$

The quantity  $\xi_0$  is called the *coefficient of lateral pressure of soil at rest*.

Using the relationships obtained, we can write the sum of normal stresses, which will be denoted by  $\Theta$

$$\Theta = \sigma_x + \sigma_y + \sigma_z$$

Since  $\sigma_z = p$ , and  $\sigma_x = \sigma_y = \xi_0 p$ , we have

$$\Theta = (1 + 2\xi_0) p \quad (2.9)$$

whence

$$p = \frac{\Theta}{1 + 2\xi_0} \quad (e_4)$$

Substituting this expression into the equation of straight section of compression curve (2.3'), we find that

$$e_i = e_0 - m_0 \frac{\Theta}{1 + 2\xi_0} \quad (e_5)$$

whence

$$e_i + \frac{m_0}{1 + 2\xi_0} \Theta = e_0 = \text{const} \quad (2.10)$$

This expression shows that the void ratio (or moisture content) of a soil mass in the given point can vary only with a variation of the sum of principal stresses  $\Theta$  in that point, or, according to N. M. Gersevanov, of the "hydrocapacity" of the soil mass. The latter formulates what is called Gersevanov's *hydrocapacity principle*.

An example of the application of this principle is the method for determining the *equivalent capillary pressure*, i.e., the average uniform pressure  $p_c$ , which replaces the action of all capillary forces.

Using the compression curve of a soil sample of disturbed structure, which is called the main branch of compression curve (Fig. 12), we find the magnitude of the compacting pressure that can transform the soil from the liquid state into the state of the given density  $e$ . Let this pressure be denoted by  $p_s$ .

For a three-dimensional compression of an element of soil mass by a capillary pressure  $p_c$ , its hydrocapacity will be

$$\Theta = \sigma_x + \sigma_y + \sigma_z = 3p_c \tag{f_1}$$

On the other hand, according to formula (2.9)

$$\Theta = (1 + 2\xi_0) p_s \tag{f_2}$$

Equating the right-hand parts of expressions (f<sub>1</sub>) and (f<sub>2</sub>) we have

$$p_c = \frac{1 + 2\xi_0}{3} p_s \tag{2.11}$$

Note that this method of determining the equivalent capillary pressure is applicable for general estimations of the average capillary pressure of clayey soils that have been formed only through their gravitational compaction in water basins *without* formation of rigid cementation bonds.

For soils having no rigid bonds, provided that we know the height of capillary lift (suction) of water  $h_c$ , i.e., the distance from the ground water level to the level of the surface of capillary menisci, the capillary pressure is found as

$$p_c = \gamma_w h_c \tag{2.12}$$

**Coefficient of lateral pressure.** In the general case the coefficient of lateral pressure  $\xi$  is the ratio of the increment of soil horizontal pressure  $dq$  to the increment of the acting vertical pressure  $dp$ , i.e.,

$$\xi = \frac{dq}{dp}$$

Separating the variables and integrating, we get

$$q = \xi p + D \tag{2.13}$$

Expression (2.13) is an equation of a straight line with an angular coefficient  $\xi$  and integration constant  $D$ , which is found from the initial conditions.

As has been found by experiments (V. G. Bulychev, N. V. Laleitin, K. Terzaghi et al.), for very loose sands having no structural

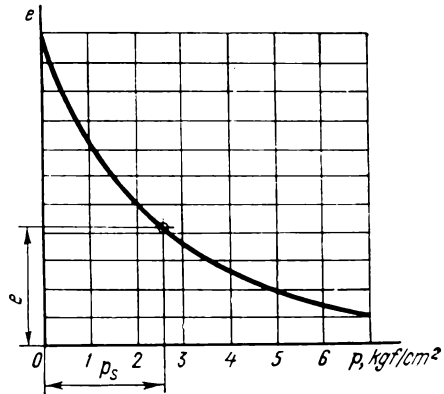


Fig. 12. Determination of "equivalent capillary pressure" on main branch of compression curve

strength, the initial pressure  $q_0 = 0$  and  $D = 0$  (Fig. 13); for preliminarily compacted sands, the initial pressure  $q_0 \neq 0$  and is a certain fraction of the compacting pressure  $p_0$ , i.e.,  $D = q_0 = \alpha p_0$  (with  $\alpha < 1$ ); for cohesive clayey soils it is less than zero and, according to Gersevanov, is equal to the capillary pressure, i.e.,

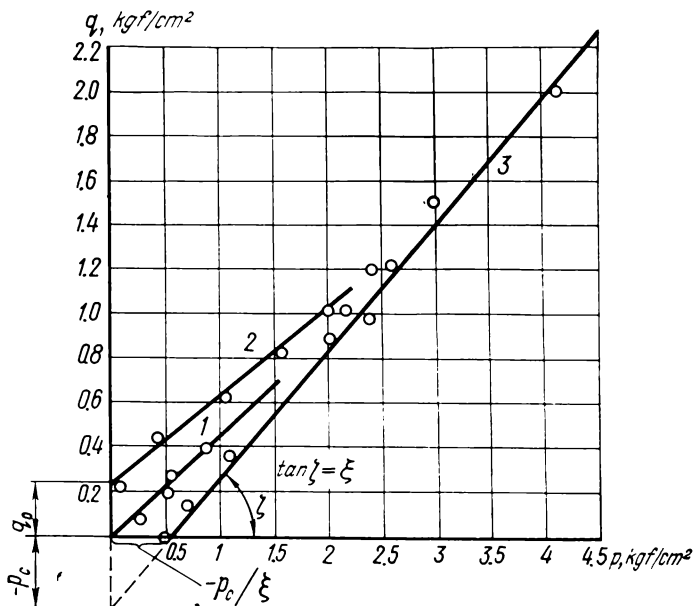


Fig. 13. Determination of coefficient of lateral pressure of soils by test results  
1—fully loose sand; 2—compacted sand; 3—water-saturated loam

$D = q_0 - p_c$ , which has been confirmed experimentally: line 3 in Fig. 13 cuts a definite section equal to  $-p_c/\xi$  on the  $p$  axis.

The coefficients of lateral pressure  $\xi$  have been found to be:  $\xi = 0.25-0.37$  for sandy soils and  $\xi = 0.11-0.82$  (depending on consistency) for clayey soils.

## 2.2. WATER PERVIOUSNESS OF SOILS. THE LAW OF LAMINAR FILTRATION

Another specific feature of soils as of disperse (finely divided) porous bodies is their water perviousness, i.e., the capability of filtering water. Filtration in soils depends on the degree of compaction, and for stiff-plastic semi-hard clays, also on the initial pressure gradient; the motion of water in soil begins only after this gradient has been overcome.

The motion of various kinds of water in soils may occur under the influence of different factors (depending on the degree of bondage of particles of water with the mineral skeleton): of vapour-phase water, under the action of a difference in vapour pressures in different points of the soil (which depends on temperature in those points); of film water, owing to a difference of osmotic pressures; of capillary water, owing to a difference of suction (adsorption) forces; and finally, of gravitational water, owing to a difference of water heads.

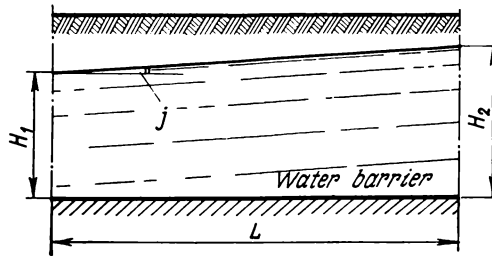


Fig. 14. Scheme of water filtration in soils

Thus, it may be generalized that a certain pressure gradient caused by some or other physical or physico-chemical factors is required to cause motion of water in soil.

Forced motion of water in soils is studied both in the theory of motion of ground water (which is of prime importance in hydraulic engineering) and in soil mechanics, where the magnitude of heads is decided not only by the position of the points in soil relative to the zero level (Fig. 14), but also by the magnitude of external pressure from a structure which also causes forced motion of free and loosely bonded porous water.

The rate of forced motion of ground waters depends on size of voids in the soil, resistances along the path of filtration, and the magnitude of acting pressures.

The motion of water is termed *laminar* if the flow lines of water (the lines of motion of water in a flow) do not intersect with each other; if flow lines intersect and form whirls, the motion is called *turbulent*.

As has been shown by experiments (Poiseul, Darcy, N. N. Pavlovsky), the motion of water in soils is laminar in most cases.

Laminar motion of water occurs with the greater rate, the greater the so-called hydraulic gradient  $i$  is or, in the simplest case, the tangent  $\tan j$  of the surface of the level of ground waters (Fig. 14).

The hydraulic gradient is equal to the ratio of the loss of head  $H_2 - H_1$  to the length of the filtration path  $L$ , i.e.,

$$i = \frac{H_2 - H_1}{L} \quad (g_1)$$

or, introducing the term "acting head"

$$H = H_2 - H_1 \quad (g_2)$$

we have

$$i = \frac{H}{L} \quad (g_3)$$

According to Darcy, the flow rate of water per unit time per unit area of cross-section of soil, or what is called the *rate of filtration*  $v_f$  is directly proportional to the hydraulic gradient  $i$ , i.e.,

$$v_f = k_f i \quad (2.14)$$

where  $k_f$  is the coefficient of filtration, which is equal to the rate of filtration with the gradient equal to unity (its dimensions may be cm/s, cm/year, etc.).

The experimental relationship (2.14) between the rate of filtration and hydraulic gradient is called the *law of laminar filtration* (Darcy, 1885).

Soil mechanics studies the motion of water mainly under the action of pressures caused in porous water by external loads, which can also be expressed through the height of a water column by the relationship

$$H = \frac{p}{\gamma_w} \quad (g_4)$$

where  $\gamma_w = 0.001 \text{ kgf/cm}^3$  is the unit weight of water.

Thus, for instance, an external pressure (load)  $p = 1.5 \text{ kgf/cm}^2$  has a corresponding acting head

$$H = \frac{1.5}{0.001} = 1500 \text{ cm} = 15 \text{ m}$$

Given below are the average coefficients of filtration for homogeneous (without caverns) clayey soils at squeezing (filtration) of water in them at a pressure of about 1-2 kgf/cm<sup>2</sup>:

Sand loams:	$k_f = r \cdot 10^{-3}$ to $r \cdot 10^{-6}$ cm/s
Loams:	$k_f = r \cdot 10^{-5}$ to $r \cdot 10^{-8}$ cm/s
Clays:	$k_f = r \cdot 10^{-7}$ to $r \cdot 10^{-10}$ cm/s

where  $r$  is any number from 1 to 9.

These values will naturally differ from the values of coefficients of filtration obtained by the method of field pumping.

In order not to use such small values, calculations in soil mechanics (for instance, in prediction of the rate of settlement of saturated soils) are often made with the coefficients of filtration expressed in cm/year, it is taken approximately that  $1 \text{ cm/s} = 3 \times 10^7 \text{ cm/year}$ .

**Initial gradient in clay soils.** Filtration of water in viscous clayey soils has some specific features caused by small size of voids and viscous resistance of water-colloidal films enveloping mineral particles of soil. The thinner these water-colloidal films (as, for instance, in compacted clayey soils), the greater resistance they provide to the forced motion of the water owing to a high viscosity of these films (according to M. P. Volarovich) and their elasticity (according to B. V. Derjagin).

According to the results of studies carried out by S. A. Roza and B. F. Rel'tov, filtration of water in viscous (stiff-plastic) clayey soils begins only when the pressure gradient attains a definite initial value at which the internal resistance to motion provided by water-colloidal films is overcome.

Figure 15 shows the experimental curves of dependence of the rate of filtration  $v_f$  on hydraulic gradient  $i$ : *I* for sands and *II* — for clays (the scale of  $v_f$  for clays has been increased by several orders).

Three different sections may be distinguished in curve *II*: the initial section 0-1, where the rate of filtration is practically equal to zero ( $v_f = 0$ ); the transition section 1-2, which is curvilinear; and finally, the straight section 2-3 of stable filtration, when the rate of filtration is proportional to the acting gradient.

For the last (main) section we have

$$v_f = k'_f (i - i'_0) \quad (2.15)$$

where  $i'_0$  is the initial pressure gradient for the given clay.

Note that because of the uncertainty in the outline and insignificant magnitude of the transition section 1-2, the magnitude of the initial pressure gradient may be taken at the intersection of the extension of the inclined straight line 3-2 with the  $i$  axis.

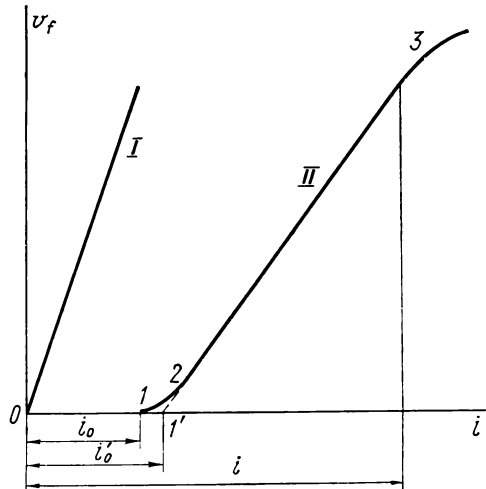


Fig. 15. Relationship between filtration rate  $v_f$  and pressure gradient  $i$   
*I*—for sand; *II*—for clay (on a different scale)

It should be noted that account of relationship (2.15) in predictions of compaction settlement of viscous clayey soils under the action of the external load (pressure) from structures being erected has a substantial effect on the magnitude of settlements obtained and makes it possible to estimate these more correctly.

**Effective and neutral pressures in soil mass.** When studying the compression of a soil mass, two systems of pressures are considered: (1) pressures in the soil skeleton  $p_z$  and (2) pressures in the porous water  $p_w$ . The first are called the *effective* pressures, since they act effectively on soil particles, compact and strengthen the soil; the second are termed *neutral* pressures, since they do not compact or strengthen the soil, but only form a water head which causes filtration of water.

For a fully saturated soil mass at any instant of time, the following relationship holds true:

$$p = p_z + p_w \quad (2.16)$$

i.e., the total pressure is equal to the sum of the effective and neutral pressures. With a variation of one of the summands (with a constant external pressure  $p$ ), the other also changes.

This may be explained by considering the pressure in a thin layer of soil mass placed into a cylindrical vessel (Fig. 16a). If a load of

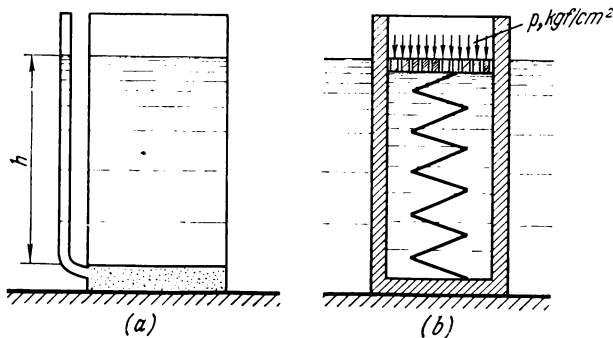


Fig. 16. Schemes of devices to explain two systems of pressures in water-saturated soils

(a) pressure transmission to soil skeleton; (b) model of compression of soil mass (the load being first fully transmitted to water and then, as compression proceeds, to soil skeleton)

intensity  $p$ ,  $\text{kgf/cm}^2$ , is applied to the surface of soil by means of a perforated stamp or a layer of lead shot, then the soil will be compacted by that load and its resistance to compression, shear, etc. will increase, i.e., the load will act *effectively* on the soil layer.

If, however, the shot is replaced with water filled to such a height  $h = p/\gamma_w$  as to ensure the same pressure, then, as has been shown by

experiments of Prof. L. Rendulic in 1943, the pressure from the water will be transmitted only to the porous water, thus increasing the head of the latter, but will not affect the compaction of the soil, i.e., it will be the *neutral pressure*.

Note that the effective pressure  $p_z$  is always transferred only through the points and areas of contact of solid particles, while the neutral pressure  $p_w$  is transferred through the *porous* water and, when positive (i.e., in excess of hydrostatic pressure), it is called the *porous pressure*.

The concept of effective and neutral pressures can be extended to any normal stresses acting in water-saturated soils. In the general case we can write

$$\sigma = \bar{\sigma} + u$$

whence

$$\bar{\sigma} = \sigma - u \quad (2.17)$$

i.e., the effective stress  $\bar{\sigma}$  in any point of a water-saturated soil is equal to the difference between the total stress  $\sigma$  and neutral stress  $u$ .

### 2.3. ULTIMATE CONTACT SHEAR RESISTANCE OF SOILS. STRENGTH CONDITIONS

Under the action of an external load, the effective stresses in individual points (regions) of the soil may overcome the internal bonds between particles, so that *slippages* (shears) of some particles or aggregations over others will arise and the continuity of the soil in a definite region may be disturbed, i.e., the strength of the soil will be exceeded.

The internal resistance that counteracts the displacement (shear) of particles in ideally loose bodies (to which pure sands may be related) is only the friction at the points of contact of particles. In perfectly cohesive soils, however, such as very viscous disperse clays, the displacement of particles will be counteracted only by the internal structural bonds and the viscosity of water-colloidal shells of particles.

Natural clays, however, possess both viscous (water-colloidal) and rigid (crystallizational) internal bonds, the role of each kind of bond being different in various clays.

Until the internal bonds are not overcome by effective stresses, a cohesive soil will behave as a quasi-solid body possessing only elastic forces of cohesion.

The forces of *cohesion* will be understood as the resistance of structural bonds to any displacement of the particles they bind together, irrespective of the magnitude of the external pressure.

If the load is such that the effective stresses exceed the strength of rigid structural bonds, then in the points of contact of mineral particles and over the surfaces of their water-colloidal (firmly bonded with mineral particles) interlayers the displacement of particles will be resisted by the water-colloidal bonds that still remain or are newly formed. It is often impossible to divide these resistances into solely friction and solely cohesion, since the friction of the particles being displaced relative to each other can take place simultaneously with the surmounting of viscous resistances which always remain in clayey soils, because with some viscous bonds overcome (if the rigid bonds have been destroyed), new bonds are being formed.

As has been shown by numerous experiments, the shear resistance of non-cohesive solid mineral particles is only their resistance to friction which is proportional to external pressure; the resistance of aggregations of particles with water-colloidal bonds is, however, a combination of the viscous resistance to slippage, whose magnitude depends on the rate of increase of shear forces and the forces of cohesion, which in turn depend on the magnitude of compacting pressures arising in the points and surfaces of contact of particles.

The characteristics of shear resistance (which are the main strength characteristics of resistance of bodies to external forces) of soils have the principal specific feature—they are *variable*, i.e., *dependent on pressure* and the conditions existing in the points of contact of particles resisting to slippage.

A correct choice of the characteristics of soil shear resistance is of prime practical importance, since it ensures a high accuracy of engineering calculations in determination of the ultimate loads on soils, the stability of soil masses, and the pressure of soils on retaining structures.

Experimental determinations of shear resistance of soils can be made by various methods: by the results of direct plane shear, simple uniaxial compression, three-axial compression, a shear along a cylindrical surface, impression, etc.

**Ultimate shear resistance of soils at a direct plane shear.** This may be determined by testing soils in a box-shear apparatus (Fig. 17); a cylindrical sample of soil (either preliminarily compacted or non-compacted, depending on the conditions of the test) is placed into a box-shear apparatus so that its one half remains stationary and the other can be displaced under the action of a horizontal shearing load, the possibility being provided for the soil sample to increase or diminish its volume at shearing.

A compressive load  $N$  normal to the surface of shear is applied to the soil sample.

For better cohesion of the stamp with soil, the stamp is provided with projections (of triangular or rectangular shape) which cut into the upper and lower surfaces of the soil sample and ensure cohesion

between the stamp and soil and a more uniform distribution of shear stresses along the plane of shear.

The shear load  $T$  tangent to the shear surface is applied to the shear box stepwise or continuously increased (for instance, by means of water jet, shot, etc.) until one portion of the sample is is

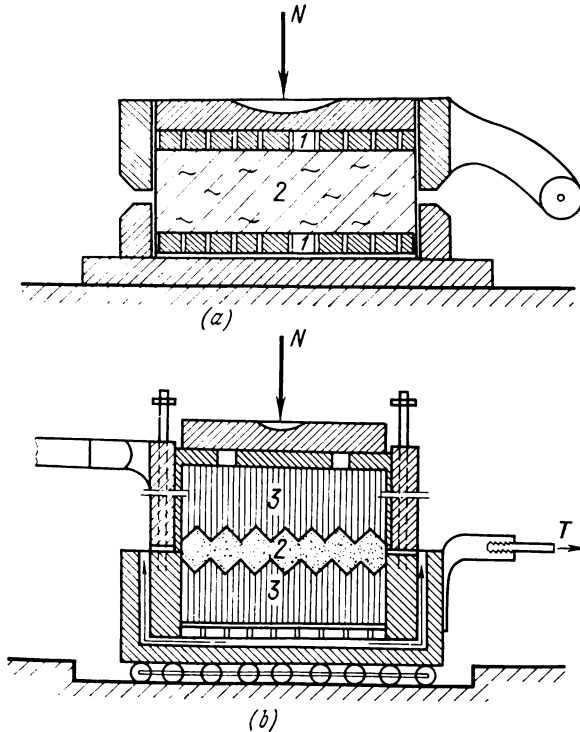


Fig. 17. Shear-box apparatus

(a) with stationary lower part; (b) with stationary upper part; 1—filters; 2—soil sample; 3—filtering stones

sheared or slips over the other. Measurements of vertical and horizontal deformations of the soil are made at the moment of application of the load and during the whole test time, which makes it possible, at tests of compacted clayey soils, to introduce a “correction for oblique shear” \* and to plot a shear diagram by the results of measurements (Fig. 18).

Figure 18*b* illustrates the effect of the initial density of a loose soil on its shear deformations at a constant rate of deformation.

\* Tsytoich N. A. Mekhanika gruntov (Soil Mechanics), 4th ed., Moscow, Stroiizdat, 1963, p. 165.

When the rate of deformation is not constant (for instance, a shear load is applied stepwise or gradually increased), the shape of shear diagram will be such as shown in Fig. 18a.

It should be noted that, as can be seen from the shear diagram (Fig. 18b), a loose soil when sheared attains a definite void ratio irrespective of whether it has been dense or loose in the initial state.

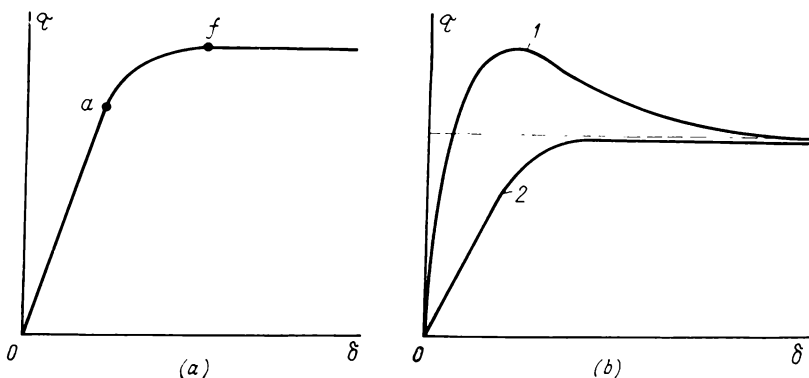


Fig. 18. Diagrams of horizontal deformations of soil at plane shearing (a) with gradually increasing load; (b) with constant deformation rate; 1—for dense sand; 2—for loose sand;  $\tau$ —shear stress;  $\delta$ —shear deformation

This ratio has been termed the *critical void ratio at shear* for the given sandy soil, since the porosity of dense soils increases at shearing, and that of more loose soils decreases.

Further, we shall consider only the maximum (ultimate) shear resistance of soils, which corresponds to point *f* in the shear diagram (Fig. 18a), i.e., to the moment when the resistance of the soil to shear forces has been completely exhausted.

**The Coulomb's law.** *Loose soils:* the density of various kinds of sand (except mica-containing sands), large-size gravelly soils, etc. varies but insignificantly with an increase of the external pressure (by a value of the order of several kilograms per square centimetre), so that in tests of loose soils for the ultimate shear resistance these variations can practically be neglected.

After loading a soil sample with a definite compressive (vertical) load, a shear (horizontal) load is applied and increased until non-attenuating progressively increasing shear deformations  $\delta$  (Fig. 19a) are formed without further increase of the shear load and one portion of the sample slips over the other. The maximum ultimate shear resistance at the given step of loading is related to the unit area of the sample cross-section, assuming the distribution of shear stresses to be uniform. An identical sample of the same soil is then loaded

with a greater pressure and the maximum shear resistance is determined again. The test is repeated with various compacting pressures  $\sigma'$ ,  $\sigma''$ ,  $\sigma'''$  and the results obtained are used for plotting the diagram of ultimate shear resistance, with the ultimate shear stresses ( $ult \tau$ ,  $\text{kgf/cm}^2$ ) being laid along the vertical axis, and the corresponding compacting pressures (compressive stresses  $\sigma$ , Fig. 19b), along the horizontal one.

As seen from the results of numerous experiments, the diagram of ultimate shear resistances for loose soils is exactly a *straight line*

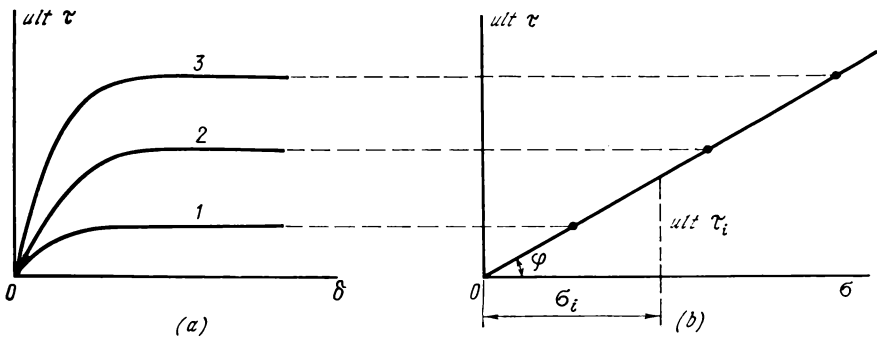


Fig. 19. Diagram of shear resistance of loose soils

(a) shear displacements (1-3—under different pressures); (b) ultimate shear resistances

passing out from the origin of coordinates (for perfectly loose soils) and inclined at an angle  $\varphi$  to the axis of pressures (Fig. 19b).

According to the shear diagram for loose soils, any ultimate shear stress  $\tau_i$  is

$$ult \tau_i = \sigma_i \tan \varphi \quad (2.18)$$

or, denoting the proportionality factor as

$$\tan \varphi = f \quad (2.19)$$

we have

$$ult \tau_i = f \sigma_i \quad (2.18')$$

Since the shear resistance of loose soils is *their resistance to friction*, the angle  $\varphi$  has been called the *angle of internal friction*, and  $f = \tan \varphi$ , the *coefficient of internal friction*.

Relationship (2.18) is the principal strength relationship for loose soils. It was established by Coulomb as far back as in 1773 and can be formulated as follows: *the ultimate shear resistance of loose soils is their resistance to friction which is proportional to the normal pressure*. In soil mechanics this relationship is called the *Coulomb's law*.

*Cohesive soils* (clays, loams, and sand loams) differ from cohesionless (loose) soils in that their particles and aggregations of particles are bonded together by plastic (water-colloidal) and partly by rigid cementation-crystallizational bonds, their shear resistance being dependent appreciably on their *cohesion* (cohesion forces).

As has been shown in Sec. 2.2, any external pressure acting on a saturated cohesive clayey soil under conditions of a free removal of the water that is squeezed by the external pressure, produces an

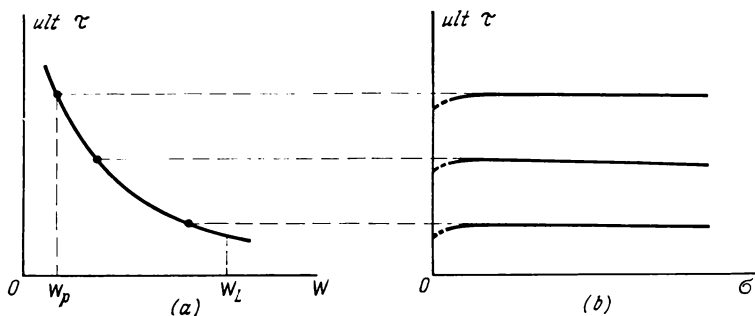


Fig. 20. Diagram of ultimate shear resistances of cohesive clayey soils in a closed system (nonconsolidated-nondrained)

(a) dependence of shear resistance on moisture content; (b) shear diagram at rapid (nondrained) shearing.

appreciable variation of their density and moisture content, which results in a variation of their total shear resistance.

The main types of shear tests of cohesive soils are tests by a *closed system* (nonconsolidated-nondrained) and tests by an *open system* (consolidated-drained).

In the former case, samples of cohesive soils must be tested under conditions of no squeezing-out of water from voids and so that their density and moisture content are not practically changed during tests; this can only be done by *rapid* shearing. Results of such a test are shown in Fig. 20, where Fig. 20a gives the dependence of the shear resistance of a cohesive (clayey) soil on its *moisture content* or density, since for fully saturated soils there exists a direct relationship between the moisture content and void ratio, which is determined by formula (1.7); Fig. 20b shows the dependence of shear resistance on the normal compacting pressure (compressive stress  $\sigma$ ).

Whereas the first curve shows that the soil density and moisture content have a substantial effect on shear resistance, the second curve (Fig. 20b) confirms the fact that under conditions of nondrained tests and with the moisture content of the soil maintained constant, the ultimate shear resistance  $ult\tau$  is practically independent of

external pressure (compressive stress  $\sigma$ ) and varies only with variations in the density and moisture content of the soil.

The shear diagram of cohesive soils tested by the open (consolidated-drained) system has a different nature.

When a cohesive soil is being tested by the same method as loose soils, i.e., a sample of soil is first compacted by a definite pressure and then tested for shear under the same pressure, then the results of a number of tests cannot be related to any *one state* of density and moisture content of the soil, since each value of pressure will have

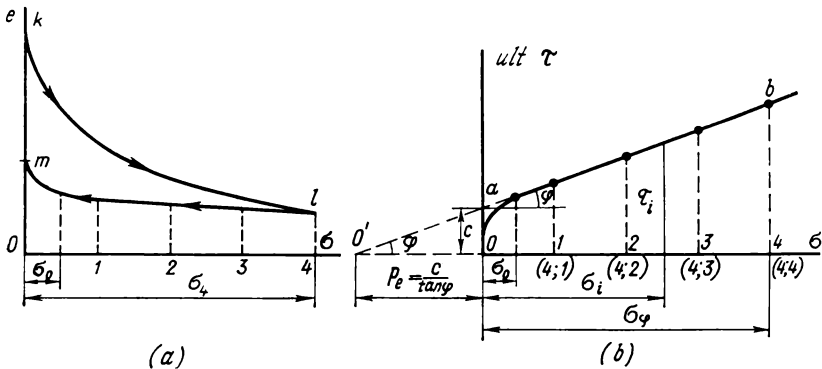


Fig. 21. Diagram of ultimate shear resistances of cohesive clayey soils in an open system (consolidated-drained)

(a) compaction ( $kl$ ) and decompaction-swelling ( $lm$ ) curves; (b) shear diagram

corresponding values of moisture content and density, so that the results of the test will characterize the shear resistance of soil samples of different densities.

In order to obtain samples of a cohesive soil of the same density (of the same void ratio), use is made of the *unloading* (swelling) *branch* of compression curve (Fig. 21a), according to which variations in the void ratio at unloading almost for all cohesive soils are rather insignificant. For that reason, a number of soil samples are usually prepared by first compacting them with the maximum pressure until settlements are fully stabilized, and are then unloaded to lower pressures (but greater than  $\sigma_0$ ) and, after the deformations of decompacting have been stabilized, they are tested under these pressures. In the latter case it may be assumed that the shear resistance of a number of samples of a cohesive soil, which are being tested under different pressures, will correspond to the density and moisture content of the soil under the maximum pressure.

It should be noted that the Author of this book has proposed another method for constructing the shear diagram of cohesive soils by a *single sample* (of natural or disturbed structure, depending on

test conditions); this method, which will be discussed below, uses the results of an independent determination of cohesion forces.

As seen from numerous tests, the diagram of consolidated shear of cohesive soils can be approximated with a linear equation in a rather wide range of pressures (from  $\sigma_0 \approx 0.5 \text{ kgf/cm}^2$  to  $\sigma_\varphi = 5-7 \text{ kgf/cm}^2$ ), which is quite satisfactory for the building practice.

With the notation according to Fig. 21b, the equation of a straight line drawn through the experimentally found points will be of the form

$$ult\tau_i = c + \tan \varphi \sigma_i \quad (2.20)$$

or, since  $\tan \varphi = f$ ,

$$ult\tau_i = c + f\sigma_i \quad (2.20')$$

Equation (2.20) expresses the Coulomb's law for cohesive soils, which may be formulated as follows: the *ultimate shear resistance of cohesive soils after their consolidation is a first power function of the normal pressure* (compressive stress).

The angular coefficient of the straight line ( $\tan \varphi = f$ ), by analogy with loose soils, is called the *coefficient of internal friction*, and the parameter  $c$ , which is explicitly independent of the external pressure, is termed *cohesion*.

The values  $f$  and  $c$  must only be regarded as *mathematical parameters* of a linear shear diagram of cohesive soils, which correspond to a definite density of the soil.

Note that for a *non-consolidated state* of completely saturated cohesive soils, i.e., when the full compaction from the given load is not yet attained, the portion of the shear resistance which is dependent on normal pressure will be lower, since not the full normal pressure, but only the effective pressure  $\bar{\sigma}$  equal to the difference between the full pressure (compressive stress  $\sigma$ ) and the neutral pressure  $u$  is transmitted to the soil skeleton. The shear resistance of a fully saturated cohesive soil at incomplete consolidation will then be an intermediate one between the shear resistance corresponding to the initial moisture content of the soil and that corresponding to the stabilized state of the soil, and can be expressed as

$$ult\tau = c + f(\sigma - u) \quad (2.21)$$

or

$$ult\tau = c + f\bar{\sigma} \quad (2.21')$$

where  $u$  = neutral (porous) pressure corresponding to the given degree of consolidation

$c$  = effective cohesion

The magnitude of the section  $c$  cut off by the shear diagram on the axis of ultimate shears  $ult \tau$  is equal to the total cohesive force of the soil which corresponds to the density and moisture of that soil.

As has been proposed by Prof. N. N. Maslov\*, the total cohesion  $c$  must be regarded to consist of two components, which can be written (under the notation adopted) as follows:

$$c = c_c + c_w \quad (2.22)$$

where  $c_c$  = structural rigid cohesion (caused by the strength of cementation-crystallizational bonds), which is irrecoverable at failure

$c_w$  = plastic cohesion caused by recoverable water-colloidal bonds

It should be noted that with a gradual increase of the shear load, destruction of both visco-plastic and rigid structural bonds occurs simultaneously, so that in a soil with purely water-colloidal bonds no plastic cohesion may be observed at small values of the initial shear resistance  $c$  (smaller than  $\sigma_0$ ), since these bonds become deformed already at low pressures. For some cohesive soils, however (for instance, silts), their shear resistance may be independent of external pressure at the beginning of loading until their structural strength is overcome.

Thus, the initial section of the shear diagram for various kinds of soil (Fig. 21b) requires special examination. The general relationship, which is described by equation (2.21), holds true within a very important range of pressures (from  $\sigma_0$  to  $\sigma_\varphi$ ) with account of the remarks made earlier.

It should also be noted that if the ultimate straight line  $ab$  is extended to intersect the pressure axis  $\sigma$  (Fig. 21b) up to point  $O'$ , then the magnitude of the parameter  $c$  can be found from triangle  $OO'a$  as

$$c = \tan \varphi p_e \quad (2.23)$$

where  $p_e$  is a certain uniform pressure replacing the action of all cohesion forces; this will be called *cohesion pressure*. It follows from (2.23) that

$$p_e = \frac{c}{\tan \varphi} \quad (2.23')$$

or

$$p_e = c \cdot \cot \varphi \quad (2.23'')$$

---

\* Maslov N. N. *Prikladnaya mekhanika gruntov* (Applied Soil Mechanics), Moscow, Stroiizdat, 1949.

Expressions (2.23') and (2.23'') are often used in problems of the theory of ultimate equilibrium of soils to calculate the values replacing the cohesion forces of cohesive soils.

**Various cases of the ultimate stress diagram at shearing.** The Coulomb's law described by equations (2.18) and (2.20) can be applied to the complex stressed state of soils if the shear diagram is regarded as an envelope of Mohr's ultimate stress circles, which is identical assuming that *Mohr's theory of strength* known from courses on Strength of Materials is valid for soils.

Indeed, the magnitude of shear stresses cannot be greater than their *ultimate value* which is determined by equation (2.18) or (2.20) and corresponds to the appearance of continuous slippage (shearing) of one portion of soil over another, i.e.,

$$ult\tau \leq \tan \varphi \sigma$$

or

$$ult\tau \leq c + \tan \varphi \sigma$$

This value of stresses corresponds to a certain experimental point  $M$  on the ultimate line which at the same time must belong to a Mohr's circle of ultimate stresses (Fig. 22). This is only possible when line  $OM$  (Fig. 22a) or  $O'M$  (Fig. 22b) is a tangent to the stress circle, i.e., makes an angle of 90 degrees with the radius of the circle in the point of contact and passes through the origin of coordinates ( $O$  or  $O'$ ).

This *condition* can be written in an analytical form.

Having found the main stresses—the maximum  $\sigma_1$  and the minimum  $\sigma_2$  (by determining them, for instance, from the stress circle as the abscissa of the intersection of the circle with the  $\sigma$  axis, if the circle has been constructed for a certain plane inclined at an angle  $\alpha$  to the axis of pressures from values of  $\tau_\alpha$  and  $\sigma_\alpha$ ; or directly from the results of corresponding tests) and noting that the triangle  $OMC$  (or  $O'MC$ ) in the shear diagram (see Fig. 22) is a rectangular one, we get:

from Fig. 22a (for loose soils)

$$\sin \varphi = \frac{CM}{OC}$$

but since

$$CM = \frac{\sigma_1 - \sigma_2}{2} \quad \text{and} \quad OC = \sigma_2 + \frac{\sigma_1 - \sigma_2}{2} = \frac{\sigma_1 + \sigma_2}{2}$$

then we have

$$\sin \varphi = \frac{\sigma_1 - \sigma_2}{\sigma_1 + \sigma_2} \quad (2.24)$$

and from Fig. 22b (for cohesive soils)

$$\sin \varphi = \frac{CM}{O'C} = \frac{\frac{\sigma_1 - \sigma_2}{2}}{c \cot \varphi + \sigma_2 + \frac{\sigma_1 - \sigma_2}{2}}$$

or

$$\sin \varphi = \frac{\sigma_1 - \sigma_2}{\sigma_1 + \sigma_2 + 2c \cot \varphi} \tag{2.25}$$

Equations (2.24) and (2.25) express mathematically the *conditions of ultimate equilibrium* (strength conditions) for *loose* (2.24) and *cohesive* (2.25) soils. These conditions find a great number of practical

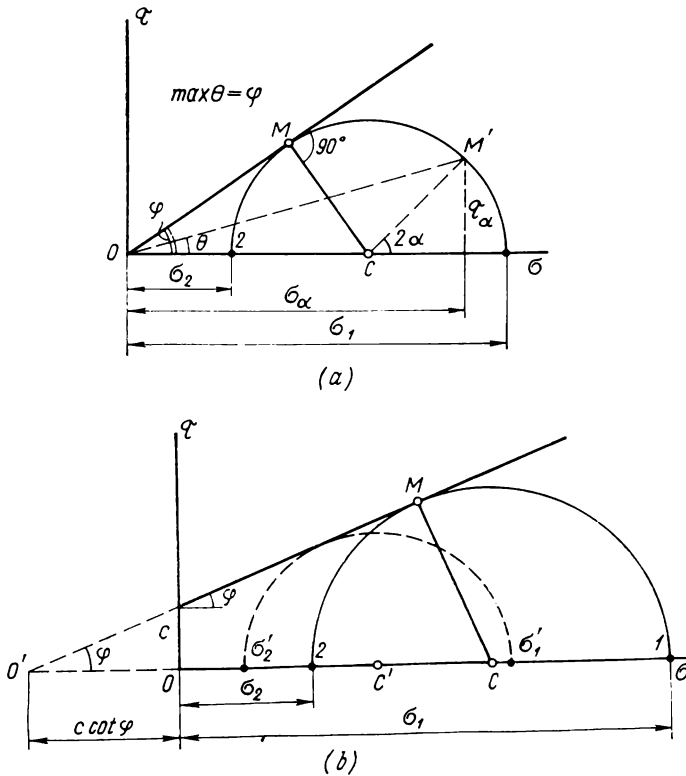


Fig. 22. Diagram of ultimate stresses of soils at shearing  
(a) for loose soils; (b) for cohesive soils

applications and are used in determinations of ultimate loads on soils, in calculations of stability of soil masses and the pressure of soils on retaining structures.

It will also be noted that the parameters of shear resistance of soils ( $c$  kgf/cm<sup>2</sup>, and  $f = \tan \varphi$ ) are only the *mathematical parameters* of a linear envelope of ultimate stress circles. But, as has been shown by detailed studies, the envelope of ultimate stress circles is a *curvilinear* one in the general case (Fig. 23), if the shear resistance of soils is considered in a wide range of variations of compacting pressures and for different stressed states (simple and complex). If, however, variations of pressures are not very large (with  $\sigma < \sigma_{\varphi} = 5-7$  kgf/cm<sup>2</sup>), a portion of the envelope curve of ultimate stresses

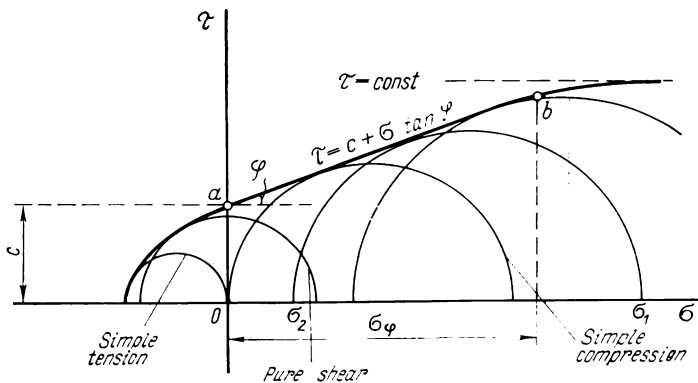


Fig. 23. The general case of the envelope of ultimate shear (rupture) stresses (by the results of tests in simple and complex stressed states)

(section  $ab$  in Fig. 23) can be reasonably assumed to be *linear*, i.e., for pressures lower than  $\sigma_{\varphi}$ , the Coulomb's law and the conditions of ultimate stressed state of soils [equations (2.24) and (2.25)] will hold true.

**Shear tests of soils under simple and triaxial compression.** Tests for simple (laterally unrestricted) compression are only possible for stiff-plastic and hard clayey soils from which cylindrical or prismatic samples can be cut. Tests for triaxial compression are applicable, however, not only to cohesive soils, but also for loose soils, since they are made with samples enclosed in thin rubber shells with application of a uniform lateral pressure and an additional (in excess of the uniform one) axial pressure.

In tests for simple uniaxial compression of soil samples (cylinders with a height 1.5-2 times their diameter) the compressive load is increased until brittle fracture of the sample occurs or the deformations in it become progressively increasing. The magnitude of breaking load is related to the unit cross-sectional area of the sample, assuming that pressures are distributed uniformly ( $\sigma_1 = P/F$ , where  $P$  is the load and  $F$ , the cross-sectional area of the sample). As

has been shown by Prof. A. N Zelenin this gives slightly conservative values of resistance, since non-uniform distribution of pressures over the edge surfaces of samples is not taken into account.

If an infinitesimal element (Fig. 24a) is separated on the axis of a sample, then the triangular prism with an angle  $\alpha$  to the axis of pressures will be subject only to the stresses indicated in Fig. 24b

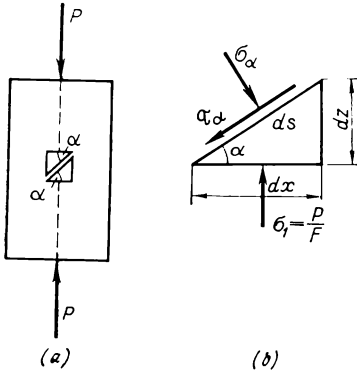


Fig. 24. Diagram of uniaxial compression test of cohesive soils

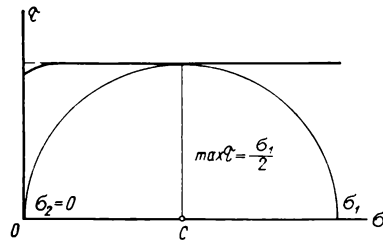


Fig. 25. Diagram of ultimate stresses at simple compression

(if the resistance to friction along the inclined face of the prism is not taken into account). By projecting all the forces onto the direction of the inclined face of the prism, we get

$$\tau_\alpha ds \cdot 1 - \sigma_1 dx \sin \alpha \cdot 1 = 0 \tag{h_1}$$

whence

$$\tau_\alpha = \sigma_1 \frac{dx}{ds} \sin \alpha \tag{h_2}$$

or

$$\tau_\alpha = \frac{\sigma_1}{2} \sin 2\alpha \tag{h_3}$$

The maximum shear stress will be observed with  $\sin 2\alpha = 1$ , i.e.,

$$\max \tau = \frac{\sigma_1}{2} \tag{2.26}$$

or, assuming that  $\max \tau = c$ , we get

$$c \approx \frac{\sigma_1}{2} \tag{2.26'}$$

The diagram of ultimate stresses for the case considered is shown in Fig. 25.

*Tests for triaxial compression* make it possible to test samples of any kind of soil precompressed with a given lateral pressure, which closer corresponds to the work of the soil under natural conditions and gives the most reliable results of determining their strength and deformation properties.

This kind of tests was first proposed by Profs. G. B. Yappu and N. V. Laletin in the USSR and is now being widely employed both in the USSR and other countries.

An apparatus for triaxial tests of soils, which is called stabilometer, is shown schematically in Fig. 26. The apparatus comprises

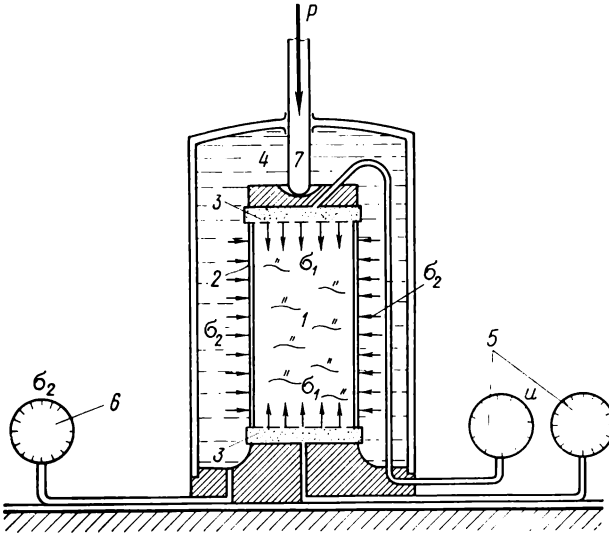


Fig. 26. An apparatus for triaxial compression tests of soils

a chamber 4 filled with liquid and communicating with a source of lateral pressures and end plates 3 (either filtering or water-impermeable, depending on the conditions of the tests), between which a sample of soil I enclosed into a thin rubber shell 2 is placed by means of a special arrangement.

The axial load is transmitted to the sample by means of a piston 7. Measurements are made during the tests of the neutral (porous) pressure of water at the ends of the sample (by means of pressure gauges 5), of the uniform pressure in the test chamber (by means of pressure gauge 6), of axial deformations (by means of an indicator), and of volume variations of the sample (by means of a volumetric tube).

The standard technique of soil tests for triaxial compression is as follows. A sample of soil placed into the test chamber is first subjected

to a uniform pressure,  $\sigma_2 = \sigma_3$ , (both in drained and non-drained tests); then after the deformations caused by the uniform pressure have attenuated, an axial load is applied in increasing steps  $\Delta\sigma_1$  until the sample breaks and loses stability.

The results of such tests make it possible to determine [by formula (2.17)] the magnitude of effective stresses at the moment of sample destruction

$$\left. \begin{aligned} \bar{\sigma}_1 &= \sigma_1 - u \\ \bar{\sigma}_2 &= \sigma_2 - u \\ \bar{\sigma}_3 &= \sigma_3 - u \end{aligned} \right\} \quad (i_1)$$

where  $u$  is the porous pressure.

In addition, the results of tests are used to determine the magnitude of the relative longitudinal deformation

$$\epsilon_z = \frac{s_i}{h} \quad (i_2)$$

where  $s_i =$  settlement from an  $i$ -th step of load  
 $h =$  initial height of the soil sample  
 and the relative volume deformation

$$\theta = \frac{\Delta V}{V} \quad (i_3)$$

where  $V =$  initial volume of the sample  
 $\Delta V =$  change of its volume (determined by means of a volumeter)

The data obtained are used to construct the diagrams (Fig. 27) of variations

$$\frac{\bar{\sigma}_1}{\bar{\sigma}_2} = f(\epsilon_z)$$

from which the maximum value  $\max \frac{\bar{\sigma}_1}{\bar{\sigma}_2}$  is found, and the diagrams of dependence of the total longitudinal and volume deformations of the soil on the increment of axial pressure  $\Delta\sigma_1$ , from which the deformability moduli are determined.

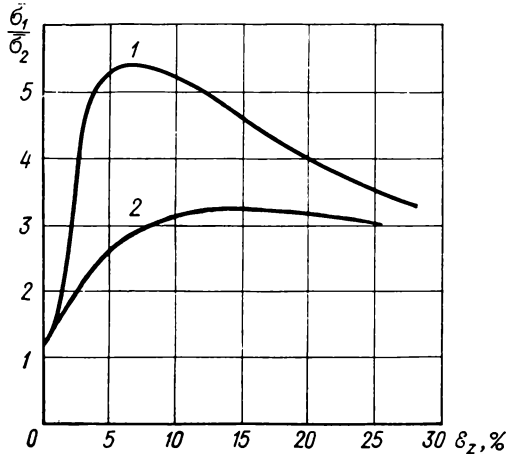


Fig. 27. Results of triaxial compression tests of soils  
 1—dense soils; 2—loose soils

Within the limits of a linear relationship between the total deformations (either longitudinal or volumetric) and the increment of axial pressure  $\Delta\delta_1$ , we have:

the modulus of total (linear) deformation

$$E_o = \frac{\Delta\sigma_1}{\Delta\varepsilon_z} \quad (2.27)$$

and the modulus of volume deformation

$$E_v = \frac{\Delta\sigma_1}{\Delta\theta} \quad (2.28)$$

As is known from the course of the Strength of Materials, the modulus of volume deformation and that of total linear deformation are linked by the following relationship:

$$E_v = \frac{E_o}{1 - 2\mu_o} \quad (j)$$

whence the *coefficient of relative lateral deformation* (analogous to the Poisson's ratio for elastic bodies) is

$$\mu_o = \frac{E_v - E_o}{2E_v} \quad (2.29)$$

Having found the maximum of the ratio  $\overline{\sigma_1}/\overline{\sigma_2}$  from the diagram in Fig. 27 and using the condition (2.24) for loose soils (in which the numerator and denominator in the right-hand part must be divided by  $\overline{\sigma_2}$ ), we get

$$\sin \varphi = \frac{\frac{\overline{\sigma_1}}{\overline{\sigma_2}} - 1}{\frac{\overline{\sigma_1}}{\overline{\sigma_2}} + 1} \quad (2.24')$$

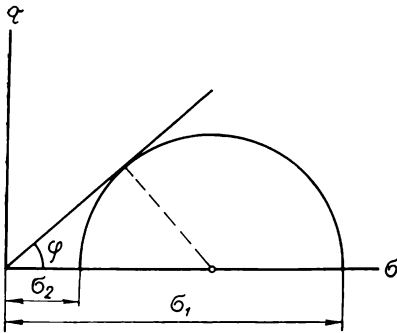


Fig. 28. Determination of the angle of internal friction of a loose soil by the results of triaxial compression tests

determined directly from the results of a test for triaxial compression (Fig. 28).

In order to determine the parameters of the shear diagram for cohesive soils, we have to know the results of triaxial tests of at least two identical soil samples under different lateral pressures

This expression is used to calculate the angle of soil internal friction  $\varphi$ .

For loose soils, the angle of internal friction can also be found from the ultimate stress circle, which is easy to construct, since  $\sigma_1$  and  $\sigma_2$  can be

$\bar{\sigma}_2 = \bar{\sigma}_3$ , and therefore, under different breaking axial (main) stresses  $\bar{\sigma}_1$ , which is made in Fig. 29.

The results of tests for triaxial compression make it possible to estimate the soil strength not only by Mohr's strength theory which is based on Coulomb's law, but also by the *octahedral strength theory*, which takes into account the three-dimensional stressed state of

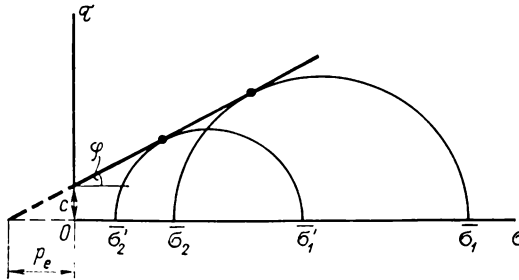


Fig. 29. Determination of shear parameters by the results of triaxial compression tests of a cohesive soil

soils along octahedral planes of *equal inclination* to the planes of main stresses.

According to the general mechanics of continuous bodies, the normal and shear stresses at these planes are respectively

$$\begin{aligned} \text{normal } \sigma_{oct} &= \frac{1}{3} (\sigma_1 + \sigma_2 + \sigma_3) \\ \text{shear } \tau_{oct} &= \frac{1}{3} \sqrt{(\sigma_1 - \sigma_2)^2 + (\sigma_2 - \sigma_3)^2 + (\sigma_3 - \sigma_1)^2} \end{aligned}$$

According to the Mises—Botkin strength theory, the octahedral shear stress *at breakage* is a direct function of the normal octahedral stress, i.e.,

$$\tau_{oct} = F(\sigma_{oct}) \tag{2.30}$$

or, following A. I. Botkin (1940) and introducing our notation, we get

$$\tau_{oct} = \tan \varphi_{oct} (p_{e\ oct} + \sigma_{oct}) \tag{2.31}$$

As has been demonstrated by experiments, the *deformations* at failure can be described with good results by a power dependence of the *second invariants* of the stressed-strained state of soils

$$T = \zeta \Gamma^m \tag{2.32}$$

where  $T = \sqrt{\frac{2}{3} (\tau_1^2 + \tau_2^2 + \tau_3^2)}$  = intensity of shear stresses

$\Gamma = \sqrt{\frac{2}{3} (\gamma_1^2 + \gamma_2^2 + \gamma_3^2)}$  = intensity of shear deformations

$\tau_1, \tau_2, \tau_3$  = maximum shear stresses

$\gamma_1, \gamma_2, \gamma_3$  = maximum (main) shear deformations

$\zeta$  and  $m$  = time-variable ( $\zeta$ ) and constant ( $m$ ) parameters for a given soil, which are determined experimentally.

**Other methods for shear tests of cohesive soils.** Apart from the principal methods for determining the ultimate shear resistance of soils which have been discussed earlier (the method of direct shear, the method of triaxial compression), there exist a number of other methods for shear tests, of which we shall discuss only those most widely employed in practice; these are the *vane tests* of plastic soils and the *method of spherical stamp*, which has been proposed by the Author of this book.

The method of vane tests by means of special vanes, which is employed in field conditions, has been proposed in Sweden and is now widely used for testing plastic weak clayey and silt soils, and also water-saturated sand loam soils whose samples are difficult to take without disturbing the structure.

A vane test apparatus designed in the USSR is shown in Fig. 30. With the height of the vane of 160 mm and diameter of 80 mm, it allows soils to be tested for an ultimate shear resistance of up to 1 kgf/cm<sup>2</sup>, and with smaller dimensions of the vane, up to 2-2.5 kgf/cm<sup>2</sup>.

In vane tests, a vane (crosspiece *I* in Fig. 30) is pressed into the soil below the lower end of case pipe, then the vane is given a complete turn (360°) by handle  $\gamma$  through a double worm gear and the soil is thus cut off along a cylindrical surface of height  $h$  and diameter  $d$ ; at the same time the maximum torque  $M_t$  applied is measured on scale  $\delta$  of a torque meter.

Assuming a triangular distribution of shear stresses  $\tau_s$  over the cross-sectional area of the shear cylinder (the upper and lower surfaces) and a uniform distribution over its side surface, we have

$$M_t = \tau_s \pi dh \frac{d}{2} + 2\tau_s \frac{\pi d^2}{4} \cdot \frac{2}{3} \cdot \frac{d}{2}$$

whence

$$\tau_s = \frac{2M_t}{\pi d^2 h \left(1 + \frac{d}{3h}\right)} \quad (2.33)$$

The vane test method is widely employed for determination of the total ultimate shear resistance of weak silt and clayey soils and corresponds to their undrained state.

It is usually assumed in calculations that the shear resistance  $\tau_s$  found in vane tests is approximately equal to the total cohesion of the soil, i.e.,  $\tau_s \approx c$ .

The method of spherical stamp (proposed by Prof. N. A. Tsytoich in 1947) is a simple and convenient means for a large-scale

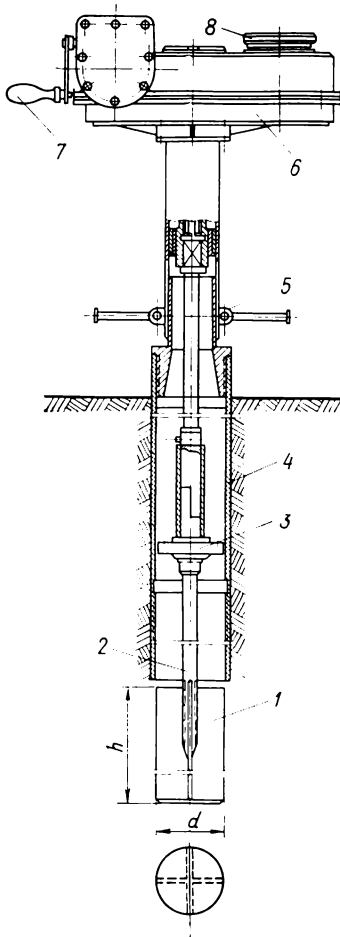


Fig. 30. An apparatus for vane tests of soils in field conditions  
1—vane with four blades; 2—rod; 3—centering sleeve; 4—casing pipe; 5—clamping device; 6—head portion of apparatus; 7—worm gear handle; 8—torsionmeter scale to indicate  $M_t$

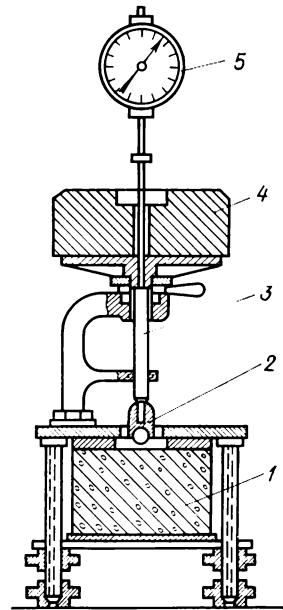


Fig. 31. Single-rod spherical stamp for measuring cohesion forces in cohesive soils by Tsytoich's method

1—soil sample; 2—spherical stamp; 3—stopper screw; 4—weight; 5—indicator

determination of cohesion forces and their time variations in disperse cohesive soils and viscous rock (silts, clays, loesses, icy soils, permafrost, etc.).

The method is based on measuring the settlements of a spherical stamp  $s$  at a definite constant load  $P$  in a laboratory apparatus (Fig. 31) or a field arrangement (Fig. 32).

As distinct from shear tests of soils, and especially from the method of trial field load, where it is required to load a flat stamp with gradually increasing steps of load, in tests by the spherical (ball) stamp it is sufficient to measure the settlements for any load

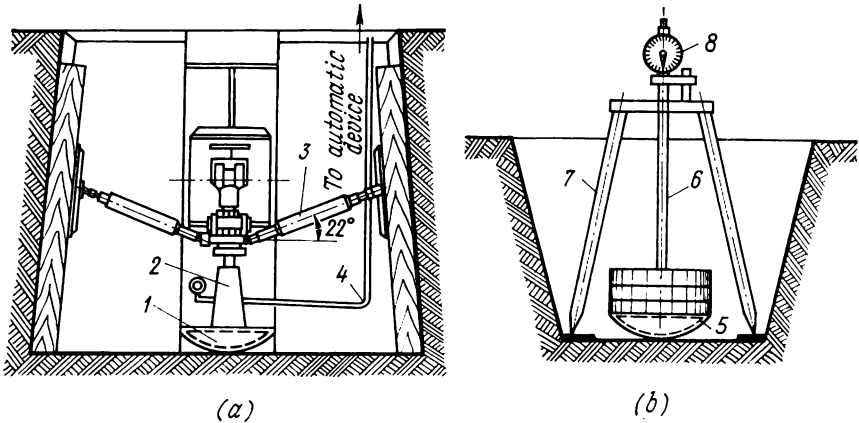


Fig. 32. Field apparatus for cohesive soil testing by Tsytovich's spherical stamp method (designed at the Byelorussian Institute of Building Construction and Architecture)

(a) for hard clayey soils; (b) for weak clayey and peat soils; 1, 5—spherical portion, 30-50 cm in diameter; 2—jack; 3—stoppers; 4—pipe connection to pump and pressure reducer to maintain a constant pressure; 6—rod with loading plate; 7—stand; 8—indicator

(not very small) so that the ratio of the settlement to the diameter of the spherical stamp is greater than approximately  $1/200$ ; elastic deformations of the soil can then be neglected.

It also follows from theoretical considerations that the ratio of settlements of a stamp  $s$  to its diameter  $D$  should be less than 0.1, i.e.,  $s/D \leq 0.1$ ; tests with spherical stamps of different diameters will then give practically identical results.

The cohesion of the soil is determined by the results of tests from the formula of the theory of plastic-viscous media

$$c_b = 0.18 \frac{P}{\pi D s} \quad (2.34)$$

The coefficient 0.18 has been found theoretically on the basis of a constant ratio of hardness to yield limit for plastic bodies, which has been established by A. Yu. Ishlinsky.

As has been shown by respective experiments, the magnitude of cohesion  $c_b$  found by the spherical stamp method [(formula (2.34)]

should be regarded as a certain complex characteristic which makes it possible to estimate not only cohesion, but for plastic soils also the internal friction to a certain extent, which can be used, for instance, for calculations of the ultimate load on clayey soils by the formulae of ideally cohesive bodies (without account of friction, since this is included in  $c_b$ ).

Determination of cohesion by the spherical stamp method makes it possible, for cohesive soils, as has been first proposed by the Author of this book, to restrict determinations of shear parameters to tests of a *single monolith* of a soil; this is of great importance in practice. The monolith is first tested at its end

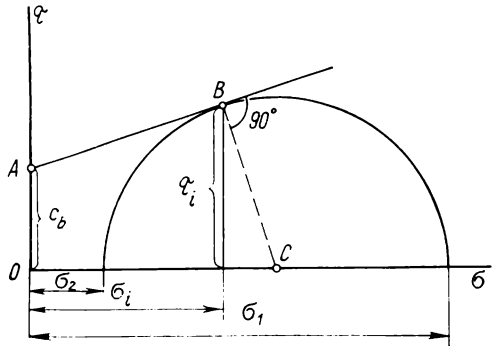


Fig. 33. Diagram of ultimate shear stresses plotted by the results of testing of a monolith of cohesive soil

means of a spherical stamp in order to determine cohesion forces (by making measurements of settlements of the stamp at intervals of 10 s from the beginning of loading), and is then subjected to direct

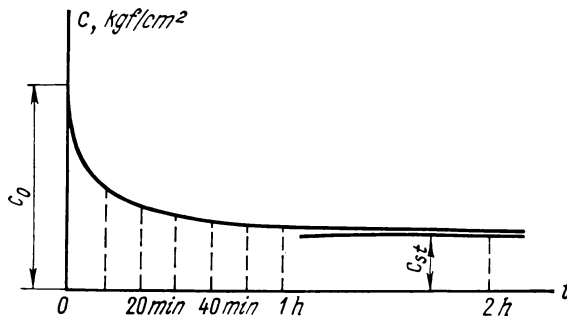


Fig. 34. Time variation curve of cohesion forces in viscous clayey soil

shear or triaxial crushing in order to determine the total shear resistance at a definite external pressure.

The results of the tests of a *single monolith* make it possible to construct a diagram of ultimate shear stresses (Fig. 33).

It should be noted that settlements of a spherical stamp in viscoplastic clays occur not instantaneously, but increase gradually and attain a certain limit (stable deformation).

From the results of measurements for different intervals of time from the beginning of loading, cohesion forces are determined, which for visco-plastic soils vary in time from the maximum (instantaneous) value  $c_0$  to the stable value  $c_{st}$  (Fig. 34); the latter is to be taken into account in calculations of strength (load-bearing capacity) of soils.

Note that determinations of long-term stable cohesion  $c_{st}$  by the spherical stamp method require not more than from one to a few hours, whereas determination of *long-term shear resistance* by the method of direct shear or triaxial compression requires as much as several months.

#### 2.4. STRUCTURAL-PHASE DEFORMABILITY OF SOILS

As has been indicated earlier in the book, soils are very complicated mineral-disperse formations consisting of diverse mutually bonded particles possessing different mechanical properties.

The application of the general theory of stresses, that has been developed for continuous elastic bodies, to soils requires special discussion. Thus, an external load in disperse soils is transmitted from one particle to another only through the points of their contact, which in most cases are located irregularly or according to a definite structural network.

A question then arises, whether it is possible to consider the internal forces in soils to be continuously distributed over sufficiently small planes in which the stresses are to be determined. As has been shown by Prof. N. M. Gersevanov in 1931, the error in determinations of the stresses in soils (for instance, in clays) by the general theory of continuous bodies will not be greater than in determining the stresses in steel which also consists of crystalline grains, though of very small size. Determination of stresses in soils is, however, a much more complicated problem than that in continuous bodies.

The most characteristic feature of the stressed-strained state of soils is that (when an external load is applied) the soil individual phases (components) resist in different ways to the effective forces and are deformed differently.

When considering the general problem, we have to study the stressed-strained state of both the soil as a whole (regarding it as a quasi-continuous and quasi-singlephase body) and its individual phases in their interaction.

As has been shown by the latest research, the earlier hypotheses on incompressibility of some soil component (for instance, porous water) and on instantaneous transmission of pressure to the soil skeleton are incorrect. In addition, it should be taken into account that not only the deformability of the soil as a whole, but also of its individual phases (solid particles, for instance) depends on the duration of load action because of the creep phenomenon.

**General stress-strain relationship.** Let us discuss the general case of relationship between the normal stress  $\sigma$  and relative strain  $\varepsilon$  for a soil as a whole. This analysis will be fully valid for the initial and final state of the soil when there is no phase redistribution in unit volume of the soil (for instance, when squeezing of water from soil voids at compaction has been finished). When considering the intermediate state, we have additionally to take into account the process of consolidation, creep of the soil skeleton, etc.

When analysing stress-strain relationships, at least two kinds of soil must be distinguished, i.e., loose (cohesionless) and cohesive.

For *loose* soils, a single loading always causes irreversible displacements and turns of soil grains relative to each other, which results in that *residual deformations* are always observed in such soils.

In *cohesive* soils the nature of their deforming depends appreciably on their structural bonds, both rigid and viscous. With rigid bonds, the soil deforms as a quasi-solid body, if the load is such that it does not disturb the strength of bonds.

With viscous (water-colloidal) bonds in soils, some bonds become destroyed (or undergo viscous flow) already at rather low loads, while others become destroyed at slightly higher loads, etc., so that both reversible and residual deformations are always observed in such soils at unloading. It is of importance to note that residual deformations can often exceed many times the reversible ones.

In most cases natural cohesive soils possess both rigid and purely viscous bonds of different strength, because of which the process of their deforming is a complicated one. The conditions for appearance of some or other kind of soil deformation (elastic deformations, residual deformations upon compaction, deformations of viscous flow, creep deformations, etc.) and the methods for their determination will be discussed in detail in Chapters 5 and 6. Here we shall only dwell on the general relationship between the normal stress  $\sigma$  and relative strain  $\varepsilon$ , since this relationship is taken as a basis for the theory of distribution of stresses in soils and determination of their deformations under the action of external forces.

In the most general case, as has been shown by numerous experiments, the stress-strain relationship for soils is non-linear (dotted curve *Oab* in Fig. 35).

In the general form this relationship can be represented by the function

$$\varepsilon = \alpha_0 \sigma_{str} + \alpha_t (\sigma_t - \sigma_{str})^m \quad (2.35)$$

where  $\alpha_0$  and  $\alpha_t$  = coefficients to be determined experimentally  
 $\sigma_{str}$  = stress not exceeding the initial strength of structural bonds ( $\sigma_{str} \leq p_{str}$ )

$(\sigma_t - \sigma_{str}) = \sigma$  = effective normal stress responsible for soil deformations at a partial or full destruction of structural bonds  
 $m$  = parameter of non-linearity to be determined experimentally

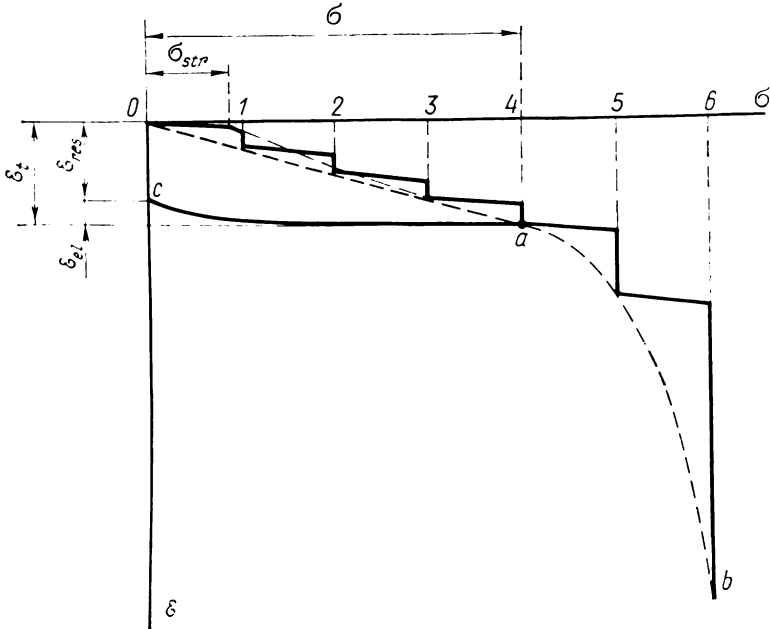


Fig. 35. Relationship between normal stresses  $\sigma$  and deformations  $\epsilon$  for soils with a stepwise increasing load

The coefficient  $\alpha_0$  may be taken as an inverse of the normal elastic modulus of the soil  $E$ , i.e.,

$$\alpha_0 = \frac{1}{E}$$

As regards the coefficient  $\alpha_t$ , its nature is appreciably more complex. If we consider only stabilized stresses, this coefficient will be dependent on the total deformation modulus  $E_0$  of soil [see formula (2.37)], which in the general case may enter the expression above with a certain power  $r$  less than or equal to unity, and also on the coefficient  $\beta$  which estimates the capability of the soil to expand

laterally (for determination of  $\beta$ , see Chap. 5), i.e., we may take that

$$\alpha_t = \frac{\beta}{E_{o(z)}^r}$$

where the parameter  $r \leq 1$  is to be found experimentally as well.

If we consider soil deformations at pressures exceeding the structural compressive strength, then relationship (2.35) can be given the following form:

$$\varepsilon = \alpha \sigma^m \quad (2.35')$$

where  $\alpha$  is a certain general proportionality factor, which in the simplest case is  $\alpha = \beta/E_o$ .

The general relationship (2.35'), even in the simple form given, is still too complicated to be used in practice.

**Principle of linear deformability.** If variations of external pressure are not very great (of the order of 1-3 kgf/cm<sup>2</sup> or, for dense and hard soils, up to 5-7 kgf/cm<sup>2</sup>), the relationship between stresses  $\sigma$  and deformations  $\varepsilon$  can be taken to be *linear* with an approximation sufficiently correct for practical purposes (see the straightened section *Oa* of the curve in Fig. 35), which largely simplifies calculations without introducing impermissible errors into them. Assuming  $m = 1$  in expression (2.35') (which is quite admissible when the stresses are lower than the *practical proportionality limit*), the relationship between the stress  $\sigma_\varepsilon$  and total deformation, with a constant modulus of total deformation, will be of the form

$$\varepsilon = \alpha \sigma \quad (2.36)$$

i.e., with small variations of stresses the *theory of linearly deformable bodies* is fully applicable to soils.

As has been demonstrated by Prof. N. M. Gersevanov in 1931, with a *linear* relationship between stresses and total deformations, the *solutions of the theory of elasticity* are fully applicable to *determination of stresses in soils*; determination of total deformations of soils, however, requires additional conditions (for instance, the relationship between the pressure and void ratio, etc.).

What has been said above enables the so-called *principle of linear deformability* to be formulated as follows: *with small variations of pressures, soils may be regarded as linearly deformable bodies, i.e., it may be taken with an accuracy sufficient for practical purposes that the relationship between stresses and total deformations in soils is a linear one.*

This principle also follows from the considered case of compression of a soil layer with a continuous load (compression of the soil) within

the range of pressures when the *law of compaction* holds true. Indeed, according to formula (2.5') we have

$$m_v = \frac{s_i}{hp_i}$$

and, since the relative strain is

$$\varepsilon = \frac{s}{h}$$

then

$$\varepsilon = m_v p_i \quad (2.36')$$

Comparing (2.36) and (2.36') and taking into account that, in the case considered,

$$\sigma = p \quad \text{and} \quad \alpha = \frac{\beta}{E_o}$$

we get

$$m_v = \frac{\beta}{E_o} \quad (2.37)$$

or

$$E_o = \frac{\beta}{m_v} \quad (2.37')$$

where  $E_o$  is the modulus of soil total deformation, which is determined from formula (2.27) by using the results of tests of soil samples for triaxial compression or the data of field tests by a trial load.

The coefficient  $\beta$ , as has been indicated earlier, depends on the coefficient of relative lateral deformation of soil (which is analogous with Poisson's ratio for elastic bodies) and approximately equals:  $\beta = 0.8$  for sands;  $\beta = 0.7$  for sand loams;  $\beta = 0.5$  for loams; and  $\beta = 0.4$  for clays (see Chap. 5).

It should be noted that the *principle of linear deformability* (which holds true for soils of medium compaction at pressures of the order of 1-3 kgf/cm<sup>2</sup> or more) is one of the main principles in modern soil mechanics, since it is used as the basis for almost all engineering calculations of stresses and strains of natural soil foundations. For weak soils, however (when their load-bearing capacity is less than 1 kgf/cm<sup>2</sup>), the *relationship* between stresses and strains must be taken to be *non-linear*.

**Deformability of individual soil phases.** The stressed-strained state of the *soil skeleton*, and also of *single-component and quasi-singlephase soils* (i.e., those in which the phase ratio in unit volume remains practically constant at deforming) can be strictly described by equations (2.35) and (2.36) only with  $t = 0$  and  $t \rightarrow \infty$ , i.e., when the process of redistribution of soil phases has not yet begun or

has already finished; for intermediate time intervals, the stressed-strained state of soils, generally speaking, is dependent on time  $t$ .

As seen from the latest research, time variations of the stressed-strained state of *soil skeleton* (and also of single-component and single-phase soils in the whole) are the result of the *rheological properties of the soil skeleton*, namely, its *creep at load*.

The experiments made by S. R. Meschyan and others have confirmed Florin's statement that the deformability of the skeleton of disperse soils (with their consolidation finished) is described quite adequately by the linear (with respect to stresses) *theory of heredity creep* proposed by Boltzmann—Volterra.

According to that theory, the relative deformation of the soil skeleton,  $\varepsilon(t)$ , (or of quasi-singlecomponent soils in the whole) is determined in the most general case by the expressions:

with a single loading during time  $\Delta t_0$  by a stress  $\sigma(t_0)$

$$\varepsilon(t) = \frac{\sigma(t)}{E_{inst}} + \bar{K}(t-t_0) \sigma(t_0) \Delta t_0 \quad (2.38)$$

and with continuous loading

$$\varepsilon(t) = \frac{1}{E_{inst}} \left[ \sigma(t) + \int_0^t K(t-t_0) \sigma(t_0) dt_0 \right] \quad (2.38')$$

where  $\bar{K}(t-t_0)$  is the so-called *creep core* which characterizes the rate of creep at a constant stress, related to unit acting pressure, with  $\bar{K}(t-t_0) = K(t-t_0)/E_{inst}$ , and  $E_{inst}$  is the modulus of instantaneous deformation.

Equations (2.38) and (2.38') show that the total relative deformation of soil skeleton depends not only on the stressed state during the time elapsed from the beginning of loading, but also on the pre-history of loading ( $t_0$ ), because of which the theory has been called the *theory of heredity creep*.

It should also be noted that equations (2.38) and (2.38') hold true for any creep core.

The simplest form of creep core, which has been proved for disperse clayey soils by direct experiments, is as follows:

$$\bar{K}(t-t_0) = \delta e^{-\delta_1(t-t_0)} \quad (2.39)$$

where  $\delta$  and  $\delta_1$  are creep parameters to be determined experimentally.

The deformability of porous water, if it is free of gas bubbles, is not large; in that case the water may be regarded as an ideally elastic body. Completely degassed water has an appreciable modulus of elasticity, of the order of 20,000 kgf/cm<sup>2</sup>.

A different case is porous water containing closed air bubbles and dissolved gases (in nature, almost any porous water contains a certain amount of gases); its deformability is appreciable and must be taken into account in calculations.

Account of the volume compressibility of gas-containing porous water has a substantial effect on the magnitude and time course of deformations of water-saturated soils (both of filtration deformations and creep deformations), which will be discussed in more detail in Chapters 5 and 6.

It has been shown\* that the coefficient of volume compressibility of gas-containing porous liquid,  $m_w$ , with a low gas content (less than 2 per cent of the volume of voids) can be approximately determined by the following simple expression:

$$m_w \approx (1 - I_w) \frac{1}{p_a} \quad (2.40)$$

where  $I_w$  = coefficient of water saturation of soil [see formula (1.6')] and

$p_a$  = atmospheric pressure, kgf/cm<sup>2</sup>

As regards the *deformability* of closed *air* bubbles proper (the third phase of soils), usually it is not taken into account separately in calculations, since closed air bubbles are enclosed in liquid and are moved and deformed together with the latter, while free air is insensitive to pressure. But, as has been indicated earlier, the deformability of an *air-water* mixture must be taken into account to the full extent.

Thus, in the most general case of studying the stressed-strained state of soils we have to take into account the deformability of all phases of the soil in their interaction, especially if time variations of the stressed-strained state are being considered. The problem becomes simpler only for the initial moment and the *stabilized state*, to which, as has been shown earlier, the simplest expression of the principle of linear deformability (2.36') is fully applicable. When studying time variations of the stressed-strained state of water-saturated soils, we must consider variations of the effective stresses in the course of *filtration consolidation*, and for tough clayey soils, the effect of the *creep of the soil skeleton* on the stressed-strained state in addition to the process of filtration consolidation. For non-saturated soils with  $I_w \leq 0.85$  and for quasi-homogeneous soils, time variations of the stressed-strained state depend exclusively on *creep* of the soil skeleton.

---

\* Tsytovich N. A. et al. Prognoz skorosti osadok osnovanii sooruzhenii (konsolidatsiya i polzuchest' mnogofaznykh gruntov) [Prediction of Settlement Rate of Structure Bases (Consolidation and Creep of Multiphase Soils)], Moscow, Stroizdat, 1967.

## 2.5. FEATURES OF THE PHYSICAL PROPERTIES OF STRUCTURALLY UNSTABLE SUBSIDENCE SOILS

Among the great diversity of soils with which civil engineering has to deal, those offering special difficulties are structurally unstable subsidence soils which can strongly alter their structure under usual conditions with the action of some additional physical effects; this may substantially worsen their physical and mechanical properties, increase settlements, reduce the load-bearing capacity, etc.

Substantial settlements of soils of this kind when their structure is disturbed can also be caused by that these soils are often undercompacted in natural conditions. The soils of this group include, in the first place, *loess* and *frozen* soils.

**Undercompacted soils.** The conditions of the formation of individual kinds of soils might be such that the action of their own weight and of the upper layers could not cause complete consolidation because of the formation of new structural bonds, for instance, formation of solid colloidal films and cementation of particles with separated salts in loess soils, cementation of particles with ice in frozen soils and permafrost, etc.

The soils in which, at incomplete consolidation, new structural bonds have been formed that prevent their further consolidation, are related to the group of undercompacted soils. With certain additional actions, such soils may become structurally unstable and undergo further compaction at destruction of the structural bonds that have been formed earlier; this can cause substantial settlement of these soils.

A local rapid settlement of undercompacted structurally unstable soils, which can be caused by a sharp variation of their structure and is usually accompanied with extrusion of the liquid-plastic masses formed laterally from the local action, is termed *subsidence*, and soils possessing such properties are related to the group of structurally unstable *subsidence soils*. Such are loess soils (their deposits being often found in regions near deserts) when they are being moistened under load; *icy frozen soils* and *permafrost* at thawing; and also *mineral-organic silts* at a rapid loading, when the rate of formation of new water-colloidal bonds is less than the rate of destruction of the existing bonds; and finally, *loose weak sands* subjected to vibrations which cause a hydrodynamic pressure and a substantial reduction of friction at contacts between mineral particles.

An important characteristic of the physical and mechanical properties of structurally unstable clayey soils is their *structural strength* and its variations under the action of external factors (moistening, thawing, vibrations, etc.) which cause the soil to settle under load.

The subsidence of soils can usually be evaluated by *relative subsidence* which is found from the expression

$$\varepsilon_s = \frac{h_p - h'_p}{h_p} \quad (k_1)$$

where  $h_p$  = height of soil sample of undisturbed structure (being tested without the possibility of lateral expansion at a pressure  $p$  equal to the pressure from the action of the external load and the dead weight of the upper soil layers)

$h'_p$  = height of the same sample at a load  $p$  after being subjected to an action disturbing its structural strength (moistening of loess soils, thawing of frozen soils, etc.)

Structurally unstable soils in which the relative subsidence  $\varepsilon_s \geq 0.02$  are related to the group of subsidence soils.

Formula (k<sub>1</sub>) can be written as follows:

$$\varepsilon_s = \frac{\Delta h_p}{h_p} \quad (k_2)$$

As has been shown by experiments (Yu. M. Abelev, N. Ya. Denisov, A. A. Mustafayev, N. A. Tsytoich et al.), the magnitude of relative subsidence  $\varepsilon_s$  does not remain constant but increases with an increase of external pressure.

According to the results of experiments carried out by A. A. Mustafayev, with large variations of external pressures (up to 4-5 kgf/cm<sup>2</sup> and more), the dependence of relative subsidence on external pressure is curvilinear and can be approximated with a *power function* [for instance, by formula (2.35) or (2.35')].

However, with pressures not very high (practically up to 2-2.5 kgf/cm<sup>2</sup> for loess soils at moistening and up to 2.5-4.0 kgf/cm<sup>2</sup> for frozen soils and permafrost at thawing), as has been shown by Author's detailed experiments with statistical treatment of results, the variation curves of the relative deformation at subsidence (i.e., of relative subsidence  $\varepsilon_s$ ) can be sufficiently accurately described by a full first-degree function of normal pressure, i.e.,

$$\varepsilon_s = A_0 + a_0 p \quad (2.41)$$

where  $A_0$  = initial parameter of linear relationship  $\varepsilon_s = f(p)$ , which is termed the *coefficient of subsidence* (for loess soils) or *coefficient of thawing* (for frozen soils and permafrost)

$a_0$  = angular coefficient of the straight line which characterizes the relative compressibility of soils in the course of subsidence

As will be shown in Chap. 5, equation (2.41) is used as the basis for calculations of subsidence of loess soils and icy permafrost.

The coefficients  $A_0$  and  $a_0$  can be found from the results of tests of two monolith twins for compression at subsidence or (by a special technique) from the results of tests of one and the same soil monolith.

Compression curves for structurally unstable subsidence soils have a rather peculiar shape (Fig. 36) and differ from the common compression curves in that the soil void ratio changes stepwise in the course of subsidence so that a discontinuity is observed on the curve.

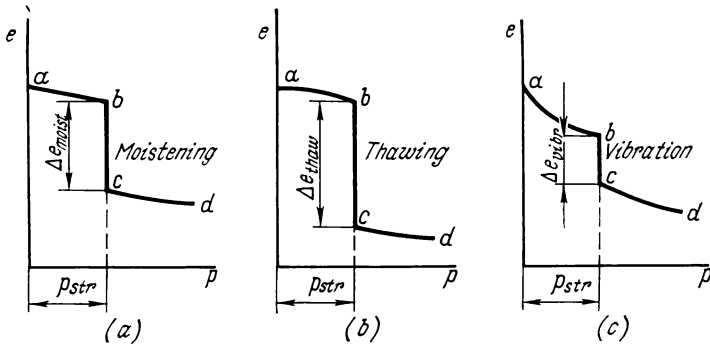


Fig. 36. Compression curves of structurally unstable soils

(a) loess soil on wetting; (b) frozen soil on thawing; (c) loose sand under vibrations

According to the results of tests (see Fig. 36), three different regions should be distinguished on compression curves of subsidence soils: region  $ab$  corresponding to compression of the soil in an undisturbed state; region  $bc$  which characterizes the *subsidence* of soil; and region  $cd$ , i.e., compression of the subsided soil with disturbed structural bonds; the greatest deformation of the soil is observed in the second region.

Compression curves of subsidence soils can be used directly for determining the variation of the void ratio of the soil at subsidence,  $\Delta e_s$ .

Since the relative deformation  $\varepsilon = s/h$ , where  $s$  is the settlement and  $h$  is the initial height of the soil sample, it follows from equation (2.1) that

$$\varepsilon = \frac{e_0 - e_i}{1 + e_0} = \frac{\Delta e}{1 + e_0}$$

Or, denoting the subsidence as  $\varepsilon_s$ , we get

$$\varepsilon_s = \frac{\Delta e_s}{1 + e_0} \quad (k_3)$$

where  $e_0$  = initial void ratio of the soil (before subsiding)

$\Delta e_s$  = variation of the void ratio in the course of subsidence

By testing samples of a soil for subsidence at two different pressures  $p_1$  and  $p_2$ , and using expression (2.41) we can obtain two equations with two unknowns from which the parameters  $A_0$  and  $a_0$  can be found.

Subsidence of loess and permafrost soils can be established either through appropriate compression tests (the existence of a step-like change of the void ratio at tests first in the natural state of the soil without disturbance of its structural bonds and then, with an external action which disturbs the structural bonds of the given soil)

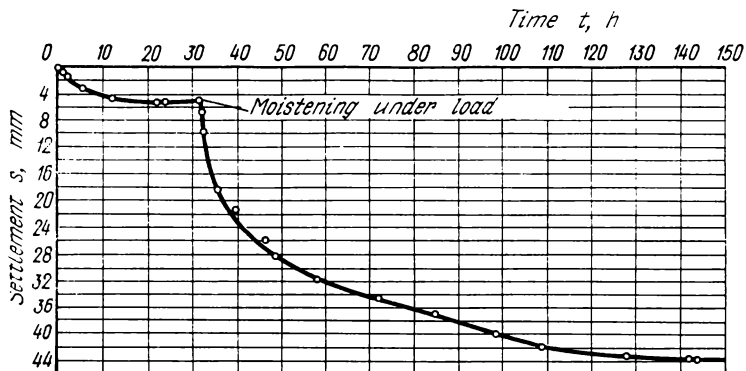


Fig. 37. Settlement of a loess subsidence soil through trial loading with moistening

or by means of a test load. Thus, shown in Fig. 37 are the results of test of a loess soil by a test load with an external pressure  $p = 1.5 \text{ kgf/cm}^2$  and moistening under load; as can be seen from the figure, settlements increase sharply at moistening. It should be noted that for *non-subsidence* clayey soils being tested with a test load under moistening no sharp increase of settlements is observed, though moistening causes a smooth growth of settlement.

The physical and mechanical properties of loess soils, as has been shown earlier, change sharply in the course of subsidence at moistening: their shear resistance reduces strongly (the angle of internal friction by 33-50 per cent, and cohesion, up to ten times); this results in a substantial decrease of the load-bearing capacity of moistened loess soils and expansion of disturbed structureless masses of the soil under load.

A *passive measure* for combatting subsidence of loess soils under structures is laying the base of a footing below the soil layer subject to subsidence (if this is technically feasible), which necessitates the employment of deep pile or column foundations (to a depth of 6 to 20 m).

*Active measures* for combatting subsidence of loess soils are reduced to their chemical cementation by means of silicatization or roasting of the load-bearing volumes of the soil with the use of special equipment, and also to the use of stamped earth piles made from the same loess soil preliminarily moistened by a special technique. Description of these methods may be found in courses on bases and foundations of structures.

**Frozen soils and permafrost.** Structurally unstable subsidence soils also include a large group of *icy frozen soils and permafrost* which at thawing are transformed into a liquefied or soft plastic mass. The physical and mechanical properties of frozen soils and permafrost are very specific and must be carefully considered in tests. Here we shall only discuss the main peculiarities of frozen soils and permafrost. More detailed discussion of the problems of mechanics of frozen soils may be found in the specialist literature\*.

Frozen soils and permafrost (the latter are soils which remain in the frozen state for many years or ages) are found on a large portion of the USSR territory (permafrost occupies 49 per cent of the whole area) and are typical *four-component systems* of particles, since apart from the common three components of soils (solid, liquid and gaseous) they include an ideally plastic component, i.e., *ice* that is formed from porous water at the point of freezing.

But not all porous water in soils freezes at 0°C; the process occurs stepwise, as it were: free water (in coarse-grain soils) freezes at temperatures close to 0°C; layers of combined water freeze at a negative temperature, which is the lower, the greater the water is bonded by mineral particles; finally, a certain amount of combined water in disperse soils always remains *unfrozen* at any negative temperature.

For that reason *frozen* soils will be termed further in the book as *soils having a negative or zero temperature in which at least part of the water has frozen*, i.e., converted into ice, thus cementing soil particles. Various soils can contain different amounts of unfrozen water (Fig. 38) depending on their composition (mainly on unit surface area of mineral particles), each kind of soil having its specific curve of the content of unfrozen water.

As has been shown by corresponding experiments, the *amount of unfrozen water and ice* in frozen soils is not constant, but varies under

---

\* See, for instance: Tsytoich N. A., Sumgin M. I. *Osnovaniya mekhaniki merzlykh gruntov* (Fundamentals of Mechanics of Frozen Soils), Moscow, USSR Academy of Sciences, 1937; Tsytoich N. A. *Printsipy mekhaniki merzlykh gruntov* (Principles of Mechanics of Frozen Soils), Moscow, USSR Academy of Sciences, 1952; Vyalov S. S. *Reologicheskie svoistva i nesushchaya sposobnost' merzlykh gruntov* (Rheological Properties and Load-Carrying Capacity of Frozen Soils), Moscow, USSR Academy of Sciences, 1959; Tsytoich N. A. *Mekhanika merzlykh gruntov (obshchaya i prikladnaya)* [Mechanics of Frozen Soils (General and Applied)], Moscow, Vysshaya Shkola Publishers, 1973, etc.

the action of external factors (negative temperature, external pressure, etc.), so that a *dynamic equilibrium* is always observed.

This is the *principle of equilibrium state of water and ice in frozen soils* (formulated by N. A. Tsytovich) which is the physical basis for investigations of the physical and mechanical properties of frozen soils.

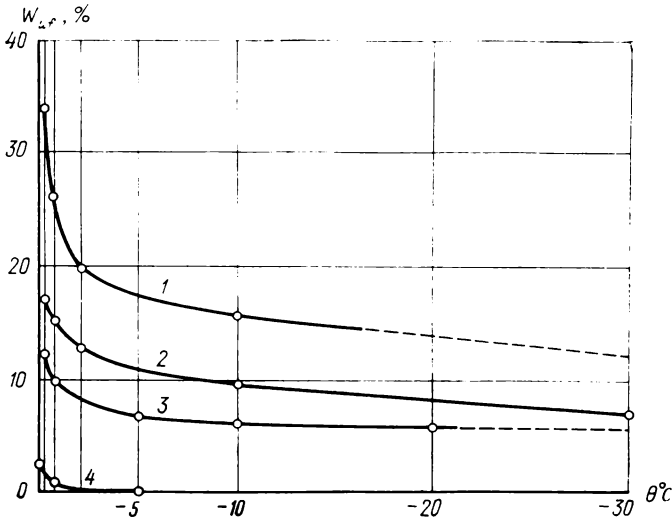


Fig. 38. The content of unfrozen water  $W_{uf}$  in frozen soils depending on subzero temperature ( $-\theta^{\circ}$ )

1—clay; 2—loam; 3—sand loam; 4—sand

The most essential effect on the physical and mechanical properties of frozen soils is produced by cementing action of ice whose total content  $i$  in the soil is determined as the ratio of the weight of the ice to the weight of the total amount of water contained in the soil, i.e.,

$$i = \frac{W - W_{uf}}{W} \quad (2.42)$$

where  $W_{uf}$  = moisture content due to the unfrozen water (in fractions of the dry weight)

$W$  = total moisture content of frozen soil related to the dry weight of soil

Note that for frozen soils it is more expedient to calculate not the weight moisture content  $W$  (related to the dry weight) but what is called the total moisture content  $W_{tot}$  (related to the whole weight of the soil), which makes it possible to exclude incomprehensible

values of moisture content in excess of 100 per cent. For instance, the weight moisture content of frozen soil of  $W = 200$  per cent corresponds to the *total moisture content* of 66 per cent, i.e., 66 per cent of the total weight of the soil is occupied by water of all kinds.

Since the total moisture content  $W_{tot}$  is equal to the ratio of the weight of water to that of all soil, then (for 1 cm<sup>3</sup> of the soil) we have

$$W_{tot} = \frac{W\gamma_d}{\gamma}$$

Substituting the volume weight of the soil skeleton  $\gamma_d$  into this expression by formula (1.3), we get

$$W_{tot} = \frac{W}{1+W} \quad (2.43)$$

Similarly we may find (for 1 cm<sup>3</sup> of frozen soil) that

$$\text{weight of solid particles } g_s = \gamma(1 - W_{tot}) \quad (2.44)$$

$$\text{weight of ice } g_i = \gamma W_{tot} i \quad (2.45)$$

$$\text{weight of water in liquid phase } g_w = \gamma W_{tot} (1 - i) \quad (2.46)$$

For a unit volume of soil the following equation will naturally hold true:

$$g_s + g_i + g_w = \gamma \quad (2.47)$$

Thus, in order to evaluate the physical properties of frozen soils, we have to know four characteristics as follows: unit weight  $\gamma$ ; specific weight  $\gamma_s$ ; total moisture content  $W_{tot}$ ; and the moisture content due to unfrozen water  $W_{uf}$ . Other characteristics can be found from the formulae given in Table 2.2.

Important characteristics of the *mechanical properties* of frozen soils and permafrost are the long-term (stable) cohesion  $c_{st}$ , which makes it possible to estimate the load-bearing capacity of a frozen soil at the given negative temperature, and the coefficient of thawing  $A_0$ , which makes it possible to calculate the expected "thawing settlement" that usually constitutes an appreciable portion (sometimes more than 90 per cent) of the total settlement of thawing bases.

The magnitude of  $c_{st}$  is determined by the method of spherical stamp (see Sec. 2.3) by formula (2.34)

$$c_{st} = 0.18 \frac{P}{\pi D s_{st}}$$

where  $s_{st}$  is the long-term (stable) settlement of the frozen soil under a spherical stamp of a diameter  $D$  under load  $P$ .

As has been shown by the studies carried out at the Institute of Permafrost Research of the Siberian Division of the USSR Academy of Sciences (1966), the long-term (stable) settlement of frozen soils in tests with a spherical stamp is approximately twice the settlement of the stamp during 30 minutes of observation, i.e.,

$$s_{st} \approx 2s_{30'} \quad (2.48)$$

Table 2.2

**Relationships Between Characteristics of Main Physical  
Properties of Frozen Soils**

Experimentally found characteristics	Characteristics to be calculated by formulac
$\gamma_s$ = specific weight	Total moisture content $W_{tot} = \frac{W}{1+W}$
$\gamma$ = unit weight	Weight ice content $i = \frac{W - W_{uf}}{W}$
	Volume ice content $i_v = \frac{\gamma}{\gamma_i} \cdot \frac{W - W_{uf}}{1+W}$
$W$ = total moisture content related to the dry weight	( $\gamma_i$ = unit weight of ice) Unit weight of soil skeleton $\gamma_d = \gamma(1 - W_{tot})$
$W_{uf}$ = moisture content due to unfrozen water in fractions of the weight of dry soil	Void ratio of frozen soil $e = \frac{\gamma_s - \gamma_d}{\gamma_d}$
	Weight of components of frozen soil (in 1 cm <sup>3</sup> ); ice $g_i = \gamma W_{tot} i$ unfrozen water $g_w = \gamma W_{tot} (1 - i)$ solid particles $g_{sk} = \gamma (1 - W_{tot})$ Volume of gases $V_0 = \left( \frac{e}{\gamma} - \frac{W}{\gamma_w} \right) \gamma_d$

When  $c_{st}$  is known, it is easy to determine the safe load on a permafrost soil at retaining its negative temperature, considering the frozen soil an ideally bonded body (see Sec. 4.3).

The coefficient of thawing  $A_0$  can be found by testing the settlement of a soil under thawing (in a pit of an area of 1 or 2 m<sup>2</sup>) under the action of only the dead weight of the soil (i.e., without load).

If the layer under thawing is of an insignificant thickness (less than 0.5 m), the maximum pressure from the dead weight of soil is also low (as a rule, less than 0.1 kgf/cm<sup>2</sup>), so that the second term in formula (2.41) can be neglected. In that case we shall have

$$A_0 \approx \frac{s_{th}}{h} \quad (2.49)$$

where  $s_{th}$  = settlement of the layer of soil under thawing  
 $h$  = depth of thawing

## Chapter Three

### DETERMINATION OF STRESSES IN SOIL

The problem of determining the stresses in soils is of particular importance for establishing the conditions of their strength and stability and determining their deformations (mainly settlements) under the action of external forces and the own weight of the soil.

The problem of distribution of stresses in soil is now solved in soil mechanics by using the theory of linearly deformable bodies. For determination of stresses by this theory, the equations and relationships of the theory of elasticity are fully applicable, since they are also based on a linear relationship between stresses and deformations in the elastic region (Hooke's law). *Hooke's law is inapplicable*, however, to soils in the general case, since external forces and pressures exceeding their structural strength cause not only elastic deformations, but also residual deformations which may largely exceed the elastic ones.

As has been shown earlier, however, the linear relationship between stresses and total deformations (and not only elastic ones) can be assumed to be valid for soils within definite limits. In order to determine total deformations (elastic and residual: compression, plastic flow, creep, etc.), the equations of the theory of plasticity are insufficient.

We then have to introduce additional conditions which follow from the physical nature of soils as disperse bodies, namely, their compressibility, creep of the soil skeleton, etc.

It should also be noted that the equations of the theory of linearly deformable bodies are valid for a mass of soil having no regions of ultimate stressed state, in which the relationship between deformations and stresses is nonlinear.

With highly developed regions of ultimate equilibrium, for instance, under structures carrying a substantial load which is close to the ultimate one, the solutions of the theory of linearly deformable bodies will be inapplicable.

An additional condition for direct application of the formulae of the theory of linearly deformable bodies for determining stresses in soils is, as has been shown earlier, the absence of time redistribution of soil phases in the volume considered, i.e., the solutions of the theory of linearly deformable bodies should comply with the

initial (undisturbed) and the final (stabilized) static state of the soil and define the *total stresses* in the soil skeleton caused by the action of external forces.

### 3.1. STRESS DISTRIBUTION IN THE CASE OF A THREE-DIMENSIONAL PROBLEM

**Effect of a concentrated force (the basic problem).** Let us analyse the action of a concentrated force  $P$  applied perpendicular to the plane limiting a *half-space* (Fig. 39). The half-space is assumed to be of a uniform structure (both along its depth and laterally) and linearly deformable.

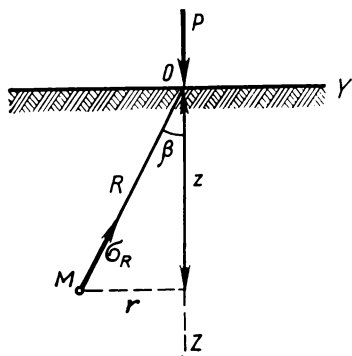


Fig. 39. Action of a concentrated force

The problem is to determine all component stresses  $\sigma_z$ ,  $\sigma_y$ ,  $\sigma_x$ ,  $\tau_{zy}$ ,  $\tau_{zx}$ ,  $\tau_{xy}$  and displacements  $w_z$ ,  $w_y$ ,  $w_x$  for any point of the half-space having the coordinates  $z$ ,  $y$ ,  $x$  or  $R$  and  $\beta$ .

For an elastic half-space (and, therefore, for any linearly deformable half-space) this problem was first solved completely by Prof. J. Boussinesq in 1885 and the determination of stresses for the planes parallel to the plane limiting the half-space was made by Prof. V. Kirpichev and the Author of this book (1923-1934). Here

we shall limit ourselves to the derivation of the formulae of stresses for planes parallel to the limiting plane, i.e., of stresses  $\sigma_z$ ,  $\tau_{zy}$ , and  $\tau_{zx}$ , since they are most often used in calculations.

We take a point  $M$  (Fig. 39) given by the polar coordinates  $R$  and  $\beta$ , and determine the normal stress  $\sigma_R$  acting along the radius  $R$ , and then, using transformation formulae, we find all component stresses for a plane drawn through the point  $M$  parallel to the limiting plane.

In order to simplify the derivation (in which the final result coincides with Boussinesq's solution), we assume without proof that the stress  $\sigma_R$  is proportional to  $\cos \beta$  and inversely proportional to the square of the distance to the point of application of a concentrated force,  $R^2$ .

Note that, as has been shown by Proctor and Moran, this principle can be strictly deduced from the Newton's law of gravitation.

Thus, we assume that

$$\sigma_R = A \frac{\cos \beta}{R^2} \quad (1)$$

where  $A$  is a factor to be determined from the equilibrium condition.

In order to write the equilibrium conditions, we draw a hemispherical section with the centre in the point of application of the concentrated force (Fig. 40). The stresses normal to the hemispherical surface are determined by formula (1) and can vary from zero at the limiting plane to the maximum at the  $Z$  axis; for an elementary

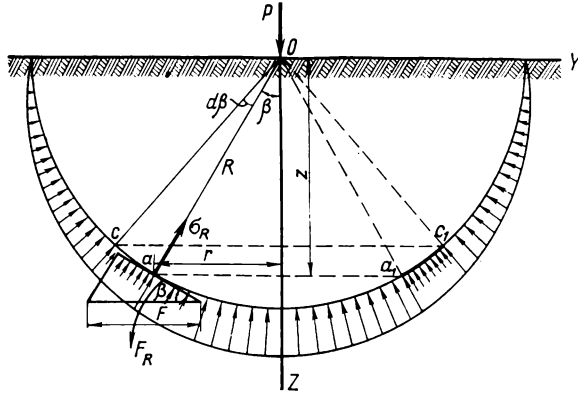


Fig. 40. Radial stresses under the action of a concentrated force

spherical belt with a central angle  $d\beta$  separated from the hemisphere, these stresses can be assumed to be constant.

The condition of equilibrium is that the sum of projections of all the forces onto the vertical axis is zero

$$P - \int_0^{\pi/2} \sigma_R \cos \beta dF = 0 \quad (m)$$

where  $dF$  is the surface area of the elementary spherical belt, which is equal to

$$dF = 2\pi (R \sin \beta) (R d\beta) \quad (n)$$

Substituting the expressions for  $dF$  and  $\sigma_R$  into equation (m), we get

$$P - A2\pi \int_0^{\pi/2} \cos^2 \beta \sin \beta d\beta = 0 \quad (o)$$

Integration and substitution of limits give

$$P - \frac{2}{3} A\pi = 0 \quad (p)$$

whence the sought-for proportionality factor  $A$  is

$$A = \frac{3}{2} \cdot \frac{P}{\pi} \quad (q)$$

Substituting  $A$  into formula (1), we have for the radial stresses

$$\sigma_R = \frac{3}{2} \cdot \frac{P}{\pi R^2} \cos \beta \quad (r)$$

Let the radial stresses be related not to the plane perpendicular to the radius, but to a plane parallel to the limiting plane and making an angle  $\beta$  with the former plane. Let this stress be denoted as  $\sigma'_R$ .

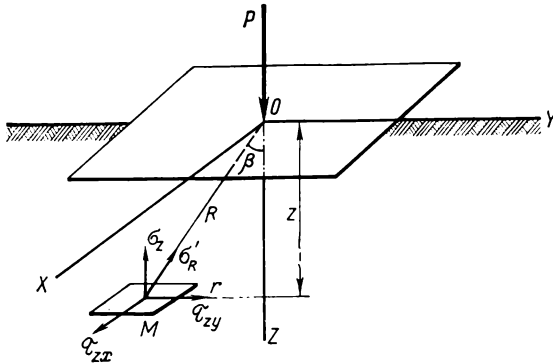


Fig. 41. Component stresses for a plane parallel to a boundary plane

It follows from the geometrical relationships that

$$\sigma'_R = \sigma_R \cos \beta \quad (s)$$

or, upon substituting  $\sigma_R$  from formula (r) and noting that  $\cos \beta = z/R$

$$\sigma'_R = \frac{3}{2} \cdot \frac{P}{\pi} \cdot \frac{z^2}{R^4} \quad (t)$$

Then, without changing the direction of the plane, we resolve the force  $\sigma'_R F$  (Fig. 41) into three directions:  $Z$ , which is perpendicular to the plane, and  $X$  and  $Y$ , lying in the plane. Then we have

$$\left. \begin{aligned} \sigma_z &= \sigma'_R \cos(\sigma'_R, Z) \\ \tau_{zy} &= \sigma'_R \cos(\sigma'_R, Y) \\ \tau_{zx} &= \sigma'_R \cos(\sigma'_R, X) \end{aligned} \right\} \quad (u)$$

Since  $\cos(\sigma'_R, Z) = z/R$ ;  $\cos(\sigma'_R, Y) = y/R$ , and  $\cos(\sigma'_R, X) = x/R$ , the stress components for the plane parallel to the limiting

plane will have the final forms

$$\left. \begin{aligned} \sigma_z &= \frac{3}{2} \cdot \frac{P}{\pi} \cdot \frac{z^3}{R^5} \\ \tau_{zy} &= \frac{3}{2} \cdot \frac{P}{\pi} \cdot \frac{yz^2}{R^5} \\ \tau_{zx} &= \frac{3}{2} \cdot \frac{P}{\pi} \cdot \frac{xz^2}{R^5} \end{aligned} \right\} \quad (3.1)$$

Note that the magnitudes of both compressive stresses  $\sigma_z$  and shear stresses  $\tau_{zy}$  and  $\tau_{zx}$  for the planes parallel to the boundary plane of the half-space are independent of elastic constants of the half-space, whereas for other planes parallel to the limiting planes  $XOZ$  and  $YOZ$  they depend on the deformability moduli  $E_o$  and  $\mu_o$  and are determined by more complicated expressions (see [14], for example).

The expressions for calculating the sum of normal stresses  $\Theta$  in any point and the displacements  $w_z$  of a limiting surface parallel to the  $Z$  axis can be written as follows:

$$\Theta = \sigma_z + \sigma_y + \sigma_x = \sigma_1 + \sigma_2 + \sigma_3 = \frac{P}{\pi} (1 + \mu_o) \frac{z}{R^3} \quad (3.2)$$

$$\boxed{w_z = \frac{P}{\pi CR}} \quad (3.3)$$

where  $C = \frac{E_o}{1 - \mu_o^2}$  is termed the *coefficient of a linearly deformable half-space* ( $E_o$  being the modulus of total deformation and  $\mu_o$ , the coefficient of relative lateral deformation, which is similar to the Poisson's ratio).

Formulae (3.2) and (3.3) are of large practical importance for calculations of settlements of foundations.

The expression for the compressive stresses  $\sigma_z$  can be given a simpler form which makes it possible to compile a supplementary table for calculation of stresses.

As seen from Fig. 41, point  $M$  can be completely determined by two coordinates:  $z$  and  $r$ . Noting that

$$R = \sqrt{z^2 + r^2} = z \left[ 1 + \left( \frac{r}{z} \right)^2 \right]^{1/2}$$

we have from the first line of formula (3.1)

$$\sigma_z = \frac{3}{2\pi \left[ 1 + \left( \frac{r}{z} \right)^2 \right]^{5/2}} \cdot \frac{P}{z^2}$$

Table 3.1

**Coefficient  $K$  to Calculate Compressive Stresses from  
a Concentrated Force Depending on  $r/z$  Ratio**

$r/z$	$K$	$r/z$	$K$	$r/z$	$K$	$r/z$	$K$
0.00	0.4775	0.50	0.2733	1.00	0.0844	1.50	0.0251
0.01	0.4773	0.51	0.2679	1.01	0.0823	1.51	0.0245
0.02	0.4770	0.52	0.2625	1.02	0.0803	1.52	0.0240
0.03	0.4764	0.53	0.2571	1.03	0.0783	1.53	0.0234
0.04	0.4756	0.54	0.2518	1.04	0.0764	1.54	0.0229
0.05	0.4745	0.55	0.2466	1.05	0.0744	1.55	0.0224
0.06	0.4732	0.56	0.2414	1.06	0.0727	1.56	0.0219
0.07	0.4717	0.57	0.2363	1.07	0.0709	1.57	0.0214
0.08	0.4699	0.58	0.2313	1.08	0.0691	1.58	0.0209
0.09	0.4679	0.59	0.2263	1.09	0.0674	1.59	0.0204
0.10	0.4657	0.60	0.2214	1.10	0.0658	1.60	0.0200
0.11	0.4633	0.61	0.2165	1.11	0.0641	1.61	0.0195
0.12	0.4607	0.62	0.2117	1.12	0.0626	1.62	0.0191
0.13	0.4579	0.63	0.2070	1.13	0.0610	1.63	0.0187
0.14	0.4548	0.64	0.2024	1.14	0.0595	1.64	0.0183
0.15	0.4516	0.65	0.1978	1.15	0.0581	1.65	0.0179
0.16	0.4482	0.66	0.1934	1.16	0.0567	1.66	0.0175
0.17	0.4446	0.67	0.1889	1.17	0.0553	1.67	0.0171
0.18	0.4409	0.68	0.1846	1.18	0.0539	1.68	0.0167
0.19	0.4370	0.69	0.1804	1.19	0.0526	1.69	0.0163
0.20	0.4329	0.70	0.1762	1.20	0.0513	1.70	0.0160
0.21	0.4286	0.71	0.1721	1.21	0.0501	1.72	0.0153
0.22	0.4242	0.72	0.1681	1.22	0.0489	1.74	0.0147
0.23	0.4197	0.73	0.1641	1.23	0.0477	1.76	0.0141
0.24	0.4151	0.74	0.1603	1.24	0.0466	1.78	0.0135
0.25	0.4103	0.75	0.1565	1.25	0.0454	1.80	0.0129
0.26	0.4054	0.76	0.1527	1.26	0.0443	1.82	0.0124
0.27	0.4004	0.77	0.1491	1.27	0.0433	1.84	0.0119
0.28	0.3954	0.78	0.1455	1.28	0.0422	1.86	0.0114
0.29	0.3902	0.79	0.1420	1.29	0.0412	1.88	0.0109
0.30	0.3849	0.80	0.1386	1.30	0.0402	1.90	0.0105
0.31	0.3796	0.81	0.1353	1.31	0.0393	1.92	0.0101
0.32	0.3742	0.82	0.1320	1.32	0.0384	1.94	0.0097
0.33	0.3687	0.83	0.1288	1.33	0.0374	1.96	0.0093
0.34	0.3632	0.84	0.1257	1.34	0.0365	1.98	0.0089
0.35	0.3577	0.85	0.1226	1.35	0.0357	2.00	0.0085
0.36	0.3521	0.86	0.1196	1.36	0.0348	2.10	0.0070
0.37	0.3465	0.87	0.1166	1.37	0.0340	2.20	0.0058
0.38	0.3408	0.88	0.1138	1.38	0.0332	2.30	0.0048
0.39	0.3351	0.89	0.1110	1.39	0.0324	2.40	0.0040
0.40	0.3294	0.90	0.1083	1.40	0.0317	2.50	0.0034
0.41	0.3238	0.91	0.1057	1.41	0.0309	2.60	0.0029
0.42	0.3181	0.92	0.1031	1.42	0.0302	2.70	0.0024
0.43	0.3124	0.93	0.1005	1.43	0.0295	2.80	0.0021
0.44	0.3068	0.94	0.0981	1.44	0.0288	2.90	0.0017
0.45	0.3011	0.95	0.0956	1.45	0.0282	3.00	0.0015
0.46	0.2955	0.96	0.0933	1.46	0.0275	3.50	0.0007
0.47	0.2899	0.97	0.0910	1.47	0.0269	4.00	0.0004
0.48	0.2843	0.98	0.0887	1.48	0.0263	4.50	0.0002
0.49	0.2788	0.99	0.0865	1.49	0.0257	5.00	0.0001

or, denoting that

$$\frac{3}{2\pi} \cdot \frac{1}{\left[1 + \left(\frac{r}{z}\right)^2\right]^{5/2}} = K$$

we have

$$\sigma_z = K \cdot \frac{P}{z^2} \quad (3.4)$$

Formula (3.4) has found a wide application for practical calculations of foundation settlements. For easier calculations, Table 3.1 gives the values of the coefficient  $K$  in the formula for vertical compressive stresses in soil, which are normal to the planes parallel to the boundary plane of the half-space. The magnitude of the coefficient  $K$  is determined for a number of values of  $r/z$  (where  $r$  is the distance along the horizontal from the  $z$  axis passing through the point of application of the concentrated force, and  $z$  is the depth of the point considered below the boundary plane).

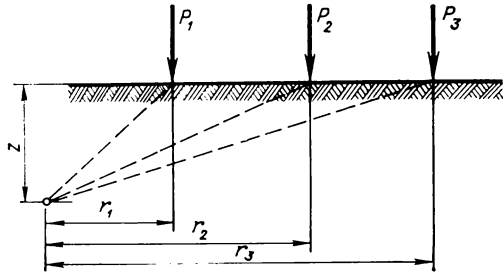


Fig. 42. Action of a number of concentrated forces

If a number of concentrated forces  $P_1, P_2, P_3, \dots$  (Fig. 42) is applied to the surface of soil, then the compressive stress in any point of soil for the horizontal planes parallel to the boundary plane can be found by simple summation, since the derivation of formula (3.4) is based on a direct proportionality between stresses and deformations

$$\sigma_z = K_1 \frac{P_1}{z^2} + K_2 \frac{P_2}{z^2} + K_3 \frac{P_3}{z^2} \quad (3.4')$$

where the coefficients  $K_i$  are found from Table 3.1 for the corresponding ratios  $r_i/z$ .

**Example 3.1.** A concentrated force  $P = 60$  t is applied to the surface of soil. Find the vertical compressive stress in point  $a$  located at a depth of 2 m below the surface and at a distance of 1 m sideways from the line of action of the force (Fig. 43).

For point  $a$  we have:  $z = 200$  cm;  $r = 100$  cm;  $r/z = 0.5$ . From Table 3.1, for  $r/z = 0.5$ ,  $K = 0.2733$ .

By formula (3.4)

$$\sigma_z = K \frac{P}{z^2} = 0.2733 \frac{60,000}{200^2} = 0.41 \text{ kgf/cm}^2$$

Similarly, we have found the compressive stresses for a number of planes located at the same depth  $z = 2$  m and at other depths along the  $Z$  axis. The results of calculation have been used to construct the diagrams of compressive stresses for a section at a depth  $z = 2$  m and for horizontal planes along the vertical axis  $Z$  ( $r_i = 0$ ). Note that the pressures found for the point of application of the concentrated force are naturally infinitely great. In practice, there

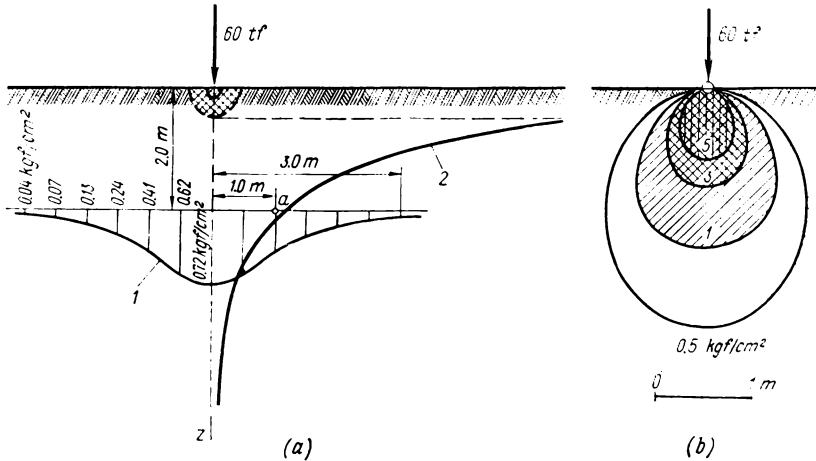


Fig. 43. To the example for determination of compressive stresses in soil under the action of a concentrated force  
(a) at depth  $z = 2$  m (1), and along the vertical axis  $Z$  (2); (b) isobars

will be no such pressures, since a high load cannot be concentrated at one point, whereas with a small area of load transfer the stresses in the place of application of the load will exceed the ultimate strength of soil; for that reason, a definite region (hatched in Fig. 43a) at the point of application of a concentrated load should be excluded from consideration.

For the stresses  $\sigma_z$  found for a number of points (areas), we have plotted the lines of equal compressive stresses, *isobars* (Fig. 43b), which visualize the "bulb" of pressures.

**Concentrated force  $Q$  applied to the surface parallel to the boundary plane of the half-space.** In this case the vertical compressive stress  $\sigma_z$  can be found from the expression

$$\sigma'_z = \frac{3}{2} \cdot \frac{Q}{\pi} \cdot \frac{yz^2}{R^5} \tag{3.1'}$$

where  $y$  = a coordinate parallel to the force  $Q$   
 $R$  = the distance to any point ( $R^2 = x^2 + y^2 + z^2$ )  
 and the sum of main stresses  $\Theta$  is determined by expression (3.2) with the coordinate  $z$  being replaced by  $y$

$$\Theta = \frac{Q}{\pi} (1 + \mu_0) \frac{y}{R^3} \tag{3.2'}$$

The expressions for the forces (the vertical force  $P$  and horizontal force  $Q$ ) being known, it is easy to find the compressive stresses and the sum of principal stresses for any obliquely acting force.

**Effect of a uniformly distributed load.** The closed exact solution of this problem has been found only for a rectangular loading surface whose deformations correspond to those of the surface of a linearly deformable half-space, i.e., to the conditions of a very elastic load transfer.

The results of the simplest solution (A. Love, 1935) will be discussed below.

The compressive stress  $\sigma_{zc}$  and the sum of main stresses  $\Theta_c$  for any point lying on the vertical below the corner of a loaded rectangle with the sides  $l$  and  $b$  (which will be termed *corner sides*) will be as follows:

$$\sigma_{zc} = \frac{p}{2\pi} \left[ \frac{lbz}{D} \cdot \frac{l^2 + b^2 + 2z^2}{D^2 z^2 + l^2 b^2} + \arcsin \left( \frac{lb}{\sqrt{l^2 + z^2} \sqrt{b^2 + z^2}} \right) \right] \quad (3.5)$$

$$\Theta_c = \frac{p}{\pi} (1 + \mu_0) \arctan \frac{\alpha}{\beta \sqrt{1 + \alpha^2 + \beta^2}} \quad (3.6)$$

where

$$\alpha = \frac{l}{b} \quad \text{and} \quad \beta = \frac{z}{b}$$

$$\left( \frac{D}{2} \right)^2 = R^2 = l^2 + b^2 + z^2$$

Using these formulae, it is easy to calculate the maximum compressive stress under the centre of the loading area,  $\sigma_z$ , and the maximum value of the sum of main stresses  $\Theta_{\max}$ .

**Determination of compressive stresses by the method of corner points.** The knowledge of the compressive stresses for the corner points under a rectangular area of loading makes it possible to calculate very quickly the compressive stresses for any point of the half-space, especially if we use the corner coefficients  $K_c$  (Table 3.2 or 3.4).

For surfaces under the centre of a loaded rectangle, the compressive stress  $\sigma_{z0}$  is

$$\sigma_{z0} = K_0 p \quad (3.7)$$

and for surfaces under the corner of a loaded rectangle

$$\sigma_{zc} = K_c p \quad (3.8)$$

where  $K_0$  and  $K_c$  = tabulated coefficients

$p$  = intensity of uniformly distributed load

The coefficients  $K_0$  and  $K_c$  are found from Table 3.2 as a function of the relative depth  $\beta = 2z/b$  or  $\beta = z/b$  (according to BC&R,  $m$ )

Table 3.2

Coefficients  $f$  and  $f'$  in Formulae (3.9) and (3.10)

$\beta$	Rectangular foundations with $\alpha = l/b$											Strip foundations with $\alpha \geq 10$	
	1	1.2	1.4	1.6	1.8	2	2.4	2.8	3.2	4	5		
0.0	1.000	1.000	1.000	1.000	1.000	1.000	1.000	1.000	1.000	1.000	1.000	1.000	1.000
0.4	0.949	0.968	0.972	0.974	0.975	0.976	0.976	0.977	0.977	0.977	0.977	0.977	0.977
0.8	0.756	0.800	0.848	0.859	0.866	0.870	0.875	0.878	0.879	0.880	0.880	0.881	0.881
1.2	0.547	0.652	0.682	0.703	0.717	0.727	0.740	0.746	0.749	0.753	0.754	0.755	0.755
1.6	0.390	0.449	0.496	0.558	0.578	0.593	0.612	0.623	0.630	0.639	0.639	0.642	0.642
2.0	0.285	0.336	0.379	0.441	0.463	0.481	0.505	0.520	0.529	0.540	0.545	0.550	0.550
2.4	0.214	0.257	0.294	0.352	0.374	0.392	0.419	0.437	0.449	0.462	0.470	0.477	0.477
2.8	0.165	0.201	0.232	0.284	0.304	0.321	0.350	0.369	0.383	0.400	0.410	0.420	0.420
3.2	0.130	0.160	0.187	0.232	0.251	0.267	0.294	0.314	0.329	0.348	0.360	0.374	0.374
3.6	0.106	0.130	0.153	0.192	0.209	0.224	0.250	0.270	0.285	0.305	0.320	0.337	0.337
4.0	0.087	0.108	0.127	0.161	0.176	0.190	0.214	0.233	0.248	0.270	0.285	0.306	0.306
4.4	0.073	0.091	0.107	0.137	0.150	0.163	0.185	0.203	0.218	0.239	0.256	0.280	0.280
4.8	0.062	0.077	0.092	0.118	0.130	0.141	0.161	0.178	0.192	0.213	0.230	0.258	0.258
5.2	0.053	0.066	0.079	0.102	0.112	0.123	0.141	0.157	0.170	0.191	0.208	0.239	0.239
5.6	0.046	0.058	0.069	0.089	0.099	0.108	0.124	0.139	0.152	0.172	0.189	0.223	0.223
6.0	0.040	0.051	0.060	0.078	0.087	0.095	0.110	0.124	0.136	0.155	0.172	0.208	0.208
6.4	0.036	0.045	0.053	0.070	0.077	0.085	0.098	0.111	0.122	0.141	0.158	0.196	0.196
6.8	0.032	0.040	0.048	0.062	0.069	0.076	0.088	0.100	0.110	0.128	0.144	0.184	0.184
7.2	0.028	0.036	0.042	0.056	0.062	0.068	0.080	0.090	0.100	0.117	0.133	0.175	0.175
7.6	0.024	0.032	0.038	0.044	0.050	0.056	0.062	0.072	0.081	0.107	0.123	0.166	0.166
8.0	0.022	0.029	0.035	0.040	0.046	0.051	0.066	0.075	0.084	0.108	0.113	0.158	0.158
8.4	0.021	0.026	0.032	0.037	0.046	0.051	0.060	0.069	0.077	0.091	0.105	0.150	0.150
8.8	0.019	0.024	0.029	0.034	0.042	0.047	0.055	0.063	0.070	0.084	0.098	0.144	0.144
9.2	0.018	0.022	0.026	0.031	0.039	0.043	0.051	0.058	0.065	0.078	0.091	0.137	0.137
9.6	0.016	0.020	0.024	0.028	0.036	0.040	0.047	0.054	0.060	0.072	0.085	0.132	0.132
10	0.015	0.019	0.022	0.026	0.033	0.037	0.044	0.050	0.056	0.067	0.079	0.126	0.126
11	0.011	0.017	0.020	0.023	0.029	0.033	0.040	0.044	0.050	0.060	0.071	0.114	0.114
12	0.009	0.015	0.018	0.024	0.026	0.028	0.034	0.038	0.044	0.051	0.060	0.104	0.104

Note: For intermediate values of  $\alpha$  and  $\beta$ , the coefficients are found by interpolation.

and the side ratio of the rectangular area of loading ( $\alpha = l/b$ ) (according to BC&R,  $n$ )

$$K_0 = f\left(\frac{2z}{b}, \frac{l}{b}\right) \quad (3.9)$$

$$K_c = \frac{1}{4} f'\left(\frac{z}{b}, \frac{l}{b}\right) \quad (3.10)$$

These expressions make it possible to use the same table for calculating both the coefficients for central points,  $K_0$ , and those for corner ones,  $K_c$ .

The corner coefficients  $K_{\theta c} = f''(z/b, l/b) \cdot (1 + \mu_0)$  for the sum of main stresses are given in Table 3.3.

The maximum compressive stress  $\max \sigma_z$  will be observed in points located under the centre of the loaded surface and can be calculated by formula (3.7).

The method of corner points is used for determination of compressive stresses when the surface of loading can be divided into such

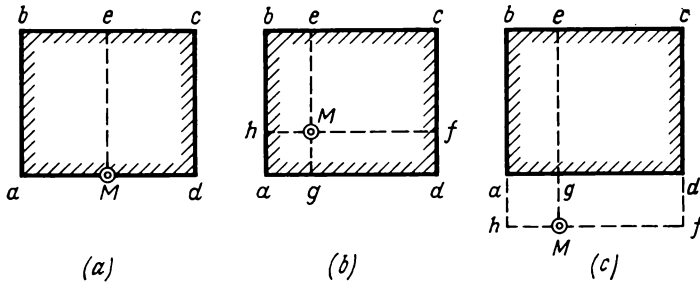


Fig. 44. Division of a rectangular loading area for determining stresses by the method of corner points

rectangles that the point considered is a *corner* point. The compressive stress in that point (for horizontal surfaces parallel to the plane boundary of the half-space) will then be equal to the algebraic sum of the stresses from the rectangular areas of loading for which this point is a corner point.

Let us explain this by discussing three main cases:

(1) point  $M$  is on the contour of the rectangle of external pressures (Fig. 44a);

(2) point  $M$  is inside the pressure rectangle (Fig. 44b);

(3) point  $M$  is outside the pressure rectangle (Fig. 44c).

In the first case the magnitude of  $\sigma_z$  is found as the sum of two corner stresses corresponding to the loading rectangles  $Mbe$  and  $Mecd$ , i.e.,

$$\sigma_z = (K_{1c} + K_{2c}) p$$

Table 3.3

Values of  $\Theta_c/(1 + \mu_0)$  in Points at Depths Located at Corner Verticals with a Load  $p$  Distributed Uniformly over a Rectangular Area (Fractions of  $p$ )

$\frac{z}{b}$	$\alpha = l/b$														
	0.2	0.4	0.6	0.8	1.0	1.2	1.4	1.6	1.8	2.0	3.0	4.0	6.0	8.0	10.0
0.0	0.5000	0.5000	0.5000	0.5000	0.5000	0.5000	0.5000	0.5000	0.5000	0.5000	0.5000	0.5000	0.5000	0.5000	0.5000
0.2	0.2439	0.3405	0.3804	0.4003	0.4114	0.4183	0.4230	0.4259	0.4281	0.4297	0.4337	0.4352	0.4363	0.4367	0.4369
0.4	0.1363	0.2280	0.2810	0.3119	0.3308	0.3430	0.3515	0.3570	0.3612	0.3643	0.3721	0.3750	0.3771	0.3779	0.3782
0.6	0.0874	0.1578	0.2074	0.2406	0.2630	0.2782	0.2890	0.2967	0.3024	0.3068	0.3179	0.3222	0.3245	0.3265	0.3270
0.8	0.0607	0.1136	0.1552	0.1812	0.2087	0.2251	0.2371	0.2458	0.2529	0.2582	0.2721	0.2776	0.2818	0.2833	0.2840
1.0	0.0443	0.0846	0.1185	0.1456	0.1667	0.1828	0.1952	0.2047	0.2121	0.2180	0.2341	0.2406	0.2457	0.2476	0.2486
1.2	0.0336	0.0649	0.0924	0.1156	0.1344	0.1495	0.1616	0.1711	0.1788	0.1850	0.2026	0.2101	0.2162	0.2182	0.2193
1.4	0.0262	0.0510	0.0735	0.0931	0.1097	0.1235	0.1348	0.1441	0.1518	0.1580	0.1766	0.1848	0.1915	0.1940	0.1952
1.6	0.0209	0.0410	0.0596	0.0762	0.0906	0.1030	0.1135	0.1223	0.1296	0.1358	0.1549	0.1638	0.1711	0.1739	0.1753
1.8	0.0171	0.0336	0.0491	0.0632	0.0758	0.0868	0.0964	0.1046	0.1116	0.1177	0.1368	0.1460	0.1540	0.1571	0.1588
2.0	0.0142	0.0280	0.0410	0.0531	0.0641	0.0739	0.0826	0.0900	0.0967	0.1024	0.1214	0.1310	0.1395	0.1428	0.1445
2.5	0.0094	0.0187	0.0276	0.0361	0.0440	0.0514	0.0581	0.0642	0.0696	0.0745	0.0921	0.1020	0.1114	0.1153	0.1173
3.0	0.0067	0.0133	0.0198	0.0260	0.0319	0.0375	0.0427	0.0475	0.0520	0.0561	0.0718	0.0814	0.0913	0.0957	0.0980
5.0	0.0025	0.0050	0.0074	0.0099	0.0122	0.0146	0.0168	0.0190	0.0212	0.0232	0.0322	0.0391	0.0481	0.0532	0.0561
7.0	0.0013	0.0026	0.0038	0.0051	0.0064	0.0076	0.0088	0.0100	0.0111	0.0124	0.0177	0.0224	0.0293	0.0339	0.0370
10.0	0.0006	0.0013	0.0019	0.0025	0.0032	0.0038	0.0044	0.0047	0.0056	0.0067	0.0091	0.0118	0.0163	0.0198	0.0224

Note:  $b$  is the width of the loaded rectangle in the plane of drawing and  $l$  is the length in the direction perpendicular to that plane.

where  $K_{1c}$  and  $K_{2c}$  = corner coefficients determined from formula (3.10) and Table 3.2 depending on the relative depth  $\beta = z/b$  and the side ratio  $\alpha = l/b$

$p$  = intensity of the external uniformly distributed load

In the second case it is necessary to sum up corner stresses from four rectangular loading areas:  $Mgah$ ,  $Mhbe$ ,  $Mecf$ , and  $Mfdg$ , i.e.,

$$\sigma_z = (K_{1c} + K_{2c} + K_{3c} + K_{4c}) p$$

In the third case the stress in point  $M$  is the sum of the stresses from the action of the load over the rectangles  $Mhbe$  and  $Mecf$ , taken with the "plus" sign, and the stresses from the action of the load over the rectangles  $Mhag$  and  $Mgdf$ , taken with the "minus" sign, i.e.,

$$\sigma_z = (K_{1c} + K_{2c} - K_{3c} - K_{4c}) p$$

where  $K_{1c}$ ,  $K_{2c}$ ,  $K_{3c}$ , and  $K_{4c}$  are corner coefficients to be determined by formula (3.10) and from Table 3.2 for the corresponding values of  $\alpha = l/b$  and  $\beta = z/b$ .

In order to facilitate calculations, Table 3.4 gives calculated values of the coefficients  $K'_c = f''(z/b, l/b)$ , which make it possible to exclude formula (3.10) and use only formula (3.8), i.e.,

$$\sigma_{zc} = K'_c p \quad (3.8')$$

**Example 3.2.** Find the magnitude of compressive stresses under the centre and under the middle of the longer side of a loaded rectangle,  $2 \times 8$  m, at a depth of 2 m from the surface with an external load of an intensity  $p = 3$  kgf/cm<sup>2</sup>.

For the area under the centre of the loaded area we have

$$z = 2 \text{ m}; \quad \beta = \frac{2z}{b} = \frac{2 \times 2}{2} = 2; \quad \alpha = \frac{l}{b} = \frac{8}{2} = 4$$

From Table 3.2,  $K_0 = 0.54$ ; then

$$\sigma_{z0} = K_0 p = 0.54 \times 3 = 1.62 \text{ kgf/cm}^2$$

For the area under the middle of the longer side of the rectangle, after dividing it into two rectangles,  $4 \times 2$  m, so that the point considered is a corner point,  $z = 2$  m;  $\beta = z/b = 1$ ; we have

$$\alpha = \frac{l}{b} = \frac{4}{2} = 2$$

Interpolating from Table 3.2 and using formula (3.10), we get

$$K_c = \frac{1}{4} \times \frac{0.870 + 0.727}{2} = 0.2 \text{ approximately}$$

$$\sigma_z = 2K_c p = 2 \times 0.2 \times 3 = 1.20 \text{ kgf/cm}^2$$

**Effect of loading area.** Stress calculations in soils have shown that the greater the area of load transfer, the slower the attenuation,



Table 3.4 (continued)

$\beta = \frac{z}{b}$	Values of $\alpha = l/b$										
	3.2	3.4	3.6	3.8	4	5	6	7	8	9	10
0.0	0.2500	0.2500	0.2500	0.2500	0.2500	0.2500	0.2500	0.2500	0.2500	0.2500	0.2500
0.2	0.2492	0.2492	0.2492	0.2492	0.2492	0.2492	0.2492	0.2492	0.2492	0.2492	0.2492
0.4	0.2443	0.2443	0.2443	0.2443	0.2443	0.2443	0.2443	0.2443	0.2443	0.2443	0.2443
0.6	0.2340	0.2340	0.2341	0.2341	0.2341	0.2342	0.2342	0.2342	0.2342	0.2342	0.2342
0.8	0.2198	0.2199	0.2199	0.2200	0.2200	0.2202	0.2202	0.2202	0.2202	0.2202	0.2202
1.0	0.2037	0.2039	0.2040	0.2041	0.2042	0.2044	0.2045	0.2045	0.2046	0.2046	0.2046
1.2	0.1873	0.1876	0.1878	0.1880	0.1882	0.1885	0.1887	0.1888	0.1888	0.1888	0.1888
1.4	0.1718	0.1722	0.1725	0.1728	0.1730	0.1735	0.1738	0.1739	0.1739	0.1739	0.1740
1.6	0.1574	0.1580	0.1584	0.1587	0.1590	0.1598	0.1601	0.1602	0.1603	0.1604	0.1604
1.8	0.1443	0.1450	0.1455	0.1460	0.1463	0.1474	0.1478	0.1480	0.1481	0.1482	0.1482
2.0	0.1324	0.1332	0.1339	0.1345	0.1350	0.1363	0.1368	0.1371	0.1372	0.1373	0.1374
2.2	0.1218	0.1227	0.1235	0.1242	0.1248	0.1264	0.1271	0.1274	0.1276	0.1277	0.1277
2.4	0.1122	0.1133	0.1142	0.1150	0.1156	0.1175	0.1184	0.1188	0.1190	0.1191	0.1192
2.6	0.1035	0.1047	0.1058	0.1066	0.1073	0.1095	0.1106	0.1111	0.1113	0.1115	0.1116
2.8	0.0957	0.0970	0.0982	0.0991	0.0999	0.1024	0.1036	0.1041	0.1045	0.1047	0.1048
3.0	0.0887	0.0901	0.0913	0.0923	0.0931	0.0959	0.0973	0.0980	0.0983	0.0986	0.0987
3.2	0.0823	0.0838	0.0850	0.0861	0.0870	0.0900	0.0916	0.0923	0.0928	0.0930	0.0933
3.4	0.0765	0.0780	0.0793	0.0804	0.0814	0.0847	0.0864	0.0873	0.0877	0.0880	0.0882
3.6	0.0712	0.0728	0.0741	0.0753	0.0763	0.0799	0.0816	0.0826	0.0832	0.0835	0.0837
3.8	0.0664	0.0680	0.0694	0.0706	0.0717	0.0753	0.0773	0.0784	0.0790	0.0794	0.0796
4.0	0.0620	0.0636	0.0650	0.0663	0.0674	0.0712	0.0733	0.0745	0.0752	0.0756	0.0758
4.2	0.0581	0.0596	0.0610	0.0623	0.0634	0.0674	0.0696	0.0709	0.0716	0.0721	0.0724
4.4	0.0544	0.0560	0.0574	0.0586	0.0597	0.0639	0.0662	0.0676	0.0684	0.0689	0.0692
4.6	0.0510	0.0526	0.0540	0.0553	0.0564	0.0606	0.0630	0.0644	0.0654	0.0659	0.0663
4.8	0.0480	0.0495	0.0509	0.0522	0.0533	0.0576	0.0601	0.0616	0.0626	0.0631	0.0635
5	0.0451	0.0466	0.0480	0.0493	0.0504	0.0547	0.0573	0.0589	0.0599	0.0606	0.0610
6	0.0340	0.0353	0.0366	0.0377	0.0388	0.0431	0.0460	0.0479	0.0491	0.0500	0.0506
7	0.0263	0.0275	0.0286	0.0296	0.0306	0.0346	0.0376	0.0396	0.0411	0.0421	0.0428
8	0.0209	0.0219	0.0228	0.0237	0.0246	0.0283	0.0311	0.0332	0.0348	0.0359	0.0367
9	0.0169	0.0178	0.0186	0.0194	0.0202	0.0235	0.0262	0.0282	0.0298	0.0310	0.0319
10	0.0140	0.0147	0.0154	0.0162	0.0167	0.0198	0.0222	0.0242	0.0258	0.0270	0.0280

(spreading over a larger area) of stresses at depth. This is natural, since, as follows from Fig. 45a, if a certain load 2 or 3 is added to load 1, then the compressive stress  $\sigma_z$  in point  $M$  will increase, but to a smaller extent than from load 1 alone, since the distance  $R$  to point  $M$  will also increase (as is known, the magnitude of additional stresses decreases with an increase of distance). The growth of stresses with an increase of the area can be established directly

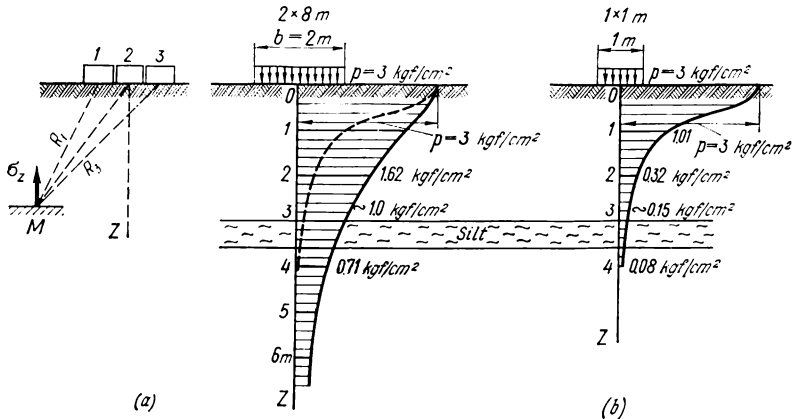


Fig. 45. An example showing the effect of the dimensions of a loaded area on the distribution of compressive stresses over the depth

from the data of Table 3.2 and may be illustrated by the following examples.

Thus, as has been found in Example 3.2, the pressure from the action of an external load of intensity  $p = 3 \text{ kgf/cm}^2$  distributed over an area,  $2 \times 8 \text{ m}^2$ , at a depth of 2 m from the boundary plane of the half-space is  $\sigma_z = 1.62 \text{ kgf/cm}^2$ . If, for the same intensity, the external load acts onto the soil surface over an area of  $1 \times 1 \text{ m}^2$ , then, noting that in such a case

$$\beta = \frac{2z}{b} = \frac{2 \times 2}{1} = 4; \quad \alpha = \frac{l}{b} = 1;$$

$$\text{and } K_0 = 0.108$$

the compressive stress at the same depth will be

$$\sigma_z = K_0 p = 0.108 \times 3 = 0.32 \text{ kgf/cm}^2$$

Diagrams of distribution of compressive stresses along the axis of loading for these two loaded areas,  $2 \times 8 \text{ m}^2$  and  $1 \times 1 \text{ m}^2$ , are shown in Fig. 45b.

As can be seen from the diagrams, for the same external pressure on the surface, the stresses with depth are different, being strongly dependent on loading area.

Thus, the greater the loading area, the slower the external pressures attenuate with depth, and compressive stresses at any given depth will be the greater, the greater the loading area. The last circumstance is of a large practical importance. Thus, for instance, with a large loading area, weak layers of soil may be subjected at a certain depth to very high pressures (greater than their load-carrying capacity), whereas with small loading areas the pressures formed are low and, therefore, have no effect on the strength and stability even of weak soils. In the example given in Fig. 45*b*, the pressure under the area  $2 \times 8$  m at a depth of 3 m is around  $1.0 \text{ kgf/cm}^2$ , while under the area  $1 \times 1$  m the pressure at the same depth is only around  $0.15 \text{ kgf/cm}^2$ .

**Method of elementary summation.** The method of corner points is inapplicable to loading areas of complicated form which cannot be divided into rectangles (for instance, those of curvilinear form or composed of triangles or more complex figures).

In such cases use is made of the method of elementary summation which consists in the following. The loading area is divided into areas of such dimensions that the loads applied to them can be considered concentrated in their centres of gravity.

As has been found by comparison with the results of an exact solution, with a loaded surface divided into elements whose longer sides  $l_0$  are smaller than *half* the distance from the centre  $R_0$  of an element to the point in which the compressive stress is being determined, the error is approximately 6 per cent, i.e., with  $\frac{l_0}{R_0} < \frac{1}{2}$ , the error  $\eta \leq 6$  per cent. Similarly, with  $\frac{l_0}{R_0} \leq \frac{1}{3}$ ,  $\eta \leq 3$  per cent and with  $\frac{l_0}{R_0} \leq \frac{1}{4}$ ,  $\eta \leq 2$  per cent.

These data provide definiteness to calculations of compressive stresses by the method of elementary summation.

It should be noted, however, that the method of elementary summation is inapplicable to determinations of main stresses and in some cases (for instance, in calculations of the effect of neighbouring foundations on settlements) the horizontal stresses should be taken into account.

In the method of elementary summation, a compressive stress is found by formula (3.4) by summing up the stresses from elementary loading surfaces

$$\sigma_z = \sum_{i=1}^{i=n} K_i \frac{P_i}{z^2} \quad (3.4'')$$

where  $K_i =$  coefficient to be found from Table 3.1 for the corresponding  $r_i/z$  ratio ( $r_i$  being the projection of the distance from the centre of gravity of the  $i$ -th element to the point considered onto the horizontal plane, and  $z$  being the depth)

$n =$  the number of elements

**Example 3.3.** Find the compressive stress  $\sigma_z$  for a horizontal plane located

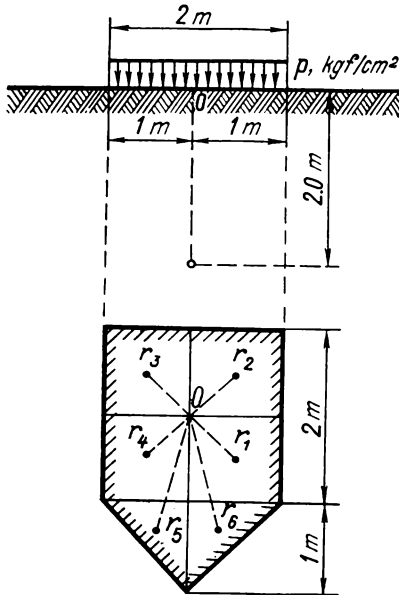


Fig. 46. To the determination of compressive stresses by the method of elementary summation

on the axis passing through the centre  $O$  of the rectangular portion of the loaded area (Fig. 46) and lying at a depth of 2 m below the surface with the action of a uniformly distributed load of intensity  $p = 3 \text{ kgf/cm}^2$ .

We divide the loaded area into 6 elements: four squares,  $1 \text{ m} \times 1 \text{ m}$ , and two rectangular triangles with catheti 1 m long.

A concentrated force  $P_i = pF_i$  ( $F_i$  being the area of an element) is assumed to be applied in the centre of each element. Since in the example considered the ratio of the larger side of each element  $l_0$  to the distance to the point considered  $R_0$  is less than two, the error in determination of  $\sigma_z$  by formula (3.44') will be less than 6 per cent towards higher pressures.

Let us determine the distances along the horizontal from the given points of application of concentrated forces (the centres of gravity of elements) to the vertical axis passing through the point considered, i.e., the magnitude of  $r_i$  (Fig. 46):

for square elements:  $r_1 = r_2 =$

$$= r_3 = r_4 = \sqrt{2}/2 = 0.71 \text{ m};$$

for triangular elements:  $r_5 =$

$$= r_6 = \sqrt{1.33^2 + 0.33^2} = 1.37 \text{ m}.$$

Then, interpolating from Table 3.1, we get

$$\text{with } \frac{r_{1-4}}{z} = \frac{0.71}{2} = 0.355$$

$$K_1 = 0.3549 \text{ and}$$

$$\text{with } \frac{r_{5-6}}{z} = \frac{1.37}{2} = 0.685$$

$$K_2 = 0.1850$$

Then

$$\sigma_z = 4K_1 \frac{P_1}{z^2} + 2K_2 \frac{P_2}{z^2}$$

or, substituting the values of  $K_1$  and  $K_2$ , and  $P_1 = 30$  tf and  $P_2 = 15$  tf, we have

$$\sigma_z = 4 \times 0.3549 \cdot \frac{30,000}{200 \times 200} + 2 \times 0.1850 \cdot \frac{15,000}{200 \times 200} = 1.2 \text{ kgf/cm}^2 \text{ approx.}$$

For more accurate determination of compressive stresses, the loaded surface must be divided into smaller elements. In the same way we can also find the magnitude of compressive stresses for any other point of a linearly deformable half-space.

### 3.2. STRESS DISTRIBUTION IN THE CASE OF A PLANAR PROBLEM

The conditions of the planar problem are observed when the stresses are distributed in a plane and are constant or equal to zero in directions perpendicular to that plane. Such conditions are found for structures very extended in one direction, such as strip and wall foundations, foundations of retaining walls, embankments, dams and the like. For such structures, the distribution of stresses in any section (except for the end portions 2 to 3 widths of the structure from its end) will be the same as in the neighbouring sections, provided that the load does not change in directions perpendicular to the plane considered.

Under conditions of the planar problem, determination of stresses becomes easier and in many cases the solution can be presented in a very convenient form.

Note that the planar problem has a very important property consisting in that all *component stresses*  $\sigma_z$ ,  $\sigma_y$  and  $\tau$  in the given plane ZOY are independent of the deformation characteristics of the linearly deformable half-space (the modulus of total deformation and the coefficient of lateral deformation), i.e., they are valid for all bodies (continuous, loose, etc.) for which the dependence between stresses and deformations can be assumed to be linear.

The planar problem of determination of stresses for linearly deformable bodies has been developed in detail in the works of Prandtl, Mitchell, Kolosov, Puzyrevsky, Gersevanov et al. We shall confine ourselves to the discussion of the solutions which are most often used in practice. These solutions have been obtained by the following method.

Using the formulae for stresses in a linearly deformable soil under the action of a linear load under conditions of the planar problem and integrating the stresses from the action of elementary forces ( $pdy \cdot 1$ ), expressions will be obtained for the component stresses  $\sigma_z$ ,  $\sigma_y$ , and  $\tau$  for various kinds of distributed load: uniform, uniformly increasing, etc.

**Effect of a uniformly distributed load.** The diagram of action of a uniformly distributed load under the conditions of the planar

problem is shown in Fig. 47. Denoting the *angle of vision* by  $\alpha$  and writing down that  $\beta = \frac{\alpha}{2} + \beta'$  ( $\beta'$  being the angle between the extreme beam and the vertical), the component stresses can be written as follows:

$$\left. \begin{aligned} \sigma_z &= \frac{p}{\pi} (\alpha + \sin \alpha \cos 2\beta) \\ \sigma_y &= \frac{p}{\pi} (\alpha - \sin \alpha \cos 2\beta) \\ \tau &= \frac{p}{\pi} (\sin \alpha \sin 2\beta) \end{aligned} \right\} \quad (3.11)$$

These expressions make it possible to easily compile a table of *influence coefficients* for calculation of component stresses after introducing the following designations:

$$\left. \begin{aligned} \sigma_z &= K_z p \\ \sigma_y &= K_y p \\ \tau &= K_{yz} p \end{aligned} \right\} \quad (3.11')$$

Table 3.5 gives the influence coefficients  $K_z$ ,  $K_y$ , and  $K_{yz}$  as a function of relative coordinates  $z/b$  and  $y/b$ .

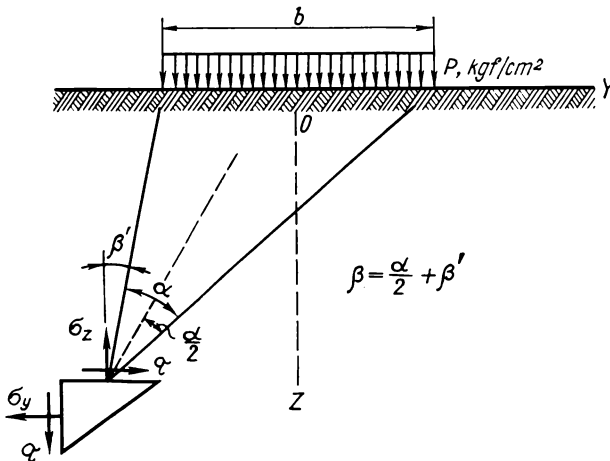


Fig. 47. Action of a uniformly distributed load under conditions of the planar problem

Using the data of the table, it is easy to plot diagrams of stress distribution over horizontal and vertical sections of soil for the

Table 3.5

Influence Coefficients  $K_z$ ,  $K_y$  and  $K_{yz}$  for Determination of Component Stresses for a Uniformly Distributed Load under Conditions of Planar Problem

$\frac{z}{b}$	Values of $y/b$																		
	0			0.25			0.5			1			1.5			2			
	$K_z$	$K_y$	$K_{yz}$	$K_z$	$K_y$	$K_{yz}$	$K_z$	$K_y$	$K_{yz}$	$K_z$	$K_y$	$K_{yz}$	$K_z$	$K_y$	$K_{yz}$	$K_z$	$K_y$	$K_{yz}$	
0.00	1.00	1.00	0	1.00	1.00	0	0.50	0.50	0.32	0	0	0	0	0	0	0	0	0	0
0.25	0.96	0.45	0	0.90	0.39	0.13	0.50	0.35	0.30	0.02	0.17	0.05	0.00	0.07	0.01	0.00	0.04	0.00	0.00
0.50	0.82	0.18	0	0.74	0.19	0.16	0.48	0.23	0.26	0.08	0.21	0.13	0.02	0.12	0.04	0.00	0.07	0.02	0.00
0.75	0.67	0.08	0	0.61	0.10	0.13	0.45	0.14	0.20	0.15	0.22	0.16	0.04	0.14	0.07	0.02	0.10	0.04	0.00
1.00	0.55	0.04	0	0.51	0.05	0.10	0.41	0.09	0.16	0.19	0.15	0.16	0.07	0.14	0.10	0.03	0.13	0.05	0.00
1.25	0.46	0.02	0	0.44	0.03	0.07	0.37	0.06	0.12	0.20	0.11	0.14	0.10	0.12	0.10	0.04	0.11	0.07	0.00
1.50	0.40	0.01	0	0.38	0.02	0.06	0.33	0.04	0.10	0.21	0.06	0.11	0.13	0.09	0.10	0.07	0.09	0.08	0.00
1.75	0.35	—	0	0.34	0.01	0.04	0.30	0.03	0.08	0.20	0.05	0.10	0.14	0.07	0.10	0.08	0.08	0.08	0.00
2.00	0.31	—	0	0.31	—	0.03	0.28	0.02	0.06	0.17	0.02	0.06	0.13	0.03	0.07	0.10	0.04	0.07	0.00
3.00	0.21	—	0	0.21	—	0.02	0.20	0.01	0.03	0.14	0.01	0.03	0.12	0.02	0.05	0.10	0.03	0.05	0.00
4.00	0.16	—	0	0.16	—	0.01	0.15	—	0.02	0.12	—	—	0.11	—	—	0.09	—	—	0.00
5.00	0.13	—	0	0.13	—	—	0.12	—	—	0.10	—	—	0.10	—	—	—	—	—	0.00
6.00	0.11	—	0	0.10	—	—	0.10	—	—	—	—	—	—	—	—	—	—	—	0.00

Note: Coefficients  $K_z = K_0$  for relative depths ( $z/b$ ) can also be found in Table 3.2 (when  $\alpha \geq 10$ ).

case of the planar problem (with a band-like uniformly distributed load).

Examples of diagrams of compressive stresses  $\sigma_z$  for horizontal and vertical sections of soil are shown in Fig. 48. Using these diagrams, it is easy to construct curves of equal stresses. Thus, Figure 49a shows the lines of equal vertical compressive stresses or pressures (*isobars*), Fig. 49b, the lines of equal horizontal stresses (*lateral*

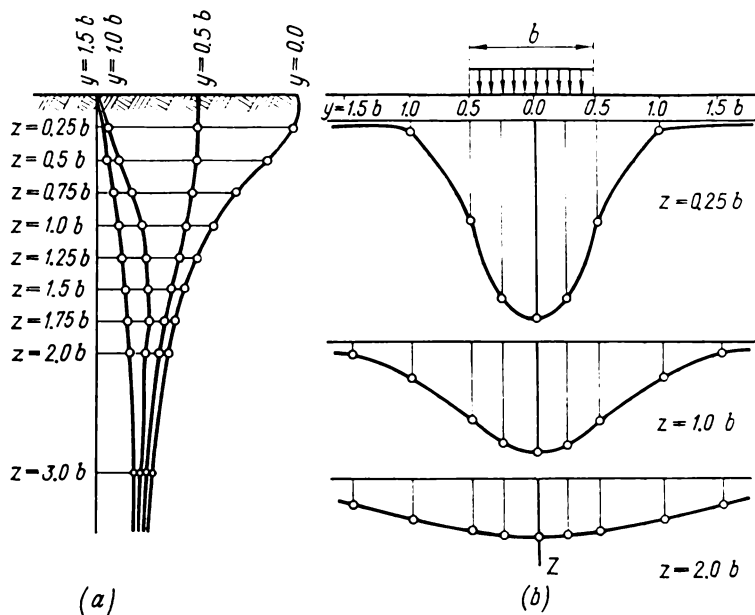


Fig. 48. Diagrams of compressive stresses  $\sigma_z$  in vertical (a) and horizontal (b) sections of a soil mass

pressures), and Fig. 49c. the lines of equal shear stresses (*shears*); these diagrams clearly characterize the total stressed region of soil under a band-like load.

It is of interest to note that, if we limit ourselves to pressures higher than  $0.1p$ , the effect of compressive stresses in the case of the planar problem will be observed to a greater depth (approximately down to  $6b$ ) than in the case of the three-dimensional problem (for a square loading surface, for instance, down to  $4b$ ).

The region of distribution of horizontal stresses extends laterally more than the width of the base of a strip foundation, and the maximum shear stresses (up to  $0.32p$ ) are observed under the edges of the base of a band-like load, while along the axis of the load the shear

stresses are equal to zero. For the principal stresses  $\sigma_1$  and  $\sigma_2$  and the maximum shear stresses  $\tau_{\max} = (\sigma_1 - \sigma_2)/2$ , the lines of equal stresses are circles passing through the edge points of the base of the band-like load.

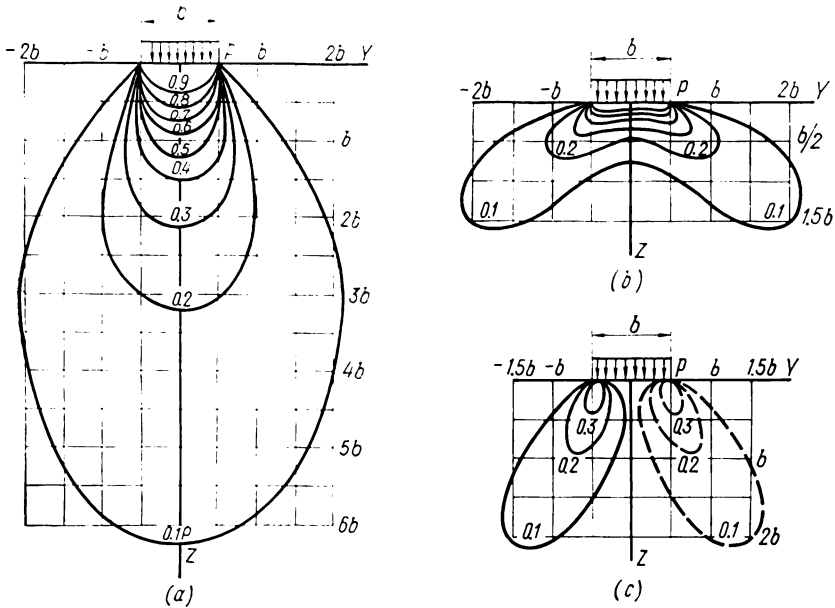


Fig. 49. Lines of equal stresses in a linearly deformable mass for the planar problem

(a) isobars  $\sigma_y$ ; (b) lateral pressure  $\sigma_y$ ; (c) shears  $\tau_{xy}$

**Principal stresses.** The principal or maximum and minimum normal stresses will be observed for surfaces located along the vertical axis of symmetry of the load. Indeed, for such surfaces, angle  $\beta' = -\alpha/2$ , and, therefore, angle  $\beta = \alpha/2 - \alpha/2 = 0$ .

Then, according to the third line of formula (3.11), the shear stress will be  $\tau = 0$ , i.e., the surfaces are the principal ones.

It may be shown that the principal surfaces are also the surfaces located along the bisectors of the vision angles and the surfaces perpendicular to them.

The magnitude of principal stresses is found from expressions (3.11) assuming  $\beta = 0$  in them

$$\left. \begin{aligned} \sigma_1 &= \frac{p}{\pi} (\alpha + \sin \alpha) \\ \sigma_2 &= \frac{p}{\pi} (\alpha - \sin \alpha) \end{aligned} \right\} \quad (3.12)$$

Formulae (3.12) are very often used for estimation of stressed state, especially of the ultimate state, in foundations of structures. They also make it possible to construct ellipses of stresses for various points of a stressed linearly deformable half-space (Fig. 50), which clearly characterize stress variations in soil under a band-like load.

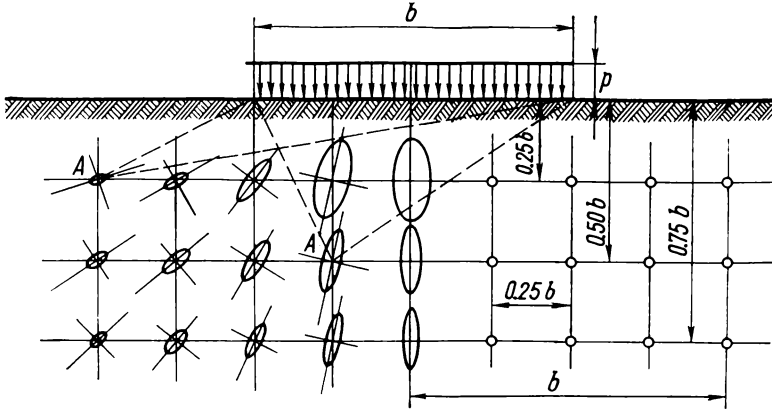


Fig. 50. Stress ellipses under the action of a uniformly distributed load in conditions of the planar problem

**Triangular load.** When determining the stresses in soils from the action of a *non-uniform load*, an important component is a triangular load, i.e., a load whose intensity varies by a triangular law.

We shall give here only the final formula (in the simplest form) for determining the compressive vertical stresses  $\sigma_z$  acting onto horizontal planes parallel to the boundary plane

$$\sigma_z = \frac{p}{2\pi} \left[ \frac{2y}{b} \alpha - \sin 2\beta' \right] \quad (3.13)$$

where  $\alpha$  and  $\beta'$  are the angles shown in Fig. 51a, radians.

Figures 51b and c show the diagrams of distribution of compressive stresses  $\sigma_z$  over horizontal and vertical sections through a linearly deformable soil under the action of a triangular load in fractions of its maximum intensity, and Table 3.6 gives the values of  $\sigma_z$  depending on  $z/b$  and  $y/b$  (Fig. 51a).

Note that the maximum compressive stresses will be in a vertical section near the centre of gravity of the triangular load.

**Effect of an arbitrary load varying by a straight-line law.** Important cases of the action of a band-like load are also loads varying by a rectangular or equilateral triangle, a trapezoidal load, etc., i.e., loads varying by a straight-line law. Formulae for calculation of stresses for such cases of loading may be found in a number

Table 3.6

Compressive Stresses for a Triangular Load (Fractions of  $p$ )

$\frac{z}{b}$	Values of $y/b$										
	-1.5	-1	-0.5	0	0.25	0.5	0.75	1	1.5	2	2.5
0.00	0.000	0.000	0.000	0.000	0.250	0.500	0.750	0.500	0.000	0.000	0.000
0.25	—	—	0.001	0.075	0.256	0.480	0.643	0.424	0.015	0.003	0.000
0.50	0.002	0.003	0.023	0.127	0.263	0.410	0.477	0.353	0.056	0.017	0.003
0.75	0.006	0.016	0.042	0.153	0.248	0.335	0.361	0.293	0.108	0.024	0.009
1.00	0.014	0.025	0.061	0.159	0.223	0.275	0.279	0.241	0.129	0.045	0.013
1.50	0.020	0.048	0.096	0.145	0.178	0.200	0.202	0.185	0.124	0.062	0.041
2.00	0.033	0.061	0.092	0.127	0.146	0.155	0.163	0.153	0.108	0.069	0.050
3.00	0.050	0.064	0.080	0.096	0.103	0.104	0.108	0.104	0.090	0.071	0.050
4.00	0.051	0.060	0.067	0.075	0.078	0.085	0.082	0.075	0.073	0.060	0.049
5.00	0.047	0.052	0.057	0.059	0.062	0.063	0.063	0.065	0.061	0.051	0.047
6.00	0.041	0.041	0.050	0.051	0.052	0.053	0.053	0.053	0.050	0.050	0.045

of handbooks on soil mechanics\*. We shall only discuss the Osterberg diagram, which is universally applicable to loads of the type considered.

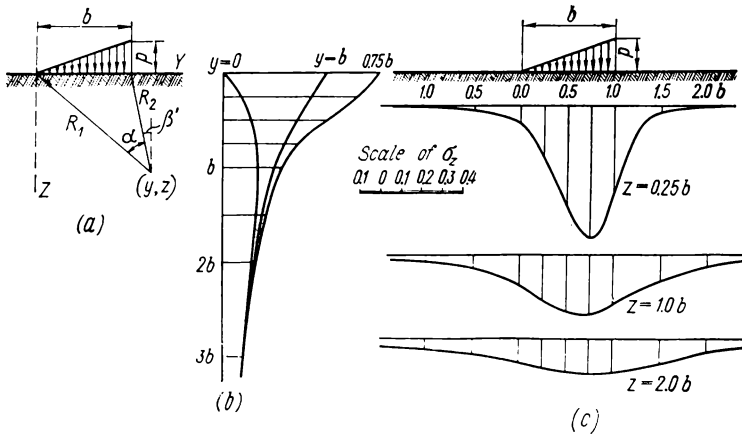


Fig. 51. Diagrams of compressive stresses in vertical and horizontal sections of a soil mass under the action of a triangular load

For a load varying by a straight-line law, the compressive stresses in soil can be calculated by the formula

$$\sigma_z = Ip$$

\* See, for example: Tsytoich N. A. *Osnovy mekhaniki gruntov* (Fundamentals of Soil Mechanics), Moscow, Stroiizdat, 1934; Maslov N. N. *Prikladnaya mekhanika gruntov* (Applied Soil Mechanics), Moscow, Mashstroizdat, 1949.

where  $I = f(a/z, b/z)$  is a function of relative quantities  $a/z$  and  $b/z$  which can be found from a graph (such as that given in Fig. 52), with  $a$  and  $b$  being the length of a triangular and rectangular load respectively, and  $z$ , the depth of the point considered.

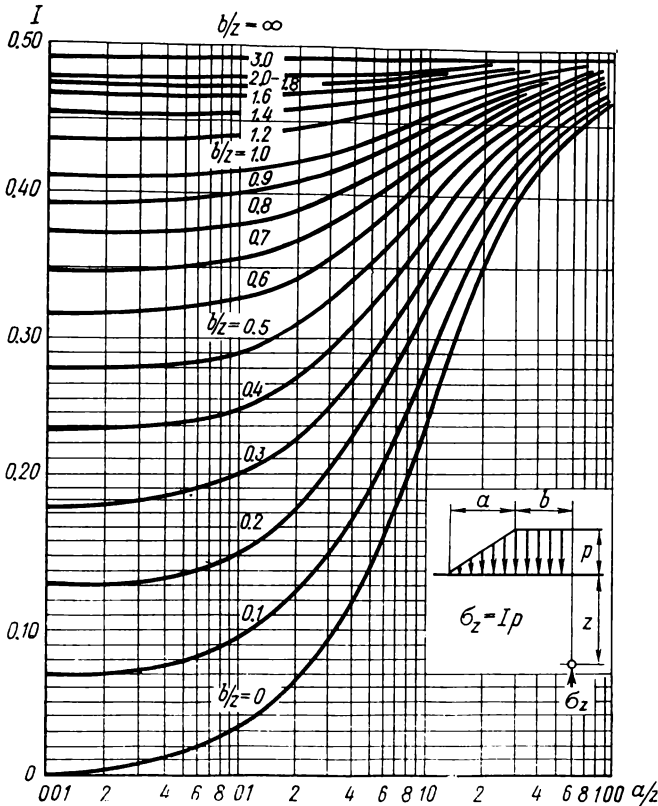


Fig. 52. A graph to determine compressive stresses from a load varying by straight-line law

In the formula above,  $I$  is found as an algebraic sum of the coefficients corresponding to the loads to the left and right from the vertical passing through the point considered.

Let this be explained by some examples.

**Example 3.4.** Find the stress  $\sigma_{z1}$  at point  $M_1$  (Fig. 53a). For the load acting at the left we have

$$\frac{a}{z} = \frac{2}{2} = 1 \text{ and } \frac{b_1}{z} = \frac{1}{2} = 0.5$$

From the diagram of Fig. 52,  $I_l = 0.397$ .  
 For the load acting at the right

$$\frac{a}{z} = \frac{2}{2} = 1 \text{ and } \frac{b_2}{z} = \frac{3}{2} = 1.5; I_r = 0.478$$

Thus,

$$\sigma_{z_1} = (I_l + I_r) p$$

or, substituting numerical values,

$$\sigma_{z_1} = (0.397 + 0.478) p = 0.875p$$

In order to determine the compressive stress  $\sigma_{z_2}$  at point  $M_2$  (see Fig. 53a),

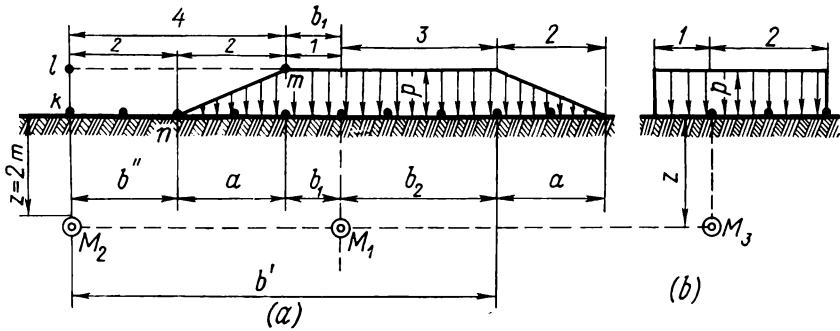


Fig. 53. Diagram of loads to explain the use of the graph in Fig. 52

we apply a fictitious load  $klmn$ . For the total load (including the fictitious one) we get

$$\frac{a}{z} = 1 \text{ and } \frac{b'}{z} = \frac{8}{2} = 4; I_r = 0.499$$

For the fictitious load

$$\frac{a}{z} = 1 \text{ and } \frac{b''}{z} = 1; I'_r = 0.455$$

Substituting numerical values and noting that the load  $klmn$  is fictitious, we obtain

$$\sigma_{z_2} = (I_r - I'_r) p = (0.499 - 0.455) p = 0.044p$$

For the case of a rectangular load (Fig. 53b)

$$\sigma_{z_3} = (I_l + I_r) p$$

Having found  $I_l$  when  $a/z = 0$  and  $b/z = 0.5$ , and  $I_r$  when  $a/z = 0$  and  $b/z = 1$ , we get

$$\sigma_{z_3} = (0.278 + 0.410) p = 0.688p$$

**Arbitrary load.** For a continuous band-like load of an arbitrary form, the diagram of external pressures is divided into rectangular and triangular elements, for instance, such as shown in Fig. 54a, and the magnitude of the compressive stress at the given point of soil is determined by summing the stresses from the rectangular and triangular elements of the pressure diagram.

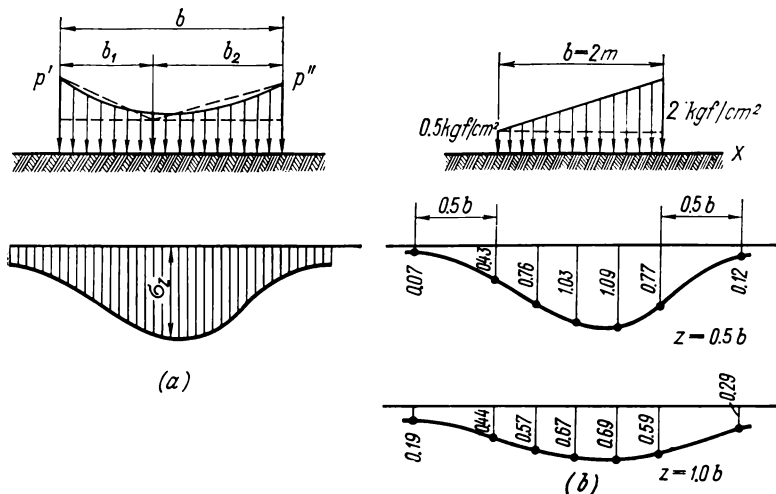


Fig. 54. Action of a non-uniform load under conditions of the planar problem (a) division of curvilinear pressure diagram into elements; (b) distribution of compressive stresses with a trapezoidal diagram of the action of external load

Figure 54b shows, as an example, the diagrams of distribution of compressive stresses  $\sigma_z$  in soil at depths  $z = 0.5b$  and  $z = 1.0b$  calculated by the method described for the case when the pressures acting on the soil surface are distributed according to a trapezoidal diagram.

The method described is applicable to any shape of the diagram of external pressures.

### 3.3. PRESSURE DISTRIBUTION OVER THE BASE OF THE FOUNDATION OF STRUCTURES (CONTACT PROBLEM)

The problem of pressure distribution over the base of structures is of high practical importance, especially for flexible foundations which are to be calculated for bending.

If we know the reactive pressure at the base of a foundation (which is usually termed the *contact pressure*), then, by applying its inverse

value to the foundation beam, we can easily find the design bending moments and shear forces by the common equations of statics.

In the previous section we have discussed the action on the soil of a distributed load which followed the deformations of the soil surface, i.e., a load which was transferred to the soil through a non-rigid body, for instance, a soil filling or the like. Most foundations of structures, however, possess a definite rigidity. It is then of importance to estimate the effect of the rigidity on the distribution of pressures and contact pressures in soil.

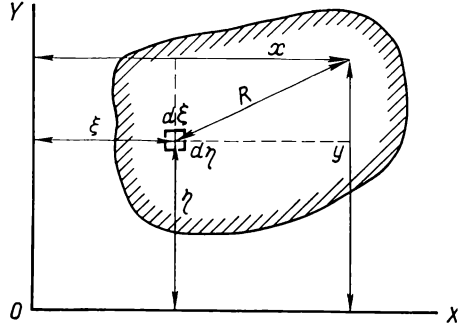


Fig. 55. Loading surface of an arbitrary shape

The starting equation for solving this problem is Boussinesq's formula (3.3) for the vertical deformation of a linearly deformable half-space under the action of a concentrated force

$$w_z = \frac{P}{\pi C_0 R}$$

For an arbitrary loading area, and using the notation of Fig. 55, we have

$$w_z = \frac{1}{\pi C_0} \iint_F \frac{p(\xi, \eta) d\xi d\eta}{\sqrt{(x-\xi)^2 + (y-\eta)^2}} \tag{3.14}$$

where  $F$  is the loading area by which integration is to be done.

With an *absolutely rigid* foundation and a central load, all points of the surface of its base will have the same vertical deformation.

Thus, the condition of absolute rigidity of a foundation gives for this case

$$w_z = \text{const}$$

or

$$w_z = \frac{1}{\pi C_0} \iint_F \frac{p(\xi, \eta) d\xi d\eta}{\sqrt{(x-\xi)^2 + (y-\eta)^2}} = \text{const} \tag{3.15}$$

The solution of this integral equation for a circular base with a central load acting on an absolutely rigid foundation is of the form

$$p_{xy} = \frac{P_m}{2 \sqrt{1 - \left(\frac{\rho}{r}\right)^2}} \quad (3.16)$$

where  $r$  = radius of the foundation base

$\rho$  = distance from the centre of the base to a given point  
( $\rho \leq r$ )

$P_m$  = mean pressure per unit area of the base

For a planar problem

$$p_{xy} = \frac{2P_m}{\pi \sqrt{1 - \left(\frac{y}{b_1}\right)^2}} \quad (3.16')$$

where  $y$  = horizontal distance from the foundation centre to a given point

$b_1$  = half-width of the foundation

For a planar problem with an off-centre load (according to V. A. Gastev)

$$p_{xy} = \frac{P}{\pi \sqrt{b_1^2 - y^2}} \left( 1 + \frac{2ey}{b_1^2} - \frac{2qb_1}{P} \right) + q \quad (3.16'')$$

where  $e$  = eccentricity of the concentrated (linear) force  $P$

$q$  = intensity of the lateral load

A diagram of distribution of contact pressures plotted for an absolutely rigid foundation on a linearly deformable half-space will have a saddle-like shape with infinitely large pressures at the ends (such as in Fig. 56a).

Indeed, when  $\rho = r$  and  $y = b_1$ ,  $p_{xy} = \infty$ . For the central axis of symmetry with a circular surface of the base

$$p_0 = \frac{P_m}{2}$$

and with a band-like surface

$$p_0 = \frac{2}{\pi} P_m$$

But, as has been shown by the solutions made with regard to the creep of the soil skeleton (N. Kh. Arutyunyan) and at the same time to the modulus of total deformation increasing with depth (Yu. K. Zaretzky), contact pressures at the base of a rigid foundation are distributed in the form of a substantially *more gradual curve*, and in addi-

tion, at the edges of the foundation they cannot be higher than the ultimate load-bearing capacity of soil, which also causes redistribution of pressures over the base (see the dotted line in Fig. 56a).

The pressure concentration at the edges of rigid foundations influences stress distribution in soil only to a small depth from the base and the whole bulb of stresses varies but slightly, as a consequence, the total settlement of a foundation depends little on its rigidity,

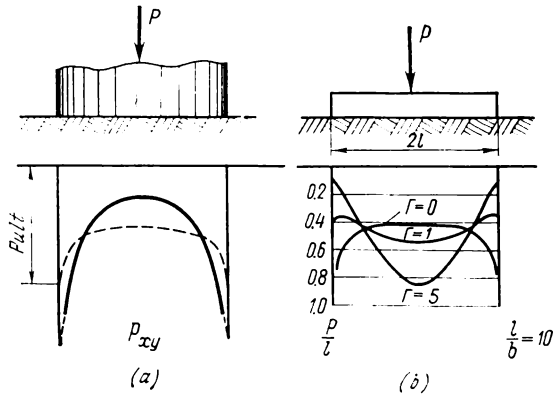


Fig. 56. Diagrams of contact pressures

(a) under an absolutely rigid foundation; (b) under foundations of various flexibilities

though the settlement of absolutely rigid foundations, as follows from the corresponding solutions (see Chap. 5), is slightly less than that of flexible ones.

This circumstance is confirmed by Fig. 57 which shows calculated isobars for an absolutely rigid and an absolutely flexible foundation.

A diagram of contact pressures for a foundation base plotted according to the solutions given in courses of Strength of Materials is rectilinear (either uniform or trapezoidal), whereas the strict solution by the theory of elasticity for absolutely rigid bodies always gives a saddle-shaped diagram; for foundations of a finite rigidity the shape of the diagram may vary from saddle-like to parabolic (see Fig. 56b).

In order to determine the contact pressures in the latter case, integral equation (3.14) is solved together with the differential equation of bending of beams. The result of such a solution shows that the distribution of contact pressures is strongly dependent on flexibility  $\Gamma$  of the foundation (according to M. I. Gorbunov-Posadov), which is found by the expression

$$\Gamma = \frac{\pi E_o l^3 b (1 - \mu_1)^2}{4 (1 - \mu_o)^2 E_1 I_1} \approx 10 \frac{E_o l^3}{E_1 b^3}$$

where  $E_o$  and  $\mu_o$  = moduli of deformability of soil

$E_1 J_1$  = rigidity of foundation beam

$l$  = half-length of beam

$h_1$  = height of the rectangular foundation beam

Figure 56b shows three curves of distribution of contact pressures depending on the flexibility of the foundation beam: with  $\Gamma = 0$  (absolutely rigid),  $\Gamma = 1$ , and  $\Gamma = 5$ .

Note that the distribution of contact pressures over the base of foundations depends not only on flexibility of foundations, but

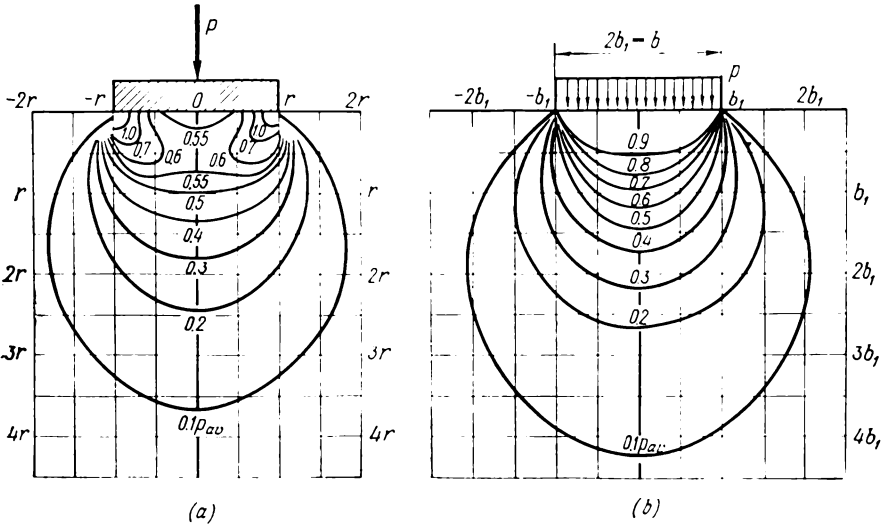


Fig. 57. Isobars in soil under foundations  
 (a) absolutely rigid foundation; (b) flexible foundation

also on depth of the foundation, the magnitude of external load (which causes plastic deformations in soil), and therefore, on the strength properties of soil.

It should be noted in conclusion that the data presented in this section may serve as the basis for the development of methods of calculation of foundation beams and plates supported by a compressible linearly deformable half-space.

**Effect of non-uniformity and anisotropy on stress distribution in soils.** The stressed state of soil under foundations is substantially affected not only by rigidity of foundations, but also by non-uniformity and anisotropy of the soil, a sharp change of the deformability modulus of individual layers of the soil, and especially by a close location of incompressible rocks. For structures having a large area in plan, when the thickness of the compressible layer (above the

rock) is of the order of the width of the loaded surface or smaller, the incompressible rock has a substantial effect on both the distribution of stresses in depth and the magnitude and distribution of contact pressures.

**Distribution of compressive stresses in a soil layer of a limited thickness on an incompressible bed.** The solution of this problem for a flexible band-like uniformly distributed load was obtained at the Institute of Foundations (K. E. Egorov, 1939); the calculated results are given in Table 3.7.

The data of this table have been used for plotting the diagram of distribution of compressive stresses along the axis of a band-like load for cases of location of an incompressible rock at a depth equal to half the width (curve 1), the width (curve 1'), and 2.5 widths (curve 1'') of the band-like load (Fig. 58). Curve 2 in the same figure is the diagram of the maximum compressive stresses for a uniform half-space (without rock bed), and curves 3, 3' and 3'' are diagrams of distribution of the same stresses in case of a less uniform bed with a variable deformability modulus, when this modulus decreases in depth and at the lower boundary of the layer is several times less than that at the load base (according to the data of the Author and V. D. Ponomarev).

It follows from an analysis of the diagrams of distribution of compressive stresses (pressures) that the presence of a rigid non-compressible layer causes concentration (growth) of stresses along the load axis, whereas an increase of the soil compressibility with depth results in a decrease of stress concentration.

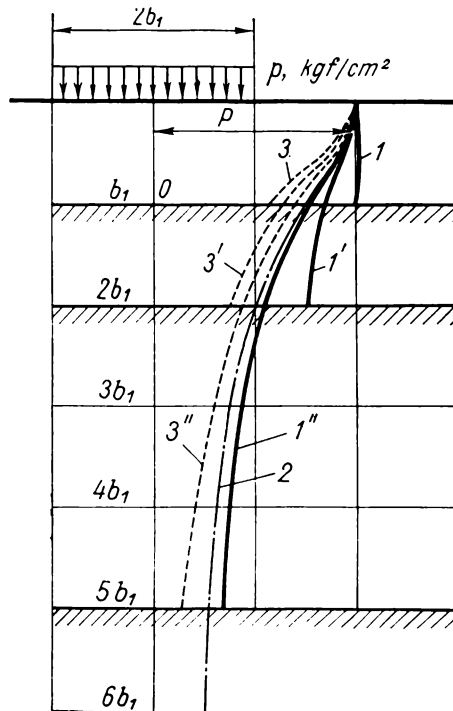


Fig. 58. Distribution of maximum compressive stresses under the centre of a flexible uniformly loaded band in a limited-thickness soil layer

1—in the presence of incompressible bed rock; 2—for a uniform half-space; 3—for a non-uniform layer with the soil compressibility increasing with depth

Table 3.7

**Maximum Compressive Stresses (Fractions of  $p$ )  
in a Soil Layer on an Incompressible Bed under  
a Strip Foundation**

$\frac{z}{h}$	With incompressible layer located at a depth		
	$h = b_1$	$h = 2b_1$	$h = 5b_1$
1.0	1.000	1.00	1.00
0.8	1.009	1.99	0.82
0.6	1.020	0.92	0.57
0.4	1.024	0.84	0.44
0.2	1.023	0.78	0.37
0.1	1.022	0.76	0.36

*Note:*  $h$  is the thickness of the compressible layer (above the rock);  $b_1$  is half the width of the uniformly distributed band-like load;  $z$  is the coordinate of the centre of the surface for which the stress is being determined (with the origin of coordinates always at the boundary between the compressible layer and rigid bed).

The distribution of contact pressures for a soil layer of a limited thickness, supported by an incompressible bed is given for *rigid foundations* in Table 3.8 (according to the data calculated at the Institute of Foundations).

For *flexible foundations*, we give Table 3.9 below for determining the contact pressures in a soil layer of a limited thickness under

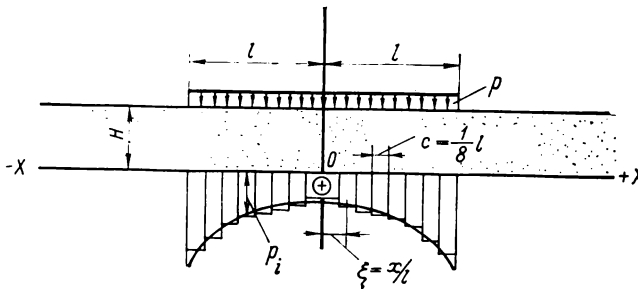


Fig. 59. Distribution of reactive pressures over the base of a flexible foundation on a limited-thickness soil layer

the action of a band-like load of intensity  $p$  (compiled by G. V. Kra-shenninnikova et al. in 1961) under assumption of the absence of friction at the contact of the elastic layer with non-compressible bed by the Zhemochkin method of stepwise summation (Fig. 59)\*.

\* A more accurate solution has been obtained by Prof. S. S. Davydov in 1939. See his book: Raschet i proektirovanie podzemnykh konstruksii (Design and Calculation of Underground Structures), Moscow, Stroizdat, 1950, pp. 133-150.

Table 3.8

**Contact Pressures under a Rigid Foundation on a Soil Layer of Limited Thickness (Fractions of  $p$ )**

$r/R$ or $y/b_1$	Thickness of layer with $h/R$ or $h/b_1$						
	0.25	0.5	1	2	3	5	10 and more
Circular foundations							
0.0	0.905	0.829	0.652	0.532	0.509	0.503	0.500
0.1	0.904	0.828	0.652	0.535	0.512	0.505	0.503
0.2	0.904	0.823	0.654	0.541	0.519	0.513	0.511
0.3	0.902	0.817	0.658	0.533	0.532	0.527	0.525
0.4	0.900	0.809	0.665	0.572	0.553	0.548	0.546
0.5	0.896	0.802	0.678	0.600	0.584	0.579	0.578
0.6	0.891	0.798	0.700	0.642	0.630	0.627	0.626
0.7	0.886	0.804	0.744	0.712	0.704	0.702	0.701
0.8	0.889	0.841	0.833	0.834	0.834	0.833	0.833
0.9	0.945	0.985	1.073	1.131	1.143	1.147	1.146
0.95	1.093	1.252	1.446	1.565	1.589	1.600	1.599
Strip foundations							
0.0	0.949	0.915	0.811	0.705	0.699	0.649	0.640
0.1	0.948	0.914	0.811	0.707	0.672	0.652	0.643
0.2	0.948	0.909	0.811	0.714	0.680	0.661	0.653
0.3	0.946	0.903	0.813	0.725	0.695	0.678	0.670
0.4	0.942	0.895	0.818	0.744	0.719	0.704	0.697
0.5	0.938	0.889	0.826	0.773	0.753	0.743	0.737
0.6	0.932	0.884	0.846	0.818	0.806	0.800	0.797
0.7	0.927	0.891	0.885	0.891	0.891	0.892	0.892
0.8	0.932	0.924	0.972	1.029	1.046	1.055	1.060
0.9	0.998	1.071	1.220	1.366	1.413	1.443	1.457
0.95	1.161	1.343	1.618	1.869	1.954	2.010	2.030

The values of reactive pressures are given in Table 3.9 for five various soil layers of limited thickness depending on the flexibility of the foundation beam, which is found by the expression

$$\Gamma \approx 10 \frac{E_o l^3}{E_1 h_1^3}$$

where  $l$  = half-span of the beam (see Fig. 59)

$E_o$  = modulus of total deformation of the soil layer

$E_1$  = elastic modulus of the material of the foundation beam

$h_1$  = height of the rectangular foundation beam

As in the cases discussed earlier, the calculated values  $\max M$  and  $\max Q$  for a foundation beam are found by the equations of statics for the known reactive pressures.

**Distribution of stresses from the dead weight of soil.** The stresses from the dead weight of soil (which are termed *natural* stresses)

Table 3.9

Reactive Pressures (Fractions of  $p$  Averaged for Sections of Length  $c = \frac{1}{8}l$ ) for Half-Span  $l$  of Flexible Uniformly Loaded Beams on a Soil Layer of Limited Thickness  $H$

± §	Γ = 0											Γ = ∞										
	Γ = 0											Γ = ∞										
	0	1/16	1/4	1/2	l	2l	∞	0	1/16	1/4	1/2	l	2l	∞	0	1/16	1/4	1/2	l	2l	∞	
	with $H$ equal to																					
1/16	1	1	0.970	0.924	0.828	0.748	0.639	1	0.996	0.990	0.958	0.876	0.786	0.733	1	1.000	1.190	1.474	1.791	2.073	2.251	
3/16	1	1	0.972	0.925	0.829	0.725	0.640	1	1.002	0.985	0.956	0.874	0.789	0.738	1	1.000	1.036	1.032	0.931	0.866	0.858	
5/16	1	1	0.976	0.929	0.836	0.744	0.668	1	1.002	0.980	0.954	0.874	0.796	0.751	1	1.001	1.008	0.981	0.923	0.866	0.821	
7/16	1	1	0.966	0.918	0.837	0.769	0.710	1	0.998	0.975	0.934	0.866	0.808	0.772	1	1.001	1.027	0.953	0.902	0.859	0.742	
9/16	1	1	0.956	0.910	0.857	0.816	0.770	1	1.001	0.960	0.916	0.870	0.836	0.814	1	1.001	1.037	0.925	0.889	0.862	0.842	
11/16	1	1	0.946	0.911	0.899	0.909	0.874	1	1.001	0.960	0.904	0.893	0.899	0.898	1	1.000	1.023	0.898	0.887	0.889	0.870	
13/16	1	1	0.960	0.927	0.987	1.059	1.070	1	1.000	0.960	0.904	0.956	1.013	1.043	1	1.000	0.970	0.881	0.915	0.956	0.980	
15/16	1	1	1.254	1.556	1.927	2.263	2.629	1	1.000	1.190	1.474	1.791	2.073	2.251	1	1.000	1.114	1.380	1.615	1.822	1.988	
	with $H$ equal to																					
	Γ = 5											Γ = 10										
± §	Γ = 5											Γ = 10										
0	1/16	1/4	1/2	l	2l	∞	0	1/16	1/4	1/2	l	2l	∞	0	1/16	1/4	1/2	l	2l	∞		
1/16	1	1.004	0.990	0.972	0.900	0.820	0.773	1	1.030	1.018	0.994	0.938	0.875	0.889	1	1.030	1.018	0.994	0.938	0.875	0.889	
3/16	1	1.006	0.988	0.969	0.895	0.819	0.775	1	1.032	1.010	0.989	0.931	0.871	0.858	1	1.032	1.010	0.989	0.931	0.871	0.858	
5/16	1	1.008	0.988	0.964	0.892	0.821	0.781	1	1.036	1.008	0.981	0.923	0.866	0.821	1	1.036	1.008	0.981	0.923	0.866	0.821	
7/16	1	0.962	0.965	0.942	0.879	0.826	0.794	1	1.027	0.920	0.925	0.902	0.859	0.742	1	1.027	0.920	0.925	0.902	0.859	0.742	
9/16	1	1.008	0.960	0.919	0.877	0.845	0.824	1	1.037	0.980	0.925	0.889	0.862	0.842	1	1.037	0.980	0.925	0.889	0.862	0.842	
11/16	1	1.006	0.960	0.901	0.890	0.895	0.893	1	1.023	0.980	0.898	0.887	0.889	0.870	1	1.023	0.980	0.898	0.887	0.889	0.870	
13/16	1	1.004	0.970	0.895	0.946	0.992	1.018	1	1.016	0.970	0.881	0.915	0.956	0.980	1	1.016	0.970	0.881	0.915	0.956	0.980	
15/16	1	1.002	1.179	1.438	1.720	1.989	2.142	1	1.004	1.114	1.380	1.615	1.822	1.988	1	1.004	1.114	1.380	1.615	1.822	1.988	

are of importance in newly made earth structures and for estimation of natural compactness of soils.

With a horizontal soil surface, the dead stresses of soil (unit weight  $\gamma_z$ ) increase with depth  $z$  and are equal to

$$\sigma_z = \int_0^z \gamma_z dz; \quad \sigma_x = \sigma_y = \xi_0 \sigma_z;$$

$$\tau_{zy} = \tau_{zx} = 0$$

where  $\xi_0 = \frac{\mu_0}{1 - \mu_0}$  is the coefficient of lateral pressure of soil at rest.

Note that the expressions for lateral pressures  $\sigma_x$  and  $\sigma_y$  are only valid for a horizontal soil surface and may vary depending on the

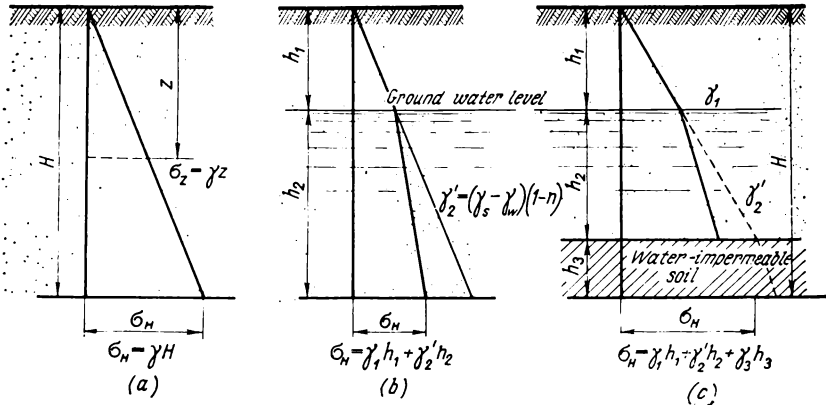


Fig. 60. Distribution of pressures from dead weight of soil (a) homogeneous soil; (b) in the presence of ground waters (at a depth  $h_1$ ); (c) in the presence of water-impermeable rock under ground waters (at a depth  $h_1 + h_2$ )

site relief, the processes of orogenesis, etc., which, however, can only be established by special field tests.

With a constant unit weight, the stresses

$$\sigma_z = \gamma z$$

For a soil mass (i.e., for a fully saturated soil with the presence of free hydraulically continuous water) the magnitude of compressive stresses is found as

$$\sigma'_z = \gamma' z$$

where  $\gamma'$  is the unit weight of soil with regard to the lifting effect of water; it is found by formula (1.8) or (1.8').

Examples of diagrams of distribution of vertical pressures from the dead weight of soil are shown in Fig. 60.

**Some general conclusions.** It may be seen from what has been said in this chapter that the theory of linearly deformable bodies has found a wide application in soil mechanics. Non-linear relationships between deformations and stresses are taken into account in special cases only. A question arises, however: how do the solutions of the theory of linearly deformable bodies correlate with the results of direct measurements?

It should be immediately pointed out that the problem of measuring the stresses (or even only pressures) in soil is technically very complicated, since immersion of a foreign body (a stress-measuring device) into soil can disturb the stressed state in the place being tested. Experiments have shown, however, that pressures in soil, for instance, should be measured by special very rigid disc-type hydraulic capsules preliminarily calibrated in identical conditions.

The distribution of pressures in soils under load has been tested in very many experiments, but the results obtained only rarely satisfy modern requirements.

Those interested in the problem may be referred to the specialist literature (for instance, [14]). We shall discuss here only the most general conclusions.

By comparing the experimental results (those obtained by G. I. Pokrovsky and I. S. Fyedorov, N. A. Tsyovich and D. S. Baranov, G. Press, S. Ya. Edelman et al.) with the data calculated by the theory of linearly deformable bodies, it can be concluded that the *calculated data are close to the measured ones* both in nature and magnitude, when the boundary conditions have been strictly observed and the measurements made in the phase of linear relationship between stresses and deformations. The results of observations on real structures are, however, preferable over those obtained in experiments with small loading surfaces.

Thus, for instance, the problem of distribution of contact pressures (which was much discussed earlier) has found quite a definite solution on the basis of both some earlier experiments (for instance, M. Burger, S. S. Vyalov, A. G. Rodstein et al.) and the newest generalizations (V. A. Florin in 1959, E. Schultz in 1965 et al.), namely: the nature of distribution of contact pressures over bases of foundations (either saddle-like or parabolic) is determined not by the kind of soil, but by the *flexibility of the foundation* and the *degree of development of plastic deformations* in the soil bed, which depends both on the unit load on soil and depth of foundation (lateral loading) and also on the area of load transfer.

In all cases, as a rule (except for shallow foundations on weak soils), the distribution of pressures over the foundation base with regard to the boundary conditions (a limited thickness of the layer of compressible soil, etc.) in the phase of linear deformability should be taken saddle-shaped.

## Chapter Four

### THE THEORY OF ULTIMATE STRESSED STATE OF SOILS AND ITS APPLICATION

The *ultimate stressed state* of soil in a given point is such that the slightest additional force can disturb the existing equilibrium and bring the soil to an unstable state: slip surfaces, discontinuities, and settlements occur in the soil and cohesion between its particles and aggregations is disturbed. Such a stressed state of soils should be regarded as utterly inadmissible for erection of structures on them.

For this reason it is very important in engineering practice to be able to estimate the maximum allowable load on the soil at which it will still be in equilibrium, i.e., will not lose its strength and stability.

The problems of strength (load-bearing capacity), stability, and pressure of soils on retaining structures are particular problems of the general *theory of ultimate equilibrium*, whose foundations already were laid down in the works of Coulomb and Prandtl, but only in the forties and fifties of this century did the Soviet scientists (V. V. Sokolovsky, S. S. Golushkevich, V. G. Berezantsev and others) develop effective general methods for solving ultimate equilibrium differential equations (formulated by F. Kötter) and in the last decade a number of closed and tabulated strict solutions were obtained (V. V. Sokolovsky et al.).

#### 4.1. STRESSED STATE PHASES OF SOILS WITH AN INCREASE IN LOAD

**Mechanical processes in soils.** Consider the mechanical processes occurring in soils under the action of a *local* gradually increasing *load*. Let a load be applied to the soil surface through a rigid stamp of limited dimensions and observations on setting of the stamp be made continuously.

In the case considered the mechanical processes will be substantially more complicated than, for instance, those occurring under compression which have been discussed earlier, when only attenuating deformations are observed, since every element of the soil in the compression device is subjected only to normal stresses and has no possibility to expand laterally.

Under the action of a *local load*, however, an arbitrarily separated element of soil is subjected, apart from normal stresses, to shear stresses, which, after reaching a definite magnitude, may cause local irreversible *slippages* (shears). For this reason, under the action of a local load, there may occur both attenuating *compaction* deformations and (with a definite magnitude of the external load) non-

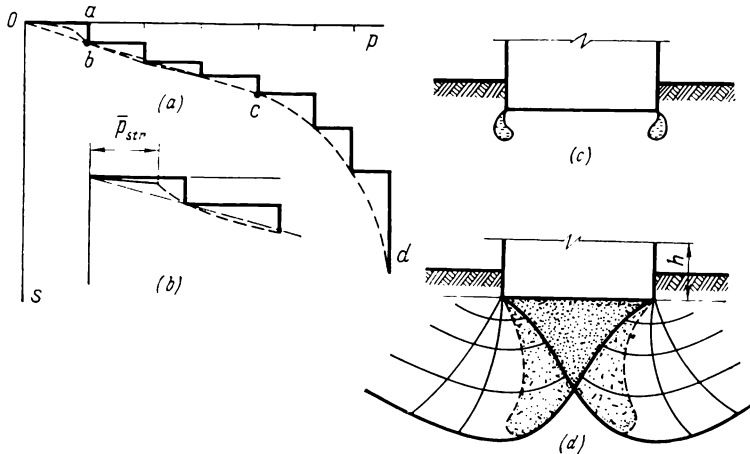


Fig. 61. Relationship between deformations and stresses with an increase in load on soil

(a) diagram of deformations with stepwise loading; (b) initial section of deformation curve; (c) end of compaction phase—beginning of shear phase; (d) slip lines and compacted core at fully developed zones of ultimate equilibrium

attenuating shear deformations, which under certain conditions may turn into plastic creep, bulging, setting, etc.

Figure 61a shows a typical curve of soil deformations under the action of a local stepwise increasing load on its surface. Let us discuss the diagram in more detail.

If the steps of load are small and the soil is cohesive, then the first sections on the deformation curve will be almost horizontal (Fig. 61b, where the initial section is shown on an increased scale), i.e., before the *structural strength* is exceeded, the soil will be subjected only to very small elastic deformations and settlement of the stamp will recover completely upon unloading.

At subsequent steps of loading (or even at the first step, but with the structural strength of the soil being exceeded) the *soil undergoes compaction* under load, i.e., its porosity in a definite region under the loaded surface decreases.

It is of value to note that, as has been shown by the results of direct experiments, there always exists a certain external pressure

when the soil is only compacted and acquires greater resistance to external forces.

**Phases of stressed state.** The *first phase* of the stressed state of soil is termed the *compaction phase*. Such a state of soil is advantageous from the standpoint of building construction, since the soil in the compaction state acquires a denser structure and is less liable to setting.

As has been indicated earlier (see Section 2.5), the relationship between total deformations and unit pressure (compressive stress) at compaction can be taken *linear* with an accuracy sufficient for practical purposes.

Compaction of soil under load may continue at several steps of loading, but when the load attains a definite magnitude ever greater number of slippages (shears) occurs between particles of the soil, since the shear resistance has been overcome in these places. There appear *slippages* between particles, which gradually form individual *slippage surfaces* and *shear zones*.

The *end of the compaction phase* (point *c* on the curve in Fig. 61*a*) and the beginning of the formation of *shear zones*, which appear initially at the edges of the loading surface (Fig. 61*c*) where shear stresses are at the maximum, are the most characteristic parameters of the mechanical properties of soils and correspond to the *initial critical load* on soil under the given loading conditions.

With a further increase in load, the *second phase* is attained, which is called the *shear phase*. This phase then transforms (according to the boundary conditions and the magnitude of the load) into plastic or progressive creep, bulging, setting and similar inadmissible deformations of the foundation.

In this phase, the relationship between deformations and stresses is *non-linear*.

It is important to note that at the end of the compaction phase (or the beginning of the shear phase), a rigid core of limited displacements of particles begins to form directly under the stamp (which

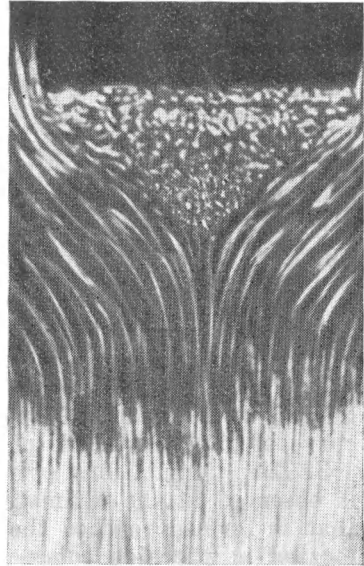


Fig. 62. The shape of rigid core in a loose soil when a stamp is pressed in (according to experiments of J. Biarez)

can be established directly by photographing the displacements by the method of Prof. V. I. Kurdyumov; see, for instance, Fig. 62 according to Prof. Biarez). This core then expands the soil laterally, thus causing a substantial settlement of the stamp. As has been found by V. G. Berezantsev and V. A. Yaroshenko in experiments with sand soils, such a core is formed completely when the soil has attained the maximum load-bearing capacity, after which it remains unchanged, but there are formed additional plastic regions of the core (see the dotted line in Fig. 61*d*) which, by varying their positions, find, as it were, the most weak places in the soil, whereas the rigid core remains unchanged and moves deeper into the soil.

With the ultimate stressed state of soil developed, lateral displacements of particles become prevailing and there *are formed continuous slip surfaces*, as a result of which the soil loses stability.

**Slip surfaces.** At attaining the ultimate load-bearing capacity of soil in the second phase (which corresponds to the end of formation of a rigid core and complete development of the zones of ultimate equilibrium), several main cases with characteristic *slip surfaces* (Fig. 63*a*) may be distinguished depending on boundary conditions (mainly the depth of foundation) and density of soils:

1. *Shallow foundations* (with  $h/b < \frac{1}{2}$ ), for which bulging of soil is characteristic at the ultimate load (line 1 in Fig. 63*a*).

2. *Medium-deep foundations* (with  $h/b = \frac{1}{2}$  to 2), for which bulging at the ultimate load is also observed, but the envelope curve of slip surfaces is of an S-shaped form (Fig. 63*a*, line 2).

3. *Deep foundations* (with  $h/b = 2$  to 4), for which no bulging is observed at the ultimate load, but the zone of ultimate shears that is formed reaches the foundation base and deforms the soil located at the side edges of the foundation (Fig. 63*a*, line 3).

4. *Very deep foundations* (with  $h/b > 4$ ), for which *settlement* of the base (rapidly occurring local settlement) is formed below the foundation base at a load exceeding the ultimate one; such a settlement is utterly inadmissible in bases of structures.

It is of interest to note that with a substantial settlement of the base, a separate rigid foundation or stamp attains after deformation (if it has not been destroyed) a new state of equilibrium corresponding to the new boundary conditions (the depth of foundation, compactness of bearing soil, etc.). But very large settlements even of a separate foundation are inadmissible, since foundations are usually connected (sometimes rigidly) with other elements of structures; such settlement can cause destruction of a structure.

Deformations of soils in the first phase (*compaction* phase) are always attenuating; in the second phase (*shear* phase) they are, as a rule, non-attenuating and result from successive slippages.

On any curve of deformations in the shear phase (Fig. 63b), we can distinguish three different sections: (1)  $Oa_1$ ;  $Oa_2$ , etc.—section

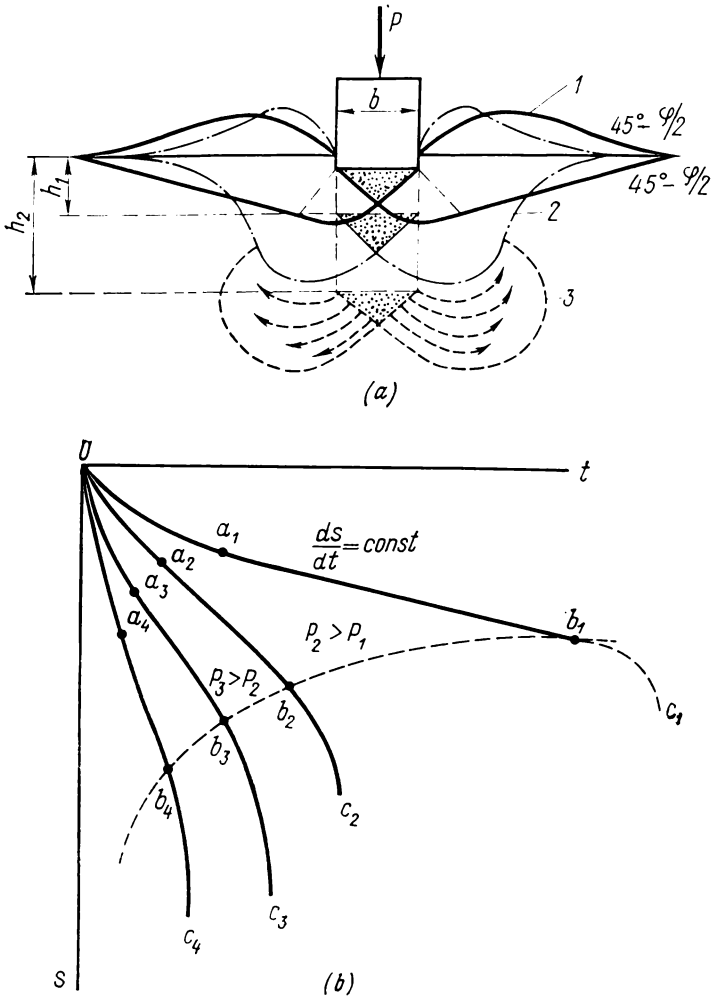


Fig. 63. Slip surfaces and deformations in a soil under a foundation with fully developed zones of ultimate equilibrium

(a) enveloping slip lines (1, 2, 3) for different foundation depths: (b) deformations of soil (creep) in shear phase

of *unstable creep*; (2)  $a_1b_1$ ,  $a_2b_2$ , etc.—section of *stable creep* or *plastic flow*, for which the rate of deformation  $ds/dt = \text{const}$ ; and (3)  $b_1c_1$ ,  $b_2c_2$ , etc.—section of *progressive flow*, for which  $ds/dt \rightarrow \infty$ ;

as has been found by direct experiments, plastic flow always transforms into progressive flow, this transformation occurring the quicker, the greater the external pressure, but only after attaining a definite shear deformation characteristic of the given soil.

By connecting the points  $b_1$ ,  $b_2$ , etc. of creep curves (Fig. 63b) corresponding to the time of beginning of progressive flow, we obtain what is called the *curve of long-time strength*, which makes it possible to determine the minimum pressure at which a creep curve (after appropriate recombination of the soil structure) becomes an *attenuating one*. This pressure determines the so-called *long-time strength* of soils.

Thus, with an increase of the load on soil, we have to distinguish at least between its two characteristic values: the first, corresponding to the *beginning* of transfer of the compaction phase into shear phase (i.e., into the phase of formation and development of zones of ultimate stressed state) and the second, when the *load-bearing capacity* of soil base is *exhausted*, the formation of the rigid core is finished, and there is observed full development of the zones of ultimate equilibrium when even a slight increase of the load results in that the soil loses its strength and stability.

#### 4.2. EQUATIONS OF ULTIMATE EQUILIBRIUM FOR LOOSE AND COHESIVE SOILS

**Angle of maximum deviation.** With a local load acting on the soil surface, normal and shear stresses will arise at any point  $M$  of the soil for any plane  $mn$  drawn through that point at an angle  $\alpha$  (Fig. 64a). When considering the problem mathematically, the normal stresses must also include cohesion forces which can be fully estimated by the cohesion pressure  $p_e$  [see formula (2.23')]. Then a normal stress  $\sigma_\alpha + p_e$  and a shear stress  $\tau_\alpha$  will act on the plane  $mn$  (Fig. 64a).

With a variation of the angle  $\alpha$ , the magnitude of component stresses will also vary and, if the shear stresses attain a certain fraction of the normal ones, then, as has been shown by shear tests, one portion of the soil will slip over another.

Thus, the condition of soil ultimate equilibrium in a given point is

$$\tau_\alpha \leq f(\sigma_\alpha + p_e)$$

or

$$\frac{\tau_\alpha}{\sigma_\alpha + p_e} \leq f$$

If  $f$  is a constant, then in the ultimate state, as has been shown in Chap. 2, it is the tangent of the straight envelope of the circles of ultimate stresses (Fig. 64b and c).

On the other hand, according to Fig. 64a

$$\frac{\tau_\alpha}{\sigma_\alpha + p_e} = \tan \theta$$

This ratio is equal to the tangent of the *angle of deviation*  $\theta$ , i.e., the angle through which the total stress  $\sigma$  for the plane deviates from the normal to that plane.

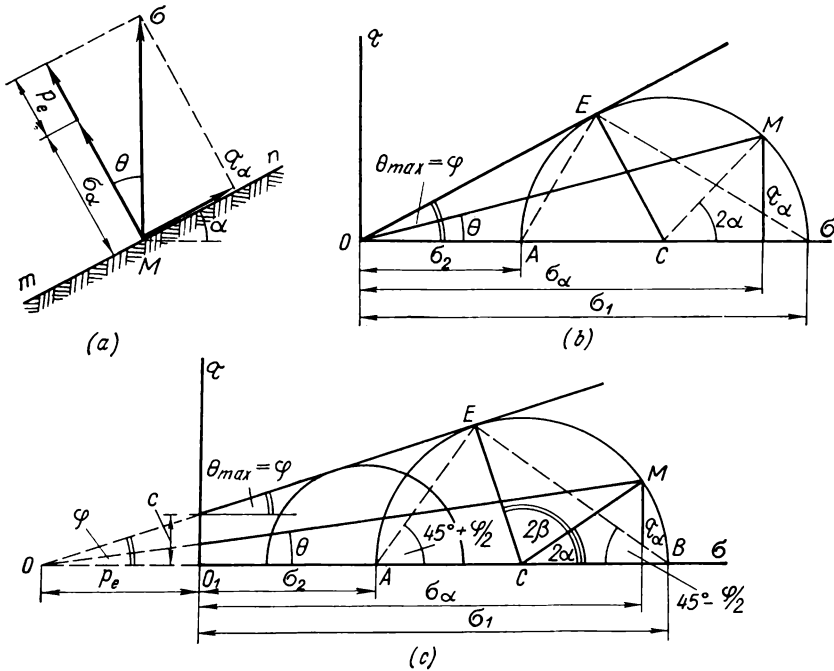


Fig. 64. Ultimate stress circles

(a) diagram of stresses in a given point; (b) shear diagram for loose soils; (c) same, for cohesive soils

Since we can draw a plurality of planes through a given point, then, obviously, we have to find the most disadvantageous plane which has the *maximum deviation angle*  $\theta_{max}$ . Then

$$\tan \theta_{max} \leq f$$

**Conditions of ultimate equilibrium.** For *loose soils*, according to the shear diagram (see Fig. 64b), the maximum angle of deviation  $\theta_{max}$  will be observed when the envelope  $OE$  touches the circle of ultimate stresses.

As has been shown earlier in the book (Section 2.4), and as follows from geometrical relationships, this condition is satisfied with the equality (2.24)

$$\frac{\sigma_1 - \sigma_2}{\sigma_1 + \sigma_2} = \sin \varphi$$

where  $\sigma_1$  and  $\sigma_2$  = principal stresses

$\varphi$  = angle of internal friction of the soil

This is the *condition of ultimate equilibrium for loose soils*. After simple trigonometrical transformations, the expression can be written in the form

$$\sigma_2 = \sigma_1 \frac{1 - \sin \varphi}{1 + \sin \varphi}$$

or

$$\boxed{\frac{\sigma_2}{\sigma_1} = \tan^2 (45^\circ \pm \varphi/2)} \quad (2.24'')$$

The last expression is widely used in the theory of soil pressure on retaining structures. The "minus" sign (in brackets) corresponds to the so-called *active* pressure, and the "plus" sign, to the *passive resistance* of loose soils.

The condition of ultimate equilibrium for loose soils is sometimes written in a different form, in which the principal stresses  $\sigma_1$  and  $\sigma_2$  are expressed through the component stresses  $\sigma_z$ ,  $\sigma_y$ , and  $\tau_{yz}$  (for the planar problem). Then we have the following expression which is identical with relationship (2.24):

$$\frac{(\sigma_z - \sigma_y)^2 + 4\tau_{yz}^2}{(\sigma_y + \sigma_z)^2} = \sin^2 \varphi \quad (2.24''')$$

For *cohesive soils*, similar to the foregoing, we can use the diagram of ultimate stresses (Fig. 64c) and find the *condition of ultimate equilibrium* in the form

$$\frac{\sigma_1 - \sigma_2}{\sigma_1 + \sigma_2 + 2p_e} = \sin \varphi \quad (2.25')$$

whence

$$\sigma_1 - \sigma_2 = 2 \sin \varphi \left( \frac{\sigma_1 + \sigma_2}{2} + p_e \right) \quad (2.25'')$$

But since, according to formula (2.23'),

$$p_e = \frac{c}{\tan \varphi} = c \cot \varphi$$

where  $c$  is the cohesion of soil, which is defined as the initial parameter of the envelope of the circles of ultimate pressures, then equation (2.25") can be written in the form

$$\frac{1}{\cos \varphi} \cdot \frac{\sigma_1 - \sigma_2}{2} - \tan \varphi \frac{\sigma_1 + \sigma_2}{2} = c \quad (2.25''')$$

The last formula is widely used in problems of the theory of ultimate equilibrium.

The condition of ultimate equilibrium for cohesive soils, when expressed in terms of the component stresses  $\sigma_z$ ,  $\sigma_y$ , and  $\tau$ , is of the form

$$\frac{(\sigma_z - \sigma_y)^2 + 4\tau_{yz}^2}{(\sigma_z + \sigma_y + 2c \cot \varphi)^2} = \sin^2 \varphi \quad (2.25^{IV})$$

Note that the circle of ultimate stresses makes it possible to determine the directions of *slip planes* for any given point.

If the point of contact of the ultimate line  $OE$  (Fig. 64c) is connected with the end of a section showing  $\sigma_2$  on a definite scale (point  $A$ ), then the direction  $EA$  will define the direction of the slip plane. According to Fig. 64c

$$\angle BCE = 2\beta = 90^\circ + \varphi$$

whence

$$\angle \beta = 45^\circ + \varphi/2$$

Thus, under conditions of ultimate equilibrium the slip planes are inclined at an angle  $\pm(45^\circ + \varphi/2)$  to the direction of the plane of the maximum principal stress, or, in other words, at an angle  $\pm(45^\circ - \varphi/2)$  to the direction of the principal stress  $\sigma_1$ .

**Differential equations of equilibrium of soils under ultimate stressed state.** *The planar problem.* In the general case of the stressed state under conditions of the planar problem the differential equations of equilibrium for any linearly deformable bodies with a horizontal boundary plane of the half-space (with the  $Y$  axis directed horizontally, and the  $Z$  axis, vertically) can be written, as is known from the theory of elasticity, in the following forms:

$$\frac{\partial \sigma_y}{\partial y} + \frac{\partial \tau_{yz}}{\partial z} = 0 \quad (a_1)$$

$$\frac{\partial \sigma_z}{\partial z} + \frac{\partial \tau_{yz}}{\partial y} = \gamma \quad (a_2)$$

where  $\sigma_z$ ,  $\sigma_y$ ,  $\tau_{yz}$  = component stresses  
 $\gamma$  = unit weight of soil

These *two* differential equations contain *three* unknowns ( $\sigma_z$ ,  $\sigma_y$ , and  $\tau_{yz}$ ); thus, the problem (without additional conditions) is

statically indeterminate. When a third equation is added to these two, for instance, (2.25<sup>IV</sup>), we get a closed system of three equations with three unknowns, but for the *ultimate stressed state*, since equation (2.25<sup>IV</sup>) is the condition of ultimate equilibrium

$$\frac{(\sigma_z - \sigma_y)^2 + 4\tau_{yz}^2}{(\sigma_z + \sigma_y + 2c \cot \varphi)^2} = \sin^2 \varphi \quad (a_3)$$

Thus, the problem, when stated generally, is statically determinate.

The solution of the differential equations of equilibrium (a<sub>1</sub>) and (a<sub>2</sub>) together with the condition of ultimate equilibrium (a<sub>3</sub>) was

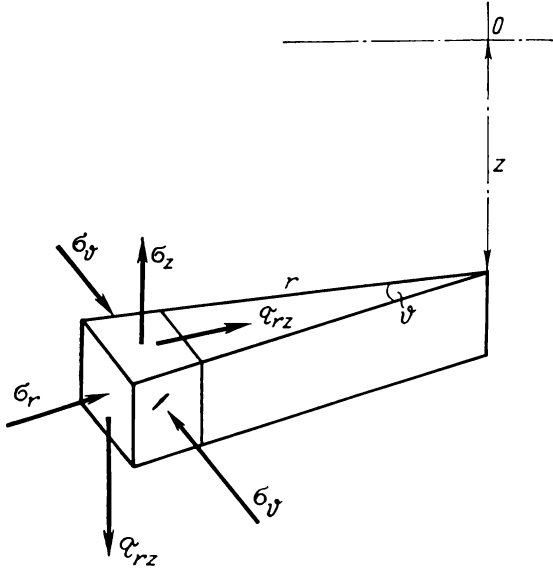


Fig. 65. Stresses for the three-dimensional axisymmetrical problem

later obtained (by Prof. V. V. Sokolovsky in 1942) as a system of hyperbolic equations.

The *three-dimensional problem* has a closed system of equations (statically determinate) only for the case of axial symmetry.

For the axisymmetrical problem, using a cylindrical system of coordinates  $(r, \vartheta)$  and the notation of component stresses as in Fig. 65, we get the following set of equilibrium equations:

$$\frac{\partial \sigma_r}{\partial r} + \frac{\partial \tau_{rz}}{\partial z} + \frac{\sigma_r - \sigma_\vartheta}{r} = 0 \quad (b_1)$$

$$\frac{\partial \sigma_z}{\partial z} + \frac{\partial \tau_{rz}}{\partial r} + \frac{\tau_{rz}}{r} = \gamma \quad (b_2)$$

In the cylindrical system of coordinates the conditions of ultimate equilibrium can be written as follows:

$$\frac{(\sigma_r - \sigma_z)^2 + 4\tau_{rz}^2}{(\sigma_r + \sigma_z + 2c \cot \varphi)^2} = \sin^2 \varphi \quad (b_3)$$

In addition, the shear stresses along the meridional planes are equal to zero because of symmetry, and therefore, the stress is the principal one and, besides, for the axisymmetrical problem

$$\sigma_\varphi = \sigma_2 = \sigma_3 \quad (b_4)$$

Equation (b<sub>4</sub>) is a supplementary one to the system of equations (b<sub>1</sub>)-(b<sub>3</sub>) and makes the latter statically determinate. The above system of equations of ultimate equilibrium (b<sub>1</sub>)-(b<sub>4</sub>) for the axisymmetrical problem (formulated by Prof. V. G. Berezantsev in 1952) corresponds to the case of deformations of soil *from the axis of symmetry OZ*. Some important cases of solution of this problem are discussed below.

#### 4.3. CRITICAL LOADS ON SOIL

In Section 4.1 we have discussed the mechanical phenomena occurring in soils with an increase of local loads and established that critical loads of two kinds can exist in soils (at pressures exceeding the structural strength): (1) a load corresponding to the *beginning of formation of shear zones* in soil and the *end of the compaction phase*, when the relationships arising between shear and normal stresses at the edge of the load result in the ultimate stressed state of the soil (first at the edges of the foundation base), and (2) a load at which *continuous regions of ultimate equilibrium* are formed under the loaded surface and the soil becomes unstable with *its load-bearing capacity being completely exhausted*.

The first load will be called the *initial critical load* which is still completely *safe* in the bases of structures, since before attaining this load the soil will always be in the *compaction phase*. The second load, at which the load-bearing capacity of the soil is completely exhausted, will be termed the *ultimate critical load* on soil under the given loading conditions.

**Initial critical load on soil.** Consider the action of a uniformly distributed load  $p$  over a band of width  $b$  in the presence of lateral surcharge  $q = \gamma h$  (where  $\gamma$  is the unit weight of soil and  $h$  is the foundation depth of the loaded surface, see Fig. 66).

The vertical compressive stress (pressure) from the soil dead weight with a horizontal boundary surface is

$$\sigma_1 = \gamma (h + z) \quad (c_1)$$

where  $z$  is the depth of location of the considered point below the plane of load application.

The problem is to find the load *in*  $p_{cr}$  at which the shear zones (zones of ultimate equilibrium) only begin to form under the loaded surface. Since for a band-shape load (planar problem) the shear stresses will be the maximum at the *edges* of the load, it is natural

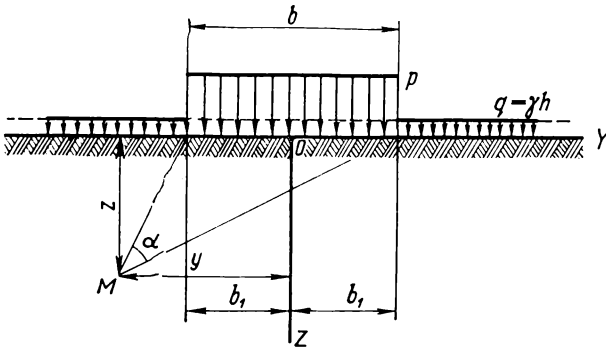


Fig. 66. Diagram of the action of a band-shape load

to expect that zones of ultimate equilibrium will be formed in these places with an increase of load.

We introduce an additional assumption that pressures from the dead weight of soil are distributed hydrostatically, i.e.,

$$\sigma_2 = \sigma_1 = \gamma (h + z) \quad (c_2)$$

With this assumption, the problem was first solved by Prof. N. P. Puzyrevsky in 1929, then by N. M. Gersevanov in 1930 and O. K. Frelich in 1934.

We apply the condition of ultimate equilibrium, for instance, in the form of expression (2.25")

$$\sigma_1 - \sigma_2 = 2 \sin \varphi \left( \frac{\sigma_1 + \sigma_2}{2} + p_e \right)$$

For an arbitrary point  $M$  (see Fig. 66) located at a depth  $z$  and characterized by a vision angle  $\alpha$ , we find the principal stresses [by formulae (3.12)] assuming that the dead weight of soil acts as a continuous load

$$\left. \begin{aligned} \sigma_1 &= \frac{p - \gamma h}{\pi} (\alpha + \sin \alpha) + \gamma (h + z) \\ \sigma_2 &= \frac{p - \gamma h}{\pi} (\alpha - \sin \alpha) + \gamma (h + z) \end{aligned} \right\} \quad (c_3)$$

Substituting these expressions for  $\sigma_1$  and  $\sigma_2$  into the condition of ultimate equilibrium (2.25'') and taking into account that  $p_e = c \cot \varphi$  [formula (2.23')], we get

$$\frac{p-\gamma h}{\pi} \sin \alpha - \sin \varphi \left( \frac{p-\gamma h}{\pi} \alpha + \gamma h + \gamma z \right) = c \cos \varphi \quad (c_4)$$

This expression can be regarded as the equation of the boundary region of ultimate equilibrium, and  $z$  as the ordinate of this region, since this expression satisfies the condition of ultimate equilibrium (2.25'').

Solving equation (c<sub>4</sub>) for  $z$  we obtain

$$z = \frac{p-\gamma h}{\pi \gamma} \left( \frac{\cos \alpha}{\sin \varphi} - \alpha \right) - \frac{c}{\gamma} \cot \varphi - h \quad (c_5)$$

We find  $z_{\max}$  by the known rules of higher mathematics

$$\frac{dz}{d\alpha} = \frac{p-\gamma h}{\pi \gamma} \left( \frac{\cos \alpha}{\sin \varphi} - 1 \right) = 0 \quad (c_6)$$

whence

$$\cos \alpha = \sin \varphi \quad \text{or} \quad \alpha = \frac{\pi}{2} - \varphi; \quad \sin \left( \frac{\pi}{2} - \varphi \right) = \cos \varphi \quad (c_7)$$

Substituting these expressions into (c<sub>6</sub>) and solving the latter for  $p = p_{cr}$ , we get

$$p_{cr} = \frac{\pi}{\cot \varphi + \varphi - \pi/2} (\gamma z_{\max} + \gamma h + c \cot \varphi) + \gamma h \quad (4.1)$$

Note that according to BC&R, the standard pressure  $R^{st}$  on soil is assumed to be such at which the zones of ultimate equilibrium under the foundation edges do not extend deeper than  $z_{\max} = b/4$  (where  $b$  is the width of the foundation). Prof. N. N. Maslov allows that  $z_{\max} = b \tan \varphi$ , i.e., that  $z_{\max}$  is still beyond the vertical planes passed through the edges of a band-shape load. At a lower pressure, it is permissible to assume that the relationship between deformations and stresses is *linear* and the soil is in the *compaction phase*.

If *no development* of zones of ultimate equilibrium is *allowed* for all points under the foundation base, then we have to assume in equation (4.1) that

$$z_{\max} = 0 \quad (c_8)$$

The maximum pressure at which no zones of ultimate equilibrium will be in any point of soil ( $z_{\max} = 0$ ) is termed the *initial critical pressure on soil*, in  $p_{cr}$ . Then we have from equation (4.1)

$$\text{in } p_{cr} = \frac{\pi (\gamma h + c \cot \varphi)}{\cot \varphi + \varphi - \frac{\pi}{2}} + \gamma h \quad (4.2)$$

This is Puzyrevsky's formula for the initial critical load on soil. The pressure found by this formula may be regarded as *completely safe* for bases of structures, so that no additional safety factors must be introduced.

The formula may be given a different form by separating the multipliers which depend only on the angle of internal friction of soil and tabulating them. But calculation of  $in p_{cr}$  by formula (4.2) also encounters no difficulties.

For *perfectly cohesive soils* (for which  $\varphi \approx 0$ ,  $c \neq 0$ ), the expression for  $in p_{cr}$  becomes still simpler.

The condition of ultimate equilibrium for soils of this kind is as follows:

$$\tau_{\max} = \frac{\sigma_1 - \sigma_2}{2} \leq c$$

whence

$$\sigma_1 - \sigma_2 \leq 2c$$

Substituting the expressions for the principal stresses [by formulae (c<sub>3</sub>) at  $z = 0$ ], we get

$$\frac{p - \gamma h}{\pi} \sin \alpha = c$$

This expression has a maximum at  $\sin \alpha = 1$  when the state of ultimate equilibrium begins to form under the edge of foundation. Then

$$in p_{cr} = \pi c + \gamma h \quad (4.3)$$

The last expression is often used to determine the standard (safe) pressure for clayey soils with a low angle of internal friction (practically with  $\varphi \leq 5$  to 7 degrees), and also for permanently frozen soils (with their temperature being always maintained below zero) taking account of the relaxation of cohesive forces, with  $c_{st}$  being substituted for  $c$ .

**Ultimate load for loose and cohesive soils.** As has been said earlier, the second critical load on soil must be the *ultimate load* corresponding to the *total exhaustion of the load-bearing capacity of the soil* and continuous development of zones of ultimate equilibrium, which for foundation bases is attained after the formation of the rigid core that deforms the base and expands the soil laterally.

The solution of the differential equations of equilibrium together with the conditions of ultimate equilibrium makes it possible to determine mathematically the exact outlines of slip surfaces. By using the latter, the magnitude of ultimate load (pressure) on soil corresponding to the *maximum load-bearing capacity* of the base can be estimated with a sufficiently high accuracy.

This problem was first solved by Prandtl and Reissner in 1920-21 for a *weightless soil* loaded with a continuous and band-shape load (the ultimate magnitude of this load being sought for), with the following expression being obtained for the ultimate load on soil:

$$\text{ult } p_{cr} = (q + c \cot \varphi) \frac{1 + \sin \varphi}{1 - \sin \varphi} e^{\pi \tan \varphi} - c \cot \varphi \quad (4.4)$$

where  $q$  is lateral surcharging;  $q = \gamma h$  ( $h$  being the depth of application of the band-shape load, see Fig. 67).

For the case considered (a band-shape flexible load with lateral surcharging and without account of the volume forces due to the

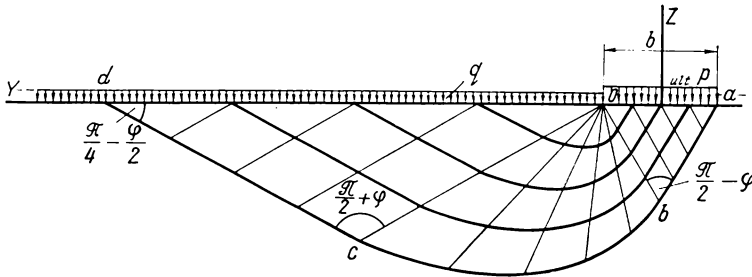


Fig. 67. Network of slip lines in soil with a band-shape load under lateral surcharging without taking into account the dead weight of soil

dead weight), the following exact outline of slip lines has been found (Fig. 67): in the triangle  $Ocd$ , two families of parallel straight lines inclined at an angle  $\pm \left( \frac{\pi}{4} - \frac{\varphi}{2} \right)$  to the horizontal; within the angle  $cOb$ , a bundle of straight lines radiating from point  $O$  and the conjugated logarithmic helices; and finally, in the triangle  $Oab$  (under the base of the load), two families of parallel straight lines inclined at an angle  $\pm \left( \frac{\pi}{4} + \frac{\varphi}{2} \right)$  to the horizontal.

The described network of slip lines, with the triangle  $Oab$  being replaced by the outline of the rigid core, was later used by a number of researchers (K. Terzaghi, A. Caquot, J. Kerisel, V. G. Berezantsev, and others) for approximate estimations of the ultimate load onto a ponderable soil under rigid foundations.

Note that for a particular case of *perfectly cohesive* soils ( $\varphi = 0$ ,  $c \neq 0$ ) the ultimate load under conditions of the planar problem (with a band-shape loading) according to Prandtl is

$$\text{ult } p_{pl} = (2 + \pi) c + q \quad (4.5)$$

or

$$\text{ult } p_{pl} = 5.14c + \gamma h \quad (4.5')$$

For an axisymmetrical three-dimensional problem (a circle or a square), the ultimate load for perfectly cohesive soils (according to A. Yu. Ishlinsky, 1947) is

$$\text{ult } p_{sq} = 5.7c + q \quad (4.6)$$

For an *obliquely acting load with lateral surcharging* on the soil possessing friction and cohesion (Fig. 68), the solution has been found by V. V. Sokolovsky (1952) as the sum of the ultimate load

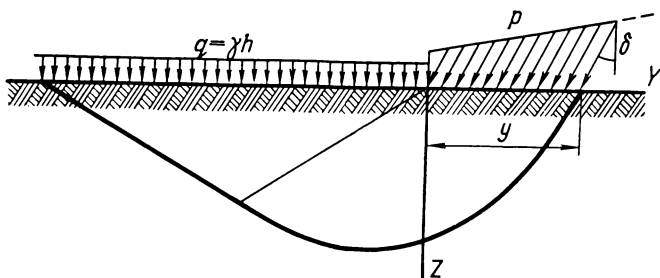


Fig. 68. Diagram of the action of an oblique load on soil

for a perfectly loose soil ( $c = 0$ ,  $\varphi \neq 0$ ,  $\gamma \neq 0$ ) with regard to the action of its dead weight and the ultimate load for a cohesive soil but without account of its dead weight ( $c \neq 0$ ,  $\varphi = 0$ ,  $\gamma = 0$ ); the solution gives the results very close to those of the exact one.

The vertical component of the ultimate load is then determined (with the notation adopted) by the following expression:

$$\text{ult } p_{cr} = N_{\gamma}\gamma y + N_q q + N_c c \quad (4.7)$$

where  $N_{\gamma}$ ,  $N_q$ , and  $N_c$  are the *coefficients of load-bearing capacity of soil*, which are determined by calculating the slip lines on the plotted network as a function of the angle of internal friction and the inclination of load.

Note that the form of equation (4.7), first proposed by Prof. K. Terzaghi in 1943, has become the canonical one and all other solutions obtained for the ultimate load on soil at different boundary conditions and different surchargings can be reduced to it.

The coefficients of load-bearing capacity  $N_{\gamma}$ ,  $N_q$ , and  $N_c$  for the case considered are given in Table 4.1 compiled at the Computing Centre of the USSR Academy of Sciences.

The horizontal component of ultimate pressure on soil under the action of a band-shape oblique load can be found by the formula

$$p_t = p_n \tan \delta \quad (4.8)$$

where  $\delta$  is the angle of inclination of the band-shape load to the vertical (see Fig. 68).

Table 4.1

## Coefficients of Load-Bearing Capacity for an Oblique Band-Shape Load

$\delta$ , degrees	Coefficients	$\varphi$ , degrees								
		0	5	10	15	20	25	30	35	40
0	$N_\gamma$	0.00	0.17	0.56	1.40	3.16	6.92	15.32	35.19	86.46
	$N_q$	1.00	1.57	2.47	3.94	6.40	10.70	18.40	33.30	64.20
	$N_c$	5.14	6.49	8.34	11.00	14.90	20.70	30.20	46.20	75.30
5	$N_\gamma$	—	0.09	0.38	0.99	2.31	5.02	11.10	24.38	61.38
	$N_q$	—	1.24	2.16	3.44	5.56	9.17	15.60	27.90	52.70
	$N_c$	—	2.72	6.56	9.12	12.50	17.50	25.40	38.40	61.60
10	$N_\gamma$	—	—	0.17	0.62	1.51	3.42	7.64	17.40	41.78
	$N_q$	—	—	1.50	2.84	4.65	7.65	12.90	22.80	42.40
	$N_c$	—	—	2.84	6.88	10.00	14.30	20.60	31.10	49.30
15	$N_\gamma$	—	—	—	0.25	0.89	2.15	4.93	11.34	27.61
	$N_q$	—	—	—	1.79	3.64	6.13	10.40	18.10	33.30
	$N_c$	—	—	—	2.94	7.27	11.00	16.20	24.50	38.50
20	$N_\gamma$	—	—	—	—	0.32	1.19	2.92	6.91	16.41
	$N_q$	—	—	—	—	2.09	4.58	7.97	13.90	25.40
	$N_c$	—	—	—	—	3.00	7.68	12.10	18.50	29.10
25	$N_\gamma$	—	—	—	—	—	0.38	1.50	3.85	9.58
	$N_q$	—	—	—	—	—	2.41	5.67	10.20	18.70
	$N_c$	—	—	—	—	—	3.03	8.09	13.20	21.10
30	$N_\gamma$	—	—	—	—	—	—	0.43	1.84	4.96
	$N_q$	—	—	—	—	—	—	2.75	6.94	13.10
	$N_c$	—	—	—	—	—	—	3.02	8.49	14.40
35	$N_\gamma$	—	—	—	—	—	—	—	0.47	2.21
	$N_q$	—	—	—	—	—	—	—	3.08	8.43
	$N_c$	—	—	—	—	—	—	—	2.97	8.86
40	$N_\gamma$	—	—	—	—	—	—	—	—	0.49
	$N_q$	—	—	—	—	—	—	—	—	3.42
	$N_c$	—	—	—	—	—	—	—	—	2.88

Approximate values of the coefficients of load-bearing capacity were calculated by K. Terzaghi in 1943 under assumption that the outline of slip lines is as for a weightless soil with the presence of a compacted triangular core whose faces are inclined at an angle  $\varphi$  to the foundation base and that the core upon setting overcomes the passive resistance of soil over plane surfaces of sliding (see Sec. 4.6 below).

In that case formula (4.7) takes the following form:

$$ult p_{cr} \approx N'_\gamma \gamma b_1 + N'_q q + N'_c \quad (4.7')$$

where  $N'_\gamma$ ,  $N'_q$  and  $N'_c$  = coefficients of load-bearing capacity determined from the graph in Fig. 69  
 $b_1$  = half-width of the foundation

Note that for the case of the planar problem the coefficients of load-bearing capacity found by Terzaghi differ only slightly from the values given by more rigorous solutions (for instance, those found by V. G. Berezantsev), but they are inapplicable to the three-dimensional problem, since certain correction factors (empirical, as recommended by Terzaghi) must be introduced.

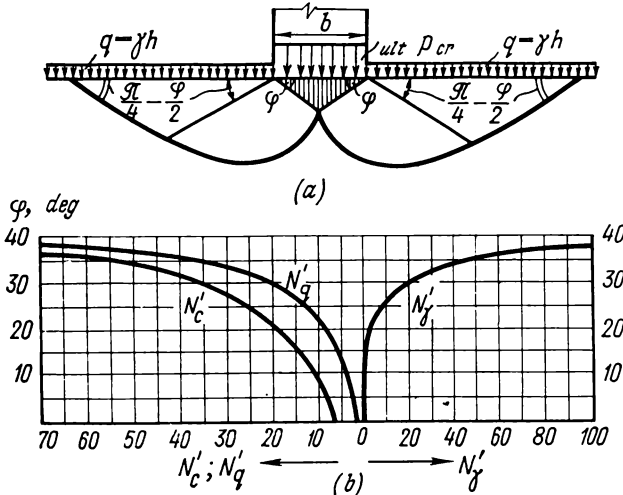


Fig. 69. Zones of ultimate equilibrium under a strip foundation (according to Terzaghi)  
 (a) slip lines; (b) diagram of coefficients of load-bearing capacity

Note that the data given in Table 4.1 make it possible to determine the ultimate load on soil also for a vertical load, i.e., when  $\delta = 0$ .

The results obtained by formula (4.7) and Table 4.1 are close to a strict solution only for an oblique semi-infinite load (see Fig. 68), which corresponds in practice only to cases of a very wide surface of the structure base.

If, however, the foundation has a finite width  $b$ , then the data of Table 4.1 can be used, with a certain approximation, for determining the ultimate load-bearing capacity of a soil base under conditions of one-sided bulging.

For the edge of an obliquely acting load (assuming  $y = 0$ ) we have

$$ult p_0 = N_q q + N_c c$$

and for the ordinate corresponding to the foundation width (i.e., with  $y = b$ ) and with no bulging to the opposite side, we get

$$ult p_b = N_\gamma \gamma b + p_0$$

Then the average magnitude of the vertical component of ultimate pressure on soil will be

$$ult p_{cr} \approx \frac{1}{2} (p_0 + p_b)$$

In order to determine the ultimate load on the soil base with a *finite width of a band-shape oblique load* (or, what is the same, with an eccentric force obliquely acting on the foundation) and different foundation depths ( $h_1$  and  $h_2$ ) to the left and right of the band-shape load (Fig. 70a), we can use M.V. Malyshev's grapho-analytical method\* and an additional table of coefficients of load-bearing capacity  $N''_\gamma$ ,  $N''_q$ ,  $N''_c$  (Table 4.2) for the right-hand portion of the ultimate load; these coefficients can be calculated by the same relationships as those in Table 4.1.

The ordinates of the trapezoidal diagram of ultimate pressures  $OO'$  and  $aa'$  (Fig. 70b) can be calculated by the formula

$$ult p = N_\gamma \gamma y + N_q \gamma h_1 + N_c c \quad (d_1)$$

and the ordinates  $aa''$  and  $OO''$ , by the formula

$$ult p = N''_\gamma \gamma (b - y) + N''_q \gamma h_2 + N''_c c \quad (d_2)$$

Table 4.2

**Coefficients of Load-Bearing Capacity for an Oblique Load Acting from the Right (Opposite to Its Inclination)**

$\delta$ , degrees	Coefficients	$\phi$ , degrees				
		0	10	20	30	40
0	$N''_\gamma$	0	0.56	3.16	15.3	86.4
	$N''_q$	1	2.47	6.40	18.4	64.2
	$N''_c$	5.14	8.34	14.8	30.1	75.3
10	$N''_\gamma$	—	0.78	5.26	31.0	136
	$N''_q$	—	1.65	7.79	23.9	90.5
	$N''_c$	—	3.69	18.7	39.7	105
20	$N''_\gamma$	—	—	7.80	41.0	176
	$N''_q$	—	—	3.05	28.3	117
	$N''_c$	—	—	5.64	47.3	139
30	$N''_\gamma$	—	—	—	46.9	251
	$N''_q$	—	—	—	6.70	141
	$N''_c$	—	—	—	9.85	167

\* Paper of M. V. Malyshev in the works of the 5th International Congress on Soil Mechanics and Foundation Engineering. Papers to the V Congress, edited by N. A. Tsytovich. Stroizdat, 1961.

where  $N_\gamma$ ,  $N_q$ , and  $N_c$  = coefficients of load-bearing capacity to be found from Table 4.1

$N_\gamma^*$ ,  $N_q^*$ , and  $N_c^*$  = same, from Table 4.2

Assuming in formulae (d<sub>1</sub>) and (d<sub>2</sub>) that  $y = 0$  and  $y = b$ , we can find the ordinates of ultimate diagrams; the values of  $p'$  and of the average ultimate load on soil (ultimate pressure) are determined graphically by the method shown in Fig. 70b.

The value of *ult*  $p_{cr}$  for the considered kind of eccentric load can be found more accurately by introducing a correction for the difference

between the eccentricity of the ultimate load (which is found from the diagram in Fig. 70b) and the actual eccentricity, which, however, can only be determined by a special experimental graph; this is done only in special cases in order to check the safety factor.

Note that the tabulated solution by the theory of ultimate equilibrium which we have discussed (Tables 4.1 and 4.2) is only applicable to a flexible or non-cohesive loading (for instance, soil filling) and a low foundation depth (with  $h/b \leq 0.5$ ) when the effect of the foundation depth is allowed to be replaced by the action of a lateral load  $q = \gamma h$ .

For *bases of massive foundations*, the ultimate load should be determined

with account of the rigid core of limited displacements, which is formed under the bottom of rigid foundations; this is a complicated mathematical problem and its closed solution has not yet been found. In such cases, use is made of an approximate technique consisting in that the outlines of slip surfaces are given in advance but such that they practically coincide with the accurate results of a numerical solution of the system of differential equations of ultimate equilibrium (in finite differences).

This technique was widely used by Prof. V. G. Berezantsev in 1952-60; the solutions obtained by him for a band-shape and axisymmetrical problems of the theory of ultimate equilibrium with account of the rigid core are discussed below.

The outline of the rigid core was taken by Berezantsev (on the basis of experimental data) in the form of a rectangular triangle

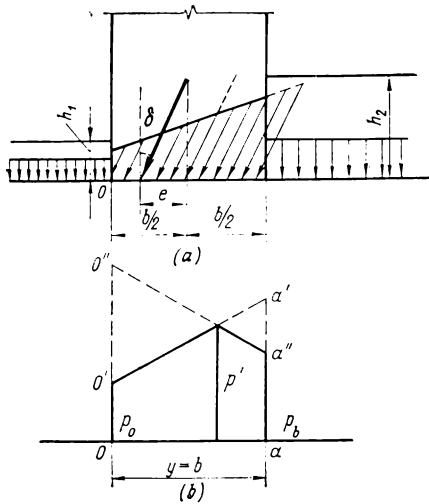


Fig. 70. Calculation diagram to determine the ultimate load on soil with an oblique eccentric load

(planar problem) or a cone (axisymmetrical three-dimensional problem) with the apex angle of 90 degrees; the depth of foundation was then taken into account by replacing it with a lateral surcharging  $q = \gamma h$ , which makes the solution applicable only to shallow foundations (with  $h/b \leq 0.5$ ).

For a *planar problem* (a band-shape load) the pattern of slip lines was taken such as that shown in Fig. 71: in triangles  $Obc$  and  $O_1b_1c_1$ , two families of conjugated straight lines inclined at an angle  $\pm(\pi/4 - \varphi/2)$  to the horizontal; in sectors  $Oab$  and  $O_1ab_1$ , bundles of straight lines radiating from  $O$  and  $O_1$  and a family of logarithmic

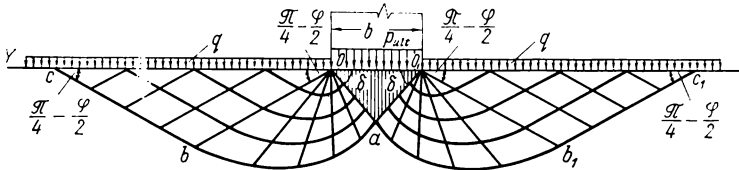


Fig. 71. Network of slip lines in soil under a rigid band-shape foundation with account of the compacted core

helices, the angle of inclination of the rigid core to the foundation base being taken approximately equal to  $\delta = \pi/4$ .

The formula obtained for the case considered can be written in its earlier form, namely,

$$ult p_{pl} = N_{\gamma pl} \gamma b_1 + N_{q pl} q + N_{c pl} c \tag{4.7"}$$

where  $N_{\gamma pl}$ ,  $N_{q pl}$ , and  $N_{c pl}$  = coefficients of load-bearing capacity for the *planar problem*, such as given in Table 4.3

- $b_1$  = half-width of the band-shape load
- $q = \gamma h$  = lateral surcharging
- $c$  = cohesion of the soil

In the case of a *three-dimensional axisymmetrical problem*, the ultimate load on soil for shallow bases and foundations (with  $h/b <$

Table 4.3

Coefficients of Load-Bearing Capacity for a Planar Problem with Account of Soil Dead Weight and Compacted Core

Coefficients	$\varphi$ , degrees												
	16	18	20	22	24	26	28	30	32	34	36	38	40
$N_{\gamma pl}$	3.4	4.6	6.0	7.6	9.8	13.6	16.0	21.6	28.6	39.6	52.4	74.8	100.2
$N_{q pl}$	4.4	5.3	6.5	8.0	9.8	12.3	15.0	19.3	24.7	32.6	41.5	54.8	72.0
$N_{c pl}$	11.7	13.2	15.1	17.2	19.8	23.2	25.8	31.5	38.0	47.0	55.7	70.0	84.7

$< 0.5$ ) was obtained by solving an appropriate equation for the outline of the envelope of slip line in the form of a logarithmic helix in the zone of radial shears and of conjugated straight lines inclined at the angles shown in Fig. 72, in the lateral zones. The formula for the ultimate load corresponding to exhaustion of the maximum load-bearing capacity of the soil may be given the former

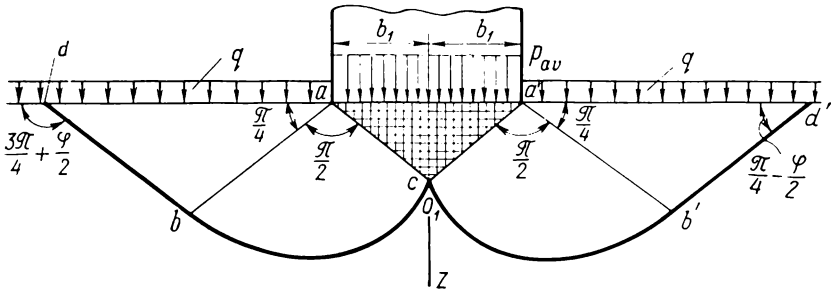


Fig. 72. Approximate outline of enveloping slip surfaces for the case of axi-symmetrical problem with account of the compacted core

shape of expression (4.7) by changing only the magnitude of the coefficients of load-bearing capacity

$$\text{ult } p_{sq} = N_{\gamma sq} \gamma b_1 + N_{q sq} q + N_{c sq} c \quad (4.7^m)$$

where  $N_{\gamma sq}$ ,  $N_{q sq}$  and  $N_{c sq}$  = coefficients of load-bearing capacity for the axisymmetrical problem, to be found from Table 4.4 (according to Berezantsev)

$b_1$  = half the side of a square (or the radius of a circular) surface of the foundation base

For medium-deep foundations (with  $0.5 < h/b < 2$ ), and even more so for deep foundations (with  $h/b \geq 2$ ), it would be incorrect to replace the effect of the foundation depth on the ultimate load of the base by the action of a non-cohesive lateral surcharging ( $q = \gamma h$ ), since the mechanical phenomena occurring on loading of deep foundations are quite different from those for shallow foundations because of the solidity of the whole mass of the soil.

For *medium-deep* foundations on loose soils, the problem of ultimate load on the base can be solved by an approximate method in which the S-shaped envelope of slip line (see Fig. 63, case 2) is approximated with straight sections and, in the zone of radial shears, with logarithmic helices, with account of the rigid core of a triangular outline with a right angle at the apex.

Table 4.4

**Coefficients of Load-Bearing Capacity for Foundations  
with a Circular or Square Surface of the Base**

Coefficients	$\varphi$ , degrees						
	16	18	20	22	24	26	28
$N_{\gamma sq}$	4.4	5.7	7.3	9.9	14.0	18.9	25.3
$N_{q sq}$	4.5	6.5	8.5	10.8	14.1	18.6	24.8
$N_{c sq}$	12.8	16.8	20.9	24.6	29.9	36.4	45.0
$\frac{l}{2b_1}$	1.44	1.50	1.58	1.65	1.73	1.82	1.91

Coefficients	$\varphi$ , degrees						
	30	32	34	36	38	40	42
$N_{\gamma sq}$	34.6	48.8	69.2	97.2	142.5	216	317
$N_{q sq}$	32.8	45.5	64.0	87.6	127.0	185	270
$N_{c sq}$	55.4	71.5	93.6	120.0	161.0	219	300
$\frac{l}{2b_1}$	1.99	2.11	2.22	2.34	2.45	2.61	2.76

Note:  $l/2b_1$  is the relative length of the bulge prism.

Using this method V. G. Berezantsev has found the solution for loose soils in the following form:

for the planar problem

$$ult p_{pl h} = A_{pl} \gamma b \quad (4.9)$$

for the three-dimensional problem (with a square or circular surface of the foundation base)

$$ult p_{sq h} = A_{sq} \gamma b_1 \quad (4.10)$$

where  $A_{pl}$ ,  $A_{sq}$  = generalized coefficients of load-bearing capacity for loose soils, which can be determined from the graphs in Figs. 73 and 74 as a function of the angle of internal friction  $\varphi$  and relative foundation depth  $h/b$

$2b_1 = b$  = side of square (or diameter of circular) surface of the foundation base

As follows from formulae (4.9) and (4.10) and similar formulae, and also from tables and graphs of coefficients of load-bearing capacity (such as those in Figs. 73 and 74), the ultimate load on soil

increases substantially with an increase of the relative depth of foundation  $h/b$  and the width  $b$  of foundation base.

With a large depth of foundation and a large area of its base, the load-bearing capacity of soils becomes so high that it cannot be utilized completely in bases of structures since very high settlements then occur (the theory of calculation of these settlements will be

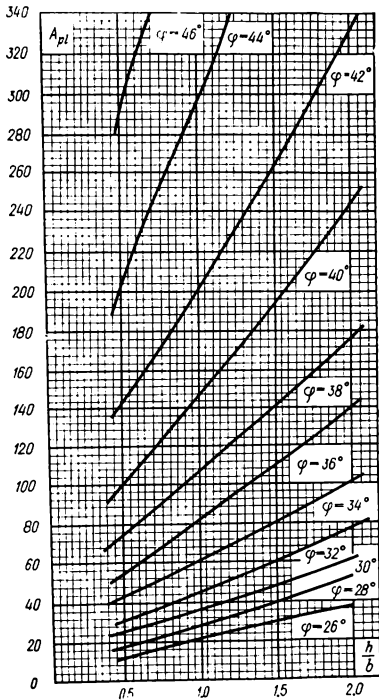


Fig. 73. Graph to determine the coefficients  $A_{pl}$  with  $0.5 < h/b < 2$

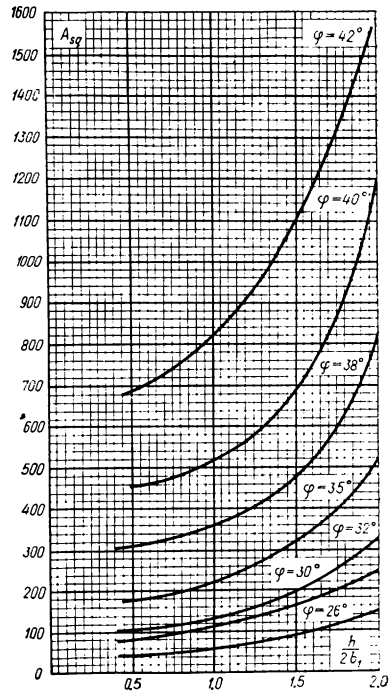


Fig. 74. Graph to determine the coefficients  $A_{sq}$  with  $0.5 < h/2b_1 < 2$

discussed in the next chapter) that are inadmissible for bases of structures.

For that reason, bases of structures are usually designed for pressures of only 25 to 50 per cent of the ultimate ones, so that the load-bearing capacity of soil bases can be completely utilized.

**Example 4.1.** Find the initial critical load  $in p_{cr}$  on soil under a strip foundation of depth  $h = 1.5$  m and base width  $b = 3.0$  m, if known: (a) the angle of internal friction of soil (loam)  $\varphi = 25^\circ$ ; (b) cohesion  $c = 0.2$  kgf/cm<sup>2</sup>; and (c) unit weight  $\gamma = 1.9$  gf/cm<sup>3</sup>.

By formula (4.2) (with  $\varphi = 25^\circ = 25\pi/180 = 0.436$ ,  $\cot \varphi = 2.145$ ;  $c = 0.2 \text{ kgf/cm}^2 = 2 \text{ tf/m}^2$ , and  $\gamma = 1.9 \text{ tf/m}^3$ ) we find

$$\begin{aligned} \text{in } p_{cr} &= \frac{\pi(\gamma h + c \cot \varphi)}{\cot \varphi + \varphi - \frac{\pi}{2}} + \gamma h = \frac{3.14(1.9 \times 1.5 + 2 \times 2.145)}{2.145 + 0.436 - 1.571} + 1.9 \times 1.5 = \\ &= 25.05 \text{ tf/m}^2 = 2.5 \text{ kgf/cm}^2 \text{ (approx.)} \end{aligned}$$

Such a unit load should be regarded as a completely safe pressure on soil and independent of the width of the foundation base, since no zones of ultimate equilibrium will be formed in points of the foundation base at this pressure and the soil will be in the compaction phase.

**Example 4.2.** Determine the ultimate load ( $ult p_{cr}$ ) on soil for the conditions of the previous example.

By formula (4.7), for the end points (with  $y = 0$  and  $y = b$ ) we have

$$ult p_0 = N_q q + N_c c \quad (e_1)$$

$$ult p_b = N_\gamma \gamma b + p_0 \quad (e_2)$$

For the vertical load ( $\delta = 0$ ) when  $\varphi = 25^\circ$ , we find from Table 4.1 that

$$N_q = 10.70$$

$$N_c = 20.70$$

$$N_\gamma = 6.92$$

Substituting these values into formulae (e<sub>1</sub>) and (e<sub>2</sub>) gives

$$ult p_0 \approx 10.7 \times 1.9 \times 1.5 + 20.7 \times 2 = 71.9 \text{ tf/m}^2$$

$$ult p_b \approx 6.92 \times 1.9 \times 3 + 71.9 = 111.3 \text{ tf/m}^2$$

Then

$$ult p \approx \frac{1}{2} (p_0 + p_b) = \frac{1}{2} (71.9 + 111.3) = 91.6 \text{ tf/m}^2 \approx 9.2 \text{ kgf/cm}^2$$

**Example 4.3.** Find the ultimate load for the same conditions but with account of formation of a rigid core under a massive foundation.

In this case, we use formula (4.7'') and the data of Table 4.3. Then

$$ult p_{pl} = N_\gamma \gamma b_1 + N_q p_l q + N_c p_l c$$

where  $b_1$  is half the width of the foundation.

For  $\varphi = 25^\circ$ , we find by interpolation from Table 4.3 that  $N_\gamma p_l = 11.7$ ,  $N_q p_l = 11.0$ ,  $N_c p_l = 21.5$ . Then

$$ult p_{pl} \approx 11.7 \times 1.9 \times 1.5 + 11.0 \times 2.85 + 21.5 \times 2 = 107.6 \text{ tf/m}^2 \approx 10.8 \text{ kgf/cm}^2$$

**Certain conclusions.** By analysing the results of numerous field and laboratory tests on determination of the ultimate load-bearing capacity of soils loaded with various stamps or foundations, which have been carried out in the last decade (see, for instance, the works of the 5th and 6th Congresses of ISSMFE), the following conclusions can be made:

(a) for perfectly cohesive clayey soils (possessing high cohesion and a very low coefficient of internal friction), the theoretical and experimental data coincide almost fully;

(b) when determining the load-bearing capacity of sand soils, the role of the initial parameter of the shear diagram must be taken into account;

(c) notwithstanding a large scatter of experimental data, the maximum load-bearing capacity of soil bases determined experimentally is, as a rule, substantially greater (often 1.5 to 2.5 times) than the calculated one, which suggests that boundary conditions (the depth of foundation, the shape and size of the rigid core under foundations, etc.) are not adequately estimated and that further studies are required, namely, of the outline of slip lines in soil above the foundation base, especially for deep foundations; of the mutual influence of zones of ultimate equilibrium and elastic zones (for a combined problem of the theory of elasticity and theory of plasticity); of the effect of the dead weight and compactness of soils, etc.;

(d) the existing rigorous methods of calculation which ensure a certain safety limit in practical calculations, require further development for more accurate account of boundary conditions, kinematical permissibility of solutions, and lamination of soils.

#### 4.4. STABILITY OF SOILS IN LANDSLIDES

**Causes of the breach of stability.** Analysis of stability of soils is of high practical importance for the design of earthen structures: embankments, cuts, dams, large open pits sometimes having the depth of 100 m and more, and similar structures.

The problem of stability of soils is a particular problem of the general theory of ultimate stressed state of soils, but has very essential peculiarities caused by the distinguishing features of the motion of soils when their stability is disturbed.

Calculations of stability of soils are a special division of the *statics* of structures. We shall discuss here only some of the main relationships which may illustrate the essence of the problems being discussed and give the most important methods for their solution which are applied in the design practice.

The most important causes of disturbance of stability of soil masses are (a) erosion processes and (b) disturbance of equilibrium.

*Erosion processes*, as a rule, occur slowly and imperceptibly. They depend on external meteorological and physico-geological conditions, and also on the properties of the soil surface; usually they are not considered in soil mechanics.

The study of the conditions of stability of soils and of their disturbance is, however, the direct object of soil mechanics.

*Breach of stability* of soil masses can occur abruptly with a slide of a large mass of soil; such disturbances are termed *landslides*. This kind of disturbance of equilibrium is the one most often observed; it occurs in various dips and natural slopes when the loads acting on the soil increase or the internal resistances decrease.

An increase of loads may take place when the pressure of the structures erected on dips and slopes exceeds a certain limit and also when the weight of the soil layers changes (increases) owing to their saturation with water after a prolonged period of rains or high-flood, or owing to retention of capillary moisture as the ground water level drops. A decrease of internal resistances may occur in

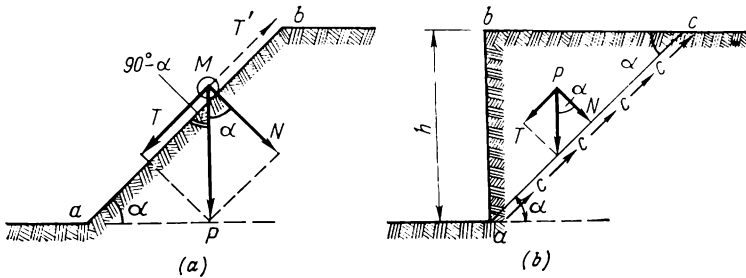


Fig. 75. Forces acting on a particle in a slope of perfectly loose soil (a) and on the vertical dip of a cohesive soil (b)

case of any destruction of natural supports in soil and also with a reduction of the effective friction (in the presence of pore-water pressure) and cohesion forces (on moistening and swelling of soils).

The following main kinds of landslides may be distinguished: (1) *rotational landslides* (with the formation of curvilinear failure surfaces); (2) *slip landslides* (with slippage along fixed surfaces); and (3) *liquefaction landslides* (sel flows of supersaturated soils along river beds and thalwegs).

We shall consider the conditions of equilibrium for landslides of each kind.

**Stability of free dips and slopes. Elementary problems.** In order to establish certain concepts, let us solve two elementary problems: (1) stability of the slope of a perfectly loose soil and (2) stability of a massif of a perfectly cohesive soil.

1. In the first case, let a solid particle  $M$  be lying freely on a slope of loose soil (Fig. 75a).

Let weight  $P$  of the particle be resolved into two components: the component  $N$  normal to the line of slope  $ab$ , and a tangential force  $T$ . Force  $T$  tends to move the particle to the slope base but is counteracted by the friction force  $T'$  which is proportional to the normal pressure, i.e.,  $T' = fN$  (where  $f$  is the coefficient of friction).

By projecting all the forces onto the inclined plane of the slope, we have

$$P \sin \alpha - fP \cos \alpha = 0$$

whence  $\tan \alpha = f$  and, since the friction coefficient  $f = \tan \varphi$ , we finally get

$$\alpha = \varphi \quad (4.11)$$

Thus, the *ultimate angle of slope of loose soils is equal to the angle of internal friction of the soil*. This angle is termed the *angle of repose*.

The concept of the angle of repose is only applicable to dry loose soils and is meaningless for cohesive clayey soils, since the angle of slope of the latter may vary from 0 to 90° depending on soil moistening and the height of the slope.

2. Consider the *conditions of equilibrium* for a perfectly *cohesive soil* ( $\varphi = 0$ ;  $c \neq 0$ ).

We assume approximately that disturbance of equilibrium at a certain ultimate height  $h$  will occur along a plane slip surface  $ac$  inclined at an angle  $\alpha$  to the horizontal (Fig. 75b).

We write an equation of equilibrium of all forces acting on a sliding prism  $abc$ . The active force here is the weight  $P$  of prism  $abc$ .

Noting that, according to Fig. 75b,  $bc = h \cot \alpha$ , we get

$$P = \frac{\gamma h^2}{2} \cot \alpha \quad (f_1)$$

Let the force  $P$  be resolved into a normal force and a force tangent to the slip surface  $ac$ . The forces that counteract slippage are only the cohesive forces  $c$  distributed over the slip plane  $ac = h/\sin \alpha$ .

Since the pressure in the upper point  $c$  of prism  $abc$  is zero and in the lower point  $a$ , at the maximum, we can take into account, on the average, only half the cohesion forces. Then, after elementary transformations, we come to a solution coinciding for the case considered with the rigorous solution by the theory of ultimate equilibrium.

By taking the sum of projections of all forces onto the direction  $ac$  and equating it to zero, we obtain the equation of equilibrium as follows:

$$\frac{\gamma h^2}{2} \cot \alpha \sin \alpha - \frac{c}{2} \cdot \frac{h}{\sin \alpha} = 0 \quad (f_2)$$

whence:

$$c = \frac{\gamma h}{2} \sin 2\alpha \quad (f_3)$$

We find the height  $h = h_{90}$  corresponding to the maximum utilization of cohesion forces. Then, evidently,  $\sin 2\alpha = 1$  and  $\alpha = 45^\circ$ .



where  $\bar{\sigma}_z$  = dimensionless ultimate pressure (Table 4.5)  
 $p_e = c \cot \varphi$  = cohesion pressure  
 $\bar{y}$  = relative coordinate (Table 4.5) whose actual value is  $\bar{y} = y \frac{\gamma}{c}$

Using the data of Table 4.5, we can easily calculate the ordinates of the diagram of ultimate pressures onto a horizontal surface of a plane slope for any values of  $\alpha$ ,  $\varphi$ ,  $c$ , and  $\gamma$ .

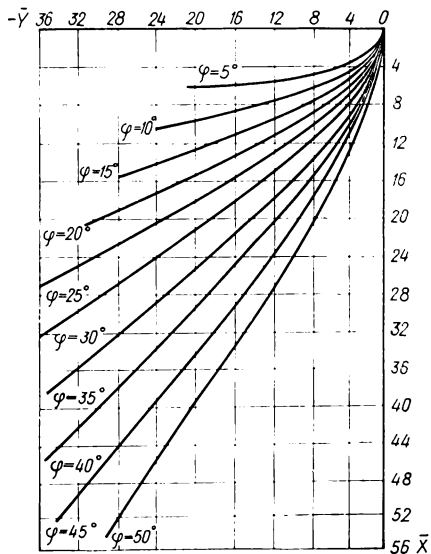


Fig. 77. The shape of outline of equistable slopes

the expression

$$p_0 = \frac{2c \cos \varphi}{1 - \sin \varphi} \quad (4.13)$$

If this load is regarded as the pressure of a soil layer, assuming that  $p_0 = \gamma h$ , then we get

$$h = \frac{2c \cos \varphi}{\gamma (1 - \sin \varphi)} \quad (4.13')$$

For a perfectly cohesive soil (when  $\varphi = 0$ ) we obtain the earlier formula (4.12)

$$h = \frac{2c}{\gamma}$$

2. The shapes of ultimate equistable slopes for a case when the soil possesses both friction and cohesion are shown in Fig. 77. These curves have been obtained by numerical solution of the differential equations of ultimate equilibrium by means of electronic computers.

The coordinates of equistable slopes are given in dimensionless units

$$x = \bar{x} \frac{c}{\gamma}, \quad y = \bar{y} \frac{c}{\gamma}$$

where  $\bar{x}$  and  $\bar{y}$  are dimensionless coordinates in Fig. 77.

The form of an equistable slope is constructed beginning from its upper edge.

According to V. V. Sokolovsky, the horizontal surface of an equistable slope can carry a uniformly distributed load determined by

Table 4.5

Dimensionless Ultimate Pressure  $\bar{\sigma}_z$  onto the Horizontal Surface of a Slope

$\bar{y}$	Values of $\bar{\sigma}_z$ at $\alpha$ , degrees															
	10				20				30				40			
	0	10	0	10	20	10	0	10	20	30	0	10	20	30	40	
0.0	8.34	7.51	14.8	12.7	10.9	30.1	24.3	19.6	15.7	75.3	55.9	41.4	30.6	22.5		
0.5	9.02	7.90	17.9	14.8	12.0	43.0	32.6	24.4	18.1	139.0	94.0	62.6	41.3	27.1		
1.0	9.64	8.26	20.6	16.6	13.1	53.9	39.8	28.8	20.3	193.0	126.0	81.1	50.9	31.0		
1.5	10.2	8.62	23.1	18.2	14.1	64.0	46.5	32.8	22.3	242.0	157.0	98.5	59.8	34.7		
2.0	10.8	8.95	25.4	19.9	15.0	73.6	52.9	36.7	24.2	292.0	186.0	115.0	68.4	38.1		
2.5	11.3	9.28	27.7	21.4	15.8	82.9	59.0	40.4	26.0	339.0	215.0	132.0	76.7	41.3		
3.0	11.8	9.59	29.8	23.0	16.7	91.8	65.1	44.1	27.8	386.0	243.0	148.0	84.9	44.4		
3.5	12.3	9.89	31.9	24.4	17.5	101.0	71.0	47.6	29.4	432.0	271.0	164.0	93.0	47.5		
4.0	12.8	10.2	34.0	25.8	18.3	109.0	76.8	51.2	31.1	478.0	299.0	179.0	101.0	50.4		
4.5	13.2	10.5	36.0	27.2	19.1	118.0	82.6	54.7	32.7	523.0	327.0	195.0	109.0	53.3		
5.0	13.7	10.8	38.0	28.7	19.9	127.0	88.3	58.1	34.3	568.0	354.0	211.0	117.0	56.2		
5.5	14.1	11.0	39.9	20.0	20.6	135.0	94.0	61.6	35.8	613.0	381.0	226.0	125.0	59.0		
6.0	14.5	11.3	41.8	31.4	21.4	143.0	99.6	65.0	37.4	658.0	409.0	241.0	132.0	61.7		

**Method of circular-cylindrical slip surfaces.** This method is widely employed in practice, since it ensures a certain reserve of stability and is based on experimental data for the shape of slip surfaces observed at rotational landslides. According to numerous natural measurements (for instance, those carried out by the Swedish geotechnical commission or the management of the Moskva-Volga channel), this shape is assumed to be *circular-cylindrical*, its most critical position being determined by calculation. Because of this and certain other assumptions (which will be discussed later), the method is an approximate one.

Let us assume that the centre of the circular-cylindrical slip surface of a sliding prism is at point  $O$  (Fig. 78a). The equation of equilibrium is  $\sum M_0 = 0$ . In order to find the equations of the moments relative to point  $O$ , the sliding prism  $ABC$  is divided by vertical planes into a number of sections, the weight  $P_i$  of each section being assumed to be applied in the point of intersection of the line of its application with the corresponding section of the arc of slip. The forces of interaction over the vertical planes of a section are neglected, assuming that the pressures from neighbouring sections are equal in magnitude and opposite in direction. After projecting the weights  $P_i$  onto the radius of rotation and its perpendicular direction, we can write an equation of equilibrium by equating to zero the moment of all the forces relative to the point of rotation

$$\sum T_i R - \sum N_i \tan \varphi R - cLR = 0 \quad (g_1)$$

Upon eliminating  $R$ , we get

$$T_i - \sum N_i \tan \varphi - cL = 0 \quad (g_2)$$

where  $L$  is the length of slip arc  $AC$ ;  $\varphi$  and  $c$  are respectively the angle of internal friction and cohesion of the soil; and  $T_i, N_i$  are component pressures from the weights of the sections, which can be determined graphically or calculated from measurements of angles  $\alpha_i$

$$T_i = P_i \sin \alpha_i; \quad N_i = P_i \cos \alpha_i$$

The coefficient of stability of a slope is expressed as the ratio of the moment of retaining forces to that of shear forces, i.e.,

$$\eta = \frac{M_{ret}}{M_{sh}} = \frac{\left( \sum_{i=1}^{i=n} N_i \tan \varphi + cL \right) R}{\sum T_i R}$$

or

$$\eta = \frac{\sum_{i=1}^{i=n} N_i \tan \varphi + cL}{\sum T_i} \quad (4.14)$$

Having thus found the coefficient of stability for an arbitrary arc of the slip surface, we have not yet solved the problem, since of all possible arcs of slip surfaces the one most critical must be chosen. The latter is found by the trial-and-error method by assuming

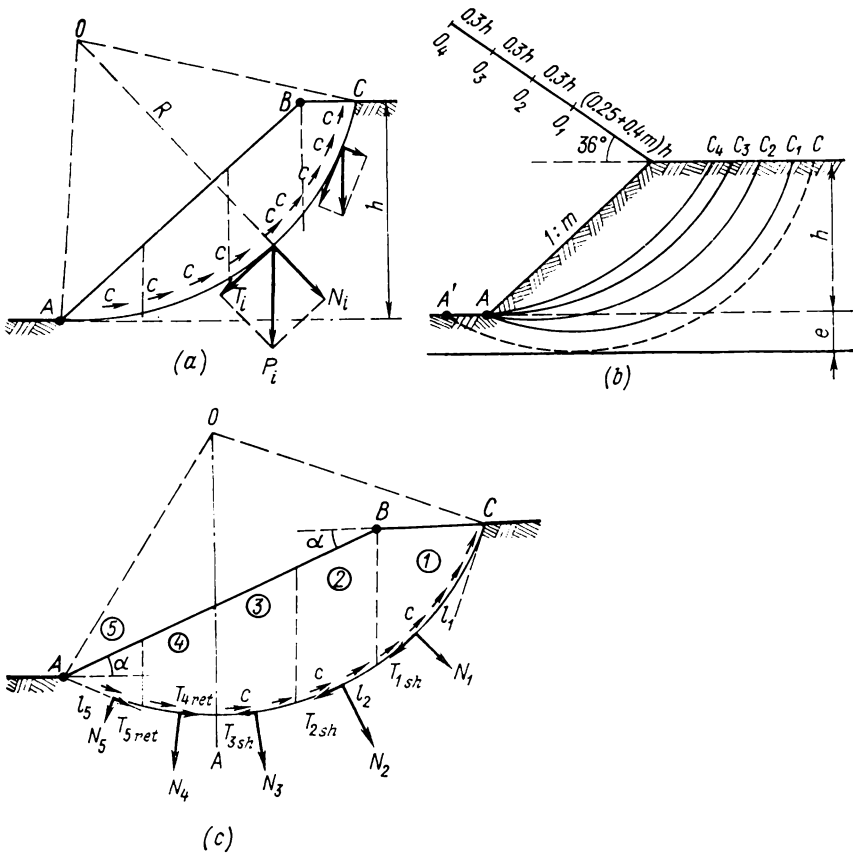


Fig. 78. To prediction of stability of a slope by circular-cylindrical slip surfaces

a) diagram of acting forces; (b) position of critical slip arcs; (c) diagram of forces acting along the slip surface

different positions of rotation points  $O$ ; the number of steps may be reduced by using certain techniques, for instance, those suggested

by Prof. Fellenius\*, or at the Moskva-Volgostroi (Fig. 78b, where the position of the critical slip arcs is indicated), etc.

For a number of selected centres of the arcs of slip surfaces ( $O_1, O_2, O_3$ , Fig. 78b), we determine the *cohesion* required by the stability condition and corresponding to the ultimate equilibrium of the given slope according to the expression following from relationship (g<sub>2</sub>), i.e.,

$$c = \frac{\sum T_i - \sum N_i \tan \varphi}{L} \quad (4.15)$$

Further, from all possible centres of slippage we select the one requiring the maximum force of cohesion. This centre is regarded as the most critical and the coefficient of stability  $\eta$  is calculated for it by formula (4.14).

It is usually assumed that a slope will be stable when  $\eta \geq 1.1-1.5$ .

As has been shown by Prof. G. M. Shakhunyants\*\*, formula (4.14) holds true only for cases when the arc of a slip surface in all its portions is *drooping* toward the possible displacement of the slope or dip, or (for a case of slippage over a cylindrical surface) when all sections of the curve of slippage are located to one side from the direction of vertical radius  $OA$  (Fig. 78c).

Denoting the shear forces directed toward slippage (shear) as  $T_{i\ sh}$  and those acting in the opposite direction (for instance,  $T_4$  and  $T_5$  in Fig. 78c) and retaining the slope from slippage as  $T_{i\ ret}$ , formula (4.14) can be given the following form:

$$\eta = \frac{\sum_{i=1}^{i=n} N_i f_i + \sum_{i=1}^{i=n} c l_i + \sum_{i=1}^{i=n} T_{i\ ret}}{\sum_{i=1}^{i=n} T_{i\ sh}} \quad (4.14')$$

This expression must be used for determining the coefficient of stability of dips and slopes in calculations by the methods of circular-cylindrical slip surfaces.

But, as has been shown by respective calculations, this method gives somewhat excessive margin in certain cases and, what is most important, does not take into account the forces acting on vertical faces of sections, which makes the calculation an approximate one and causes additional assumptions to be made.

Prof. G. I. Ter-Stepanyan and M. N. Goldstein have made certain improvements and simplifications in the calculation method of circular-cylindrical slip surfaces (by introducing a variable scale, but in the same statement of the problem). The formula recommen-

\* See Tsytoich N. A. *Mekhanika gruntov* (Soil Mechanics), 4th ed., Moscow, Stroizdat, 1963.

\*\* *Stroitelstvo zheleznykh dorog*, No. 2, 1941.

ded by Goldstein for the coefficient of stability is as follows:

$$\eta = fA + \frac{c}{\gamma h} B \quad (4.16)$$

where  $A$  and  $B$  are coefficients depending on geometrical dimensions of the sliding wedge, expressed as fractions of the slope height  $h$ ; numerical values of these coefficients are given in Table 4.6 (according to Goldstein).

Table 4.6

**Coefficients  $A$  and  $B$  for Approximate Prediction of Stability of Slopes**

Slope ratio 1 : m	Slip surface passes through lower edge of slope		Slip surface passes through the base and has a horizontal tangent at a depth of							
			$e = \frac{1}{4} h$		$e = \frac{1}{2} h$		$e = h$		$e = 1 \frac{1}{2} h$	
	A	B	A	B	A	B	A	B	A	B
1 : 1.00	2.34	5.79	2.56	6.40	3.17	5.92	4.32	5.80	5.78	5.75
1 : 1.25	2.64	6.05	2.66	6.32	3.24	6.62	4.43	5.86	5.86	5.80
1 : 1.50	2.64	6.50	2.80	6.53	3.32	6.13	4.54	5.93	5.94	5.85
1 : 1.75	2.87	6.58	2.93	6.72	3.41	6.26	4.66	6.00	6.02	5.90
1 : 2.00	3.23	6.70	3.10	6.87	3.53	6.40	4.78	6.08	6.10	5.95
1 : 2.25	3.49	7.27	3.26	7.23	3.66	6.56	4.90	6.16	6.18	5.98
1 : 2.50	3.53	7.30	3.46	7.62	3.82	6.74	5.08	6.26	6.26	6.02
1 : 2.75	3.59	8.02	3.68	8.00	4.02	6.95	5.17	6.36	6.34	6.05
1 : 3.00	3.59	8.81	3.93	8.40	4.24	7.20	5.31	6.47	6.44	6.09

The height  $h$  is found from expression (4.16) as follows:

$$h = \frac{cB}{\gamma(\eta - fA)} \quad (4.16')$$

Using formulae (4.16) and (4.16') and the data of Table 4.6, it is easy to find the coefficient of stability  $\eta$  of a slope or the ultimate height  $h$  for the adopted coefficient of stability.

For cohesive soils with an insignificant angle of internal friction ( $\varphi < 5-7^\circ$ ), with a dense soil located at a certain depth  $e$  (Fig. 78b, the arc of slip surface  $A'C'$ ), the calculation is made under an assumption that the base bulges out beyond the outline of the slope.

**Example 4.4.** Find the ultimate height of a slope of gradient 1:2 for  $\eta = 2$ ,  $\varphi = 22^\circ$ ,  $c = 1.2$  tf/m<sup>2</sup>, and  $\gamma = 1.8$  tf/m<sup>3</sup>. Having found the values of coefficients  $A$  and  $B$  from Table 4.6 and substituting them into formula (4.16'), we obtain

$$h = \frac{cB}{\gamma(\eta - fA)} = \frac{1.2 \times 6.7}{1.8(2 - 0.404 \times 3.23)} \approx 6.4 \text{ m}$$

**Slip landslides and liquid-flow landslides.** *Slip landslides* can occur over fixed slip surfaces, for instance, in *overlaid slopes* when the soil during construction is laid on the surface of existing compacted slopes of earthen structures or when natural slopes or embankments slide owing to disturbance of equilibrium along the *fixed rock* or other dense soil surface.

*Liquid-flow landslides* occur in mountainous regions during catastrophic rainfalls or at a rapid thawing of snow. They are usually in the form of mud and rock streams called *torrents*. The torrents are divided into *cohesive* (structural) and *turbulent* (non-structural) flows.

Cohesive (structural) flows are such mud flows when no noticeable intermixing of sliding masses occurs in the core of a moving flow. Structural flows are only responsible for positive accumulation and do not form scours.

Turbulent mud and rock flows, in which soil masses are being strongly intermixed, are often observed in mountainous regions.

The problem of motion of mud flows is considered on the basis of hydrological calculations and the theory of motion of viscous liquids and constitutes a special field of calculations, which is beyond the scope of soil mechanics.

The *general case* of calculation of *stability of overlaid dips and slopes* is widely employed in the design of structures to be built on slopes and in extension of earthen structures, such as dams, banks, etc.

As has been shown by G. M. Shakhunyants, the coefficient of stability of an overlaid massif can be determined in this case from equations of equilibrium, if the massif is divided into a number of sections so that the slip surface within individual sections is plane and passes along the fixed surface of denser undisturbed soil. The *landslide pressure*  $E_i$ , which is required for the design of landslide-retaining structures, can also be determined comparatively easily for any section.

Let us consider the conditions of equilibrium of an  $i$ -th section (for instance, the second one in Fig. 79).

All external forces, including the load applied to the surface of the section, the soil dead weight in the volume of the section, etc., can be reduced to a single resultant force  $Q_i$ . The resultant force is then resolved in the point of its application into a normal force  $N_i$  and a tangent force  $T_i$  relative to the fixed slip surface  $nm$ .

If the slope or dip is also subjected to the action of seismic forces which deviate the resultant of external forces through a definite angle  $\theta_i$  from the vertical, we then have

$$N_i = Q \cos(\alpha_1 + \theta_i) \text{ and } T_i = Q_i \sin(\alpha_1 + \theta_i) \quad (\text{h}_i)$$

With the slip surface  $nm$  directed toward the possible slippage

of the section, the angles  $\alpha_i$  are taken with the "plus" sign, as also the angles  $\theta_i$  that deviate the resultant  $Q_i$  in the direction of slippage.

The effect of the neighbouring sections is replaced by the forces of landslide pressure  $E_{i-1}$  and  $E_i$  (see Fig. 79) directed at the angles  $\beta_{i-1}$  and  $\beta_i$  along the normals to the side faces of the section. Further,

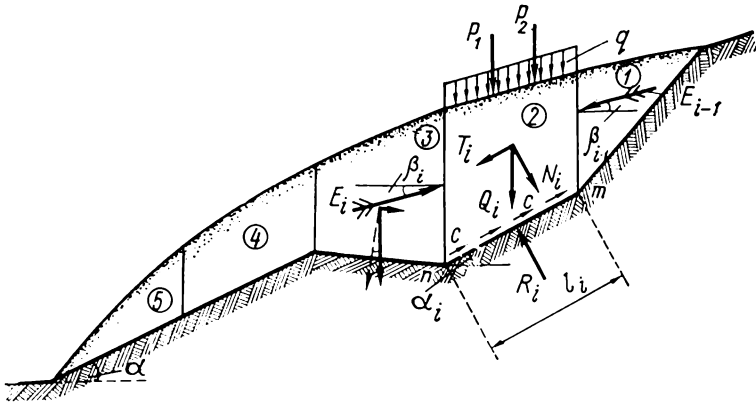


Fig. 79. Diagram of forces to determine landslide pressure

denoting the normal component of the reaction of the base of section  $nm$  by  $R_i$  and projecting all forces onto the normal to the section base and onto the direction of the section proper, we get

$$R_i = N_i + [E_i \sin(\alpha_i - \beta_i) - E_{i-1} \sin(\alpha_i - \beta_{i-1})] \quad (h_2)$$

$$T_i = c_i l_i + f_i R_i + [E_i \cos(\alpha_i - \beta_i) - E_{i-1} \cos(\alpha_i - \beta_{i-1})] \quad (h_3)$$

Substituting (h<sub>2</sub>) into (h<sub>3</sub>) and multiplying the shear force  $T_i$  by the stability coefficient  $\eta$ , we have

$$\eta T_i = c_i l_i + f_i N_i + E_i [f_i \sin(\alpha_i - \beta_i) + \cos(\alpha_i - \beta_i)] - E_{i-1} [f_{i-1} \sin(\alpha_i - \beta_{i-1}) + \cos(\alpha_i - \beta_{i-1})] \quad (h_4)$$

Solving equation (h<sub>4</sub>) for  $E_i$  and taking into account that

$$f = \tan \varphi \text{ and } f \sin(\alpha - \beta) + \cos(\alpha - \beta) = \frac{\cos(\alpha - \beta - \varphi)}{\cos \varphi}$$

and also denoting by  $T_{i \text{ sh}}$  the component  $T_i$  which promotes shear of the section, and by  $T_{i \text{ ret}}$  the force which retains the section, we get

$$E_i = \frac{(\eta T_{i \text{ sh}} - f_i N_i - c_i l_i - T_{i \text{ ret}}) \cos \varphi_i}{\cos(\alpha_i - \beta_i - \varphi_i)} + E_{i-1} \frac{\cos(\alpha_i - \beta_{i-1} - \varphi_i)}{\cos(\alpha_i - \beta_i - \varphi_i)} \quad (4.17)$$

Note that  $T_{i \text{ ret}}$  in formula (4.14') must be assumed to be zero for sections in which  $T_i = T_{i \text{ sh}}$ .

When determining  $E_i$ , calculations should be started from the uppermost section ( $I$  in Fig. 79), for which  $E_{i-1} = 0$ .

For determination of the coefficient of stability  $\eta$  of free slopes and dips, G. M. Shakhunyants recommends to select a definite value of  $\eta_1$  and determine by formula (4.17) the magnitude of the landslide pressure  $E_{end}$  for the end section. If this pressure is other than zero, then a different coefficient of stability  $\eta_2$  must be chosen so as to obtain  $E_{end}$  of the other sign. After that, by interpolation between  $\eta_1$  and  $\eta_2$  we can find the sought-for value of  $\eta$  when  $E_{end} = 0$ .

This method makes it possible to find the section (along the slope outline) where it is most advantageous to locate landslide-retaining structures (in places of the minimum  $E_i$  and not very large thickness of the landslide). In Fig. 79, for instance, this place is at the end of the third section.

If a landslide slope or overlaid slope moves as an integral whole and the contact forces of cohesion and friction between sections are inactive, then it must be assumed that  $\beta_i = 0$ ; otherwise,  $\beta_i$  and  $\beta_{i-1}$  can be assumed to be equal to the corresponding angles of internal friction of the soil.

**Landslide prevention.** The loss of stability of soil masses is often accompanied with substantial damage to roads, bridges, residential and industrial buildings and other structures, and sometimes with human victims, which necessitates the development and implementation of active measures for combating landslides and other disturbances of stability of soil masses.

Measures for combating these disturbances (landslides, mud streams, etc.) are planned on the basis of careful studies of the natural physico-geological conditions, the main causes of instability, and analytical calculations of the ultimate equilibrium of the soil masses being considered.

The main methods for improving the stability of soil massifs and combating landslides are as follows:

(1) *restoration and reinforcement* of natural supports of sliding masses (reinforcement of banks against erosion, construction of bank-protection works, application of retaining walls and bulkheads, structures for guiding mud streams, etc.);

(2) *control of water-flow conditions* of soil massifs (drainage of landslide-hazardous areas, construction of surface culverts, regulation of channels, application of deep horizontal and vertical drainage means, etc.); and

(3) *reduction of load gradient* (diminishing the gradient of slopes according to calculations based on experimental determination of shear resistance of soil; reduction of external loads; etc.).

#### 4.5. SOME PROBLEMS OF THE THEORY OF SOIL PRESSURE ON RETAINING WALLS

The problems of pressure of soils on retaining walls are most important in engineering calculations and are solved on the basis of the general theory of ultimate stressed state of soils.

If the steepness of a free slope is greater than the ultimate one (Fig. 80), a necessity arises to reinforce the soil with a *retaining wall*.

The problems of pressure of soils on retaining walls have been discussed in a great number of works beginning from the time of

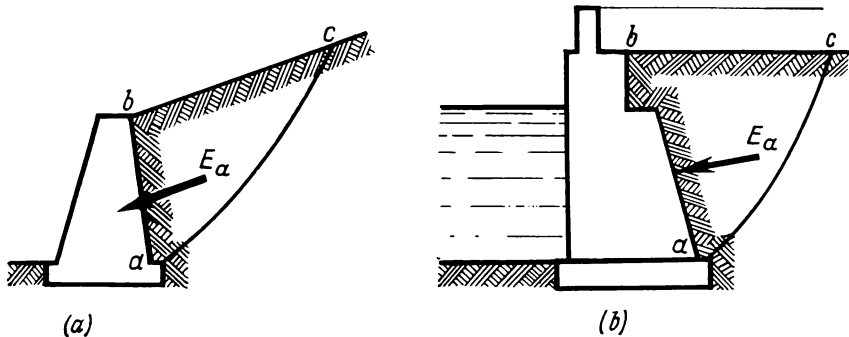


Fig. 80. Two types of retaining walls

Coulomb (18th century) and up to the present times. We shall limit ourselves to discussion of the principal problems on determination of soil pressure on massive retaining walls\*.

As has been shown by experiments, the soil pressure on retaining walls depends not only on properties of the filling ground and their variation with time (compaction, relaxation), but also on dimensions of the walls and the magnitude of their possible displacements.

With a certain flexibility of the base of a retaining wall, the latter may deflect away from the filling ground; at a definite magnitude of this deflection, the ground behind the wall attains the ultimate stressed state and two conjugate families of curvilinear slip surfaces are formed in it.

The problem is to determine the maximum pressure of soil on the retaining wall. An exact mathematical solution of this problem is possible if we know accurately the outline of slip surfaces, which is determined by solving a system of differential equations of ultimate equilibrium [see formulae (a<sub>1</sub>)-(a<sub>3</sub>) in Sec. 4.2].

\* The problems of soil pressure on retaining structures are now studied in the courses of structural mechanics.

However, in some practical applications it can be assumed without large error (and for smooth massive retaining walls, exactly) that the slip surfaces behind the wall are plane with the trace of the failure surface passing through the lower face of the wall.

**Loose soils.** With the assumption of plane slip surfaces, the *maximum pressure of loose soils* on retaining walls is determined from the following simple considerations.

Any horizontal plane in the soil behind a smooth vertical wall with a horizontal surface of filling is subject only to a compressive stress (the normal principal stress  $\sigma_1$ ) which is equal to the weight of the soil column between the surface and the plane being considered, i.e.,

$$\sigma_1 = \gamma z \cdot 1 \quad (i_1)$$

The lateral pressure  $\sigma_2$  on the wall can be found from the condition that the soil behind the wall is in the ultimate equilibrium.

From the equation of ultimate equilibrium (2.24') we get

$$\frac{\sigma_2}{\sigma_1} = \tan^2 \left( 45^\circ - \frac{\Phi}{2} \right) \quad (i_2)$$

Noting expression (i<sub>1</sub>), we have

$$\sigma_2 = \gamma z \tan^2 \left( 45^\circ - \frac{\Phi}{2} \right) \quad (4.18)$$

The diagram of distribution of pressures over the rear face of the wall will have the form of a triangle (Fig. 81).

Note that in the case when the wall moves toward the soil (moves onto the soil), the soil will offer *passive resistance* to this motion and the sign in the brackets of formula (4.18) will change to the positive one. The magnitude of the passive pressure can be found as

$$\sigma_{2p} = \gamma z \tan^2 \left( 45^\circ + \frac{\Phi}{2} \right) \quad (4.18')$$

The resultant of the soil active pressure on the wall,  $E_a$ , will be equal to the area of the pressure diagram

$$E_a = \frac{\max \sigma_2 H}{2}$$

or

$$E_a = \frac{\gamma H^2}{2} \tan^2 \left( 45^\circ - \frac{\Phi}{2} \right) \quad (4.19)$$

The resultant force  $E_a$  is directed horizontally and applied to one-third of the wall height from below.

When a continuous uniformly distributed load  $q$ ,  $\text{kgf/cm}^2$ , acts on the surface of soil, we determine the reduced height of the soil layer  $h = q/\gamma$ , which replaces the action of the load, extend the rear face of the wall to the intersection with the new line of filling (Fig. 82), and plot the general triangular diagram of pressures.

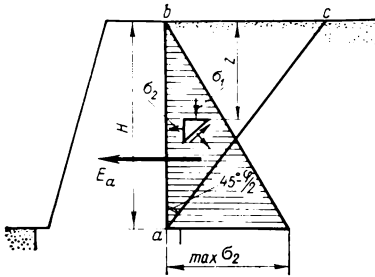


Fig. 81. Diagram of forces and lateral pressures of cohesionless soil for a smooth retaining wall

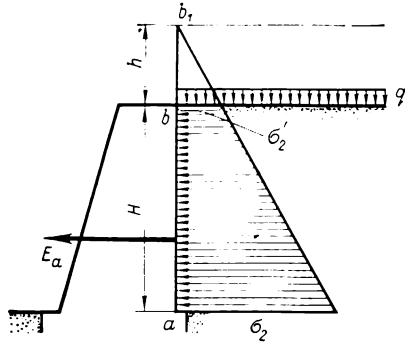


Fig. 82. Distribution of pressures over the rear face of a retaining wall under the action of uniformly distributed load and dead weight of soil

The wall will be subjected to the action of only the hatched portion of the pressure diagram (see Fig. 82). Then

$$E'_a = \frac{\sigma_2 + \sigma'_2}{2} H$$

or

$$E_a = \frac{\gamma}{2} (H^2 + 2Hh) \tan^2 \left( 45^\circ - \frac{\varphi}{2} \right) \quad (4.20)$$

**Cohesive soils.** If the soil possesses *cohesion*, the action of cohesive forces can be replaced with a uniform *cohesion pressure* ( $p_e = c/\tan \varphi$ ) applied to the free faces of the soil (Fig. 83); then, reducing the action of this pressure to an equivalent soil layer  $h$  and taking into account the oppositely directed action of the cohesion pressure  $p_e$ , we obtain as in the former case

$$\sigma_2 = \gamma (H + h) \tan^2 \left( 45^\circ - \frac{\varphi}{2} \right) - p_e \quad (j_1)$$

or, noting that

$$h = \frac{c}{\gamma \tan \varphi} \quad \text{and} \quad p_e = \frac{c}{\tan \varphi}$$

we get

$$\sigma_2 = \gamma \left( H + \frac{c}{\gamma \tan \varphi} \right) \tan^2 \left( 45^\circ - \frac{\varphi}{2} \right) - \frac{c}{\tan \varphi} \quad (j_2)$$

whence, after some simple transformations, we have

$$\sigma_2 = \gamma H \tan^2 \left( 45^\circ - \frac{\varphi}{2} \right) - 2c \tan \left( 45^\circ - \frac{\varphi}{2} \right) \quad (4.21)$$

Formula (4.21) can be written in the form

$$\sigma_2 = \sigma_{2\varphi} - \sigma_{2c} \quad (j_3)$$

where

$$\sigma_{2\varphi} = \gamma H \tan^2 \left( 45^\circ - \frac{\varphi}{2} \right); \quad \sigma_{2c} = 2c \tan \left( 45^\circ - \frac{\varphi}{2} \right)$$

Thus, *cohesion reduces the lateral pressure of the soil on the wall by a magnitude  $\sigma_{2c}$  which is the same over the whole height of the wall. At a definite depth  $h_c$  the total pressure is zero.*

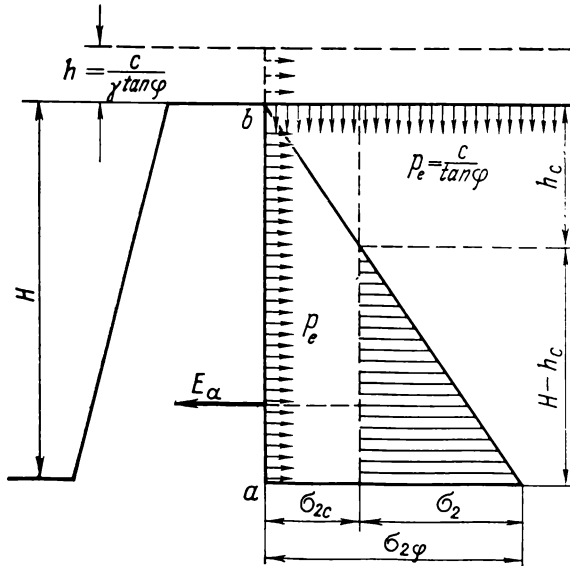


Fig. 83. Diagram to determine pressure of cohesive soils on a retaining wall

Having found the depth  $h_c$  from the condition that  $\sigma_2 = 0$ , we then determine the total active pressure of a cohesive soil on a retaining wall as the area of a rectangular triangle with the sides  $\sigma_2$  and  $H - h_c$  (Fig. 83)

$$E_\alpha = \frac{\sigma_2 (H - h_c)}{2} \quad (4.22)$$

In the case considered, the active pressure can also be found (when  $h_c < H$ ) by the formula

$$E_a = \frac{\gamma H^2}{2} \tan^2 \left( 45^\circ - \frac{\varphi}{2} \right) - 2cH \tan \left( 45^\circ - \frac{\varphi}{2} \right) + \frac{2c^2}{\gamma} \quad (4.22')$$

Let us make a *graphical construction* based on an assumption that the *slip surfaces* are plane, which is valid for the *general case* of soil

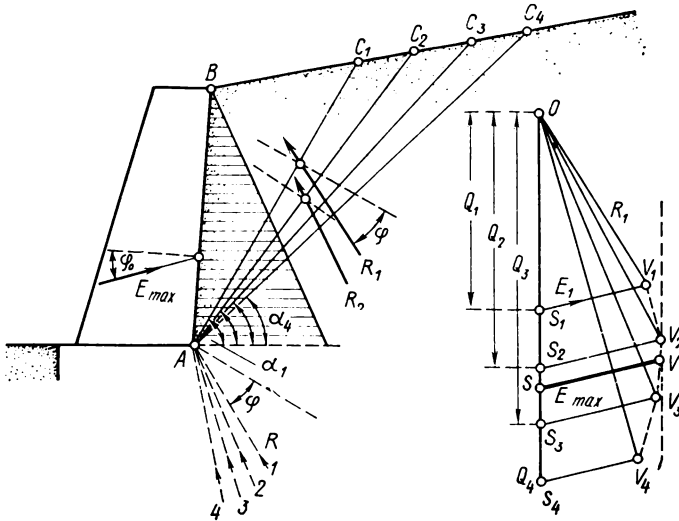


Fig. 84. Graphical determination of the maximum pressure of soil on a retaining wall

filling behind a wall, any shape of the filling, and any inclination of the wall rear face.

We draw a number of possible slip planes  $AC_1, AC_2, AC_3$ , etc., through the lower edge  $A$  of the retaining wall (Fig. 84). For each of the failure prisms, for instance, prism  $ABC_1$ , we construct a triangle of forces by laying from a definite point  $O$  an interval  $OQ_1$  representing, on a definite scale, the weight of prism  $ABC_1$ , and draw a line parallel to the reaction of the immovable portion of the soil mass,  $R_1$ , which is directed at an angle  $\varphi$  to the perpendicular of the slip plane  $AC_1$ , and a line parallel to the reaction of the wall,  $E_1$ , directed at an angle  $\varphi_0$ , which is the angle of friction of the wall over the soil.

From the condition of closure of the force triangle, we find  $R_1$  and  $E_1$  to scale of forces. Further, we construct force triangles for failure prisms  $ABC_2, ABC_3$ , etc., with the direction of the wall

Table 4.7

Dimensionless Coefficients  $\bar{q}_0$  and  $\delta$  (Radians) for Determination of Active Pressure of Soils

$\theta$ , degrees	Coefficients	$\varphi$ , degrees											
		10			20			30			40		
		$\varphi_0$ , degrees											
		0	5	10	0	10	20	0	15	30	0	20	40
0	$\bar{q}_0$	0.00	0.00	0.00	0.00	0.00	0.00	0.00	0.00	0.00	0.00	0.00	0.00
	$\delta$	0.00	0.00	0.00	0.00	0.00	0.00	0.00	0.00	0.00	0.00	0.00	0.00
10	$\bar{q}_0$	0.17	0.17	0.17	0.17	0.17	0.17	0.17	0.17	0.17	0.17	0.17	0.17
	$\delta$	0.00	0.05	0.05	0.00	0.09	0.09	0.00	0.12	0.12	0.00	0.14	0.14
20	$\bar{q}_0$	0.34	0.33	0.33	0.33	0.33	0.33	0.32	0.32	0.32	0.32	0.32	0.32
	$\delta$	0.00	0.09	0.10	0.00	0.17	0.17	0.00	0.23	0.23	0.00	0.27	0.27
30	$\bar{q}_0$	0.47	0.47	0.47	0.45	0.44	0.45	0.44	0.43	0.44	0.42	0.43	0.44
	$\delta$	0.00	0.09	0.14	0.00	0.17	0.25	0.00	0.26	0.33	0.00	0.35	0.40
40	$\bar{q}_0$	0.58	0.57	0.57	0.54	0.52	0.53	0.50	0.48	0.51	0.46	0.47	0.50
	$\delta$	0.00	0.09	0.16	0.00	0.17	0.31	0.00	0.26	0.43	0.00	0.35	0.52
50	$\bar{q}_0$	0.67	0.64	0.64	0.59	0.56	0.57	0.52	0.50	0.53	0.46	0.45	0.51
	$\delta$	0.00	0.09	0.17	0.00	0.17	0.34	0.00	0.26	0.49	0.00	0.35	0.62
60	$\bar{q}_0$	0.72	0.68	0.68	0.60	0.57	0.57	0.50	0.47	0.50	0.42	0.40	0.46
	$\delta$	0.00	0.09	0.17	0.00	0.17	0.35	0.00	0.26	0.52	0.00	0.35	0.69
70	$\bar{q}_0$	0.73	0.70	0.70	0.58	0.54	0.54	0.46	0.43	0.45	0.35	0.34	0.38
	$\delta$	0.00	0.09	0.17	0.00	0.17	0.35	0.00	0.26	0.52	0.00	0.35	0.70
80	$\bar{q}_0$	0.72	0.70	0.68	0.54	0.50	0.50	0.40	0.37	0.38	0.29	0.27	0.29
	$\delta$	0.00	0.09	0.17	0.00	0.17	0.35	0.00	0.26	0.52	0.00	0.35	0.70
90	$\bar{q}_0$	0.70	0.67	0.65	0.49	0.45	0.44	0.33	0.30	0.31	0.22	0.20	0.22
	$\delta$	0.00	0.09	0.17	0.00	0.17	0.35	0.00	0.26	0.52	0.00	0.35	0.70
100	$\bar{q}_0$	0.65	0.61	0.59	0.42	0.38	0.37	0.26	0.24	0.24	0.16	0.14	0.15
	$\delta$	0.00	0.09	0.17	0.00	0.17	0.35	0.00	0.26	0.52	0.00	0.35	0.70
110	$\bar{q}_0$	0.58	0.54	0.52	0.35	0.31	0.30	0.20	0.18	0.17	0.11	0.09	0.10
	$\delta$	0.00	0.09	0.17	0.00	0.17	0.35	0.00	0.26	0.52	0.00	0.35	0.70
120	$\bar{q}_0$	0.49	0.45	0.44	0.27	0.24	0.23	0.13	0.12	0.11	0.06	0.05	0.05
	$\delta$	0.00	0.09	0.17	0.00	0.17	0.35	0.00	0.26	0.52	0.00	0.35	0.70

Note:  $\theta$  = angle between the rear face of the wall and the horizontal, calculated from the rear face clockwise;  $\varphi$ ,  $\varphi_0$  = angle of internal friction of soil and angle of friction between soil and wall;  $\delta$  = angle between the direction of soil pressure and the normal to the rear face (for steep walls, it is close to  $\varphi$ ).

reaction remaining the same and the direction of reaction  $R_i$  varying depending on the angle of inclination  $\alpha_i$  of the slip plane.

The construction can be conveniently arranged as shown in Fig. 84. From this construction, it is easy to determine  $E_{max}$  at the point of contact between a straight line drawn parallel to  $Q$  and the curve

$V_1 V_2 V_3$  of variations of pressure  $E$ . In order to find the magnitude of  $E_{\max}$ , we should draw a straight line parallel to the direction of  $E$  through the point of contact thus found and measure the interval obtained to scale of forces.

Since the total pressure on the wall is equal to the area of the triangular diagram of lateral pressures, the unit pressure at the lower edge of the rear face of the wall will be found as

$$\max \sigma_2 = \frac{2E_{\max}}{H} \quad (4.23)$$

where  $H$  is the length of the rear face of the retaining wall.

To conclude this section, let us give the *results of the exact solution* (made by Prof. V. V. Sokolovsky) of the problem of active pressure of loose soils on retaining walls. These results have been obtained by numerical integration of reduced non-linear differential equations of the theory of ultimate equilibrium by the method of finite differences (Table 4.7).

The active pressure is calculated by the formula

$$\sigma_2 = \bar{q}_0 (\gamma z + q) \quad (4.24)$$

where  $q$  = intensity of the load uniformly distributed over the horizontal surface of filling

$\bar{q}_0$  = dimensionless coefficient (Table 4.7).

#### 4.6. SOIL PRESSURE ON UNDERGROUND PIPELINES

The vertical pressure at a depth  $z$  in a soil massif having the unit weight  $\gamma$  is (Fig. 85a)

$$\sigma_z = \gamma z \quad (k_1)$$

The lateral pressure at the same depth is

$$\sigma_x = \xi \gamma z \quad (k_2)$$

where  $\xi$  is the coefficient of lateral pressure of soil under conditions of natural compaction; it is equal to the ratio  $\sigma_x/\sigma_z$ .

If the soil in the zone of the contour of a pipeline is exactly replaced by the pipeline proper (Fig. 85b), then this pipeline will naturally be subjected to the pressure which is determined by relationships (k<sub>1</sub>) and (k<sub>2</sub>).

The pressure is transferred onto the pipeline from above and from the sides and causes an equal and opposite reaction of the base; this pressure is taken in the form of an average uniformly distributed pressure, the vertical one of intensity  $p$  and the horizontal one of intensity  $q$  (Fig. 85b), with the inequality  $p > q$  holding true.

According to the data of structural mechanics, the bending moments  $M$  and normal forces  $N$  in a circular pipeline of radius  $R$  loaded with pressures  $p$  and  $q$  respectively are

$$\left. \begin{aligned} M &= \frac{p-q}{4} R^2 \cos 2\theta \\ N &= \frac{R}{2} [p+q] - (p-q) \cos 2\theta \end{aligned} \right\} \quad (4.25)$$

where  $\theta$  is the angle between the vertical and the radius drawn from the centre of the pipeline to the given point.

It follows from formulae (4.25) that for pipes whose material equally resists both to tension and compression (for instance, steel) the

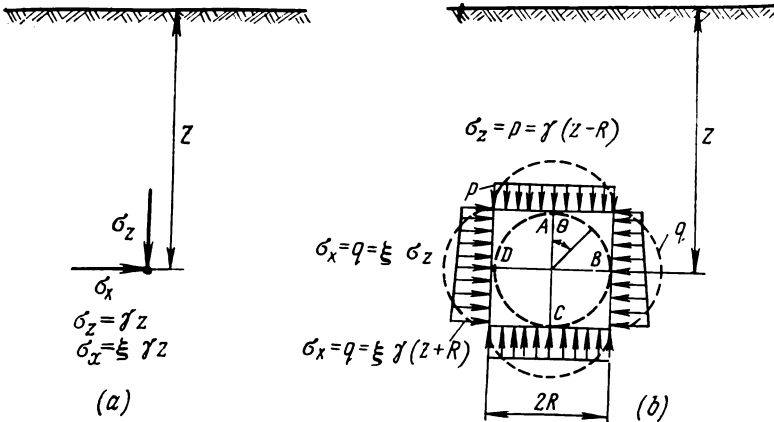


Fig. 85. Vertical and horizontal pressures of soil in a volume bounded by a horizontal plane  
(a) in an individual point; (b) when laying pipelines

most critical sections are  $B$  and  $D$  (Fig. 85b), since maximum compressive stresses are formed in them; if the material is substantially less resistive to tension (such as concrete), the most critical sections are  $A$  and  $C$ , since tensile stresses are at the maximum in them.

The most critical is the case when the pressure is transferred to the pipeline in a single point. If the pipe is assumed to be loaded from above by a load  $P = 2pR$  and supported from below in a single point by a rigid base, the moment from below

$$M = \frac{(2pR)}{\pi} R$$

will be 2.54 times that from above.

Three different methods of pipe-laying are used: (1) in trenches (Fig. 86a); (2) under a filling (Fig. 86b); and (3) in tunnelled drifts

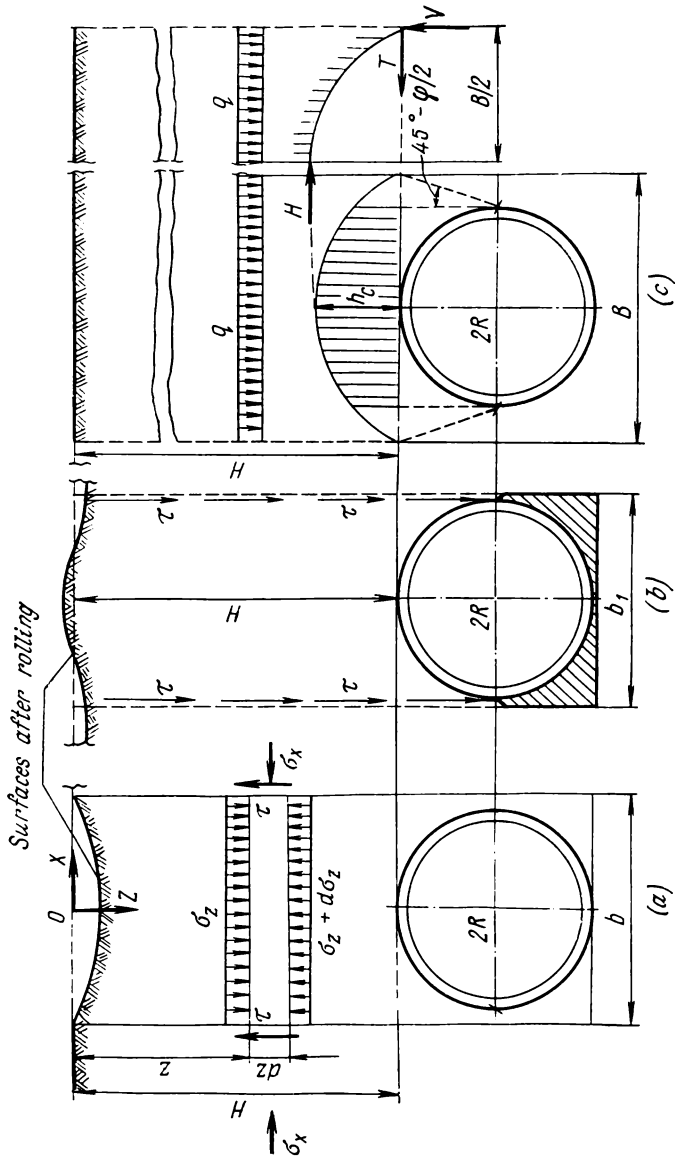


Fig. 86. Determination of soil pressures on underground pipelines  
 (a) pipelines laid in trenches; (b) pipelines laid under fillings; (c) pipelines laid in tunnelled drifts at a considerable depth ( $H \gg h_c$ )

(Fig. 86c). The soil pressure on the pipeline (for the same depth  $H$ ) will be different in these three methods, i.e.,  $p < \gamma H$  for trench laying;  $p > \gamma H$  for laying under filling, and  $p = \gamma H$  for tunnelled drifts when  $H$  is comparatively small or  $p < \gamma H$  for greater values of  $H$ .

The reasons for this are as follows. If a pipeline is being laid in a trench (this is the most widely used method of pipe-laying), then the soil being filled into the trench at backfilling will be loose and not compacted by its dead weight, whereas the soil at the sides of the trench has been compacted by its weight. Because of this, friction forces are formed at the sides of trenches during compaction and settlement of soil filling. These forces counteract compaction, so that the soil filling will be suspended, as it were, at the sides of the trench, this suspension being the greater, the deeper the trench is.

Let us determine the *soil pressure on pipelines* being laid in *trenches*, assuming that the vertical pressure of the soil filling at any depth is distributed uniformly and that friction forces are formed at the side faces of the trench.

We write the conditions of equilibrium for an elementary layer  $dz$  separated at a depth  $z$  (see Fig. 86a). This element is subjected to the action of the dead weight of the soil layer,  $\gamma b dz$ , the vertical pressure of soil filling from above,  $\sigma_z$ , and from below,  $\sigma_z + d\sigma_z$ , the shear resistance of soil at the trench sides per unit area being  $\tau = c + \sigma_x \tan \varphi_0$  (where  $c$  is cohesion and  $\varphi_0$  is the angle of friction over the trench side). Further, the coefficient of lateral pressure of soil is assumed to be constant, i.e.,

$$\xi = \frac{\sigma_x}{\sigma_z} = \text{const} \quad (1)$$

By projecting the forces onto the vertical axis  $Z$ , we obtain

$$\gamma b dz + \sigma_z b - (\sigma_z + d\sigma_z) b - 2cdz - 2\xi\sigma_z \tan \varphi_0 dz = 0$$

After reduction of like terms and integration for the boundary conditions ( $z = 0, \sigma_z = 0$ ), we obtain the total pressure of soil at a depth  $z$ , whose maximum value can be presented (by introducing an overloading coefficient  $n \approx 1.2$ ) as follows\*:

$$p_1 = nK_{tr}\gamma H \quad (4.26)$$

where  $K_{tr}$  is the coefficient of soil pressure on the pipeline *in a trench*, which is equal to

$$K_{tr} = \frac{b}{H} \cdot \frac{1 - \frac{2c}{\gamma b}}{2\xi \tan \varphi_0} \left( 1 - e^{-\frac{2H}{b}\xi \tan \varphi_0} \right) \quad (4.27)$$

---

\* Klein G. K. Raschet podzemnykh truboprovodov (Design of Underground Pipelines), Moscow, Stroizdat, 1969.

For pipes being laid in trenches, the coefficient  $K_{tr}$  cannot be greater than a unity ( $K_{tr} \leq 1$ ); this is the condition of applicability of formula (4.27).

For approximate determination of  $K_{tr}$ , use may be made of the curves of Klein's diagram (Fig. 87, curves 1 and 2), which give  $K_{tr}$  somewhat on the conservative side (under assumption that  $c = 0$ ). Taking into account, however, that for many kinds of soil the product  $\xi \tan \varphi_0$  is approximately the same for common  $H/b$  ratios, we can limit ourselves to the determination of only two average values of  $K_{tr}$ : for sand and sand-loam fillings (curve 1 in Fig. 87) when  $\xi \tan \varphi_0 = 0.43 \tan 25^\circ \approx 0.20$ , and for clay fillings (curve 2 in Fig. 87) when  $\xi \tan \varphi_0 \approx 0.54 \tan 15^\circ \approx 0.145$ .

Having found the value of  $K_{tr}$  by formula (4.27) or the diagram in Fig. 87, we can determine the soil pressure on the pipeline laid into a trench.

For pipelines being laid under fillings, the friction forces of the soil will have an opposite direction (see Fig. 86b), since pipes are more rigid than the soil nearby, the latter being compacted under the action of its dead weight.

In that case the vertical pressure of the soil is greater than  $\gamma H$  and corresponds to the expression

$$p_2 = K_f \gamma H \tag{4.26'}$$

where  $K_f$  is the coefficient of soil pressure on the pipeline under filling,  $K_f \geq 1$ .

The values of  $K_f$  can be found from the curves of Klein's diagram (curves 3-7 in Fig. 87).

For pipelines being laid in tunnelled drifts the pressure is taken equal to  $\gamma H$  for a small depth, and assumed as rock pressure with

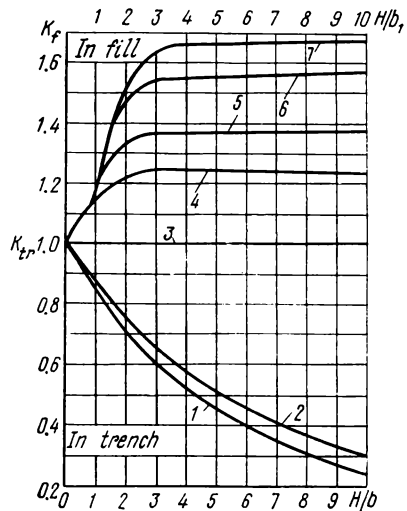


Fig. 87. Diagram to determine pressure coefficients of soil for pipelines laid in trenches ( $K_{tr}$ ) or in fillings ( $K_f$ ) (according to G. K. Klein)

- (1) for sand and sand-loam filling; (2) for clay filling; (3) for loose dusty sands and liquid clays; (4) for fine-grain dense sands and soft-plastic clays; (5) for medium- and coarse-grain dense sands and plastic clays; (6) for dense coarse-grain and gravelly sands and stiff-plastic and hard clays; (7) for semi-rock soils and fissured rocks

account of what is called the *arch of destruction* (see Fig. 86c), for a greater depth\*.

Let us write the equation of equilibrium for the forces acting on half the arch of destruction (see Fig. 86c, left-hand portion), namely: the load  $q$  (which is assumed to be distributed uniformly), the lateral pressure  $H$  (from the removed half the arch) and the components of the support reaction: the vertical  $V$  and horizontal force of friction  $T$ , equal to  $T = fV$ , where  $f$  is the coefficient of friction. According to Prof. M. M. Protodiakonov\*\* the latter is assumed for cohesive soils to be equal to the strength coefficient

$$f' = \frac{\tau}{\sigma} = \frac{c}{\sigma} + \tan \varphi$$

Assuming the arch to be parabolic, we have from the conditions of equilibrium

$$\left. \begin{aligned} H &= T = fV \\ V &= \frac{qB}{2} \\ h_c &= \frac{qB^2}{8H} = \frac{B}{4f} \end{aligned} \right\} \quad (4.28)$$

where  $B$  is the width of the arch of destruction and  $h_c$  is its maximum ordinate.

Assuming, according to M.M. Protodiakonov, that vertical pressure is distributed uniformly (over the maximum ordinate) and taking into account only half the friction force (for safety), the design height of the relieving arch will be found as

$$h_c \approx \frac{B}{2f} \quad (4.29)$$

and the vertical pressure on the pipeline as

$$p_3 \approx \gamma h_c = \frac{\gamma B}{2f} \quad (4.30)$$

It will be noted that calculations of the arch of destruction according to M. M. Protodiakonov give quite reliable results.

**Constructional features of pipe-laying.** There are three methods of supporting pipelines: common (Fig. 88a), where a pipeline is laid onto a flat unprofiled bottom of a trench (in that case, care should be taken to see that the pipeline bears against the soil uniformly along its length, and not in some points only); an improved method (Fig. 88b), where the bottom of a trench is profiled to the

\* Tsytovich N. A. *Mekhanika gruntov* (Soil Mechanics), 4th ed., Moscow, Stroizdat, 1963.

\*\* Protodiakonov M. M. *Davlenie gornykh porod i rudnichnoe kreplenie* (Rock Pressure and Mine Roofing), Part 1, Moscow, Geolizdat, 1930.

contour of the pipe and embraces the latter along an arc of 75-90°, and finally, placing the pipe on a concrete foundation, also embracing a part of the pipe perimeter (Fig. 88c). In the latter method, which is the most labour-consuming and expensive, with the pipe laid on a mortar layer, its lower portion acts integrally with the foundation

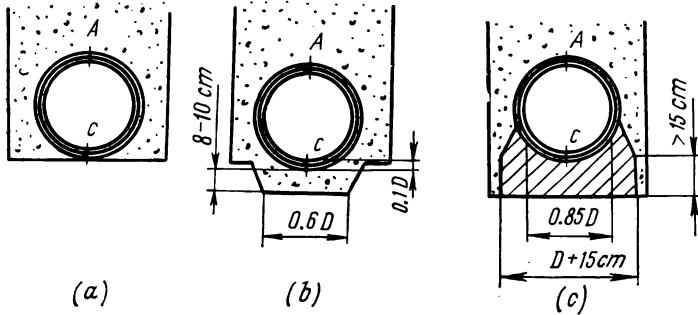


Fig. 88. Designs of pipeline bases

(a) without special preparation; (b) specially profiled; (c) with a concrete footing

and therefore the section  $c$  is no more the critical one. The method of laying a pipeline on a profiled base (Fig. 88b) provides better results than the common one. Here, we tend to fulfill the condition that the moments in point  $c$  be equal to the moments in point  $A$ , but do not exceed them, as is the case with the common method of pipeline-laying (Fig. 88a).

It should be noted that external loads on underground pipelines are taken as in road construction, dynamic effects being accounted only for pipelines laid at depths less than 0.7 m.

## Chapter Five

### SOIL DEFORMATIONS AND SETTLEMENT OF FOUNDATIONS

#### 5.1. KINDS AND CAUSES OF DEFORMATIONS

Analysis of soil deformations under the action of external forces is of great importance for practical design of foundations of structures.

The factors that determine durability of structures are, properly speaking, not the stresses in soil (provided that these do not attain their ultimate values), but deformations of bases and their *settlements*, which are usually understood as vertical displacements of soil bases. A uniform settlement of a whole structure cannot cause additional stresses in its members, but different settlements of individual parts of the base can strongly affect the strength of foundations and upper structures. As seen from appropriate observations, the greater the absolute settlement of a base, the greater, as a rule, will be the difference in settlements of bases, then it is of great importance to know both the absolute settlement and the difference in settlements of individual parts of structures.

In last decades, the progress in the theory of settlement of earth bases (to which a great contribution has been made by the Soviet scientists) and the results of statistical analysis of numerous measurements of settlements and differences in settlements of various structures on various kinds of soil provided the possibility of development of the most advanced method of calculation of foundations *by the ultimate deformations of bases*, which ensures full safety and a substantial economic effect.

This method, which has found wide application in the Soviet design practice, is based on the following conditions:

$$\left. \begin{aligned} s_{des} &\leq s_{ult} \\ \Delta s_{des} &\leq \Delta s_{ult} \end{aligned} \right\} \quad (5.1)$$

i.e., the design settlement of foundation bases  $s_{des}$  and the difference in settlements of neighbouring foundations  $\Delta s_{des}$  must not exceed certain ultimate values  $s_{ult}$  and  $\Delta s_{ult}$  established by an analysis of the results of numerous observations on settlements of bases of structures and specified by respective standards (for instance, BC&R).

As has been shown earlier (see Sec. 2.4), soils are complex multi-phase systems of particles whose deformations depend both on the

total variation of their volume (caused by compaction, swelling, etc.) and the deformability of all their components (phases) which make up the soil (creep of the skeleton, compressibility of porous water and vapour and gaseous inclusions, etc.), and also on their interaction.

Various kinds of deformation of soils and their causes are systemized in Table 5.1.

Table 5.1

Main Physical Causes of Soil Deformations

Kind of deformation	Causes
Elastic: volume variations  shape distortions	Molecular elastic forces of solid particles and of thin films of water and closed air bubbles Molecular elastic forces, distortions of structural lattice
Non-elastic residual deformations: compaction  swelling  creep purely residual	Reduction of porosity (compression properties) Wedging effect as a result of the action of electromolecular forces Mutual shear of particles Destruction of structure, breakage of particles

In practice, *elastic* deformations may be of prime importance in some cases, for instance, at dynamic loads (including seismic effects) and in calculations of flexible foundations for combined operation with a compressible base; in other cases *inelastic* deformations (compaction and swelling) may be critical, for instance, in calculations of massive foundations by the ultimate deformations of bases (in order to determine the total settlement of soil bases and attenuation of settlements with time), and sometimes *purely residual* deformations become important, for instance, for the formation of tracks in improved earth pavements, etc.

## 5.2. ELASTIC DEFORMATIONS OF SOILS AND METHODS FOR THEIR DETERMINATION

**Conditions for development of elastic deformations in soils.** Though elasticity is a property inherent in all natural bodies, soils can be regarded as elastic bodies only under definite conditions, since they are complex disperse natural formations.

If a soil is loaded and unloaded with a local load (which is greater than its structural strength), both elastic and residual deformations will be observed in it, the magnitude of residual deformations being many times that of elastic ones; with a repeated loading and unloading, however, the soil will gradually acquire an *elastically compacted* state which is characterized by that its elastic properties are constant (for the given loading conditions).

If the load on the soil is increased above that causing its elastically compacted state, appreciable residual deformations will again appear in it, so that after a sufficiently large number of cycles of loading and unloading the soil will acquire a new elastically compacted state with a greater modulus of elasticity (with the curve of soil deformations on unloading having a smaller slope to the axis of pressures). It is natural that such increase of loading can be performed only to a definite value until the limit of the *compaction* phase of the soil is attained and a new phase of development of *shears* sets in.

Thus, under definite conditions of loading a soil can acquire an *elastically compacted state*.

Until the load does not destroy the structural bonds, and with small displacements of particles and structural elements, a cohesive soil behaves as an elastic body, which is confirmed by natural observations on propagation of elastic oscillations (vibrations, seismic waves, etc.) in soils; if, however, cyclic loading destroys structural bonds, the soil after certain cycles of loading and unloading will come to a new elastically compacted state.

Among the methods for determining elastic deformations of soils we should distinguish the *method of total elastic deformations* which takes into account the elastic displacements not only of points below a loaded surface, but also of those *beyond it*; the *method of local elastic deformations*, when only the deformations directly *in the place of application of the load* are considered, while the total elastic deformations of the soil mass are disregarded; and some *generalized methods* which take into account both total reversible deformations, including elastic ones, and local residual deformations.

*The method of total elastic deformations* is based on rigid solutions of the theory of elasticity for an elastic half-space and an elastic layer of a limited finite thickness supported by an incompressible base.

The solutions obtained by this method will also hold true for determination of *total deformations* (both elastic and residual) of a *linearly deformable* half-space and a linearly deformable layer of finite thickness.

The initial relationship for the determination of total elastic deformations of a half-space is Boussinesq's formula for vertical displacements of points lying in a plane limiting the half-space

( $z = 0$ ) under the action of a concentrated force  $P$  on that half-space [see Sec. 3.1, formula (3.3)]

$$w_z = \frac{P}{\pi CR}$$

where the *coefficient of elastic half-space*

$$C = \frac{E}{1 - \mu^2}$$

Note that if a *linearly deformable half-space* is considered, the modulus of soil elasticity  $E$  should be replaced with the modulus of total deformation (both elastic and residual)  $E_o$ , and the Poisson's ratio  $\mu$ , with the coefficient of total relative lateral deformation  $\mu_o$ .

With a *local load*  $p$ , uniformly distributed over the area  $F$  acting on the plane limiting an elastic half-space, the settlements of any point are determined by integration of the expression for vertical displacements of the point of the elastic half-space under the action of an elementary concentrated force  $p d\xi d\eta$  (Fig. 89).

Denoting the coordinates of the point considered by  $x$  and  $y$  and using formula (3.3), we get

$$s_{el} = \frac{p}{\pi C} \iint_F \frac{d\xi d\eta}{\sqrt{(x-\xi)^2 + (y-\eta)^2}} \quad (5.2)$$

Solutions of equation (5.2) have been obtained both for circular and elliptical planes of loading (Boussinesq et al.) and for any rectangular plane (F. Schleicher, V. G. Korotkin et al.): for the maximum settlements in the centre of a loaded rectangle, for settlements of the corners of a rectangular loading plane, for the average settlement over the whole loading area, for the settlement of a plane loaded with a rigid foundation, etc.

All the solutions obtained can be given a unified form, namely,

$$s_{el} = \frac{\omega'}{C} p \sqrt{\bar{F}} \quad (5.3)$$

where  $\omega'$  is an integral coefficient which is constant for the given shape of the base plane and the location of the point considered (it can be easily tabulated).

Expression (5.3) shows that the settlements of a homogeneous elastic (or linearly deformable) *half-space* are directly proportional ( $\omega'/C$  being the coefficient of proportionality) to the unit pressure on soil  $p$  and the *square root from the area*  $\sqrt{\bar{F}}$ .

It is important to note that the natural experiments on studying the settlements of earth bases for areas of 0.5 m<sup>2</sup> to 15 m<sup>2</sup> on a homo-

geneous silt-laden sand of a thickness of about 12 m (Kh. R. Khakimov, 1939) and also the experiments on homogeneous loess-like sand loams with areas from 0.25 m<sup>2</sup> to 8 m<sup>2</sup> (D. E. Polshin et al.) give the following empirical expression within the limits of linear relationship between pressure and settlement:

$$s = Ap\sqrt{\bar{F}} \quad (5.3')$$

Thus, with an external pressure not exceeding the practical limit of proportionality, the theoretical formula (5.3) for soils which are

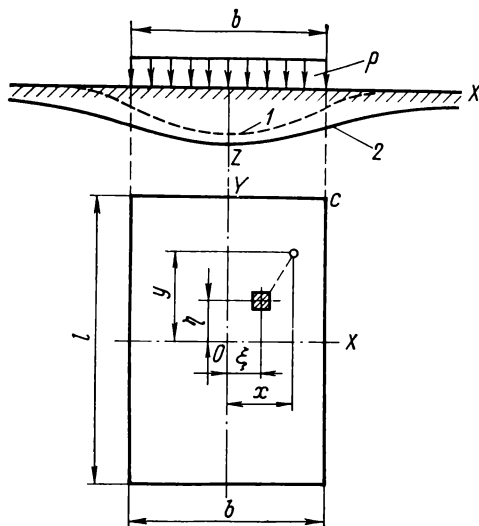


Fig. 89. Action of a local load (the method of total elastic deformations)

(1) deformations of a finite-thickness elastic layer supported by an incompressible base; (2) deformations of an elastic half-space

homogeneous to a sufficient depth is completely confirmed by the results of experiments (though the coefficient of proportionality  $A$  in some cases may somewhat differ from the theoretical one,  $\omega'/C$ ).

With a wide range of variation of areas, however, the dependence of settlement on the magnitude of the loading area is expressed by a more complicated relationship, as has been shown by natural experiments.

Thus, Fig. 90 shows a generalized curve of the average results of numerous experiments on studying the settlements of earth bases (at an average degree of compaction) for the same pressure on soil but

with different areas of loading. Three different regions may be distinguished on the curve: *I*—the region of small loading areas (approximately up to 0.25 m<sup>2</sup>) where soils at average pressures are predominantly in the *shear phase*, with the settlement being reduced with an increase of area (just opposite to what is predicted by the theory of elasticity for the phase of linear deformations); *II*—the region of areas from 0.25-0.50 m<sup>2</sup> to 25-50 m<sup>2</sup> (for homogeneous soils of medium density, and to higher values for weak soils), where settlements are strictly proportional to  $\sqrt{\bar{F}}$  and at average pressures on soil correspond to the *compaction phase*, i.e., are very close to the theoretical ones; and *III*—the region of areas larger than 25-50 m<sup>2</sup>,

where settlements are smaller than the theoretical ones, which may be explained by an increase of the soil modulus of elasticity (or a decrease of deformability) with an increase of depth. For very loose and very dense soils these limits will naturally be somewhat different.

The data given can be used for establishing the limits of applicability of the theoretical solutions obtained for homogeneous massifs to real soils, which is of especial importance in developing rational methods of calculation of foundation settlements.

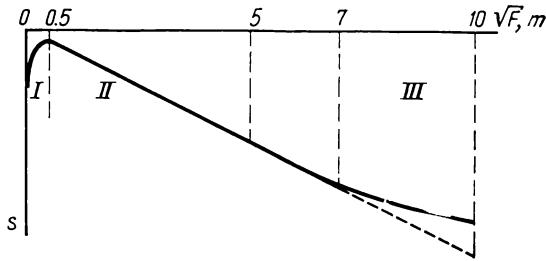


Fig. 90. Relationship between settlement of natural soils and dimensions of loading area

For convenience in use, let the main dependence of settlement on the loading area and the effective external pressure [formula (5.3)] be written in a different form (which has become generally adopted) by introducing the ratio of the length to width of a rectangular loading area  $\alpha = l/b$  (and therefore,  $l = \alpha b$  and  $F = \alpha b^2$ ) and denoting  $\omega' \sqrt{\alpha}$  through  $\omega$

$$s_{el} = \frac{\omega p b (1 - \mu^2)}{E} \quad (5.4)$$

where  $\omega$  = coefficient of the shape of the base area and of the rigidity of foundation (which may be either the same for the whole loading area or different for its various points)

$b$  = width of a rectangular, or diameter of a circular, area of the base

$p$  = unit pressure on soil

$E, \mu$  = moduli of elasticity (deformability) of the half-space

In order to simplify calculations, Table 5.2 gives the values of the shape coefficient  $\omega$  for a circle and rectangles of various side-to-side ratios  $\alpha = l/b$  (where  $l$  is the length and  $b$ , the width of a rectangular base area).

Note that formula (5.4) is also used for trial determinations of the modulus of total deformation of soil  $E_0$  (kgf/cm<sup>2</sup>) from results of a field trial loading (on an area of 5000 cm<sup>2</sup>).

Table 5.2

Values of Coefficients  $\omega$ 

Side ratio $\alpha = l/b$	$\omega$ for half-space				$\omega_{mh}$ for finite-thickness layer at $h/b$				
	$\omega_c$	$\omega_0$	$\omega_m$	$\omega_{const}$	0.25	0.5	1	2	5
1 (circle)	0.64	1.00	0.85	0.79	0.22	0.38	0.58	0.70	0.78
1 (square)	$\frac{1}{2} \omega_0$	1.12	0.95	0.88	0.22	0.39	0.62	0.77	0.87
2 (rectangle)	$\frac{1}{2} \omega_0$	1.53	1.30	1.22	0.24	0.43	0.70	0.96	1.16
3 Same	$\frac{1}{2} \omega_0$	1.78	1.53	1.44	0.24	0.44	0.73	1.04	1.31
4 Same	$\frac{1}{2} \omega_0$	1.96	1.70	1.61	—	—	—	—	—
5 Same	$\frac{1}{2} \omega_0$	2.10	1.83	1.72	—	—	—	—	—
10 Same	$\frac{1}{2} \omega_0$	2.53	2.25	2.12	0.25	0.46	0.77	1.15	1.62

Note: The coefficients  $\omega$  for half-space are given according to F. Schleicher with the Author's corrections, and for a finite-thickness layer, according to M. I. Gorbunov-Posadov. The table gives the following coefficients:

$\omega_c$  for settlements of corner points of a rectangular loading area;

$\omega_0$  for the maximum settlement under the centre of a loaded area;

$\omega_m$  for the average settlement over the whole loaded area;

$\omega_{const}$  for settlement of absolutely rigid footings;

$\omega_{mh}$  for the average settlement of rectangular loading areas on a finite-thickness soil layer.

Denoting the moduli of total deformability with a subscript "o", we find from formula (5.4) that

$$E_o = \frac{\omega pb (1 - \mu_o^2)}{s_o} \quad (5.4')$$

where  $s_o$  is the total settlement (both residual and elastic) of a stamp, but within the limits of the linear relationship between settlements  $s_o$  and pressure  $p$ .

The coefficient of relative lateral deformation  $\mu_o$  is usually taken according to the experimental data, namely: 0.1-0.15 for hard and semi-hard clays and loamy soils; 0.20-0.25 for stiff plastic clays; 0.30-0.40 for plastic and liquid-plastic clays; 0.45-0.50 for liquid clays; 0.15-0.30 for sand loams (depending on their consistency); and 0.20-0.25 for sands.

It has been earlier assumed [Chap. 2, formula (2.37')] that

$$E_o = \frac{\beta}{m_v}$$

where  $m_v$  = coefficient of relative compressibility of soil  
 $\beta$  = coefficient characterizing lateral expansion of soil  
 (function of  $\mu_o$ )

The coefficient  $\beta$  can be found as follows. It is known from the course of Strength of Materials, that the relative deformation  $\epsilon_z$  of a linearly deformed elementary prism being compressed along three mutually perpendicular directions is

$$\epsilon_z = \frac{\sigma_z}{E_o} - \frac{\mu_o}{E_o} (\sigma_x + \sigma_y) \quad (m_1)$$

And since, for the conditions of no lateral expansion of soil with a continuous load

$$\sigma_x = \sigma_y = \frac{\mu_o}{1 - \mu_o} p \quad \text{and} \quad \sigma_z = p$$

then

$$\epsilon_z = \frac{p}{E_o} \left( 1 - \frac{2\mu_o^2}{1 - \mu_o} \right) \quad (m_2)$$

The multiplier in the parentheses is usually denoted through  $\beta$ , i.e.,

$$\beta = 1 - \frac{2\mu_o^2}{1 - \mu_o} \quad (5.5)$$

But, since  $m_v = \frac{s}{hp} = \frac{\epsilon_z}{p}$  according to formula (2.5'), then expression (m<sub>2</sub>) gives formula (2.37')

$$E_o = \frac{p\beta}{\epsilon_z} = \frac{\beta}{m_v}$$

Under the action of a local load, deformations of an elastic half-space appear not only directly under the load (over its base), but are spread laterally to substantial distances, thus forming an "elastic crater" (see Fig. 89). Experiments show, however, that the elastic crater under the load in real soil conditions spreads to a substantially smaller distance than that obtained by the theory of elastic half-space. The latter can evidently be explained by that not the whole soil mass (half-space), but only its limited portion participates in the work under the load.

This circumstance, and also actually shallow location of incompressible rocks in some practical cases have led to a problem of stresses and deformations of a finite-thickness elastic layer supported by a non-deformable rock base. The solution of this problem is the object of a number of works of both Soviet (M. I. Gorbunov-Posadov, O. Ya. Schechter, K. E. Egorov, and others) and foreign researchers (Marger, J. Sovinc, and others).

M. I. Gorbunov-Posadov has solved the problem by the method of approximate integration of the general equation of deformations and determination of a number of values of the coefficients  $\omega_{mh}$  averaged for the whole area of loading at different depths of the compressible soil layer  $h$ , expressed in fractions of the load width  $b$  (see Table 5.2).

As follows from the data given in Table 5.2, with small thicknesses of a finite-thickness elastic layer ( $h/b \leq 0.25$ ), the shape of the base area has almost no effect on the vertical deformations of the layer; with the soil layer thickness  $h \geq 2b$ , however, as has been shown by appropriate calculations, the stresses in the soil layer, and especially the *contact pressures*, differ only slightly from the pressures found by the theory of homogeneous elastic half-space.

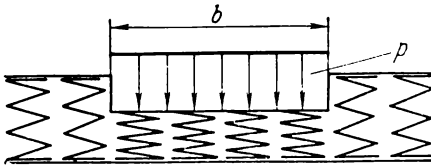


Fig. 91. A model of a local elastic base

With a layer of compressible soil supported by an incompressible base having a thickness  $h \leq 2b$  or  $h \geq 0.1b$ , its finiteness must be fully taken into account.

The *method of local elastic deformations* takes into account only the elastic deformations directly in the place of load application and is based on a hypothesis according to which the pressure in a given point is directly proportional only to the local elastic settlement of the soil in that point, i.e.,

$$p = C_z z \quad (5.6)$$

where  $p$  = unit pressure, kgf/cm<sup>2</sup>

$z$  = vertical elastic displacement (local elastic settlement), cm

$C_z$  = coefficient of local elasticity of the base, sometimes called the *modulus of subgrade reaction*, kgf/cm<sup>3</sup>

According to equation (5.6), elastic settlement is

$$z = \frac{p}{C_z} \quad (5.6')$$

Equation (5.6') shows that elastic settlement of soil occurs only in the place of load application; it is evident that  $z = 0$  in the place where  $p = 0$ . This condition can be simulated by a base formed by vertical elastic springs not connected together (Fig. 91), whose settlement will be strictly proportional to the pressure applied. The

neighbouring springs (outside the loading area) will not be subjected to pressure. This model of elastic base is naturally very conditional and can be applied only in special cases.

Note that the hypothesis (5.6) is used as the basis for the derivation of the main differential equation of bending of foundation beams and plates supported by a continuous (Winckler) elastic base by the method of local deformations. As is known from the courses of Strength of Materials and theory of elasticity, this differential equation has the form as follows:

$$EI \frac{d^4 z}{dy^4} = -C_z z \quad (5.7)$$

where  $EI$  = rigidity of foundation beam  
 $z$  = its elastic deflection

Solution of differential equation (5.7) when  $C_z = \text{const}$  encounters no special difficulties but contains four integration constants which must be determined from the initial conditions of bending of a beam supported by a continuous base.

Direct experiments show, however, that the coefficient  $C_z$  of natural soil bases is not constant, but depends on both the unit pressure on the soil and the area of load transfer, which must be taken into account in calculations and can be expressed analytically\*.

For structures having a constant area of the base and subjected to the same range of variation of external pressures (for instance, railroad sleepers), the method of local elastic deformations is completely applicable.

For foundations of structures having a large area in plan, the following must be taken into account: as has been demonstrated by both theoretical research (for instance, by an analysis of the work of a finite-thickness elastic layer on an incompressible support) and experimental data, the method of local elastic deformations is only applicable with a certain approximation when the thickness of the compressible soil layer is less than the width of the foundation strip supported by the soil, and it gives sufficiently accurate results when the thickness of the soil layer does not exceed *one-fourth of the strip width*, i.e., for rather small thicknesses of the compressible soil layer. These ranges can be taken somewhat wider for strongly compressible soils with a low deformation modulus.

*The generalized methods for determination of soil deformations* take into account both the total elastic and local inelastic deformations of soils.

---

\* Savinov O. A. *Fundamenty pod mashiny (Machine Foundations)*, Moscow, Stroiizdat, 1955; see also Sec. 7.4 of this book.

Among the generalized methods those worth mentioning here are Pasternak — Vlasov's method\* of a two-parameter elastic base, according to which a soil base is characterized by a subgrade reaction coefficient  $C_1$  (kgf/cm<sup>3</sup>) and the coefficient of local elastic shear  $C_2$  (kgf/cm) [the equations of deformations include both  $C_1$ ,  $C_2$  and  $\sqrt{C_1/C_2}$ ], and Cherkasov — Klein's method of structurally reversible deformations, which takes into account the total reversible deformations (elastic and adsorptional) and residual (structural) deformations].

In the latter method, reversible deformations are assumed to be linearly deformable and are characterized by a coefficient similar to the coefficient of elastic half-space

$$C_r = \frac{1 - \mu_r^2}{E_r} \quad (a_1)$$

and structural deformations are determined by the theory of dimensions from the following exponential relationship:

$$p = A \left( \frac{s_{res}}{D} \right)^n \quad (a_2)$$

where  $A$  = hardness number, kgf/cm<sup>2</sup>

$s_{res}$  = residual deformation, cm

$D$  = diameter of circular loaded area, cm

$n$  = degree of strengthening (dimensionless parameter)

$p$  = external unit pressure (load), kgf/cm<sup>2</sup>

The total settlement for a circular loaded area is expressed by this method as follows:

$$s_o = \frac{\pi}{4} C_r p D + D \sqrt[n]{\frac{p}{A}} \quad (a_3)$$

and the settlement of the points on the soil surface outside the loaded plane is

$$s_r = \frac{D}{2} C_r p \arcsin \frac{D}{2r} \quad (a_4)$$

where  $r$  is the distance from the point considered on the soil surface to the centre of the circular loading area.

Note that the method described is used in calculations of non-rigid road pavements.

---

\* Pasternak P. L. Osnovy novogo metoda rascheta zhestkikh i gibkikh fundamentov na uprugom osnovanii (Fundamentals of a New Method of Calculation of Rigid and Flexible Foundations on Elastic Bases). In: Proceedings of the Moscow Civil Engineering Institute, No. 14, ed. by Prof. N. A. Tsytoich, Moscow, Stroiizdat, 1956. Vlasov V. Z., Leontyev N. N. Tekhnicheskaya teoriya rascheta fundamentov na uprugom osnovanii (Technical Theory of Calculation of Foundations on Elastic Bases), Moscow, Stroiizdat, 1956.

### 5.3. ONE-DIMENSIONAL PROBLEM OF THE THEORY OF SOIL CONSOLIDATION

The physical aspect of the problem of soil consolidation has been discussed in detail in Chap. 2, so that here we shall consider only the principal physical prerequisites underlying the statement and solution of some or other problems in the theory of soil consolidation.

The one-dimensional problem of the theory of soil consolidation, first formulated by Prof. Terzaghi in 1925, has been developed mainly by Profs. N. M. Gersevanov (1931-48) and V. A. Florin (1937-64), who have considered a wide circle of problems, and also in the works of other Soviet and foreign researchers who have studied a number of important particular problems in the theory of soil consolidation.

Finally, the latest works in this field are devoted to further development of the *theory of consolidation and creep of soils* on the basis of accounting of the natural compaction and structure of soils and the deformability of all components (creep of the skeleton, compressibility of porous water, etc.) that form soils according to Biot—Florin's generalized theory of volume forces\*.

**Settlement of a soil layer under a continuous load (the principal problem).** Under the action of a continuous load (spreading laterally to substantial distances) a soil layer (Fig. 92) will be subject only

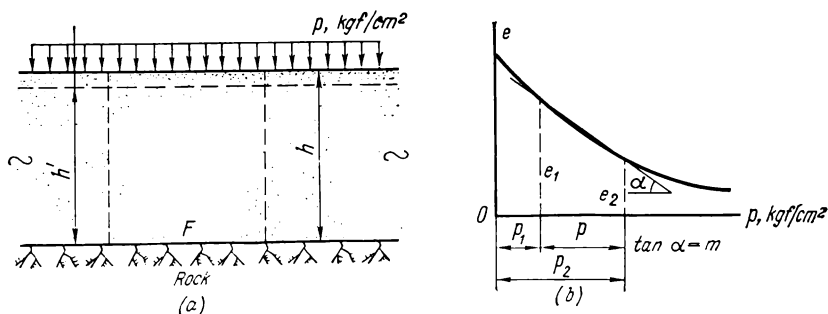


Fig. 92. Scheme of compression of a soil layer with a continuous load  
(a) scheme of load; (b) compression curve

to compression without having the possibility of lateral expansion, which is quite similar to compression in a low cylinder with rigid walls. Under the conditions considered we shall have a one-dimen-

\* Tsytoich N. A., Zaretsky Yu. K. et al. *Prognoz skorosti osadok osnovanii sooruzhenii (konsolidatsiya i polzuchest' mnogofaznykh gruntov)* [Prediction of Settlement Rates of Structure Bases (consolidation and creep of multi-phase soils)], Moscow, Stroizdat, 1967.

sional problem of compression of soils, and the total stabilized settlement of the soil layer can be determined by using the results of compression tests (see Chap. 2).

The settlement of the soil will evidently occur through variation of its volume owing to a reduction of the porosity with an increase of external pressure, the volume of solid particles of the soil then remaining practically invariable.

In the considered layer of height  $h$  we separate a cylinder of a cross-sectional area  $F$ . Taking into account that the volume of solid particles in unit volume of soil [according to formula (1.5)] is  $m = \frac{1}{1+e}$ , we equate the volume of solid particles of the soil in the separated cylinder before the application of the load to the volume after complete compression under load. Then we have

$$\frac{1}{1+e_1} Fh = \frac{1}{1+e_2} Fh' \quad (b)$$

where  $e_1$  = initial void ratio of the soil, corresponding to the conditions of naturally compacted soils; it is found from the data on unit weight  $\gamma$ , moisture content  $W$ , and specific weight  $\gamma_s$  as follows:

$$e = \frac{\gamma_s - \gamma_d}{\gamma_d} \quad \text{where} \quad \gamma_d = \frac{\gamma}{1+W}$$

$e_2$  = void ratio corresponding to an increase of pressure on the soil by the magnitude of the external load  $p$  (it is determined from a compression curve, see Fig. 92b)

$h'$  = final (stabilized after compression) height of the soil layer

Cancelling both parts of equation (b) by  $F$  (which remains constant because of the impossibility of lateral expansion) and solving the equation for  $h'$ , we get

$$h' = h \frac{1+e_2}{1+e_1}$$

But since the settlement  $s$  is equal to the difference in soil heights before and after compaction under load, we have

$$s = h - h' = h \left( 1 - \frac{1+e_2}{1+e_1} \right)$$

or finally

$$s = h \frac{e_1 - e_2}{1 + e_1} \quad (5.8)$$

This is the formula for the total stabilized settlement of a soil layer under a continuous load.

Noting that the void ratio varies in direct proportion to pressure variation [formula (2.7)], i.e.,  $e_1 - e_2 = m(p_2 - p_1) = mp$ , we get

$$s = h \frac{mp}{1 + e_1} \quad (5.8')$$

The value  $\frac{m}{1 + e_1} = m_v$  is the *coefficient of relative compressibility* of soil [formula (2.5)]. Substituting it into (5.8) gives the simplest form of the formula for the settlement of a soil layer under a continuous load

$$s = hm_v p \quad (5.9)$$

but, since  $m_v = \beta/E_o$  according to expression (2.37), then

$$s = h \cdot \frac{\beta}{E_o} p \quad (5.9')$$

Note that expressions (5.8)-(5.9') are identical and hold true for any kind of soil within the limits of a linear relationship between stresses and total deformations.

For strongly compressible soils at very large variations of their void ratio under load and a wide range of variation of external pressures, we have to take into account that the void ratio will then vary by a curvilinear law, for instance, by a logarithmic equation (2.2)

$$e_0 - e_1 = C_c \ln \frac{p_i}{p_0}$$

which upon substitution into formula (5.8) gives

$$s = \frac{h}{1 + e_0} C_c \ln \frac{p_i}{p_0} \quad (5.10)$$

where  $C_c$  = coefficient of compression

$e_0$  = initial void ratio of the soil

$p_0$  = initial pressure on soil

**Time variations of settlements.** Settlements of soils do not stop after complete erection of building structures (the only exception being pure sands), but continue to proceed afterwards, so that the total settlement, determined by formulae (5.8) and (5.9), is attained at a different, sometimes rather long, time depending on the kind of soil (from a few years to tens and even hundreds of years).

The time picture of settlements is affected both by the water permeability of the soil (under conditions of saturation) and the creep of the soil skeleton, and also by the deformability of all the components of the soil (porous water, air inclusions, vapours and gases, organic matter, etc.).

*Water-saturated* plastic and especially liquid-plastic (weak) clayey soils give the highest settlements which sometimes attenuate very

slowly; this offers the highest difficulties for construction. Settlements of structures on such soils can attain hundreds of centimeters and proceed for tens and hundreds of years.

A very important characteristic is the *rate of settlement*, since various building structures possess different capabilities of redistributing the forces arising at non-uniform settlements of their bases. At high rates of settlement, *brittle* (breakdown) *failures* of structures can occur, and at lower rates, slow creep deformations.

The settlement rates can be determined only after their time picture has been studied.

For fully saturated soils, the theory that is most widely used at present and enables the problems set to be solved, is the *theory of filtration consolidation of soils*.

**The assumptions underlying this theory are as follows:**

(1) the theory considers *fully saturated soils* ("soil masses") with free incompressible and hydraulically continuous water present in their voids;

(2) the soil skeleton is assumed to be linearly deformable, the deformations in it being formed instantaneously in response to stresses;

(3) a soil is assumed to have no structure, an external pressure applied to it being completely transferred to the water at the initial instant of time; and

(4) seepage of water in soil voids fully obeys the Darcy's law.

Thus, the theory of filtration consolidation of soils (without additional conditions) is applicable to uncompacted fully saturated (weak) clayey soils.

It will be noted that a number of improvements and additions to the theory of filtration consolidation have been made by some scientists; these improvements take into account the properties of natural clayey soils of various consistency and establish the limits of applicability of particular solutions, which will be discussed later in the book.

**Differential equation of the one-dimensional problem in the theory of filtration consolidation.** This equation makes it possible, under the assumptions made earlier, to formulate the problem of time variations of settlements of a fully saturated soil layer during compaction by a continuous uniformly distributed load under conditions of unidirectional filtration of water. It is assumed that the variation of the flow rate of the water squeezed from the soil voids is described rather accurately by the *filtration law*, and the corresponding variation of the porosity, by the *compaction law*.

We assume that at the initial instant of time the soil mass is in a *static state*, i.e., the pore water pressure is zero. Let us denote by  $p_w$  the pore water pressure in excess of the hydrostatic pressure, and by  $p_z$ , the pressure transmitted to solid particles (effective pressure).

It is then evident that

$$p_z + p_w = p \quad (c_1)$$

i.e., the pressure in the pore water plus that in the soil skeleton is equal to the external pressure  $p$  at any instant of time and at any depth from the draining surface  $z$  (Fig. 93).

At the initial instant, the external pressure is fully transmitted to the pore water (if it is incompressible, which can be assumed when

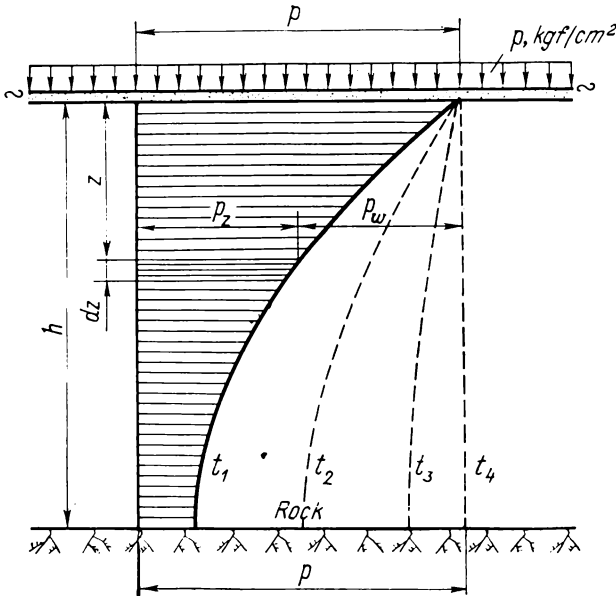


Fig. 93. Distribution of pressures in soil skeleton ( $p_z$ ) and porous water ( $p_w$ ) in a layer of saturated soil with a continuous load for a definite time interval

no air and vapour bubbles are in it), but at the subsequent intervals of time the pressure in the water will diminish, and that in the soil skeleton increase until all the load will be transmitted to the skeleton (see the model of compression of a soil mass in Fig. 16b).

For an elementary layer  $dz$  at a depth  $z$  in the soil mass, an increase of the flow rate of water  $q$  is equal to the decrease of the porosity of soil  $n$ , i.e.,

$$\frac{\partial q}{\partial z} = - \frac{\partial n}{\partial t} \quad (c_2)$$

This main relationship for the derivation of the differential equation of consolidation is a particular case of the condition of conti-

ñuity of the three-dimensional problem of motion of ground waters. It was proposed by Acad. N. N. Pavlovsky in 1922, whereas K. Terzaghi (1925) described the process of consolidation by analogy between thermal conduction and filtration.

Let us transform the left- and right-hand parts of equation (c<sub>2</sub>). For the *left-hand part*, noting the direction of motion of the pore water, we have by the filtration law

$$q = -k_f \frac{\partial H}{\partial z} \quad (c_3)$$

and therefore

$$\frac{\partial q}{\partial z} = -k_f \frac{\partial^2 H}{\partial z^2} \quad (c_4)$$

Taking into account that the head  $H$  in water is equal to the pressure  $p_w$  divided by unit weight of water  $\gamma_w$ , and noting expression (c<sub>1</sub>), we get

$$p_w = p - p_z; \quad H = \frac{p_w}{\gamma_w} \quad \text{or} \quad H = \frac{p - p_z}{\gamma_w}$$

whence

$$\frac{\partial^2 H}{\partial z^2} = -\frac{1}{\gamma_w} \cdot \frac{\partial^2 p_z}{\partial z^2} \quad (c_5)$$

or, noting expression (c<sub>4</sub>)

$$\frac{\partial q}{\partial z} = \frac{k_f}{\gamma_w} \cdot \frac{\partial^2 p_z}{\partial z^2} \quad (c_6)$$

For the *right-hand part* of equation (c<sub>2</sub>), noting that soil porosity  $n = \frac{e}{1+e}$  and neglecting the variation of the void ratio in the denominator of this expression as compared with unity, we can take a certain average value of this coefficient  $e_{av}$  and get

$$\frac{\partial n}{\partial t} \approx \frac{1}{1+e_{av}} \cdot \frac{\partial e}{\partial t} \quad (c_7)$$

By the compaction law (see Chap. 2)

$$\frac{\partial e}{\partial t} = -m \frac{\partial p_z}{\partial t} \quad (c_8)$$

and therefore, we have for the right-hand part of equation (c<sub>2</sub>)

$$\frac{\partial n}{\partial t} = -\frac{m}{1+e_{av}} \cdot \frac{\partial p_z}{\partial t} \quad (c_9)$$

where  $\frac{m}{1+e_{av}} = m_v$  is the *coefficient of relative compressibility* of soil [see formula (2.5)],  $m$  being the relationship between the variation of the void ratio and the pressure exerted.

Substituting the values  $\partial q/\partial z$  and  $dn/dt$  thus found and carrying over the constant values into the left-hand part, we obtain

$$\frac{k_f}{m_v \gamma_w} \cdot \frac{\partial^2 p_z}{\partial z^2} = \frac{\partial p_z}{\partial t} \quad (5.10)$$

Denoting the constant multiplier in the left-hand part by  $c_v$  (which will be called the *coefficient of soil consolidation*), i.e.,

$$c_v = \frac{k_f}{m_v \gamma_w} \quad (5.11)$$

we finally have

$$c_v \frac{\partial^2 p_z}{\partial z^2} = \frac{\partial p_z}{\partial t} \quad (5.12)$$

This is the differential equation of the one-dimensional problem in the theory of filtration consolidation (compaction under load) of soils.

Taking into account that the effective head is

$$H = \frac{p_w}{\gamma_w}$$

and

$$p_w = p - p_z$$

the differential equation can be written in the form

$$\frac{\partial \dot{H}}{\partial t} = c_v \frac{\partial^2 H}{\partial z^2} \quad (5.13)$$

As is known from the course of higher mathematics, differential equation (5.12) can be solved by using Fourier series and superposing certain initial and boundary conditions which can be more simply formulated if we consider a mathematically identical problem of compression of a soil layer  $2h$  thick, but under conditions of two-way filtration (both upward and downward), i.e., by supplementing the layer considered, as it were, with its mirror image.

For the case of a uniform (in a stabilized state) distribution of compacting pressures over the depth, the solution of equation (5.12) can be represented in the form as follows:

$$p_z = p \left[ 1 - \frac{4}{\pi} \sin \frac{\pi z}{2h} e^{-N} - \frac{4}{3\pi} \sin \frac{3\pi z}{2h} e^{-9N} - \frac{4}{5\pi} \sin \frac{5\pi z}{2h} e^{-25N} - \dots \right] \quad (5.14)$$

where

$$N = \frac{\pi^2 c_v}{4h^2} t \quad (5.15)$$

For some practical cases, of essential importance is the pressure in the soil skeleton that is transmitted to the subgrade rock, i.e., the pressure with  $z = h$ , and also the shear resistance at the contact with the subgrade rock which is proportional to that pressure. Assuming that  $z = h$  in formula (5.14) and limiting ourselves to the first term of the series, we get

$$p_h \approx p \left[ 1 - \frac{4}{\pi} e^{-N} \right] \quad (5.16)$$

and the shear resistance is

$$\tau = p_h \tan \varphi + c \quad (5.17)$$

Of the highest practical importance, however, is the formula of settlement of a soil layer under a continuous load for any instant of time from the beginning of loading, i.e., the settlement  $s_t$ .

In order to determine this value, we introduce the concept of the *degree of consolidation*.

If the degree of consolidation corresponding to the full stabilized settlement is taken as unity and the fraction of the total compression (i.e., the degree of consolidation for any instant of time) is denoted by  $U$ , then the latter can be found as the ratio of the area of a diagram of pressures in soil skeleton for time  $t$  to the area of the total (stabilized) diagram of pressures (when  $t = \infty$ ). Mathematically, this can be written as follows:

$$U = \int_0^h \frac{p_z dz}{F_p} \quad (5.18)$$

where  $F_p$  is the area of the total stabilized diagram of compacting pressures ( $F_p = ph$  in the case considered).

Substituting the expression for pressures  $p_z$  in the soil skeleton from formula (5.14) into equation (5.18) and integrating within the limits specified (with the degree of consolidation for the case considered being denoted as  $U_0$ ), we obtain

$$U_0 = 1 - \frac{8}{\pi^2} \left( e^{-N} + \frac{1}{9} e^{-9N} + \frac{1}{25} e^{-25N} + \dots \right) \quad (5.19)$$

Since  $e^{-N}$  is a proper fraction, then we can limit ourselves to the first term of the series in many practical cases (for instance, with  $U_0 > 0.25$ ). We then have

$$U_0 \approx 1 - \frac{8}{\pi^2} e^{-N} \quad (5.19')$$

Since the full stabilized settlement corresponds to full compaction, and the settlement during time  $t$ , to a fraction of full compaction,

Table 5.3

Values of  $e^{-x}$  Versus  $x$ 

$x$	$e^{-x}$	$x$	$e^{-x}$	$x$	$e^{-x}$	$x$	$e^{-x}$
0.000	1.000	0.40	0.670	0.90	0.407	1.40	0.247
0.001	0.999	0.41	0.664	0.91	0.403	1.41	0.244
0.002	0.998	0.42	0.657	0.92	0.399	1.42	0.242
0.003	0.997	0.43	0.651	0.93	0.394	1.43	0.239
0.004	0.996	0.44	0.644	0.94	0.391	1.44	0.237
0.005	0.995	0.45	0.638	0.95	0.387	1.45	0.235
0.006	0.994	0.46	0.631	0.96	0.383	1.46	0.232
0.007	0.993	0.47	0.625	0.97	0.379	1.47	0.230
0.008	0.992	0.48	0.619	0.98	0.375	1.48	0.228
0.009	0.991	0.49	0.613	0.99	0.372	1.49	0.225
		0.50	0.607	1.00	0.368	1.50	0.223
0.01	0.990	0.51	0.601	1.01	0.364	1.51	0.221
0.02	0.980	0.52	0.595	1.02	0.351	1.52	0.219
0.03	0.970	0.53	0.589	1.03	0.357	1.53	0.217
0.04	0.961	0.54	0.583	1.04	0.353	1.54	0.214
0.05	0.951	0.55	0.577	1.05	0.350	1.55	0.212
0.06	0.942	0.56	0.571	1.06	0.346	1.56	0.210
0.07	0.932	0.57	0.566	1.07	0.343	1.57	0.208
0.08	0.923	0.58	0.560	1.08	0.340	1.58	0.206
0.09	0.914	0.59	0.554	1.09	0.336	1.59	0.204
0.10	0.905	0.60	0.549	1.10	0.333	1.60	0.202
0.11	0.896	0.61	0.543	1.11	0.330	1.61	0.200
0.12	0.887	0.62	0.538	1.12	0.326	1.62	0.198
0.13	0.878	0.63	0.533	1.13	0.323	1.63	0.196
0.14	0.869	0.64	0.527	1.14	0.320	1.64	0.194
0.15	0.861	0.65	0.522	1.15	0.317	1.65	0.192
0.16	0.852	0.66	0.517	1.16	0.313	1.66	0.190
0.17	0.844	0.67	0.512	1.17	0.310	1.67	0.188
0.18	0.835	0.68	0.507	1.18	0.307	1.68	0.186
0.19	0.827	0.69	0.502	1.19	0.304	1.69	0.185
0.20	0.819	0.70	0.497	1.20	0.301	1.70	0.183
0.21	0.811	0.71	0.492	1.21	0.298	1.71	0.181
0.22	0.803	0.72	0.487	1.22	0.295	1.72	0.179
0.23	0.795	0.73	0.482	1.23	0.292	1.73	0.177
0.24	0.787	0.74	0.477	1.24	0.289	1.74	0.176
0.25	0.779	0.75	0.472	1.25	0.286	1.75	0.174
0.26	0.771	0.76	0.467	1.26	0.284	1.76	0.172
0.27	0.763	0.77	0.463	1.27	0.281	1.77	0.170
0.28	0.756	0.78	0.458	1.28	0.278	1.78	0.169
0.29	0.748	0.79	0.454	1.29	0.275	1.79	0.167
0.30	0.741	0.80	0.449	1.30	0.273	1.80	0.165
0.31	0.733	0.81	0.445	1.31	0.270	1.81	0.164
0.32	0.726	0.82	0.440	1.32	0.267	1.82	0.162
0.33	0.719	0.83	0.436	1.33	0.264	1.83	0.160
0.34	0.712	0.84	0.431	1.34	0.262	1.84	0.159
0.35	0.705	0.85	0.427	1.35	0.259	1.85	0.157
0.36	0.698	0.86	0.423	1.36	0.257	1.86	0.156
0.37	0.691	0.87	0.419	1.37	0.254	1.87	0.154
0.38	0.684	0.88	0.415	1.38	0.252	1.88	0.152
0.39	0.677	0.89	0.411	1.39	0.249	1.89	0.151

Table 5.3 (continued)

$x$	$e^{-x}$	$x$	$e^{-x}$	$x$	$e^{-x}$	$x$	$e^{-x}$
1.90	0.150	2.00	0.135	2.10	0.122	2.6	0.074
1.91	0.148	2.01	0.134	2.15	0.116	2.7	0.067
1.92	0.147	2.02	0.133	2.20	0.111	2.8	0.061
1.93	0.145	2.03	0.131	2.25	0.105	2.9	0.055
1.94	0.144	2.04	0.130	2.30	0.100	3.0	0.050
1.95	0.142	2.05	0.129	2.35	0.095	4.0	0.018
1.96	0.141	2.06	0.127	2.40	0.091	5.0	0.007
1.97	0.140	2.07	0.126	2.45	0.086	6.0	0.002
1.98	0.138	2.08	0.125	2.50	0.082	7.0	0.001
1.99	0.137	2.09	0.124	2.55	0.078	10.0	0.000

then the *degree of consolidation* can be expressed by the following equation:

$$U = \frac{s_t}{s} \quad (5.20)$$

where  $s_t$  = settlement during the given time

$s$  = full stabilized settlement, for instance, determined by formulae (5.8) and (5.9)

From relationship (5.20), we find

$$s_t = sU \quad (5.21)$$

For the case considered, which may be termed the *fundamental* one, we get

$$s_t = sU_0 \quad (5.21')$$

or, noting expressions (5.9) and (5.8), the settlement at any time  $t$  for the principal case (with uniform distribution of compacting pressures over the depth) is found as

$$s_t = hm_v p \left[ 1 - \frac{8}{\pi^2} \left( e^{-N} + \frac{1}{9} e^{-9N} + \dots \right) \right] \quad (5.22)$$

The calculations can be simplified by using the values of  $e^{-x}$  versus  $x$  given in Table 5.3.

**Example 5.1.** Find the settlements of a soil layer at various intervals: 1 year, 2 years, and 5 years, if the pressure on the soil  $p = 2 \text{ kgf/cm}^2$ , the thickness of the layer  $h = 5 \text{ m}$ , the coefficient of relative compressibility  $m_v = 0.01 \text{ cm}^2/\text{kgf}$ , and the coefficient of filtration  $k_f = 1 \times 10^{-8} \text{ cm/s}$ .

By formula (5.15) we find the constant multiplier  $N$

$$N = \frac{\pi^2 c_v}{4h^2} t$$

Preliminarily, we find the values of consolidation coefficient  $c_v$ , noting that  $1 \text{ cm/s} \approx 3 \times 10^7 \text{ cm/year}$  and  $\gamma_w = 1 \text{ gf/cm}^3 = 0.001 \text{ kgf/cm}^3$

$$c_v = \frac{k_f}{m_v \gamma_w} \approx \frac{1 \times 10^{-8} \times 3 \times 10^7}{0.01 \times 0.001} = 30,000 \text{ cm}^2/\text{year}$$

Then

$$N \approx \frac{9.87 \times 30,000}{4 \times 500^2} t \approx 0.3t$$

The total stabilized settlement of the soil layer under a continuous load is found by formula (5.9)

$$s = hm_v p = 500 \times 0.01 \times 20 = 10 \text{ cm}$$

The settlement  $s_1$  one year after loading is found by substituting the following values (taken from Table 5.3) into formula (5.22):

$$e^{-N} = e^{-0.3 \times 1} = 0.741; \quad e^{-9N} = e^{-9 \times 0.3 \times 1} = 0.067$$

Then the settlement of the layer considered one year after loading will be

$$s_1 = hm_v p \left[ 1 - \frac{8}{\pi^2} \left( e^{-N} + \frac{1}{9} e^{-9N} \right) \right] = 10 [1 - 0.81 (0.741 + 0.007)] = 3.9 \text{ cm}$$

The settlement after two years is found from the same formula (5.22) by neglecting all the terms except the first one

$$e^{-N} = e^{-0.3 \times 2} = 0.549$$

$$s_2 = hm_v p \left[ 1 - \frac{8}{\pi^2} e^{-N} \right] = 10 (1 - 0.81 \times 0.549) = 5.6 \text{ cm}$$

For  $t = 5$  years we have

$$s_5 = 10 (1 - 0.81 e^{-0.3 \times 5}) = 8.2 \text{ cm}$$

The curve of time variations of settlements constructed from the data of this example is shown in Fig. 94.

**Other cases of the one-dimensional problem of consolidation.** Earlier, we have considered the *fundamental case 0* when the diagram of compacting pressures in the depth of a soil layer is a rectangle (Fig. 95a), i.e., the total pressure from the action of an external load does not vary with depth (for instance, under the action of a continuous load), other cases of practical importance are *case 1*, when the compacting pressure increases with depth by a triangle law (Fig. 95b); *case 2*, when the pressure decreases with an increase of depth by a triangle law (Fig. 95c); and *combined cases* with trapezoidal diagrams of compacting pressures (either increasing or decreasing with an increase of depth).

Case 1, with the pressure increasing linearly with depth, may take place, for instance, under compaction of the soil by its dead weight (Fig. 95b), when

$$p_z = \frac{p}{h} z$$

Solution of the differential equation of consolidation (5.12) for the case considered (with boundary conditions:  $p_w = 0$  when  $z = 0$ ,

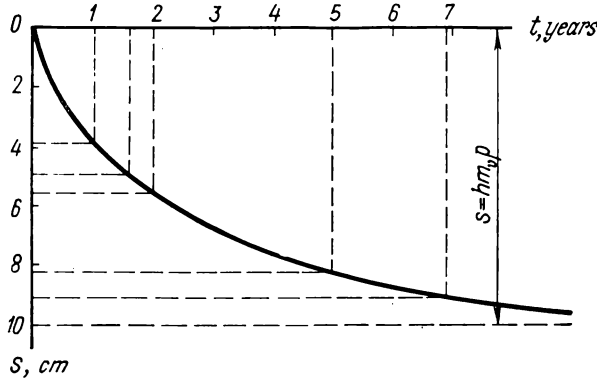


Fig. 94. Diagram to Example 5.1

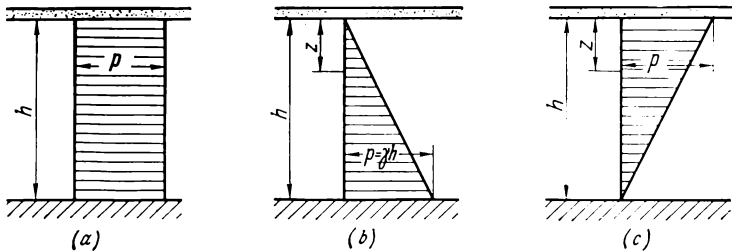


Fig. 95. Various cases of distribution of compacting pressures over the depth for the one-dimensional problem  
 (a) case 0; (b) case 1; (c) case 2

and  $dp/dz = 0$  when  $z = h$ ) makes it possible to find the expression for the pore water pressure  $p_w$  and then the degree of consolidation  $U_1$

$$U_1 = 1 - \frac{32}{\pi^3} \left( e^{-N} - \frac{1}{27} e^{-9N} + \frac{1}{125} e^{-25N} \mp \dots \right) \quad (5.23)$$

The settlement of the soil layer under the action of compacting pressures increasing with depth by a triangle law will then be found

for any time  $t$  (noting that the average pressure is  $p/2$ ) as

$$s_1 = \frac{hm_v p}{2} \left[ 1 - \frac{32}{\pi^3} \left( e^{-N} - \frac{1}{27} e^{-9N} \pm \dots \right) \right] \quad (5.24)$$

Case 2 can be reduced to those discussed earlier, since

$$p_z = p - \frac{p}{h} z$$

Solution of differential equation (5.12) and equation (5.18) for the case considered gives\*

$$U_2 = 1 - \frac{16}{\pi^2} \left[ \left( 1 - \frac{2}{\pi} \right) e^{-N} + \frac{1}{9} \left( 1 + \frac{2}{3\pi} \right) e^{-9N} + \dots \right] \quad (5.25)$$

The settlement for any time is

$$s_2 = \frac{hm_v p}{2} \left\{ 1 - \frac{16}{\pi^2} \left[ \left( 1 - \frac{2}{\pi} \right) e^{-N} + \frac{1}{9} \left( 1 + \frac{2}{3\pi} \right) e^{-9N} + \dots \right] \right\} \quad (5.26)$$

By comparing the expressions for the degree of consolidation obtained for various cases of compacting pressures, it can be shown that the following relationship holds true:

$$U_2 = 2U_0 - U_1 \quad (5.27)$$

Expression (5.27) enables  $U_2$  to be calculated for the known  $U_0$  and  $U_1$  without using formula (5.25).

Note that the case 2 considered has wide application in calculations of settlement of foundations, as will be shown later.

To simplify the prediction, Table 5.4 gives the values of  $N$  depending on the degree of consolidation  $U$  for various cases of com-

Table 5.4

Values of  $N$  for Prediction of Settlements of Soils  
as a Function of Time

$U = \frac{s_t}{s}$	Values of $N$ for cases			$U = \frac{s_t}{s}$	Values of $N$ for cases		
	0	1	2		0	1	2
0.05	0.005	0.06	0.002	0.55	0.59	0.84	0.32
0.10	0.02	0.12	0.005	0.60	0.71	0.95	0.42
0.15	0.04	0.18	0.01	0.65	0.84	1.10	0.54
0.20	0.08	0.25	0.02	0.70	1.00	1.24	0.69
0.25	0.12	0.31	0.04	0.75	1.18	1.42	0.88
0.30	0.17	0.39	0.06	0.80	1.40	1.64	1.08
0.35	0.24	0.47	0.09	0.85	1.69	1.93	1.36
0.40	0.31	0.55	0.13	0.90	2.09	2.35	1.77
0.45	0.39	0.63	0.18	0.95	2.80	3.17	2.54
0.50	0.49	0.73	0.24	1.00	$\infty$	$\infty$	$\infty$

\* Tsytoich N. A., Zaretsky Yu. K. et al. Prognoz skorosti osadok osnovanii sooruzhenii (Prediction of Settlement Rates of Structure Bases), Moscow, Stroizdat, 1967.

compacting pressures: uniform (case 0) and varying by triangle law (cases 1 and 2).

If the distribution of compacting pressures in a soil layer is close to a trapezoidal one,  $U$  and  $N$  are found by interpolation between the tabulated values of  $N$  for cases 0 and 1 (if pressures increase with depth) or for cases 0 and 2 (with decreasing pressures).

The interpolation coefficients  $I$  and  $I'$  are given in Table 5.5 and are found depending on the ratio  $V$  of compacting pressures when  $z = 0$  and  $z = h$ .

Table 5.5

Values of  $I$  and  $I'$ 

Case 0-1	$V$	0	0.1	0.2	0.3	0.4	0.5	0.6	0.7	0.8	0.9	1.0
	$I$	1	0.84	0.69	0.56	0.46	0.36	0.27	0.19	0.12	0.06	0
Case 0-2	$V$	1	1.5	2.0	2.5	3.0	3.5	4	5	7	10	20
	$I'$	1	0.83	0.71	0.62	0.55	0.50	0.45	0.39	0.30	0.23	0.13

The values of  $N$  for trapezoidal distribution of compacting pressures are found by the expressions:

for case 0-1

$$N_{0-1} = N_0 + (N_1 - N_0)I \quad (d_1)$$

for case 0-2

$$N_{0-2} = N_2 + (N_0 - N_2)I' \quad (d_2)$$

To calculate settlements by means of the tables, we have to select the degree of consolidation (for instance,  $U = 0.2; 0.4; 0.6; \text{etc.}$ ), find the corresponding value of  $N$  from Table 5.4 and, using the relationship for  $N$  [formula (5.15)], determine the time  $t$  corresponding to this degree of consolidation

$$t = \frac{4h^2}{\pi^2 c_v} N \quad (5.28)$$

Note that, as could be expected, the calculations of settlements directly by formulae (5.22) and (5.26) and by means of the tables give identical results.

**Example 5.2.** For the previous example of consolidation of a soil layer (of a thickness of  $h = 5$  m), determine the settlement and the time corresponding to 0.5 and 0.9 of the total settlement.

It has been found in the previous example that the total settlement  $s = 10$  cm and the coefficient of consolidation  $c_v = 30,000$  cm<sup>2</sup>/year.

For  $U_0 = s_t/s = 0.5$ , the settlement  $s_t = U_0 s = 0.5 \times 10 = 5$  cm and  $N_0 = 0.49$  according to Table 5.4; then

$$t = \frac{4h^2}{\pi^2 c_v} N_0 = \frac{4 \times 500^2}{9.87 \times 30,000} \times 0.49 \approx 1.6 \text{ years}$$

Similarly, for the degree of consolidation  $U_0 = 0.9$ ,  $s_t = 0.9 \times 10 = 9$  cm, and  $N_0 = 2.09$ , and the corresponding time is

$$t = \frac{4 \times 500^2}{9.87 \times 30,000} \times 2.09 \approx 6.9 \text{ years}$$

If the settlements obtained are plotted on the earlier diagram (see Fig. 94) then, as could be expected, the new points will exactly coincide with the curve constructed by the analytical formulae.

**Consideration of soil structure and compressibility of gas-containing pore water.** According to Terzaghi — Gersevanov's theory of filtration consolidation, the external pressure at the initial moment of application of a load is completely transmitted to pore water. But if the soil possesses structural bonds, then, as has been shown experimentally, the pressure transmitted to water is only a *fraction* of the external pressure, and the more discrete the structure of the soil and the greater its preliminary compaction, the smaller this fraction will be. The compaction may be characterized by the *coefficient of initial pore-water pressure*  $\beta_0$  which is determined by the expression\*

$$\beta_0 = \frac{p_{w0}}{p} \quad (5.29)$$

where  $p_{w0}$  is initial pore-water pressure in a saturated soil under a load  $p$  (a function of the structural compressive strength of soil), which is determined in compression tests of soil samples of undisturbed structure by measuring the initial pore-water pressure.

As has been given in Chap. 2, gas-containing pore water possesses a substantial compressibility, the coefficient of compressibility [formula (2.40)] being equal to

$$m_w = (1 - I_w) \frac{1}{p_a}$$

where  $I_w =$  coefficient of water saturation of soil

$p_a =$  atmospheric pressure (1 kgf/cm<sup>2</sup>)

Note that if the coefficient  $\beta_0$ , soil porosity  $n$ , and the coefficient of instantaneous compressibility  $m_{inst}$  are known, the coefficient of compressibility of pore water  $m_w$  can be found (with a greater accuracy) by the formula

$$m_w = \frac{m_{inst} (1 - \beta_0)}{\beta_0 n} \quad (5.30)$$

\* See the footnote on p. 197.

Solution of the differential equation of consolidation (5.12) with regard to an incomplete transmission of pressure to pore water and the compressibility of the gas-containing pore water (see the footnote on p. 197) makes it possible to determine the degree of consolidation and settlement for any instant of time by the earlier formulae through introducing some corrections into them, in particular, by assuming that

$$c_w = \frac{k_f}{m_v \gamma_w} \beta_0 \quad (5.34)$$

where

$$\beta_0 = \beta_{str} B \quad (5.32)$$

$$B = \frac{1}{1 + \frac{m_w}{m_v} n \beta_{str}} \quad (5.33)$$

where  $\beta_{str}$  = coefficient of influence of structural bonds on pore-water pressure

$B$  = coefficient of influence of the compressibility of pore water on pore-water pressure

The expressions for settlements  $s_t$  then take the following forms: for the fundamental case

$$s_{0(t)} = hm_v p \left[ 1 - \frac{8}{\pi^2} B \left( e^{-N} + \frac{1}{9} e^{-9N} + \dots \right) \right] \quad (5.22')$$

for case 1

$$s_{1(t)} = \frac{hm_v p}{2} \left[ 1 - \frac{32}{\pi^3} B \left( e^{-N} - \frac{1}{27} e^{-9N} - \dots \right) \right] \quad (5.24')$$

for case 2

$$s_{2(t)} = \frac{hm_v p}{2} \left\{ 1 - \frac{16}{\pi^2} B \left[ \left( 1 - \frac{2}{\pi} \right) e^{-N} + \frac{1}{9} \left( 1 + \frac{2}{3\pi} \right) e^{-9N} + \dots \right] \right\} \quad (5.26')$$

where

$$N = \frac{\pi^2 c_w}{4h^2} t$$

Note that for structureless and weakly structural soils  $\beta_{str} = 1$ ; then we have from equation (5.32) that  $B = \beta_0$ . If, however,  $m_w = 0$ , then the earlier expression (5.11) employed in the theory of purely filtration consolidation will hold true for the coefficient of consolidation.

**Secondary consolidation.** The degree of consolidation of soils, even when determined for a fully saturated soil, can truly reflect the process of compaction only after the consolidation attains a

definite magnitude (which is different for soils of various compaction and compressibility), since, with a long duration of compaction, the process of consolidation will be affected both by the newly formed structural water-colloidal bonds and the *secondary effects* caused by the *creep* of the mineral skeleton of soil and of thin water-colloidal shells of solid particles. Here we shall only indicate the range of applicability of filtration consolidation according to the degree of compaction attained, since the problems of soil creep caused by soil rheological properties will be specially discussed in Chap. 6 of the book.

With an external load applied to a water-saturated soil, an *instantaneous compression* (adiabatic compression caused by the com-

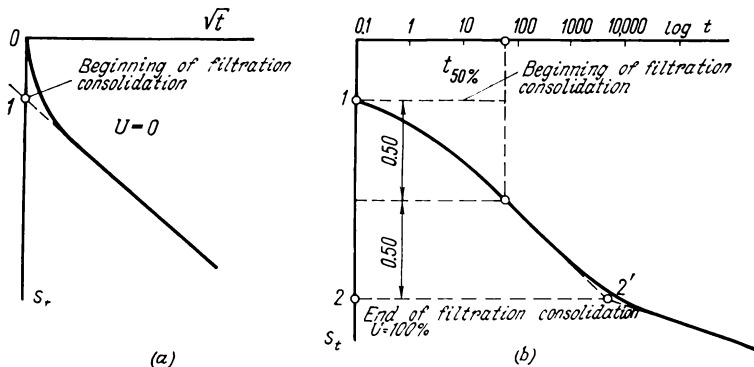


Fig. 96. Determination of filtration stage of compaction of water-saturated soils

(a) beginning of filtration consolidation; (b) end of filtration consolidation

pressibility of pore water) is first observed, and then the *process* of filtration *compaction* which is caused by squeezing water from soil voids; finally, this is supplemented by the *process* of secondary consolidation or *creep* of the soil skeleton, which is caused by irreversible *shear* of particles, aggregations, water-colloidal shells, etc., when squeezing of water becomes insignificant.

For an approximate determination of the beginning of the filtration compaction stage, let us briefly discuss Taylor's method.

The *beginning of filtration consolidation* is determined by the initial section of the consolidation curve plotted in the coordinates  $s_t$  and  $\sqrt{t}$  (Fig. 96). Since the process of filtration settlement occurs proportionally to  $\sqrt{t}$ , then, by extending the straight section of the compaction curve to the axis of settlements (Fig. 96a), we obtain the point corresponding to the beginning of filtration consolidation (i.e.,  $U = 0$ ).

The end of filtration consolidation ( $U = 100$  per cent) is determined (according to A. Casagrande) on the same curve, but plotted in semi-logarithmic coordinates ( $s_t$  and  $\log t$ ), by finding the point of intersection of the lower section of the filtration consolidation curve and the curve last section which corresponds to the secondary consolidation (Fig. 96b); according to experimental data for long intervals of time it will be linearly dependent on  $\log t$ .

Within the range thus found, we can assume that the process of compaction of saturated soils is determined mainly by filtration consolidation and further proceeds owing to secondary consolidation.

The magnitude of filtration settlement is determined by section 1-2 on the axis of settlements (Fig. 96b).

The end of the filtration consolidation process is easy to establish experimentally by careful measurement of the excess pore-water pressure. If the increment of pore-water pressure is practically equal to zero, the process of filtration consolidation can be assumed to be finished, and further settlement of the soil should be regarded as creep deformation of the skeleton.

#### 5.4. PLANAR AND THREE-DIMENSIONAL PROBLEMS IN THE THEORY OF FILTRATION CONSOLIDATION OF SOILS

**Differential equations of consolidation.** In the previous section, we have discussed the differential equation of consolidation for the one-dimensional problem and obtained its solution for a number of cases. For convenience of analogy with the following discussion, this equation will be written through the head function [formula (5.13)] as follows:

$$\frac{\partial H}{\partial t} = c_v \frac{\partial^2 H}{\partial z^2}$$

where  $c_v = \frac{k_f}{m_v \gamma_w}$  is the coefficient of consolidation for the one-dimensional problem [formula (5.11)].

For the planar and three-dimensional problems, the differential equations of the theory of filtration consolidation have been formulated in the simplest form by Prof. V. A. Florin:

for the planar problem

$$\frac{\partial H}{\partial t} = \frac{1}{2\gamma_w} \cdot \frac{\partial \Theta}{\partial t} + c'_v \nabla^2 H \quad (5.34)$$

where  $c'_v = \frac{k_f(1+2\xi_0)}{2\gamma_w m_v}$  = coefficient of consolidation for the planar problem

$\xi_0$  = coefficient of lateral pressure of soil at rest

$\Theta$  = sum of the principal stresses in the point considered from the action of external load  
for the three-dimensional problem

$$\frac{\partial H}{\partial t} = \frac{1}{3\gamma_w} \cdot \frac{\partial \Theta}{\partial t} + c_v'' \nabla^2 H \quad (5.35)$$

where  $c_v'' = \frac{k_f(1+2\xi_0)}{3\gamma_w m_v}$  = coefficient of consolidation for the three-dimensional problem

$$\nabla^2 H = \frac{\partial^2 H}{\partial x^2} + \frac{\partial^2 H}{\partial y^2} + \frac{\partial^2 H}{\partial z^2} = \text{Laplacian operator}$$

Note that when calculating the coefficients of consolidation by formulae (5.13), (5.34) and (5.35), the characteristics entering these formulae, i.e., the coefficients of filtration, lateral compressibility, lateral pressure of soil at rest, etc., are to be taken as certain average values.

The method of accounting of the variability of the coefficients characterizing the properties of compressible soils has found no wide application because of its extreme complexity. But there exists a general method (proposed by Prof. V. A. Florin) for numerical integration of the differential equations of the planar and three-dimensional problems of soil consolidation, which enables the variability of soil characteristics to be taken into account. Closed and tabulated solutions have been found only for some particular cases.

If, by solving an appropriate differential equation of consolidation, we can find the head for the given time  $t$ , then the settlement  $s_t$  in the point considered will be determined by the formula

$$s_t = s - (1 - \mu_0) \gamma_w m_v \sum_1^{h_a} H \Delta z \quad (5.36)$$

where  $s$  = total final (stabilized) settlement

$h_a$  = active depth of compression (see the next section)

**Action of a load uniformly distributed over rectangular area.** The problem of consolidation of a saturated soil under the action of a local uniformly distributed load under conditions of the three-dimensional problem of a uniform *half-space* was considered by Gibson and McNamee\*, with the following expression being found for the degree of consolidation  $U_c$  at a corner point of a rectangular sur-

---

\* Proceedings of the 4th International Congress on Soil Mechanics and Foundation Engineering, London, 1957.

face of loading :

$$U_c = \frac{\int_0^T \frac{1}{\sqrt{t}} \operatorname{erf} \frac{1}{2\sqrt{t}} \operatorname{erf} \frac{\lambda}{2\sqrt{t}} dt}{\int_0^\infty \frac{1}{\sqrt{t}} \operatorname{erf} \frac{1}{2\sqrt{t}} \operatorname{erf} \frac{\lambda}{2\sqrt{t}} dt} \quad (5.37)$$

where  $T = \frac{c_v'' t}{L^2}$  = time factor

$c_v''$  = coefficient of consolidation

$t$  = time

$L$  = length of the rectangular surface of loading

$\lambda$  = side ratio of the rectangular surface of loading  
(width-to-length ratio)

The calculations may be simplified by using a graph, such as shown in Fig. 97, which makes it possible to determine the degree

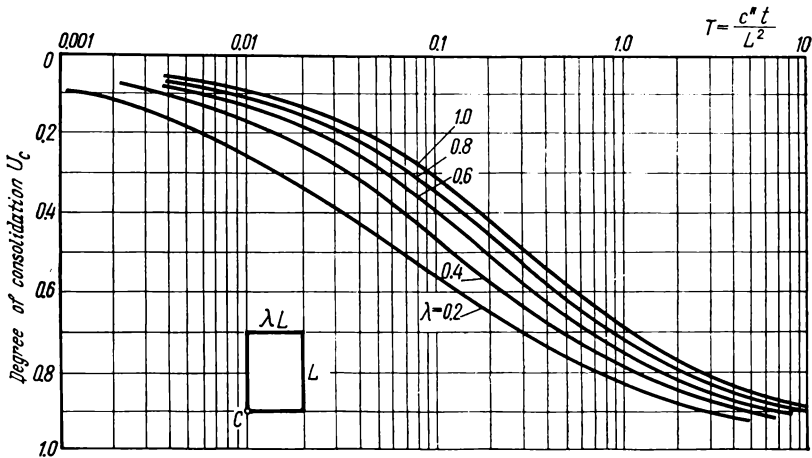


Fig. 97. Diagram to determine the degree of consolidation of a water-saturated soil under a corner point  $C$  of a rectangular loaded surface (according to Gibbson)

of consolidation  $U_c$  for the given values of  $T = c_v'' t / L^2$  and  $\lambda$  (from 0.2 to 1.0).

As regards the total settlement  $s_c$  of soil under a corner of the rectangular loading surface, it can be found by formula (5.4) for a linearly deformable space, which now takes the following form:

$$s_c = \frac{\omega_c p b (1 - \mu_0^2)}{E_0} \quad (5.4')$$

where  $\omega_c$  = form factor for the corner point  $C$  (see Table 5.2)

$p$  = unit load on the rectangular surface of loading

$b$  = width of the loading surface

When the settlement  $s_c$  and degree of consolidation  $U_c$  are known, the settlement of a corner point corresponding to any time  $t$  is easily found as follows:

$$s_t = s_c U_c \quad (5.21')$$

Using the method of corner points and the diagram given in Fig. 97, we can find the settlement for any point of the soil.

Note that calculations of  $s_c$  can be substantially simplified by using the coefficients of an equivalent soil layer (see Sec. 5.6, Tables 5.6-5.8 below).

**Axisymmetrical problem in the theory of consolidation.** This problem is of a high practical importance, for instance, in the design of a vertical drainage which is employed for quicker consolidation and strengthening of weak saturated soils.

For the case of vertical drainage, the differential equation for the three-dimensional problem of consolidation can be represented in the form

$$\frac{\partial p_w}{\partial t} = c_r \left( \frac{\partial^2 p_w}{\partial z^2} + \frac{1}{r} \cdot \frac{\partial p_w}{\partial r} \right) + c_z \frac{\partial^2 p_w}{\partial z^2} \quad (5.38)$$

where  $c_r$  and  $c_z$  = coefficients of consolidation (radial and vertical—axial)

$r$  = radius of vertical drain

The solution of equation (5.38) is based on the theorem of resolution of a three-dimensional radial flow into planar and linear flows (Carrillo, 1942), which makes it possible, by using the method of numerical integration, to obtain data for construction of the graphs of degree of consolidation, first of the radial  $U_r$  and axial  $U_z$  consolidation, and then of the total consolidation  $U_\Sigma^*$

$$U_\Sigma = 1 - (1 - U_r)(1 - U_z) \quad (5.39)$$

The problem becomes substantially more complicated if we have to take into account the structural compressive strength of drained soils,  $p_{st,r}$ , and the phenomenon of the initial pressure gradient  $i_0$ .

Here, we shall only give the closed solution found for the case of "equal vertical deformations", which is rather convenient for practical calculations.

When the surface of a soil mass being drained is covered by a water-permeable layer (usually of a thickness not less than the diameter of drains, see Fig. 98), then, as has been shown experimen-

---

\* Tsyтович N. A. Mekhanika gruntov (Soil Mechanics), 4th ed., Moscow, Stroiizdat, 1963.

tally, this layer will equalize the settlements, so that in calculations of vertical drainage we can use the *condition of equal deformations*, i.e., assume that the settlement is always the same for the whole surface of the drained portion of the soil mass.

In this case equation (5.38) can be replaced by an approximate first-order differential equation whose closed solution (according

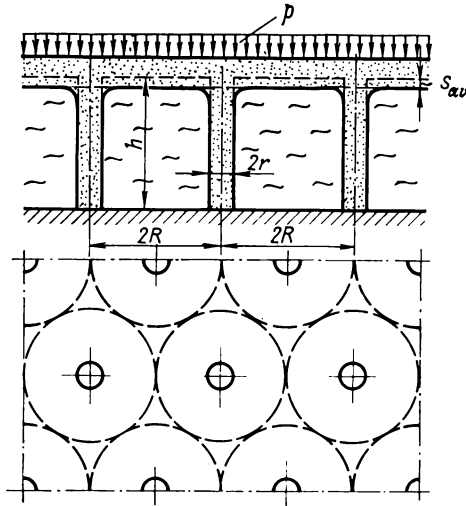


Fig. 98. Diagram of vertical draining

to M. Yu. Abelev\*) can be given for an average value of the degree of radial consolidation  $U_r$  of the whole layer being drained in the form as follows:

$$U_r \approx \left[ 1 - \frac{p_{str}}{p} - \frac{2}{3} \cdot \frac{\gamma_w i_0}{p} \left( R - \frac{r^3}{R^2} \right) \right] (1 - e^{-M't}) + \frac{p_{str}}{p} \quad (5.40)$$

where

$$M' \approx \frac{k_f}{m_o \gamma_w \left( \frac{R^2}{2} \ln \frac{R}{r} - \frac{3}{8} R^2 \right)}$$

$R$  = influence radius of drains (half the distance between the axes of drains)

$r$  = radius of drains<sup>m</sup>

$p$  = uniformly distributed external pressure (unit load)

If the initial pressure gradient is zero ( $i_0 = 0$ ), which in many cases is true of weak soils, then equation (5.40) assumes the following

\* See the footnote on p. 197.

simpler form:

$$U_r = \left[ 1 - \frac{P_{str}}{p} \right] (1 - e^{-M't}) + \frac{P_{str}}{p}$$

or

$$U_r \approx 1 - \frac{P - P_{str}}{p} e^{-M't}$$

The degree of consolidation  $U_z$  (vertical) is found from expression (5.19)

$$U_z \approx 1 - \frac{8}{\pi^2} e^{-M't}$$

where

$$M = \frac{\pi^2 c_z}{4h^2}$$

In the case considered, the settlement for any time is determined, as before, by formula (5.21)

$$s_t = sU_\Sigma = hm_v p U_\Sigma \quad (5.21'')$$

where  $U_\Sigma$  is to be found by formula (5.39).

It will be noted that the differential equation of the axisymmetrical problem of consolidation has been also solved on condition that the settlements near the drains are not equal to the settlements outside the drains, but with account of the structural strength of soils  $p_{str}$  and the initial pressure gradient  $i_0$ ; this solution, however, is of a more complicated form involving Bessel and Neumann zero- and first-order functions\*.

#### 5.5. PREDICTION OF FOUNDATION SETTLEMENTS BY THE LAYERWISE SUMMATION METHOD

Calculations of foundation settlements are of enormous practical importance, since without the knowledge of the calculated settlement it is impossible to design foundations by the ultimate deformations of their bases according to the standard requirements.

The *vertical displacements* of foundations caused by the *deformation of their bases* under the action of the load from the foundation are termed the *foundation settlements*.

The total settlement of modern foundations is composed of three components: (1) *non-elastic* completely residual *settlement* owing to remoulding of the upper soil layer during preparation of pits by

---

\* See the footnote on p. 197.

earth-digging machines; (2) *plastic local extrusions* of the soil (owing to roughness of surface) during the installation and charging of foundations; and (3) *slow compaction settlements* and attenuating creep of the compressed zone of the soil under the foundations.

The first two components of the total settlement, though they appear in the initial stage of construction, are characterized by non-uniformity, which can cause additional stresses not predicted in the design of the structure; these settlements should be avoided, where possible, for which purpose the pits for foundations must be carefully prepared.

The third component of settlement, i.e., the slow deformation of base compaction, is the greatest of the three in magnitude and depends on the properties of soil of the whole *active compression zone* under the foundations, the zone thickness in turn depends on the size and rigidity of the foundations and the compaction degree of the soil.

It is important to note that predictions of settlements of soil bases will only then correspond to reality when the design characteristics of soils are determined with sufficiently high accuracy and reproducibility and the boundary conditions for the rigid solution of the problem are specified correctly.

Before calculating the settlements of foundation bases, we have to know:

(1) the *geological structure* of the construction site and the thickness of the individual layers of the soil, the level of ground waters and, what is indispensable, the *physical and mechanical properties* of the soil of the base over the whole active compression zone (the void ratio, the coefficients of compressibility, shear resistance, and for cohesive soils, also the coefficients of filtration, structural strength, initial pressure gradient, and for dense and tough clays, the creep parameters).

(2) the *size and shape of the foundations* (according to preliminary calculations) and the sensitivity of structures to non-uniform settlements;

(3) the data on the *depth of foundations* and the load on the soil from upper structures.

The final criterion of the applicability of some or other method of calculation of foundation settlements is the results of direct natural observations on foundation settlements and their comparison with the calculated data.

**Direct application of the one-dimensional problem.** For structures having a large area in plan and to be erected on a layer of a compressible soil supported by rock with an insignificant thickness of the soil layer (with  $h \leq b/4$  for a strict solution or with  $h < b/2$  for the solution with a certain approximation), the settlements and their time attenuation can be determined, without introducing

much error, by solving the *one-dimensional problem of compaction* considered earlier (Fig. 99).

It should be emphasized, however, that all the above formulae for settlements of soil bases will hold true only for the compaction phase of soil, i.e., a necessary condition of their applicability is

$$p \leq in p_{cr} \tag{5.41}$$

where  $p$  = load (external pressure) acting on the soil

$in p_{cr}$  = initial critical pressure [see formula (4.2)], i.e., the pressure at which no zones of ultimate equilibrium (shear zones) are formed under the foundation

In the case considered, the total stabilized settlement of foundations can be found by formula (5.9) or an identical formula (5.9').

Thus, the following principal relationships will hold true:

$$s = hm_v p$$

or

$$s = h \frac{\beta}{E_o} p$$

Attenuation of settlements of water-saturated clayey soils with time can be calculated by formula (5.22) derived earlier

$$s_t = s \left[ 1 - \frac{8}{\pi^2} \left( e^{-N} + \frac{1}{9} e^{-9N} \right) \right]$$

If the soil possesses structural strength  $p_{str}$ , its settlement may be regarded consisting of two components, i.e.,

$$s' \approx hm'_v p_{str} + hm_v (p - p_{str}) \tag{5.9''}$$

where  $m'_v$  is coefficient of relative compressibility at pressures below  $p_{str}$ .

Since always  $m'_v < m_v$ , we can neglect the first very small term in expression (5.9''); then, denoting  $p - p_{str} = p_0$ , we get

$$s' \approx hm_v p_0 \tag{5.9''}$$

For cohesive and compacted soils, which are characterized by a certain coefficient of the initial pore-water pressure  $\beta_0$ , we have to introduce a factor  $B$  before the parentheses in formula (5.22) to take an account of an incomplete transfer of pressure to the soil

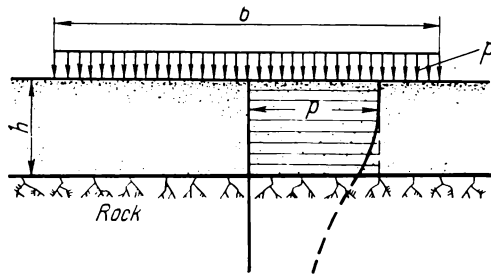


Fig. 99. Diagram of application of the one-dimensional problem of compaction

skeleton and the discrete structure of the soil [formulae (5.22') and (5.33)].

**Effect of the initial pressure gradient.** If filtration in a cohesive soil can appear only at a gradient which is greater than a certain initial pressure gradient  $i_0$ , then a layer of compressible soil (even in the case of the one-dimensional problem with a compacting pres-

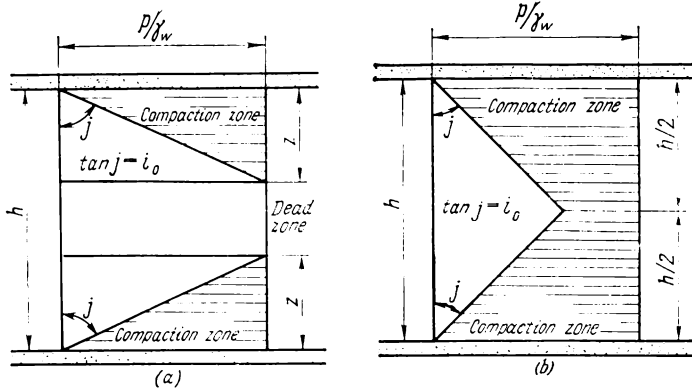


Fig. 100. Compaction of soil with an initial pressure gradient  
(a) compaction zone does not reach  $h/2$ ; (b) compaction zone extends to the whole depth, but compaction is incomplete

sure  $p$  being invariable with depth) will be deformed not completely, but only partially.

Figure 100 shows the diagrams of final pressures in a soil layer for *two-way filtration* (both upward and downward) and the action of a uniform pressure  $p$  (kgf/cm<sup>2</sup>).

In the diagram of excess pressures  $p/\gamma_w$ , the initial gradient can be shown by the tangent of angle  $j$ , i.e.,

$$\tan j = i_0 \quad (e_1)$$

Filtration of water and compaction of soil can only occur in the regions where the gradient is greater than the initial one ( $i > i_0$ ), with two following cases being possible (see Fig. 100a and b).

For the first case (Fig. 100a), we can find from the figure that

$$z = \frac{p}{\gamma_w} \cot j = \frac{p}{\gamma_w} \cdot \frac{1}{\tan j} = \frac{p}{\gamma_w i_0} \quad (e_2)$$

In that case the depth  $z$  is less than half the thickness of the layer, and the total settlement will be equal to the area of the hatched triangles multiplied by  $m_v$ , i.e.,

$$s_1 = 2m_v \frac{zp}{2} \quad (e_3)$$

or

$$s_i = z m_v p \quad (e_4)$$

Substituting the value of  $z$  from expression (e<sub>2</sub>) we get

$$s_1 = m_v \frac{p^2}{i_0 \gamma_w} \quad (5.42)$$

Similarly, for the second case (Fig. 100b), at a lower magnitude of  $i_0 = \tan j$ , and taking into account that the settlement of the soil is equal to the area of effective pressures (i.e.,  $ph - F_w \gamma_w$ , where  $F_w$  is the area of the diagram of excess pressures in pore water) multiplied by the coefficient of relative compressibility  $m_v$ , we have

$$s_2 = m_v h \left( p - \frac{1}{4} i_0 h \gamma_w \right) \quad (5.43)$$

Thus, the settlement of cohesive soils in the cases considered will be less than that determined by the principal formula (5.9).

Note that, as can be shown analytically, the determination of the degree of consolidation  $U$  in the cases of two-way filtration reduces to the principal case 0 discussed earlier [see formula (5.22)], and for one-way filtration (only upward) for the diagram in Fig. 100a, reduces to the case 2 and for the diagram of Fig. 100b, to the case 0-2 of distribution of compacting pressures over the depth.

**Method of elementary layerwise summation.** This method consists in that the soil settlement under the action of the load from a structure is determined as the sum of settlements of elementary soil layers of a thickness for which it is possible, without introducing a large error, to assume the average values of effective stresses and the average values of the coefficients characterizing the soil.

Let us consider the soils that are uniform to a substantial depth and also the stratified soils, both kinds being characterized by the same parameters of compressibility and other properties to the whole depth or for each individual layer. In all cases, the stresses will be *different* for the various sections of the soil thickness at different distances from the point of load application.

As regards the account of stresses for individual separated elements (strata) of a soil layer being compressed, we have to consider two main methods: (1) account of only axial compressive stresses  $\sigma_z$  and (2) account of all normal stresses  $\sigma_z, \sigma_y, \sigma_x$ .

1. *Account of only axial compressive stresses* is recommended by the USSR Building Code and Regulations (BC&R); this method will be discussed in detail.

The principal prerequisites of this method are the determination of soil settlements from the *condition of no lateral expansion* of soil and account of only axial *maximum compressive stresses*  $\sigma_z$  in calculations of settlements.

The account of the maximum compressive stresses compensates to some extent for the *neglect* of the lateral expansion (lateral deformations of soil which may constitute a substantial portion of the total settlement), so that the calculated settlement (for medium-dense and dense soils) turns out to differ not very largely from that observed in nature, though it is almost always smaller than the latter (except for stiff-plastic and hard clays, for which  $i_0$  and  $p_{str}$  must be taken into account).

When determining the settlements from the *condition of no lateral expansion of soil*, a vertical prism of unity cross-sectional area and

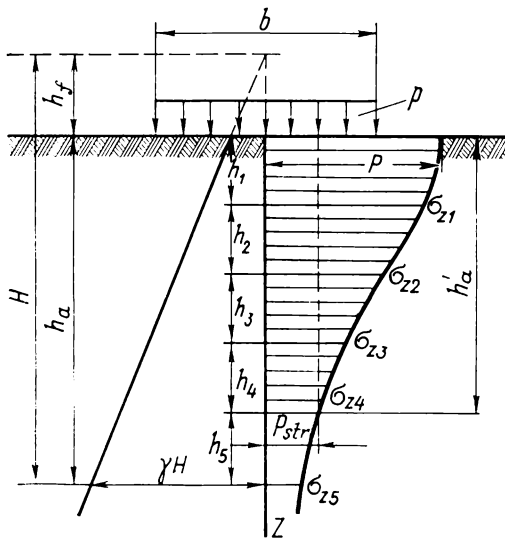


Fig. 101. Diagram to calculate compressive stresses by the method of layer-wise summation

of a depth extending from the base level to the *depth of the active compression zone* (Fig. 101) or to the bedrock is mentally separated in the soil below the centre of the foundation base. Then the maximum compressive stresses  $\sigma_z$  are found for various sections of the prism (horizontal planes) by the theory of linearly deformable bodies (see Chap. 3).

Further, it is assumed that each element of the soil will be subjected only to vertical compression through the action of an average pressure (the maximum compressive stress  $\sigma_z$ ) and will have no possibility for lateral expansion. The settlement of an individual element, without account of the structural compressive strength, can then

be found by formula (5.9) or (5.9')

$$s \approx hm_v \sigma_z \quad \text{or} \quad s \approx h \frac{\beta}{E_o} \sigma_z$$

and for the whole thickness of the layer

$$s = \sum_{i=1}^{i=h_a} h_i m_{vi} \sigma_{zi} \quad (5.44)$$

or, what is the same thing,

$$s = \sum_{i=1}^{i=h_a} h_i \frac{\beta_i}{E_{oi}} \sigma_{zi} \quad (5.44')$$

where  $h_i$  = thickness of individual soil layers (see Fig. 101)

$m_{vi}$  = coefficient of relative compressibility of a soil layer

$\beta_i$  = coefficient depending on lateral expansion of the soil [formula (5.5)]; it is different for various soils but, according to BC&R, is taken equal to 0.8 for all soils (as "a dimensionless coefficient characterizing the simplified calculation scheme")

$E_{oi}$  = modulus of the soil total deformation

The summation sign in formulae (5.44) and (5.44') holds true for the whole depth of the active compression zone  $h_a$ .

The *depth  $h_a$  of the active compression zone* is such a depth below which the deformations of the soil layer (in calculations of settlements of foundations of given dimensions) can be neglected.

According to BC&R, this depth must satisfy the requirement

$$\max \sigma_z \leq 0.2\gamma H \quad (f_1)$$

i.e., the maximum pressure from the external load must be less than 20 per cent of the pressure from the dead weight of the soil layer of thickness  $H$  from the natural relief to the active compression depth  $h_a$  (Fig. 101).

According to BC&R (for hydrotechnical structures with a large base area), the depth of the active compression zone for structures being built on clays is determined by a different inequality

$$\max \sigma_z \leq 0.5\gamma H \quad (f_2)$$

whereas some authors, mainly foreign ones, assume that

$$\max \sigma_z \leq 0.1p \quad (f_3)$$

where  $p$  is the external load.

It is evident from what has been said above that all these recommendations are *conditional* calculation techniques. An analysis of this problem carried out by the Author of this book has shown that the magnitude of the active compression zone depends on the

stresses in the depth of the soil, the *compactness* of soils (the density of sand soils or consistency of clayey soils), and the *structural strength* of soils; the recommendations according to BC&R can be considered valid only for foundations of a small base area (approximately between 1 and 25 m<sup>2</sup>) built on dense sands or coarse-skeleton soils. For clayey soils, the active compression zone  $h'_a$  may be recommended to be found from the condition (Fig. 101)

$$\max \sigma_z \leq p_{str} \quad (f_4)$$

i.e., compression of soil strata is taken into account only to a depth  $h'_a$  below which the compressive stresses will be higher than the structural strength of the soil; for viscous, stiff-plastic and hard clays, the decreasing effect of the initial pressure gradient must also be taken into account (see Sec. 5.6 below); the values of the active compression zone thus obtained may differ from those obtained by the usual recommendations, but correspond more properly to the physical nature of the phenomenon, which is confirmed by the results of natural observations.

Note that for layers of cohesive *structurally unstable* soils (loess soils, permafrost, etc.) only their *residual structural strength* (after moistening of loess soils or thawing of permafrost) must be taken into account.

For foundations on structurally unstable soils, the formula of final stabilized settlement (5.44) becomes somewhat more complicated.

Indeed, according to formulae (5.8) and (5.41) (the latter being true only for pressures between 0.5 kgf/cm<sup>2</sup> and 2.5-4.0 kgf/cm<sup>2</sup>), we have

$$s = h \frac{e_1 - e_2}{1 + e_1}$$

and

$$\frac{e_1 - e_2}{1 + e_1} = \frac{\Delta e_s}{1 + e_1} = \varepsilon_s = A_0 + m_v p$$

Substituting the value of  $\frac{e_1 - e_2}{1 + e_1}$  for subsidence soils (equal to  $A_0 + m_v p$ ) into the former expression and assuming that  $p = \sigma_z$ , we obtain the formula for determination of their stabilized settlement

$$s \approx \sum_{i=1}^{i=n} A_0 h_i + \sum_{i=1}^{i=n} m_{vi} h_i \sigma_{zi} \quad (5.45)$$

where  $A_0$  = coefficient of *thawing* for permafrost or coefficient of *subsidence* for loess soils after moistening

$m_{oi}$  = coefficient of relative compressibility of soils during subsidence

$n$  = number of soil layers from the foundation base to the depth of the settled mass

2. *The account of the components of normal stresses* in the method of layerwise summation gives more reliable results compared with the approximate method of accounting of only axial compressive stresses discussed earlier.

The relative deformation of an element separated along the axis in the general case is known to be

$$\varepsilon_z = \frac{1}{E_o} [\sigma_z - \mu_o (\sigma_x + \sigma_y)] \quad (g_1)$$

Dividing the right-hand part of expression (g<sub>1</sub>) into two summands and denoting

$$\sigma_{av} = \frac{1}{3} (\sigma_z + \sigma_y + \sigma_x) = \frac{\Theta}{3} \quad (g_2)$$

where  $\Theta$  is the sum of normal stresses (the first invariant of stresses), we find after simple transformations that

$$\varepsilon_z = \frac{1 + \mu_o}{E_o} \sigma_z - \frac{\mu_o}{E_o} \Theta \quad (g_3)$$

Supplementary tables have been compiled for calculation of  $\sigma_z$  and  $\Theta$  (see Chap. 3), because of this formula (g<sub>3</sub>) is very convenient in use.

Since  $\varepsilon_z = s/h$ , the settlement of a foundation determined by the method of layerwise summation with *account* of all normal stresses, and therefore, of *lateral deformations* of the soil, can be found by the formula

$$s = \frac{1 + \mu_o}{E_o} \sum_{i=1}^{i=ha} \sigma_{zi} h_i - \frac{\mu_o}{E_o} \sum_{i=1}^{i=ha} \Theta_i h_i \quad (5.46)$$

Prof. N. N. Maslov\* proposed formulae for calculation of the total stabilized settlement, where the characteristic of compressibility is the so-called modulus of settlement  $\varepsilon_p$ , i.e., the magnitude of the relative deformation ( $\varepsilon_p = s/h$ ) at the given external pressure  $p$  under conditions of no lateral expansion of the soil; this modulus makes it possible to take into account that soil deformations are in a curvilinear dependence on load.

The settlement of an elementary soil layer of thickness  $h$  under the action of compressive stresses along three mutually perpendicu-

\* Maslov N. N. *Osnovy mekhaniki gruntov i inzhenernoi geologii* (Fundamentals of Soil Mechanics and Engineering Geology), Moscow, Vysshaya Shkola Publishers, 1968.

lar directions and under condition of no lateral expansion of soil (noting that  $s = h\varepsilon_p$ ) will be

$$s = h[\varepsilon_{pz} - \mu_o(\varepsilon_{px} + \varepsilon_{py})] \tag{5.47}$$

where  $\varepsilon_{pz}$ ,  $\varepsilon_{px}$ ,  $\varepsilon_{py}$  are moduli of settlement (relative deformations) for a direct and separate action of normal stresses on a soil element, these moduli being dependent on these stresses.

When determining  $\varepsilon_{pz}$ ,  $\varepsilon_{px}$  and  $\varepsilon_{py}$  directly from the results of compression tests [from curves  $\varepsilon_p = f(p)$ ], a certain error is allowed, since the soil will really have a *limited* lateral expansion, rather than *no lateral expansion* at all. To pass over from the conditions of no lateral expansion to those of a limited expansion, Prof. Maslov introduces a coefficient  $M_o = 1/\beta$  into the right-hand part of expression

(5.47), where  $\beta$  has the same meaning as before [see formula (5.5)].

The settlement of an elementary soil layer will then be

$$s = M_o h[\varepsilon_{pz} - \mu_o(\varepsilon_{px} + \varepsilon_{py})] \tag{5.47'}$$

If lateral expansion is not to be taken into account, then  $\mu_o = 0$  and  $M_o = 1$ . Hence

$$s = h\varepsilon_{pz} \tag{5.47''}$$

The settlement of the whole active zone of soil is calculated by summing the settlements of elementary layers.

It should be noted that in the method of equivalent layer discussed below (see Sec. 5.6), all components of normal stresses are accounted for by simpler (and for homogeneous soils, by more strict) relationships, the results for the whole active zone being obtained in closed form requiring no summation.

For a soil layer of *limited thickness* (Fig. 102) on an incompressible rock base, Davis and Taylor\* have found the strict solution of the problem of determining the displacements of a corner point of a rectangular loading surface along any direction, the solution including eight matrices of influence coefficients; the values of these

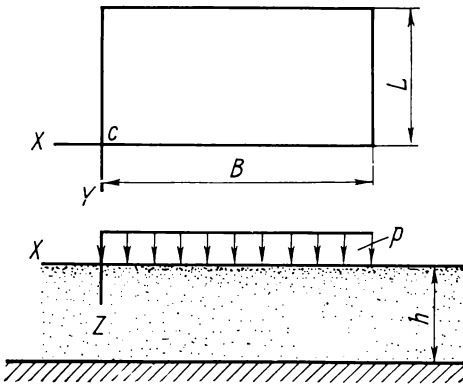


Fig. 102. Action of a local load on a finite-thickness soil layer

\* Tsyтович N. A. Teoriya i praktika fundamentostroeniya (K itogam V Mezhdunarodnogo kongressa) [Theory and Practice of Foundation Engineering (Review of the V International Congress)], Moscow, Stroizdat, 1964.

coefficients found by means of an electronic computer enabled the authors to compile calculation graphs such as the one shown in Fig. 103.

The soil *settlement* under a corner point *c* of a rectangular loading surface of a layer of limited thickness (see Fig. 102) is found by the formula

$$s_c = \frac{h}{E_o} (1 + \mu_o) [(1 - \mu_o) m_{zz} + (1 - 2\mu_o) n_{zz}] p \quad (5.48)$$

where  $m_{zz}$ ,  $n_{zz}$  are matrices of influence coefficients for vertical displacement of the corner point under a rectangular loading surface

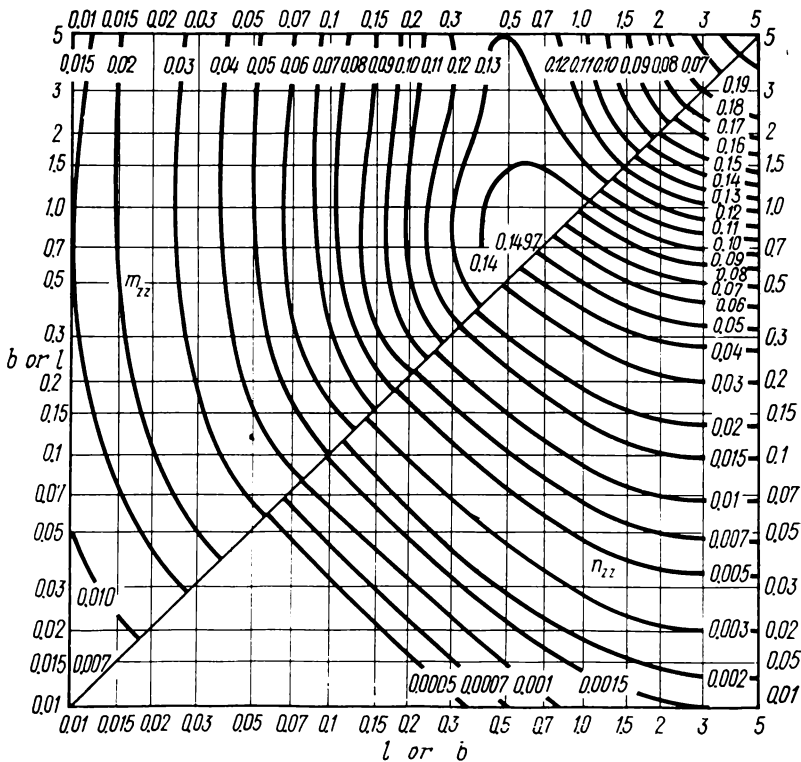


Fig. 103. Graph of matrices of influence coefficients  $m_{zz}$  and  $n_{zz}$

of a layer of limited thickness, these matrices being determined according to the relative length  $l$  and relative width  $b$  of the loaded section, with  $l = L/h$  and  $b = B/h$  (see Fig. 102).

Graphs for all other matrices of influence coefficients may be found in the Author's work cited; they make it possible to determine the *displacement* of a corner point of a layer of limited thickness in any direction under the action of a local uniformly distributed load on a rectangular surface and then, by the method of corner points, the displacement of any point of the layer.

The *settlements of a stratified soil mass* can be determined by the method of layerwise summation using the same formulae (5.44)-(5.46) derived earlier in the book; we only have to select the boundaries of elementary layers so as to make them coincident with the interfaces of the layers of different compressibility and, naturally, to take into account that moduli of deformability are different for various layers of the soil.

**Time changes of the rate of settlement**, in the layerwise summation method, can be determined only approximately for homogeneous

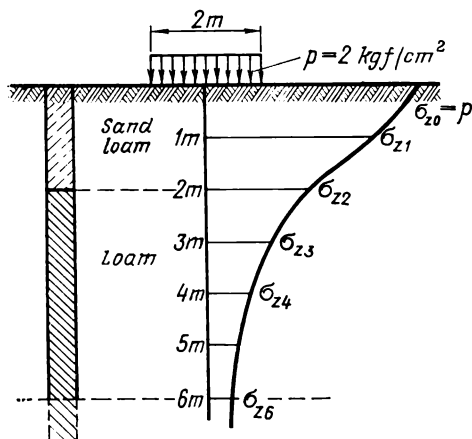


Fig. 104. Distribution of the maximum compressive stresses in soil under foundation

soils and with a shallow location of the bedrock, the diagram of compressive stresses (compacting pressures) being *approximately* taken to be *trapezoidal* (as for the case 0-2 of compacting pressures); various points under the loaded surface will then have different diagrams of compacting pressures. Strict solutions of the three-dimensional problem of compression (as has been noted earlier) have been obtained only for a few cases of homogeneous soils.

se sand loam of a thickness of 2 m supported by a homogeneous loam of high thickness (Fig. 104).

Given: the pressure on the foundation base  $p = 2 \text{ kgf/cm}^2$ , the coefficient of relative compressibility for the sand loam  $m_{v1} = 0.005 \text{ cm}^2/\text{kgf}$  and for the loam,  $m_{v2} = 0.01 \text{ cm}^2/\text{kgf}$ .

Using Table 3.2, we find the coefficients  $K_0$  to calculate  $\sigma_z$  by formula (3.9) by interpolation of close values of  $2z/b$  and  $l/b$  for various depths (from 0 to 6 m) from the foundation base.

We then have:  $\sigma_{z0} = 2 \text{ kgf/cm}^2$ ;  $\sigma_{z1} = 1.60 \text{ kgf/cm}^2$ ;  $\sigma_{z2} = 0.96 \text{ kgf/cm}^2$ ;  $\sigma_{z3} = 0.59 \text{ kgf/cm}^2$ ;  $\sigma_{z4} = 0.38 \text{ kgf/cm}^2$  and  $\sigma_{z5} = 0.19 \text{ kgf/cm}^2$ .

At depths below 6 m, compaction of soil layers is neglected.

The settlement of the foundation will then be found by the method of elementary summation (without account of lateral expansion of the soil) by formula

5.44) as follows:

$$s = \sum_{i=1}^{i=n} h_i m_{vi} \sigma_{zi} = 0.005 \left( \frac{2+1.60}{2} \times 100 + \frac{1.60+0.96}{2} \times 100 \right) + \\ + 0.01 \left( \frac{0.96+0.59}{2} \times 100 + \frac{0.59+0.38}{2} \times 100 + \frac{0.38+0.19}{2} \times 200 \right) \approx 3.4 \text{ cm}$$

## 5.6. PREDICTION OF FOUNDATION SETTLEMENTS BY EQUIVALENT SOIL LAYER METHOD

The method of an equivalent soil layer, as the other methods of prediction of foundation settlements discussed earlier, is based on the theory of linearly deformable bodies, but greatly simplifies the calculation procedure for both homogeneous and laminar soil beddings and makes it possible to determine not only the final stabilized settlement of a foundation, but also time variations of settlements. In this method, the extremely complex three-dimensional problem of the theory of consolidation is reduced to an equivalent one-dimensional problem\*.

For soils which are homogeneous to an appreciable depth, the total stabilized settlement of foundations is found as the strict solution of the theory of compaction of a linearly deformable half-space; prediction of settlements of foundations erected on stratified soils and of time changes of settlements is determined under certain simplifying approximations confirmed by comparing the results obtained with available particular cases of the strict solution (for instance, Gibson's) and the data on natural observations on settlements of structures (this is especially important); this makes it possible to regard the equivalent layer method as the one sufficiently reliable for practical purposes.

**Derivation of the principal relationship.** Let us agree that an *equivalent soil layer* is the one whose settlement under a continuous load is exactly equal to that of a foundation on a thick soil massif (half-space).

To find the thickness of the equivalent soil layer  $h_{eq}$ , we equate the vertical deformation  $s_o$  of an individual soil stratum under a continuous load to the vertical deformation  $s_{hs}$  under a local load on a half-space, i.e.,

$$s_o = s_{hs} \quad (h_1)$$

---

\* The principal relationships of the equivalent layer method were proposed by the Author as far back as 1934 and substantially improved in later years (1940-68).

Since the relative deformation of a soil layer under a continuous load [see Sec. 5.2, formula (m<sub>2</sub>)] is

$$\varepsilon_z = \frac{p}{E_o} \left( 1 - \frac{2\mu_o^2}{1-\mu_o} \right)$$

then, by multiplying the relative deformation by the total thickness  $h_{eq}$  of the layer, we have

$$s_o = \frac{ph_{eq}}{E_o} \left( 1 - \frac{2\mu_o^2}{1-\mu_o} \right) \quad (h_2)$$

On the other hand, according to formula (5.4)

$$s_{hs} = \frac{\omega pb (1-\mu_o^2)}{E_o} \quad (h_3)$$

Substituting (h<sub>2</sub>) and (h<sub>3</sub>) into (h<sub>1</sub>) and solving the equation for  $h_{eq}$ , we find

$$h_{eq} = \frac{(1-\mu_o)^2}{1-2\mu_o} \cdot \omega b \quad (5.49)$$

Denoting the constant coefficient for the given soil by a single symbol

$$A = \frac{(1-\mu_o)^2}{1-2\mu_o} \quad (5.50)$$

we obtain the following simple formula for determining the thickness of an equivalent soil layer:

$$h_{eq} = A\omega b \quad (5.51)$$

which shows that the thickness of an equivalent soil layer depends on lateral expansion of soil (coefficient  $A$ ), the shape and rigidity of the foundation (coefficient  $\omega$ ), and is proportional to the width  $b$  of the foundation base.

With the thickness of the equivalent soil layer being known, the settlement of the foundation of the given dimensions and shape can be determined by formula (5.9) by substituting  $h_{eq}$  for  $h$ , i.e.,

$$s = h_{eq} m_v p \quad (5.52)$$

This relationship is very convenient for practical purposes, especially if use is made of Table 5.6 compiled by the Author, which contains the values of equivalent layer coefficients  $A\omega$  both for the maximum and average settlements of flexible foundations (found in terms of  $A\omega_0$  and  $A\omega_m$ ) and the settlements of absolutely rigid foundations (in terms of  $A\omega_{const}$ ).

Note that settlements of foundations having a circular base can be determined, without great error, by the following relationship:

$$\omega_{cir} \approx \omega_{sq} \sqrt{\frac{\pi}{4}} \approx 0.887 \omega_{sq}$$



where  $\omega_{cir}$  = form factor for foundation with a circular base  
 $\omega_{sq}$  = same, for foundation with a square base (when  $\alpha = l/b = 1$ )

In addition, the coefficients of an equivalent soil layer for the centre of a rectangular surface of an absolutely flexible load and for its corner point are linked by the following simple relationship:

$$A\omega_c = \frac{1}{2} A\omega_0$$

where  $A\omega_c$  is the equivalent layer coefficient for corner points of a rectangular loading surface.

The settlements of foundations having a *rectangular surface* of the base are determined by using the *method of corner points* (see also

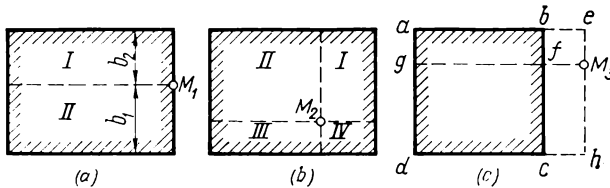


Fig. 105. Rectangles of loading in determination of settlements by the method of equivalent layer of corner points

Chap. 3), according to which the point considered is located so as to make it *corner* point; the *settlement* of any point of the soil surface under a uniformly distributed load will be equal to the *algebraic sum* of soil settlements under the rectangular loading surfaces for which that point is a corner one.

Three different cases must be considered here:

- (1) point  $M_1$  (Fig. 105a) is on the contour of the loaded rectangle;
- (2) point  $M_2$  is inside that rectangle (Fig. 105b); and
- (3) point  $M_3$  is outside that rectangle (Fig. 105c).

In the first case, the settlement of point  $M_1$  is the sum of the settlements of the corner points of rectangles I and II, i.e.,

$$s_1 = (h_{eqI} + h_{eqII}) m_0 p$$

where

$$h_{eqI} = (A\omega_c)_I b_2; \quad h_{eqII} = (A\omega_c)_{II} b_1$$

In the second case, the loaded surface is divided into four rectangles so that point  $M_2$  becomes a corner one (Fig. 105b); then

$$s_2 = (h_{eqI} + h_{eqII} + h_{eqIII} + h_{eqIV}) m_0 p$$

where  $h_{eqi}$  is the thickness of the equivalent layer for the corresponding loading surfaces.

Table 5.7

Values of  $\Delta\omega_c$ 

$\alpha$	Values of $\mu_0$					
	0.10	0.20	0.25	0.30	0.35	0.40
1.0	0.568	0.598	0.631	0.687	0.790	1.010
1.1	0.595	0.627	0.662	0.720	0.828	1.059
1.2	0.621	0.654	0.690	0.751	0.863	1.104
1.3	0.611	0.679	0.716	0.780	0.896	1.146
1.4	0.667	0.702	0.740	0.806	0.927	1.185
1.5	0.687	0.724	0.764	0.832	0.956	1.222
1.6	0.707	0.745	0.785	0.855	0.988	1.257
1.7	0.725	0.764	0.806	0.878	1.009	1.289
1.8	0.743	0.783	0.825	0.899	1.033	1.321
1.9	0.760	0.800	0.844	0.919	1.057	1.350
2.0	0.775	0.817	0.862	0.938	1.079	1.379
2.1	0.791	0.833	0.878	0.957	1.100	1.406
2.2	0.805	0.848	0.895	0.974	1.120	1.431
2.3	0.819	0.863	0.910	0.991	1.139	1.456
2.4	0.832	0.877	0.925	1.007	1.158	1.480
2.5	0.845	0.890	0.939	1.022	1.176	1.502
2.6	0.857	0.903	0.953	1.037	1.193	1.524
2.7	0.869	0.916	0.966	1.052	1.209	1.546
2.8	0.881	0.928	0.979	1.066	1.225	1.566
2.9	0.892	0.940	0.991	1.079	1.241	1.586
3.0	0.903	0.951	1.003	1.092	1.256	1.605
3.2	0.923	0.972	1.026	1.117	1.284	1.641
3.4	0.942	0.993	1.047	1.140	1.311	1.675
3.6	0.961	1.012	1.067	1.162	1.336	1.708
3.8	0.978	1.030	1.086	1.183	1.360	1.738
4.0	0.994	1.047	1.105	1.203	1.383	1.767
4.2	1.009	1.064	1.122	1.222	1.404	1.795
4.4	1.025	1.079	1.139	1.239	1.425	1.821
4.6	1.039	1.094	1.154	1.257	1.445	1.847
4.8	2.052	1.109	1.169	1.273	1.464	1.871
5.0	1.065	1.122	1.184	1.289	1.482	1.894
5.5	1.096	1.155	1.218	1.326	1.524	1.948
6.0	1.124	1.184	1.249	1.360	1.568	1.998
6.5	1.150	1.211	1.277	1.391	1.599	2.044
7.0	1.178	1.236	1.304	1.420	1.632	2.086
7.5	1.195	1.259	1.328	1.446	1.663	2.125
8.0	1.216	1.281	1.351	1.472	1.692	2.162
8.5	1.236	1.302	1.373	1.495	1.719	2.197
9.0	1.251	1.321	1.393	1.517	1.744	2.230
9.5	1.272	1.340	1.413	1.538	1.769	2.261
10.0	1.288	1.357	1.431	1.558	1.792	2.290
11.0	1.319	1.389	1.465	1.595	1.831	2.344
12.0	1.347	1.419	1.496	1.629	1.873	2.394
13.0	1.372	1.446	1.525	1.661	1.909	2.440
14.0	1.396	1.471	1.551	1.689	1.942	2.482
15.0	1.418	1.494	1.576	1.716	1.973	2.522
16.0	1.439	1.516	1.599	1.741	2.002	2.559
17.0	1.459	1.537	1.621	1.765	2.029	2.594

Table 5.7 (continued)

$\alpha$	Values of $\mu_o$					
	0.10	0.20	0.25	0.30	0.35	0.40
18.0	1.477	1.556	1.641	1.787	2.055	2.626
19.0	1.495	1.575	1.661	1.808	2.079	2.657
20.0	1.511	1.592	1.679	1.828	2.102	2.687
25.0	1.583	1.668	1.759	1.915	2.202	2.814
30.0	1.642	1.730	1.824	1.986	2.284	2.912
35.0	1.692	1.782	1.880	2.047	2.353	3.007
40.0	1.735	1.827	1.927	2.099	2.413	3.084
50.0	1.807	1.903	2.007	2.186	2.513	3.212
60.0	1.865	1.965	2.072	2.257	2.594	3.316
70.0	1.915	2.017	2.128	2.317	2.664	3.404
80.0	1.958	2.063	2.176	2.369	2.723	3.481
100.0	2.030	2.139	2.256	2.456	2.824	3.600

In the third case the settlement is the algebraic sum of the settlements of corner points of loaded rectangles (Fig. 105c), i. e.

$$I + aeM_3g; \quad II + gM_3hd; \quad III - beM_3f; \quad IV - fM_3hc$$

The settlement of the point  $M_3$  considered will then be

$$s_3 = (h_{eqI} + h_{eqII} - h_{eqIII} - h_{eqIV}) m_v p \quad (i_3)$$

Values of the equivalent layer coefficient  $A\omega_c$  for any rectangular loaded surfaces with the side ratio  $\alpha = l/b$  ( $l$  being the length and  $b$ , the width of a rectangular loaded surface) are given in Table 5.7, which largely facilitates calculations of foundation settlements.

**Example 5.4.** Find the final stabilized settlement of a massive foundation with the base area of  $2 \times 6$  m and unit pressure on soil of  $2.5 \text{ kgf/cm}^2$ , if the coefficient of relative compressibility of the soil is  $m_v = 0.004 \text{ cm}^2/\text{kgf}$  and the coefficient of lateral deformation,  $\mu_o = 0.3$ .

From Table 5.6 we find for  $\alpha = l/b = 6/2 = 3$  and  $\mu_o = 0.3$  that

$$A\omega_m = 1.89$$

Then, by formula (5.51), the thickness of the equivalent soil layer is

$$h_{eq} = A\omega_m b = 1.89 \times 2 = 3.78 \text{ m}$$

and, by formula (5.52), the stabilized settlement of the foundation of the given dimensions, with account of soil lateral expansion and the whole compressed zone under the foundation, is

$$s = h_{eq} m_v p = 378 \times 0.004 \times 2.5 = 3.8 \text{ cm}$$

**Example 5.5.** Find the settlement of an existing foundation with the base area of  $2.5 \times 5.0$  m, caused by building in its vicinity of a new foundation with the base area of  $5 \times 5$  m and pressure on soil  $p = 1$  kgf/cm<sup>2</sup>, if the soil is characterized by the coefficients:  $m_v = 0.01$  cm<sup>2</sup>/kgf and  $\mu_o = 0.3$ .

Using the method of corner points, we construct supplementary rectangles so that points 1 and 2 are corner points (Fig. 106). For point 1, for each of the two loaded rectangles of  $2.5 \times 5$  m when  $a = l/b = 5/2.5 = 2$  and  $\mu_o = 0.3$ , the equivalent layer coefficient is found from Table 5.7 as  $A\omega_c = 0.938$ . The settlement of that point will then be

$$s_1 = 2 (A\omega_c b) m_v p = 2 \times 0.938 \times 250 \times 0.01 \times 1 \approx 4.69 \text{ cm}$$

For point 2, the equivalent layer is twice the difference of the equivalent layers for the foundation with the base area of  $2.5 \times 7.5$  m and that with the base area of  $2.5 \times 2.5$  m.

Using the coefficients of Table 5.7, we get

$$s_2 = [2 (1.092 - 0.687) 250] 0.01 \times 1 = 2.02 \text{ cm}$$

Thus, the older foundation will have a non-uniform settlement  $\Delta s = 4.69 - 2.02 = 2.67$  cm in the direction of the new foundation.

**Time variations of settlements.** The prediction of time variations of settlements, i.e., determination of foundation settlements for any time  $t$  from the beginning of loading is a very complicated three-dimensional problem (see Sec. 5.4) which has been solved only for some particular cases.

We shall now discuss the general engineering method of approximate prediction of time variations of foundation settlements. This method uses an averaged generalized diagram of compacting pressures decreasing with depth and is based on account of the main direction of filtration of the water squeezed by a load from voids of saturated soil.

The diagram of compacting pressures of a soil mass under foundations is assumed to have a *triangular form* (which largely simplifies calculations of settlements) with the base located at the loaded surface and equal to the intensity of the external load and with the height determined from the condition of invariability of the final stabilized settlement according to the strict solution of the theory of linearly deformable bodies. This assumption enables the closed solution of the main differential equation of the one-dimensional problem of consolidation to be employed for the case of a non-uniform distribution of compacting pressures over the depth.

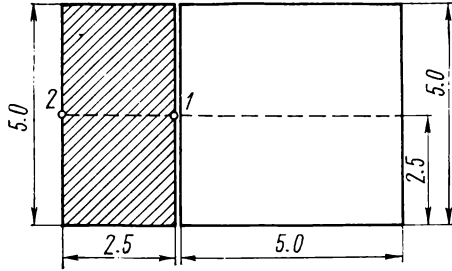


Fig. 106. Scheme to Example 5.5

The replacement of the very complicated actual diagrams of compacting pressures (or more correctly, of those calculated by the theory of uniform isotropic half-space) by a simplest *equivalent triangular diagram* of compacting pressures is quite accurate for practical purposes; this has been verified by comparing calculated settlements with the strict solution (for instance, Gibbison—McNamy solution)

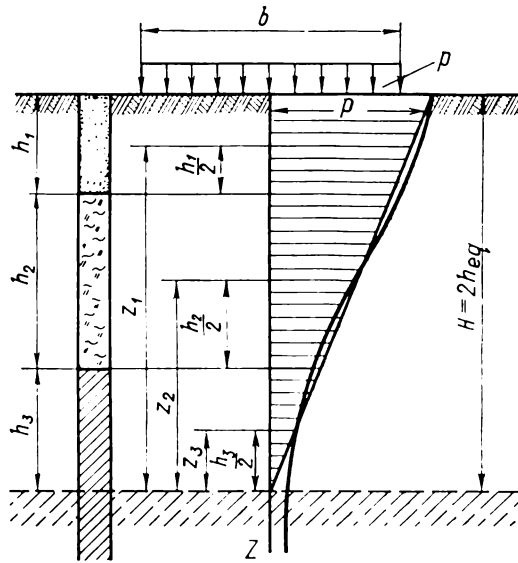


Fig. 107. Scheme of construction of an equivalent diagram of compacting pressures

and also by comparing calculated settlements with those actually observed.

The height of the triangular *equivalent diagram* of compacting pressures (Fig. 107) is

$$H = 2h_{eq} \quad (5.53)$$

According to Fig. 107, the average settlement is

$$s = H m_v \frac{p}{2}$$

On the other hand, according to the strict solution [formula (5.52)]

$$s = h_{eq} m_v p$$

Equating the right-hand parts of these two expressions gives formula (5.53).

The equivalent diagram of compacting pressures corresponds to the settlement of foundation, obtained with account of the whole compressed zone under the foundation in conditions of restricted lateral expansion of soil.

Assuming the equivalent diagram of compacting pressures to have a triangular form, let us predict time variations of settlements: (1) for *one-way filtration* (only upward), as for the earlier considered case 2 of compacting pressures decreasing with depth by a triangle law with a height  $H = 2h_{eq}$  and (2) for *two-way filtration* (both upward and downward with the presence of a filtrating soil layer having a free outlet of water at a depth  $2h_{eq}$  or less), as for the *main case 0*, i.e., for a uniform distribution of compacting pressures (which is mathematically identical with the case of triangular distribution of compacting pressures, but with two-way filtration), with the calculated thickness of soil layer equal to  $h_{eq}$ .

Thus, we shall have:

for *one-way filtration* of water (only upward), the settlement of the foundation for any time  $t$ , taking into account expression (5.25), will be expressed as

$$s_t = h_{eq} m_v p \left\{ 1 - \frac{16}{\pi^2} \left[ \left( 1 - \frac{2}{\pi} \right) e^{-N} + \frac{1}{9} \left( 1 + \frac{2}{3\pi} \right) e^{-9N} + \dots \right] \right\} \quad (5.54)$$

where, for the case considered,

$$N = \frac{\pi^2 c_v}{4H^2} t \quad \text{and} \quad H = 2h_{eq}$$

For the case of *two-way filtration* of water with the same diagram of compacting pressures (with the base equal to  $p$  and height  $2h_{eq}$ ), the settlement of the foundation for any time  $t$ , noting expression (5.19), will be

$$s_t = h_{eq} m_v p \left[ 1 - \frac{8}{\pi^2} \left( e^{-N} + \frac{1}{9} e^{-9N} + \dots \right) \right] \quad (5.55)$$

where

$$N = \frac{\pi^2 c_v}{4h_{eq}^2} t; \quad c_v = \frac{k_f}{m_v \gamma_w}$$

Note that calculations of settlements  $s_t$  can be made not only by formulae (5.54) and (5.55) using the values of  $e^{-x}$  from Table 5.3, but also by assuming some or other degree of consolidation,  $U_2$  or  $U_0$  (depending on the boundary conditions of filtration), and determining from Table 5.4 the respective values of  $N$ ; the time for

attaining the given percentage of consolidation will then be found as follows:

for one-way filtration

$$t = \frac{4H^2}{\pi^2 c_v} N_2 \quad (5.28')$$

for two-way filtration

$$t = \frac{4h_{eq}^2}{\pi^2 c_v} N_0' \quad (5.28'')$$

It should also be noted that in calculations of foundation settlements the pressure  $p$  must be taken only as an *additional pressure* or a pressure in excess of the pressure caused by the dead weight of the soil at the level of the foundation base, assuming that the soil has already been deformed under its dead weight, i.e.,

$$p = p_0 - \gamma h_f \quad (5.56)$$

where  $p_0$  = total pressure from the building at the level of the foundation base or (with account of an invariable structural strength of the soil) with subtraction of the structural strength

$\gamma h_f$  = pressure from the dead weight of the soil at the level of the foundation base  $h_f$

**Example 5.6.** Construct the curve of time variations of the settlements of a massive foundation. Given: foundation base area  $2 \times 3$  m; soil—homogeneous clay characterized by the coefficients:  $m_v = 0.006$  cm<sup>2</sup>/kgf;  $\mu_0 = 0.4$ ;  $k_f = 0.15$  cm/year; pressure on soil  $p = 2.5$  kgf/cm<sup>2</sup>.

By using Table 5.6 (for  $a = l/b = 3/2 = 1.5$ ,  $A\omega_m = 2.07$ ), we find the thickness of the equivalent soil layer

$$h_{eq} = A\omega_m b = 2.07 \times 2 = 4.14 \text{ m} = 414 \text{ cm}$$

The total stabilized settlement will then be

$$s = h_{eq} m_v p = 414 \times 0.006 \times 2.5 \approx 6.2 \text{ cm}$$

The height of the equivalent diagram of compacting pressures is

$$H = 2h_{eq} = 2 \times 414 = 828 \text{ cm}$$

The settlements corresponding to any time (for instance,  $t = 1$  year, 3 years, 5 years and 10 years) can be calculated by using formula (5.54).

Preliminarily, we find that

$$c_v = \frac{k_f}{m_v \gamma_w} = \frac{0.15}{0.006 \times 0.001} = 25,000 \text{ cm}^2/\text{year}$$

$$N = \frac{\pi^2 c_v}{4H^2} t = \frac{9.87 \times 25,000}{4 \times 828^2} t \approx 0.09t$$

For  $t = 1$  year

$$s_t = 6.2 \left\{ 1 - \frac{16}{\pi^2} \left[ \left( 1 - \frac{2}{\pi} \right) e^{-0.09 \times 1} + \frac{1}{9} \left( 1 + \frac{2}{3\pi} \right) e^{-9 \times 0.09 \times 1} \right] \right\}$$

Using Table 5.3, we find  $e^{-x}$ ; then

$$s_1 = 6.2 \left[ 1 - 1.62 \left( 0.363 \times 0.914 + \frac{1}{9} \times 1.212 \times 0.445 \right) \right] = 2.2 \text{ cm}$$

In further calculations, we take only the first term in the square brackets. For  $t = 3$  years, 5 years, and 10 years we get respectively

$$s_3 = 6.2 \left[ 1 - \frac{16}{\pi^2} \left( 1 - \frac{2}{\pi} \right) e^{-N} \right] = 6.2 [(1 - 1.62 \times 0.363e^{-0.09 \times 3})] \approx 3.4 \text{ cm}$$

$$s_5 = 6.2 (1 - 0.556e^{-0.09 \times 5}) = 3.9 \text{ cm}$$

$$s_{10} = 6.2 (1 - 0.556e^{-0.09 \times 10}) = 4.7 \text{ cm}$$

The curve of time variations of settlements constructed by the data obtained is shown in Fig. 108.

Note that the settlements calculated by the equivalent layer method are very close to those found by the strict solution (see Gibbons's diagram in Fig. 97). But with a large degree of consolidation

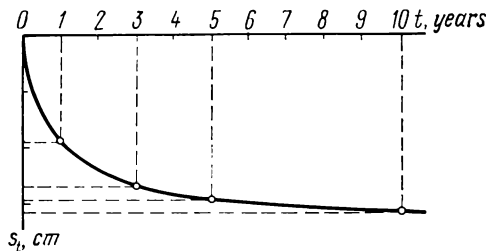


Fig. 108. Curve of time attenuation of settlements of a foundation base

(when  $U > 0.8$  to  $0.9$ ), especially for dense clays, the settlement due to *creep* of the soil skeleton, which is not taken into account in the theory of filtration consolidation, becomes of importance; this will be discussed in the next chapter.

**Determination of the active compression zone by the equivalent layer method.** In the case of non-compacted soils the depth of the active compression zone  $h_a$  may be taken equal to the height of the equivalent diagram of compacting pressures  $H = 2h_{eq}$ ; then, as evident from theoretical considerations and comparison with the data observed, this value must be considered as  $\max h_a$ , i.e.,

$$\max h_a \approx 2h_{eq} \quad (5.53')$$

Since for hard and dense soils the coefficient  $\mu_o = 0.1-0.2$  and for weak (undercompacted and liquid-plastic) soils,  $\mu_o = 0.35-0.45$ , then according to the data of Table 5.6, the maximum depth of the active compression zone effecting the settlement of a foundation, as determined by formulae (5.51) and (5.53'), will be substantially

greater for weak soils than for dense and hard ones, which is fully confirmed in practice.

For soils possessing structural strength ( $p_{str} > 0$ ), the active compression zone will be smaller and, as has been indicated earlier, will correspond only to the depth where the compressing stresses are greater than  $p_{str}$ ; this makes it possible, for the given values of  $p_{str}$ , to determine the corresponding depth of the active zone  $h'_a$  from the equivalent diagram of compacting pressures (Fig. 109); if filtration of water in a given soil begins only at the gradients  $i = \tan j > i_0$ , then, noting that the final head in the soil below the foundation is  $H = (p - p_{str}) \frac{1}{\gamma_w}$ , we get the active compression zone decreased to  $h''_a$ .

Assuming that  $p - p_{str} = p_0$ , it follows from the geometrical relationships of Fig. 109 (at constant values of  $p_{str}$  and  $i_0 = \tan j$  and taking them simultaneously into account) that the depth of the active compression zone  $h_a$  is determined in the general case by the expression

$$h''_a = 2h_{eq} \left( 1 - \frac{i_0}{i_0 + \frac{p}{2h_{eq}\gamma_w}} \right) \frac{p_0}{p} \quad (5.57)$$

If, however, only  $p_{str}$  is taken into account, then we have

$$h'_a = 2h_{eq} \frac{p - p_{str}}{p} \quad (5.57')$$

It should be noted that in all the cases considered, the shape of the diagram of compacting pressures remains triangular, which makes it possible to determine the stabilized settlement of foundations (which is equal to the area of the diagram of compacting pressures times the coefficient of relative compressibility) by the formula

$$s = \frac{h_a m_v p_0}{2} \quad (5.58)$$

The degree of consolidation must, however, be determined by the formulae given earlier: for one-way filtration only upward, as for case 2 of compacting pressures [for instance, by formula (5.25)] and for two-way filtration, both upward and downward, as for case 0 [by formula (5.19)].

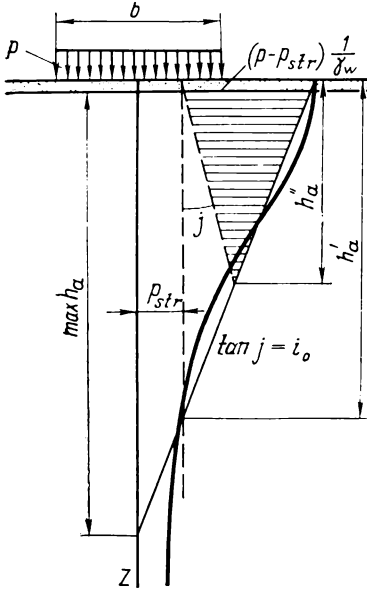


Fig. 109. Determination of active compression zone by the equivalent layer method

**Approximate account of the finiteness (finite depth) of the layer being compressed.** If incompressible rock is located at a definite depth under a foundation, an additional boundary condition, i.e., the finite depth of the layer being compressed, must be taken into account.

Further, it may be assumed that *soils are incompressible below the depth  $2h_{eq}$*  for the given dimensions of the loaded surface, since settlements at such a depth are not taken into account. In addition, if the structural strength of a soil at a certain depth below the foundation base is greater than the pressures arising from the action of an external load on the foundation, the soil can be regarded incompressible under these pressures.

With a limited thickness of the layer being compressed the coefficient  $\omega$  in the formula for the equivalent soil layer (5.51) is a variable and depends on the ratio of the thickness of the layer to the width of the foundation. By using the available solutions, B. I. Dalmatov has determined the values of  $A\omega'$  for an approximate account of the limited thickness of the soil layer from the condition that incompressible soils are located at a *depth exactly equal to twice the thickness of the equivalent layer*. The magnitude of the equivalent layer for a limited-thickness layer of soil will then be

$$h'_{eq} = A\omega'b \quad (5.51')$$

where  $A\omega'$  is the coefficient of equivalent layer for a limited thickness of the layer being compressed; its values, found by the method of successive approximations, are given in Table 5.8.

Table 5.8

**Values of  $A\omega'$  for a Limited Thickness of the Layer Being Compressed**

$\mu_o$	Side-to-side ratio of rectangular base surface $\alpha = l/b$						
	1	1.5	2	3	5	7	10
0.1	0.60	0.76	0.82	0.94	1.02	1.07	1.14
0.2	0.67	0.83	0.92	1.05	1.15	1.23	1.26
0.3	0.83	1.00	1.13	1.29	1.44	1.53	1.59
0.4	1.34	1.67	1.85	2.12	2.49	2.65	2.79

The total stabilized settlement in that case is determined by the formula

$$s = h'_{eq}m_v p \quad (5.52')$$

By comparing the values of the equivalent layer coefficient  $A\omega'$  given in the table with the main ones, for instance, when  $\mu_o = 0.3$  (see Table 5.6), it can be seen that the thickness of the active zone

of soil compression, which affects settlements of foundations, becomes substantially smaller when the finiteness of the layer being compressed is taken into account.

If the actual depth of incompressible rock  $h_{rock}$  is less than the value  $2h'_{eq}$  determined from the conditions of finiteness of the layer being compressed, then the design thickness of the equivalent layer must be calculated taking into account the actual depth of incompressible rock and the magnitude of  $\omega$ , which will be denoted as  $\omega_{mh}$ , must be determined as a function (of the ratio  $h_{rock}/b$ ,  $l/b$ ) in the right-hand portion of Table 5.2.

The approximate account of the finiteness of compressible layer may be recommended for a shallow depth (less than or equal to  $2h_{eq}$ ) of rock or generally incompressible soils and a substantial (greater than 25-50 m<sup>2</sup>) base area of a foundation, since the method of equivalent layer for a homogeneous soil layer and a large loading surface, and especially with account of the effect of neighbouring foundations, gives somewhat increased values of settlements.

**Prediction of foundation settlements on a stratified soil bedding.** With a stratified soil bedding, the method of the equivalent layer is *not a strict one*, as it was in the case of a homogeneous half-space (other strict solutions are, however, non-existent), but if the soil is reduced to a *quasi-homogeneous* state (on the basis of the theorems on the average relative coefficient of compressibility and the average coefficient of filtration of a stratified soil), then the method can be used with an accuracy sufficient for practical purposes as an engineering method for prediction of foundation settlements.

Denoting the average values of the quantities being determined with the subscript  $m$  and taking the depth of the active zone  $H = 2h_{eq}$  as the thickness of the soil layer which affects settlements, we can derive formulae for the average values of the coefficient of relative compressibility  $m_{vm}$  and the coefficient of filtration  $k_{fm}$ .

*The theorem on the average relative coefficient of compressibility* in this derivation must take into account the compressibility of individual strata of the soil in the whole active compression zone, their thickness and the pressures from an external load acting on each stratum.

Taking an equivalent triangular diagram of compacting pressures as the basis for the derivation (see Fig. 107), we can assume that the average reduced pressure in the middle of each stratum is

$$p_i = \frac{pz_i}{2h_{eq}} \quad (j_1)$$

where  $p$  = external pressure at the level of foundation base  
 $z_i$  = distance from the point at the depth  $2h_{eq}$  to the middle of the stratum considered (see Fig. 107)

The latter is valid, since the coefficient of compressibility is usually taken in calculations to be independent of external pressure, so that a slight error in the determination of pressures will have almost no effect on the magnitude of the calculated settlement, whereas, on the other hand, this scheme largely simplifies calculations.

The total settlement of the whole compressed zone of the soil is evidently equal to the sum of the settlements of the individual strata.

Taking the thickness of the active compression zone as  $2h_{eq}$  and the pressure acting on each stratum of the soil equal to  $p_i$  on the average [expression (j<sub>1</sub>)], we have

$$h_{eq}m_{vm}p = h_1m_{v1} \cdot \frac{pz_1}{2h_{eq}} + h_2m_{v2} \cdot \frac{pz_2}{2h_{eq}} + \dots \quad (j_2)$$

Cancelling out  $p$  and solving for  $m_{vm}$ , we get

$$m_{vm} = \frac{\sum_{i=1}^{i=n} h_i m_{vi} z_i}{2h_{eq}^2} \quad (5.59)$$

If the depth of active compression zone  $h_a$  is known [for instance, has been determined by formula (5.57')], then we obtain

$$m'_{vm} = \frac{2 \sum h_i m_{vi} z_i}{h_a^2} \quad (5.59')$$

The theorem on the average coefficient of filtration  $k_{fm}$  is derived proceeding from the assumption that the loss of head in the whole thickness of soil considered is equal to the sum of head losses in individual strata, i.e.,

$$\Delta H = \Delta H_1 + \Delta H_2 + \Delta H_3 + \dots \quad (k_1)$$

Since, according to the law of filtration, the flow rate of water  $q_f$  per unit cross-sectional area is

$$q_f = k_{fi} \frac{\Delta H_i}{H} \quad (k_2)$$

where  $k_{fi}$  is the coefficient of filtration and  $H$  is the length of flow path, then we have

$$\Delta H = \frac{q_f H}{k_{fm}}; \quad \Delta H_1 = \frac{q_f h_1}{k_{f1}}; \quad \text{and} \quad \Delta H_2 = \frac{q_f h_2}{k_{f2}} \quad (k_3)$$

where  $h_1, h_2$ , etc. are thickness of individual strata.

According to equation (k<sub>1</sub>), we obtain

$$\frac{q_f H}{k_{fm}} = \frac{q_f h_1}{k_{f1}} + \frac{q_f h_2}{k_{f2}} + \frac{q_f h_3}{k_{f3}} + \dots \quad (k_4)$$

whence

$$k_{fm} = \frac{H}{\sum_{i=1}^{i=n} \frac{h_i}{k_{fi}}} \tag{5.60}$$

Note that  $H$  should be taken as the thickness of the whole active zone of compression.

Having determined  $m_{vm}$  and  $k_{fm}$ , it is easy to find the stabilized settlement  $s_m$  and the settlement for any time  $t$ , i.e.,  $s_t$  for the whole stratified layer, assuming the latter to be quasi-homogeneous

$$s_m = h_{eq} m_{vm} p \tag{5.52"}$$

$$s_t = s_m U \tag{5.21"}$$

where the degree of consolidation  $U$  is determined depending on whether the main filtration flow of porous water occurs in only one or two ways, and also on the coefficient of consolidation which in that case is

$$c_{vm} = \frac{k_{fm}}{m_{vm} \gamma_w} \tag{5.11"}$$

**Example 5.7.** Find the total stabilized settlement of a foundation having a rectangular base surface ( $b = 1.6$  m,  $l = 3.2$  m) for the foundation depth of

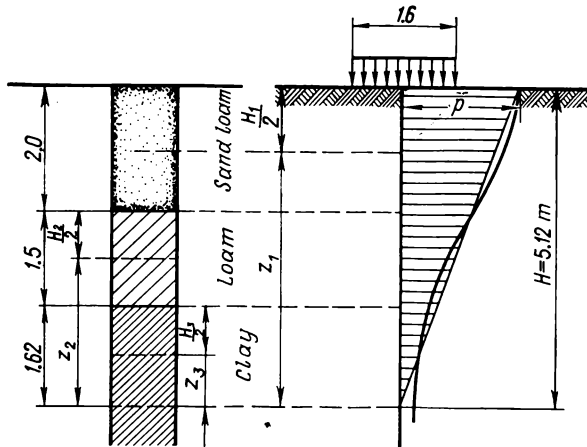


Fig. 110. Scheme to Example 5.7

$h_f = 1.5$  m, the pressure on soil  $p_0 = 2.0$  kgf/cm<sup>2</sup>, and the unit weight of soil above the base  $\gamma = 1.8$  tf/m<sup>3</sup>.

The foundation is to be built on a stratified soil layer (the thicknesses of strata are given in Fig. 110), the individual strata being characterized by the following data: 1st stratum (sand loam),  $m_{v1} = 0.008$  cm<sup>2</sup>/kgf; 2nd stratum

(loam),  $m_{v2} = 0.012 \text{ cm}^2/\text{kgf}$ ; and 3rd stratum (a thick layer of clay),  $m_{v3} = 0.015 \text{ cm}^2/\text{kgf}$ .

With the side-to-side ratio of the base surface  $\alpha = l/b = 3.2/1.6 = 2$ , we find from Table 5.6 for the average settlement (with  $\mu_0 = 0.3$ )

$$A\omega_m = 1.6$$

Then the thickness of the equivalent soil layer is

$$h_{eq} = A\omega_m b = 1.6 \times 1.6 = 2.56 \text{ m}$$

The height of the equivalent diagram of compacting pressures is

$$2h_{eq} = 2 \times 2.56 = 5.12 \text{ m}$$

The design pressure (in excess of the natural pressure) on the soil is found by formula (5.56) as

$$p = p_0 - \gamma h_f = 2 - 0.0018 \times 150 = 1.73 \text{ kgf/cm}^2.$$

To find the total stabilized settlement of the foundation, we have to know the average relative coefficient of compressibility for the whole active compression zone.

From the profile of soil strata (Fig. 110), we determine the distance  $z$  from the middle of each stratum to the depth  $2h_{eq}$ :  $z_1 = 5.12 - 1 = 4.12 \text{ m}$ ;  $z_2 = 5.12 - 2.0 - 0.75 = 2.37 \text{ m}$ , and  $z_3 = 1.62/2 = 0.81 \text{ m}$ .

The average relative coefficient of compressibility is calculated by formula (5.59)

$$\begin{aligned} m_{vm} &= \frac{\sum_{i=1}^{i=n} h_i m_{vi} z_i}{2h_{eq}^2} = \\ &= \frac{2 \times 0.008 \times 4.12 + 1.5 \times 0.012 \times 2.37 + 1.62 \times 0.015 \times 0.81}{2 \times 2.56^2} = \\ &= 0.0098 \text{ cm}^2/\text{kgf} \end{aligned}$$

The total stabilized settlement of the foundation will then be

$$s = 256 \times 0.0098 \times 1.73 \approx 4.3 \text{ cm}$$

**Some comparisons.** Let us compare the calculated settlements of foundations with the results of certain natural measurements.

Figure 111 shows the plan view of the foundations for a school building, for which the settlements have been calculated and during two years natural measurements of settlements made.

The soils of the base of these foundations consist of three strata (a sand loam stratum, 5.3 m thick; a loam stratum, 1.9 m thick; and a stratum of band clay of a thickness of more than 4 m) characterized by an average relative coefficient of compressibility for the whole active compression zone  $m_{vm} = 0.0223 \text{ cm}^2/\text{kgf}$ \*, which gives the calculated total stabilized settlement  $s = 13.5 \text{ cm}$  and the time

\* For a detailed calculation of settlements of the foundation considered, see the book: Tsytoovich N. A. Mekhanika gruntov (Soil Mechanics), 4th ed., Moscow, Stroizdat, 1963, pp. 604-8.

Table 5.9

**Settlements  $s_t$  of Foundation No. 2 (see Fig. 111)  
Calculated by the Equivalent Layer Method**

Degree of consolidation $U$	0.25	0.40	0.50	0.70	0.80	0.85	0.90
Settlement $s_t$ , cm	3.4	5.4	6.7	9.4	10.8	11.5	12.2
Time $t$ , days	13	57	106	305	477	600	787

variations of settlements according to the data given in Table 5.9. The measured values of the foundation settlements are given in Table 5.10.

Comparison of the actual (measured) settlements with the calculated data for various intervals of time from the beginning of construction of the building, which are shown in Fig. 112, shows that the calculated data (by the method of equivalent layer) agree well with the naturally measured settlements of the foundation, even

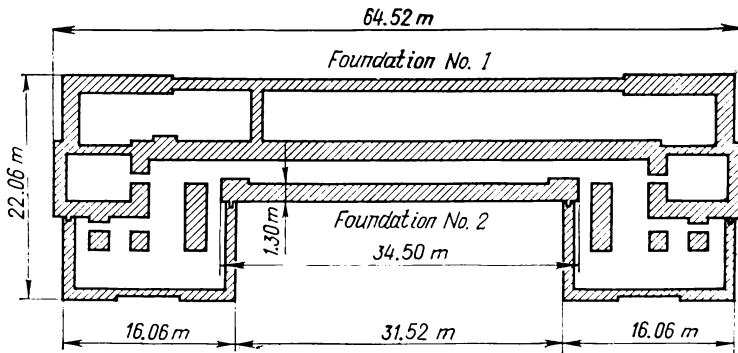


Fig. 111. Plan of foundations of a school building

for a stratified soil layer as in the case considered. Some discrepancies at the beginning of observations may be explained by that the calculation of foundation settlements has been made for the full load from the very beginning of construction of the foundation, whereas in nature the load was increasing gradually during around 5 months.

Let us also give some data obtained most recently. Thus, according to the data published in the materials of the Tallin Conference on Building Construction on Weak Soils (1965), particularly in reports of B. I. Dalmatov, S. N. Sitnikov, and others, the measured settlements were in good agreement with those calculated by the equivalent layer method for a large number of objects. For instance, for

Table 5.10

## Actual Settlements of Foundation No. 2

$s_t$ , cm	2.3	5.1	7.6	8.3	8.7	9.8	10.4	11.4
$t$ , days	30	88	136	171	220	313	404	572

the House of Soviets building in Leningrad, the settlement calculated according to BC&R (by the method of elementary summation without account of lateral expansion of soil) was 20.8 cm, that measured during 26 years (the measurements being repeated many times, since settlements were increasing gradually), 38.8 cm, and the stabilized

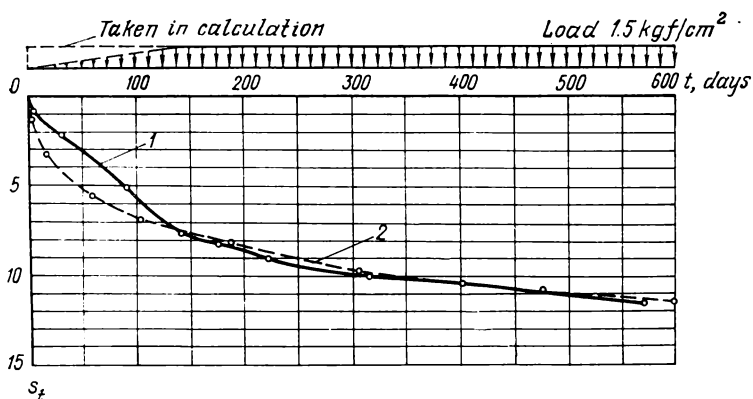


Fig. 112. Comparison of actual settlements 1 with those calculated by the equivalent layer method 2 for foundation No. 2 (see Fig. 111)

settlement calculated by the equivalent layer method, 42 cm; for the hotel "Rossiya" building in Leningrad, the settlement according to BC&R was 15 cm, that calculated by the equivalent layer method, 43 cm, and the total measured settlement, 45.3 cm; for a 12-storey residential building (approximately in the same soil conditions), the settlement according to BC&R was 31 cm, that calculated by the equivalent layer method, 51 cm, and the settlement measured one year after the beginning of construction of the foundations, 35 cm.

Thus, it may be taken for established that the predicted values of settlements correspond to those observed in nature with an accuracy sufficient for practical purposes if the design characteristics of the soils have been determined with an adequate accuracy and the boundary conditions of the problem (calculation schemes) selected properly.

## Chapter Six

### RHEOLOGICAL PROCESSES IN SOILS AND THEIR SIGNIFICANCE

The branch of science dealing with time variations of deformations of materials under the action of forces applied to them, but without changes of their composition, is called *rheology*, or the *science of flow of materials* (from the Greek “ $\rho\epsilon\omicron$ ”—to flow).

Studies into some problems of rheology were started long ago (E. Bingham in 1922, M. Reissner in 1943, and others), but only in the last decades were widely developed in connection with the use of various materials under high pressures and temperatures, the application of plastics, resins, etc. Such studies have become of special importance in geology and soil mechanics, in problems related to very long actions of loads, when appreciable *creep deformations* can be accumulated in soils and rocks or when a reduction of stresses (*relaxation*) occurs in them.

Knowledge of the reduction of soil strength is needed for selection of design resistances of soils in foundation bases or earthen materials for erection of building structures. For some kinds of soil, creep deformations may attain substantial magnitudes at certain pressures, owing to which they become dangerous for structures, especially for those subjected to permanent shear loads.

Thus, for instance, as has been shown by the experiments carried out at the Moscow Civil Engineering Institute\*, creep deformations for heavy clays may attain 36.4 to 165 per cent (see Table 6.1 below) of the deformations in the state of filtration consolidation, i.e., such values that must be accounted for, especially for structures being built on stiff-plastic, semi-hard and hard clays.

The need to account for the creep of clayey soils in calculations of stability and strength of retaining structures and natural slopes was emphasized by Prof. N. P. Puzyrevsky as far back as 1934. These problems were discussed in a number of works of other Soviet researchers (N. N. Maslov, M. N. Goldstein, G. I. Ter-Stepanyan), and the problems of the general rheology of frozen soils and permafrost (the importance of studying these problems was shown in 1937 by N. A. Tsytoovich and M. I. Sumgin in their book\*\*, where

\* Osnovaniya, fundamenti i mekhanika gruntov, No. 5, 1965.

\*\* Tsytoovich N. A., Sumgin M. I. Osnovaniya mekhaniki merzlykh gruntov (Fundamentals of Mechanics of Frozen Soils), Moscow, USSR Academy of Sciences, 1937.

they first gave rheological curves of permafrost at uniaxial compression) and later, of dense clayey soils, in the works of S. S. Vyalov, S. R. Meschyan, Yu. K. Zaretsky, and others. The works of Zh. S. Erzhanov and Yu. K. Zaretsky discuss the problems of rock mechanics, and the works of P. A. Rebinder, M. P. Volarovich, and I. M. Gor'kova deal with the problems of rheology of disperse bodies.

This brief and incomplete list of the Soviet researchers studying the problem of rheology in soil mechanics can serve as an indication to that the problem is of high actuality. This problem was discussed in recent years at a number of conferences and symposia (for instance, the International Symposium on Rheology in Soil Mechanics, Grenoble, France, 1964; Coordination Conference on Rheology in 1966; etc.).

The present chapter will discuss the rheological processes occurring mainly in clayey soils, and also their significance in soil mechanics.

In water-saturated soils these processes occur simultaneously with filtration consolidation, yet do not stop with the latter but proceed further, sometimes for a rather long time, after filtration consolidation has already stopped. Creep of the soil skeleton "in pure form" can only be studied after completion of filtration consolidation.

Let us discuss the *physical causes* of the principal rheological processes in clayey soils; these are *stress relaxations* and *creep deformations*.

The results of direct experiments on uniaxial and triaxial compression, shear and torsion of soils show that the resistance of cohesive clayey soils to external forces depends on the time of load action; with a rapid increase of the load it will be at the maximum, whereas with a slow increase and a long action of the load it diminishes, but deformations (creep) increase with time, even with an invariable physical state of the soil.

As has been shown in earlier chapters, clayey soils are very complicated systems of disperse particles with internal bonds of two kinds: rigid bonds (cementation-crystallizational) and viscous bonds (water-colloidal), the non-uniformity of internal bonds in soil being the cause of the presence of aggregates of particles of different cohesion and different strength.

With a prolonged action of external loads, rigid bonds are gradually destroyed as the forces applied to them become greater (weak bonds being destroyed first and stronger ones, later), so that *micro-fissures* are formed in aggregates of soil particles with simultaneous appearance of new water-colloidal and molecular-contact bonds, which become of tangible significance because of reduced distances between soil particles.

A reduction of the strength of soils occurs in the process of their deformation. Let us consider the curve of deformations of clayey

soils varying with time with a practically invariable physical state of these soils (when the process of filtration consolidation has already stopped) and at a load greater than *in*  $p_{cr}$ .

Apart from the instantaneous deformation  $Oa$ , three stages may be distinguished on the creep curve (see Fig. 113 and also Sec. 4.1): stage *I* (section  $ab$ ) of unstable creep; stage *II* (section  $bc$ ) of stable creep, or plastic flow with a practically constant deformation rate;

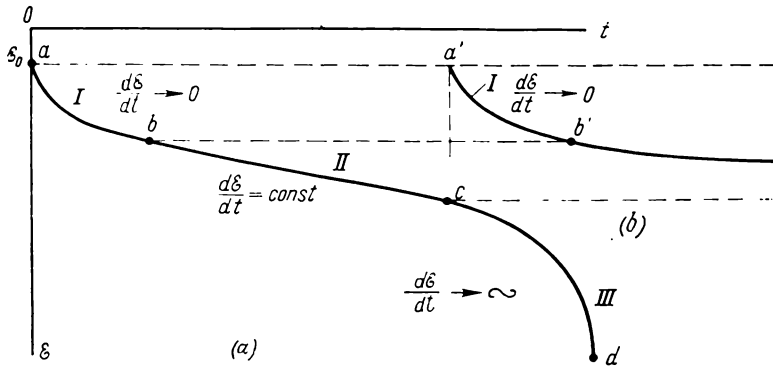


Fig. 113. Creep curves  
(a) non-attenuating; (b) attenuating

and stage *III* (section  $cd$ ) of progressively developing creep with ever increasing deformation rate.

As shown by corresponding experiments, including crystallo-optical experiments (carried out by M. N. Goldstein and S. S. Babit-skaya; E. P. Shusherina, S. S. Vyalov, N. K. Pekarskaya and R. V. Maksimyak; A. K. Larionov; the Author's experiments at the Moscow Civil Engineering Institute, etc.), the main factors responsible for the creep stages are *recombination of the soil structure* (with breakage of the old structural bonds and formation of new ones) and the *formation and development of microfissures*.

At the *first stage* (of attenuating creep) there occurs closing of existing microfissures, with the soil volume being observed to diminish.

At the *second stage* (of plastic-viscous flow) there occurs only a recombination of the structure with a practically invariable volume of the soil, the disturbance of the existing rigid and semi-rigid structural bonds being fully compensated for by the appearance of new water-colloidal and molecular-contact bonds, and the proceeding viscous deformation (mainly of water-colloidal shells which are firmly bonded with mineral particles) results in the formation of a new structure which resists ever less and less to external forces; aggregates of particles and separate particles line up, as it were, along the

direction of the acting forces, so that *microshears* occur between flaky clay particles in the direction of these forces (experiments of A. Ya. Turovskaya and others).

At the *third stage* (of progressive creep), the volume of soil increases and its total resistance decreases owing to the appearance (at a definite magnitude of relative displacements of particles and aggregates in soil) of new microfissures which continue to grow together with the existing defects and microfissures, thus being responsible for an accelerated deformation because of which the soil undergoes either *brittle* fracture or *viscous* flow which is accompanied with extrusion of the soil sideward from the loaded surface.

As shown by S. S. Vyalov in 1959 and confirmed by later researches, stable creep is always transformed into *progressive* creep, but with a different duration of load action: the greater the time of load action, the less will be the load at which progressive creep begins and, according to the experiments of Tsytoovich et al., only when the deformation attains a definite value for the given soil and for its physical state.

It should be noted that, as has been shown by experiments on frozen soils (E. P. Shusherina, 1964-66), the coefficient of relative lateral deformation  $\mu_o$  is not constant in the course of creep, but depends on the degree of deformation and for progressive creep can exceed 0.5, i.e.,  $\mu_o \geq 0.45-0.5$ , which is an indication that the soil becomes *decompacted* at the stage of progressive creep.

Let it also be recalled that the magnitude of  $\mu_o$  for clays depends on their consistency, varying in the *compaction phase* from  $\mu_o = 0.1$  (hard clays) to  $\mu_o = 0.5$  (liquid clays).

It should be mentioned, however, that *stable creep* occurs only at stresses exceeding a definite limit; at smaller effective stresses (loads), creep will not pass into the flow stage (stable creep), i.e., the soil will possess *long-term strength*, so that its deformations will be attenuating at any duration of load action (Fig. 113b).

## 6.1. STRESS RELAXATION AND LONG-TERM STRENGTH OF COHESIVE SOILS

**Physical background.** Since deformations of clayey soils in the creep phase increase with time, a given deformation may be maintained with an ever decreasing effective stress. The process of reduction of effective stresses with time at a permanent deformation is termed *stress relaxation*.

The stress relaxation caused by destruction of structural bonds in cohesive (clayey, frozen, etc.) soils always takes place in the course of creep, but stresses decline not to zero, but to a definite magnitude which further remains constant. An opinion existed, however (S. R. Meschyan, N. V. Zhukov, and others), that the strength of

clayey soils in the course of creep does not drop at shear, but, on the contrary, increases; this, however, contradicts the results of the special experiments carried out by S. S. Vyalov and N. K. Pekar-skaya in 1966 at the Research Institute of Foundations; as follows from these experiments, the resistance of clayey soils in the course of creep under rather long-term loads is always lower than the instantaneous resistance.

In accordance with what has been said above, we must distinguish between the following strength characteristics of soils possessing rheological properties: the *instantaneous strength*  $\sigma_0$ , i.e., practically

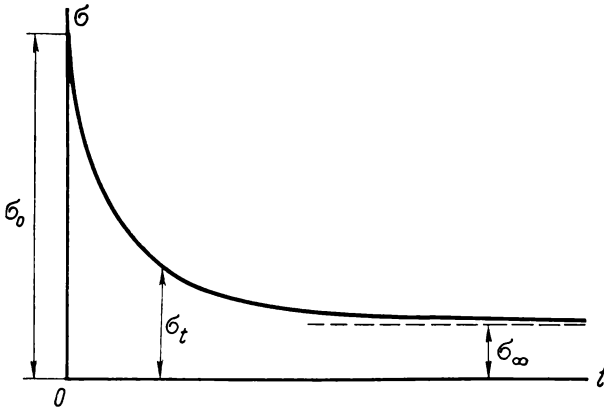


Fig. 114. Curve of long-term strength of frozen soils

an instantaneous resistance of soil at the very beginning of loading; *time-dependent strength*  $\sigma_t$ , which causes failure of soil at a given interval of time  $t$ ; and *long-term strength*  $\sigma_\infty$ , i.e., the lowest ultimate strength at stress relaxation (Fig. 114), below which the resistance decreases no more.

For predictions of time variations of soil strength  $\sigma_t$ , use can be made of the formulae proposed by S. S. Vyalov (6.1) or Yu. K. Zaretsky (6.2)

$$\sigma_t = \frac{b}{\ln t/B} \quad (6.1)$$

$$\sigma_t = \sigma_0 - (\sigma_0 - \sigma_\infty) \frac{t}{T_p + t} \quad (6.2)$$

where  $b$ ,  $B$ , and  $T_p$  are parameters to be determined experimentally\*.

\* See: Tsytoovich N. A. *Mekhanika merzlykh gruntov (obshchaya i prikladnaya)* [Mechanics of Frozen Soils (general and applied)], Moscow, Vysshaya Shkola Publishers, 1973, Chapter 3.

The degree of reduction of stresses with a constant deformation (relaxation) can be rather different for soils of various structure and consistency: up to 10-20 per cent for hard and semi-hard clays; up to 30-60 per cent for plastic clays; up to 80 per cent for liquid-plastic clays; and even 5 times and more for icy frozen soils and permafrost.

**Experimental studies.** Studies of stress relaxation and determinations of long-term strength of soils can be done by several methods: (1) method of direct measurement of stress relaxation (proposed by E. V. Kosterin in 1957); (2) method of dynamometric measurements of strength variations (S. S. Vyalov, 1966); and (3) method of spherical stamp (N. A. Tsytovich, 1947).

The first method is mainly employed in laboratory research works, because it requires high-precision measuring instruments; the second and the third methods are very simple and provide the possibility of determining the long-term strength of cohesive soils almost automatically by using a single monolithic sample; these two methods can be recommended for practical application, since they are rather convenient and require not much time (though more than is required in long-term tests); the latter method, that of a spherical-stamp test, is successfully employed in practice.

*The method of direct measurement of stress relaxations* uses an apparatus as the one shown in Fig. 115, which differs from a common compacting press in that the tie-rods are made in the form of tubes cut longitudinally into four equal portions, with resistance wire strain gauges being glued onto them for measuring stress relaxations in a soil sample with a constant value of its deformation.

As has been shown by experiments, the following relationship holds true for conditions of unrestricted lateral expansion of cohesive soils (with a correction for  $\sigma_\infty$ ):

$$(\sigma_t - \sigma_\infty) = (\sigma_0 - \sigma_\infty) t^{-n} \quad (6.3)$$

where  $\sigma_t$  = stress at the given instant of time  
 $t$  = time elapsed from the beginning of the test  
 $\sigma_0$  = initial stress  
 $\sigma_\infty$  = ultimate long-term stress  
 $n$  = parameter characterizing the rate of stress relaxation ( $n < 1$ )

It is of interest to note that the stress relaxation parameter for high-molecular compounds (according to the data of B. V. Deryagin et al.) is also less than unity.

In addition, it has been shown by experiments carried out at the Moscow Civil Engineering Institute that structural bonds become destroyed at a definite magnitude of the relative deformation of a soil.

In the *dynamometric method*, use is made of the apparatus (designed by V. F. Ermakov) shown in Fig. 116\*, which, when used by the Vyalov's method, enables the long-term strength of cohesive soils to be determined directly and almost automatically. For this, a load is applied to a soil sample by means of a dynamometer (this load being slightly less than the instantaneous strength), and measurements of deformations of the soil sample and records of the dynamo-

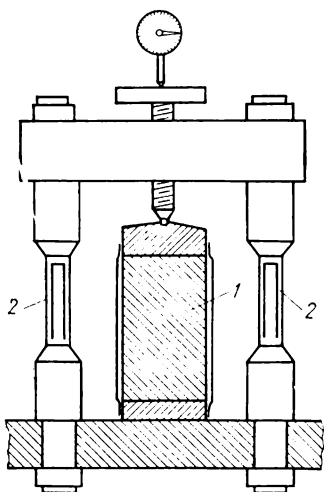


Fig. 115. An apparatus for direct measurements of stress relaxation in samples of clayey soils

1—sample to be tested; 2—measuring rods with resistance strain gauges glued onto them

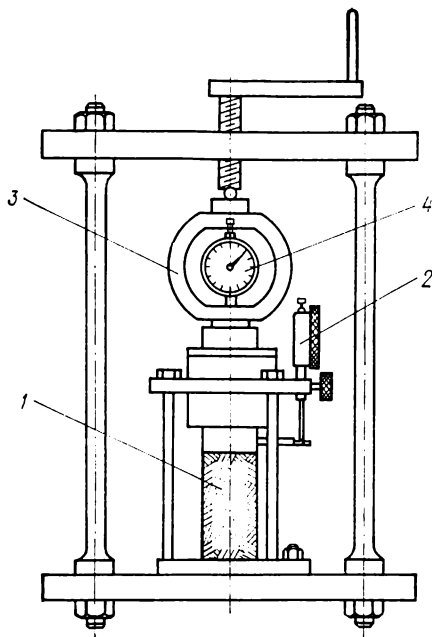


Fig. 116. A dynamometric apparatus  
1—soil sample; 2—indicator of sample deformations; 3—dynamometer; 4—dynamometer indicator

meter readings are made until the long-term strength of the soil is achieved (under a stabilized state).

The results of direct measurements make it possible to determine:  
 $\lambda_0^*$  = initial deformation of the soil sample  
 $\lambda_f^*$  = final deformation of the dynamometer

\* A similar apparatus for studies of mechanical properties of frozen soils was proposed by the Author as far back as 1938 (Proceedings of the Committee on Permafrost, Vol. 10, 1940).

$P_0$  = initial load on the soil sample

$P_f$  = final (stabilized) load on the soil sample (read off the dynamometer)

The long-term strength of the soil,  $P_\infty$ , with account of a correction for the deformability of the dynamometer (according to Vyalov) will then be

$$P_\infty = P_f \frac{P_0}{A_0 (\lambda'_f)^m} = P_f \left( \frac{\lambda''_0}{\lambda'_f} \right)^m \tag{6.4}$$

or, per unit area  $F$

$$p_\infty = \frac{P_\infty}{F} \tag{6.4'}$$

where the parameters  $A_0$  (initial deformation modulus of soil) and  $m$  (coefficient of strengthening) are determined from a diagram constructed in logarithmic coordinates of the pressure  $P_i$  and soil deformation  $\lambda''_i$  measured directly (see Fig. 117).

$$A_0 = e^{y_0}$$

$$m = \frac{\Delta(\ln P_0)}{\Delta(\ln \lambda''_0)}$$

The method of spherical stamp has been described in Chap. 2 in the paragraph dealing with cohesion of soils. It will only be noted here that after a spherical stamp has been loaded with a certain constant load (whose preferred limits corresponding to the invariance of the values obtained have been given in Chap. 2), deformations of the soil (or settlements of the stamp) must be measured before their stabilization; the deformations will stop *by themselves* as soon as the stamp comes to an equilibrium. The unit pressure thus found is the *long-term resistance* of the soil.

The average pressure on a spherical imprint in soil is

$$p_{av} = \frac{P}{\pi D s_t} \tag{6.5}$$

where  $P$  = external load on the spherical stamp

$s_t$  = settlement of the spherical stamp in the soil at any instant of time

$D$  = diameter of the stamp

If  $s_\infty$ , i.e., long-term stabilized settlement, is substituted for the settlement  $s_t$ , and it is taken into account that the ultimate pressure

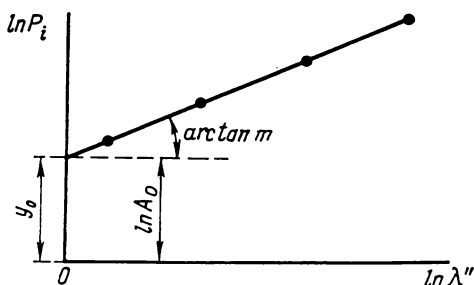


Fig. 117. Determination of stress relaxation parameters by means of a logarithmic graph

(strength) of soil increases with depth by at least the magnitude of the lateral surcharging  $\gamma h_f$  (where  $h_f$  is the depth of foundation), we finally have

$$ult p_{\infty} = \frac{P}{\pi D s_{\infty}} + \gamma h_f \quad (6.5')$$

Note that formula (6.5) determining the ultimate long-term resistance of cohesive soils (which is greater than *in p<sub>cr</sub>*) is fully applicable for estimation of long-term resistance of soils and enables this complex characteristic of their rheologic properties to be determined uniquely. This has been confirmed by numerous experiments with cohesive soils, including frozen soils\*. The simple test by means of a spherical stamp must naturally be repeated so many times as to obtain well averaged results, but this presents no special difficulties. As an example, Fig. 34 (see Chap. 2) shows a relaxation curve of cohesion forces in a cohesive soil at a long-term action of a load.

Note that, according to the data of some researches (B. F. Rel'tov et al.), stress relaxation in soils must be assumed to be caused by the fact that a part of elastic (recoverable) deformations pass with time into plastic irrecoverable deformations, mainly owing to a weakening (according to N. N. Maslov) of the cohesion forces in soils.

## 6.2. CREEP DEFORMATIONS IN SOILS AND METHODS FOR THEIR DESCRIPTION

As has been shown in the previous section, of essential practical significance (especially for stiff-plastic, semi-hard and hard clays) are the *attenuating creep* (stage *I* in Fig. 113) and, in some cases (for structures for which a definite deformation of the base, accumulated with time during the life of the structure may be allowed), the *stable creep* (stage *II* in Fig. 113), or plastic-viscous flow of the base soil with a constant speed; the *progressive creep* (stage *III* in Fig. 113) should by no means be allowed in bases of structures, since it may result in catastrophic deformations of the bases.

When studying the attenuating unstable creep of soils, distinction must be made between the volume creep (occurring at a local or total compression) and the shear creep at constantly acting horizontal forces in the bases of structures (for instance, in retaining structures: retaining walls, dams, embankments, etc.)

The *attenuating creep* occurs in the bases of structures only when the external pressures do not exceed a definite magnitude corresponding to the beginning of the stage of plastic-viscous flow.

\* Vyalov S. S. Reologicheskie svoystva i nesushchaya sposobnost' merzlykh gruntov (Rheological Properties and Load-Bearing Capacity of Frozen Soils), Moscow, USSR Academy of Sciences, 1959.

In the course of attenuating creep, the viscosity of clayey soils increases ever more owing to compaction and strengthening of water-colloidal shells of mineral particles, closure of microfissures, and appearance of new structural bonds.

Let us consider the attenuating creep of clayey soils which is responsible for what is called the *secondary* (visco-creep) *consolidation*.

As has been indicated earlier, a visco-creep deformation appears owing to *creep* deformations of the *soil skeleton*. Among many theories of creep, the one most suitable for clayey soils (as has been confirmed by numerous experiments of S. R. Meschyan et al.) is the integral theory of linear hereditary creep (formulated generally by Boltzmann and Volterra, first applied to soils by V. A. Florin, and interpreted by G. N. Maslov and N. Kh. Arutyunyan,) which is of more generalized nature compared with the multi-element rheological models of creep.

In solving problems by the linear theory of *hereditary creep*, the main equations are the *equations of state* of the soil skeleton [for instance, expression (2.38)] and equations of compressibility of gas-containing pore water [formula (2.40)].

The equation of stressed and strained state of soils with the attenuating creep and a single loading [formula (2.38)] is

$$\varepsilon(t) = \frac{\sigma(t)}{E_{inst}} + \bar{K}(t-t_0) \sigma(t_0) \Delta t_0$$

where the first term in the right-hand part is the instantaneous deformation at instant  $t$  (with the instantaneous deformation modulus  $E_{inst}$ ), the second term is the deformation which is accumulated with time and is proportional to the stress  $\sigma(t_0)$ , the interval of time of action  $\Delta t_0$ , and a certain function  $\bar{K}(t-t_0)$  which is dependent on the time elapsed from the instant  $t_0$  (creep core).

With a continuous loading [formula (2.38')] ]

$$\varepsilon(t) = \frac{1}{E_{inst}} \left[ \sigma(t) + \int_0^t K(t-t_0) \sigma(t_0) dt_0 \right]$$

where  $K(t-t_0) = \bar{K}(t-t_0) E_{inst}$ .

The creep core for clayey soils is described by the following expression which is most close to experimental results, as has been indicated earlier [see formula (2.39)]:

$$\bar{K}(t-t_0) = \delta e^{-\delta_1(t-t_0)}$$

where  $\delta$  and  $\delta_1$  are *creep parameters* (creep core coefficient  $\delta$  and creep attenuation coefficient  $\delta_1$ ) to be determined experimentally.

**Determination of creep parameters.** When determining the creep parameters of clayey soils by the results of drained compression

tests, one has to ensure that soil samples are fully saturated with water, i.e., the pore water will have no air bubbles (saturation of soil samples is to be made in vacuum). Then we can determine for each stage of loading:

(1) the coefficient of initial pore pressure [formula (5.29)]

$$\beta_0 = \frac{p_{w0}}{p}$$

where  $p_{w0}$  = initial pore water pressure measured directly after loading

$p$  = total pressure at the given stage of loading

(2) the coefficient of relative compressibility of the soil in the final stabilized state for the given stage of loading (i.e., the coefficient of final relative compressibility)  $m_v^f$ , which is found by the expression

$$m_v^f = \frac{s_\infty}{p_i h_i}$$

where  $s_\infty$  = stabilized settlement of the soil for the given stage of loading

$p_i$  = total pressure for the given stage of loading

$h_i$  = thickness of the soil layer being tested

(3) the coefficient of relative compressibility at the moment of load application (i.e., the coefficient of initial relative compressibility)  $m_v'$ , which is determined according to the compression and filtration properties of the soil by the formula following from expression (5.11)

$$m_v' = \frac{k_f}{\gamma_w c_v}$$

where  $k_f$ ,  $c_v$  are coefficients of filtration and consolidation at the beginning of compression (for instance, at the degree of consolidation  $U_0 = 0.2$  or  $U_0 = 0.3$ ).

Having found the parameters  $\beta_0$ ,  $m_v^f$ , and  $m_v'$  from the results of observation of settlements of the soil sample being tested after the pore water pressure has dropped to zero ( $p_w = 0$ ), we can determine the relative rates of settlement owing to creep of the soil skeleton for different intervals of time and from them, the *creep attenuation coefficient*  $\delta_1$ .

For this purpose, we plot a diagram (such as in Fig. 118) of the logarithm of relative settlement per unit pressure  $\left( \ln \frac{\dot{s}(t)}{hp} \right)$ , where  $\dot{s}(t) = \frac{\Delta s}{\Delta t}$  as a function of time  $t$ ; then the tangent of the semilogarithmic line obtained with the  $t$ -axis will be numerically equal (as follows from the adopted shape of the creep core) to the creep

attenuation coefficient  $\delta_1$ ,  $\text{min}^{-1}$ \*. Thus

$$\delta_1 = \tan \zeta \quad (\text{min}^{-1}) \quad (6.6)$$

With the creep attenuation coefficient  $\delta_1$  being known, the creep core coefficient  $\delta$  can be found by the formula

$$\delta = \delta_1 \cdot \frac{m_v''}{m_v'} \quad (6.7)$$

where  $m_v''$  is the secondary coefficient of relative compressibility (owing to creep of the soil skeleton).

According to the adopted exponential relationship for the attenuating creep core, the latter quantity is determined by the expression

$$m_v'' = \frac{m_v^f - m_v'}{1 - e^{-\delta_1 t_f}}$$

where  $t_f$  is the time when the settlement is practically fully stabilized (for the given stage of loading).

The expressions derived above make it possible to uniquely determine the parameters of attenuating creep which are required for description of the creep process by the linear (as regards stresses) theory of hereditary creep; these expressions are used for calculations of supplementary settlements of soil bases caused by creep of soils, which will be discussed in more detail in the next section.

It should be noted, however, that determinations of the creep parameters  $\delta$  and  $\delta_1$  by the results of drained compression tests require much time (several days) and rather accurate measurements of settlements of the soil samples being tested.

As has been shown by N. A. Tsytoovich and Z. G. Ter-Martirosyan\*\*, the time of observations can be reduced to around one day, if the creep parameters are determined from the results of *undrained tests* (by a closed system) of samples of not completely saturated (gas-

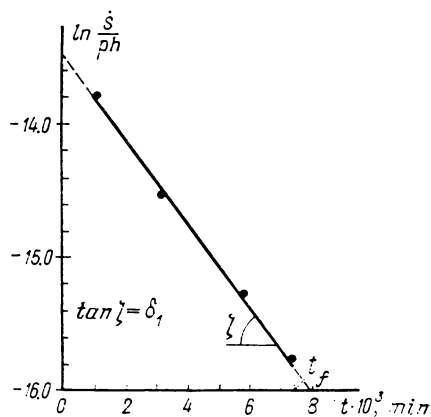


Fig. 118. Determination of the coefficient of creep attenuation through  $\ln s/\rho h$  and  $t$

\* See the footnote on page 197.

\*\* Osnovaniya, fundamenty i mekhanika gruntov, No. 3, 1966.

containing) soils with the pore water pressure being measured additionally in the course of tests.

**Stable creep at shearing.** For many retaining structures subject to a constant action of shear forces (embankments, dams, retaining walls, etc.), of essential importance is the *stable creep of soils at shearing*.

Time variations of the relative shear deformation (the ratio of the absolute deformation to the thickness of the soil layer being subject to shear) under the action of a constant shear load can be depicted by a curve similar to that shown in Fig. 113a (with relative shear deformations being laid off instead of relative compression deformations) and described in the general form by the equation

$$\Gamma = \Gamma_{rst} + \omega(t)$$

where  $\Gamma_{rst}$  = instantaneous (restorable) shear deformation

$\omega(t)$  = measure of creep (non-linear function of  $t$ ) which describes both the attenuating and stable portions of shear deformations

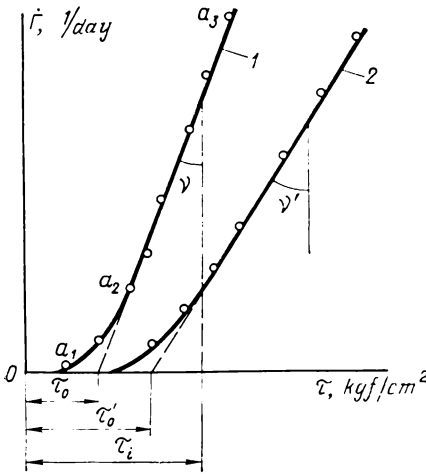


Fig. 119. A rheologic curve of a clayey soil at shearing

1—at a pressure  $p = 1 \text{ kgf/cm}^2$ ; 2—at a pressure  $p = 2 \text{ kgf/cm}^2$

The attenuating creep deformations at shearing can be described by an equation similar to equation (2.38), but the deformations of plastic-viscous flow, being the most critical for retaining structures, require a more detailed discussion.

If we lay off relative deformation rates  $\dot{\Gamma}$  (per unit thickness of the layer subject to shearing) along one of the coordinate axes (vertical), and shear stresses  $\tau$ , along the other axis (horizontal), we shall get what is called the *rheologic curve at shearing* (Fig. 119). Three characteristic sections may be distinguished on such a curve:

- $Oa_1$  = initial ultimate shear resistance (or creep threshold at shearing);
- $a_1a_2$  = initial section of creep; and
- $a_2a_3$  = stable plastic-viscous flow.

According to Fig. 119, we have for the stage of stable plastic-viscous flow

$$\tau_i - \tau_0 = \dot{\Gamma} \tan v$$

where  $\tau_0$  is the initial shear resistance. Denoting  $\tan v = \eta$ , the viscosity corresponding to the given physical state of the soil, we have

$$\tau_i = \tau_0 + \eta \dot{\Gamma} \quad (6.8)$$

This exactly is Bingham—Shvedov's equation of stable plastic-viscous flow. The applicability of this equation to clayey soils within a wide range of variation of their moisture content (consistency) has been proved by works of numerous researchers (P. A. Rebinder and his disciples; N. N. Maslov; M. N. Goldstein; E. V. Kosterin; N. V. Zhukov; A. Sh. Patvardkhan et al.).

Since the relative (per unit thickness of the layer being subject to shear) rate of shear deformations is

$$\dot{\Gamma} = \frac{v}{z}$$

then the rate of displacements at shearing,  $v$ , will be

$$v = \frac{\tau_i - \tau_0}{\eta} z \quad (6.9)$$

where  $z$  = thickness of the soil layer being subject to shearing ( $\tau_i - \tau_0$ ) = shear stress increment (in excess of the initial stress)

Note that the initial shear resistance is taken in calculations as the ultimate long-term shear resistance, i.e., it is assumed that  $\tau_0 = \tau_\infty$ .

If we consider plane shear at a certain depth  $z$  in the soil layer, then  $\tau_{zx}$  should be substituted for  $\tau_i$ , and  $\tau_{0z}$ , for  $\tau_0$

$$v_z = \frac{\tau_{zx} - \tau_{0z}}{\eta} z \quad (6.9')$$

When calculating the rate of displacements of retaining structures by Maslov's method\*, the quantity  $\tau_{zx}$  is found by the theory of linearly deformable bodies, and the initial shear resistance, or the creep threshold  $\tau_{0z}$ , corresponds to the ultimate shear resistance at a non-drained and non-consolidated state of the soil of the given moisture content. For the conditions of the planar problem we have

$$\tau_{zx} = \frac{2q}{\pi} \left( \arctan \frac{bz}{z^2 + b_1^2} \right)$$

---

\* Maslov N. N. *Osnovy mekhaniki gruntov i inzhenernoi geologii* (Fundamentals of Soil Mechanics and Engineering Geology), Moscow, Vysshaya Shkola Publishers, 1968.

where  $q$  = uniformly distributed horizontal load  
 $b_1$  = half-width of the base of retaining structure

$$\tau_{0z} \geq (\sigma + \gamma z) \tan \varphi_w + c_s$$

where  $\sigma$  = average compressive stress for the soil layer considered  
 (with a small thickness of the layer subject to shearing,  
 it can be taken equal to the external pressure  $p$ )

$\varphi_w$  = angle of internal friction for a non-drained and non-  
 consolidated state at the given moisture content of the  
 soil

$c_s$  = structurally irreversible (brittle, crystallizational) co-  
 hesion (viscous cohesion  $c_w$  is assumed to relax to  
 zero, i.e.,  $c_w \rightarrow 0$ ).

Having determined the depth  $d$  of the active zone of stable creep  
 at shearing by the condition that  $\tau_{zx} = \tau_{0z}$  and substituting  $\tau_{zx}$   
 and  $\tau_{0z}$  into expression (6.9'), we obtain the rate of displacement of  
 the retaining structure at shearing

$$v = \frac{d}{\eta} \left\{ \frac{2q}{\pi} \arctan \frac{b_1}{d} - \left[ \left( \sigma + \frac{\gamma d}{2} \right) \tan \varphi_w + c_s \right] \right\} \quad (6.10)$$

Note that the second term in the right-hand part (in square brackets)  
 can be replaced with the average value of the ultimate long-term  
 shear resistance  $\tau_\infty$  for the soil layer considered.

**Variation of soil viscosity during shearing.** In the derivation of  
 formula (6.10), viscosity is taken to be constant. But, as has been  
 shown by later investigations (N. N. Maslov, S. N. Sotnikov,  
 S. E. Mogilevskaya, A. Sh. Patvardkhan, N. A. Tsytoich, and  
 others), the viscosity  $\eta$  can vary appreciably during plastic-viscous  
 flow of clayey soils.

If the viscosity is assumed to vary according to Maslov's formula

$$\eta_t = \eta_f - (\eta_f - \eta_0) e^{-rt}$$

where  $\eta_0$  and  $\eta_f$  = initial and final viscosity of clayey soil

$r$  = a parameter depending on the soil properties:

$$r = \frac{1}{t} \ln \frac{\eta_f - \eta_0}{\eta_f - \eta_t}$$

then the displacement of a retaining structure, taking into account  
 that the rate of displacement is  $v = d\lambda/dt$  ( $\lambda$  being the displacement  
 of the structure), can be expressed as follows:

$$\lambda = d \left\{ \left[ \frac{2q}{\pi} \arctan \frac{b_1}{d} \right] - \left[ \left( \sigma + \frac{\gamma d}{2} \right) \tan \varphi_w + c_s \right] \right\} \left\{ \frac{t}{\eta_f} + \frac{1}{r\eta_f} \ln \frac{[\eta_f - (\eta_f - \eta_0)] e^{-rt}}{\eta_0} \right\} \quad (6.11)$$

The results of long-term observations on displacements of retaining structures (for instance, the Farkhad hydroelectric station) carried out at the All-Union Research Institute of Soils agree well with the data of calculations (S. E. Mogilevskaya) by formula (6.11).

### 6.3. ACCOUNT OF SOIL CREEP IN PREDICTIONS OF FOUNDATION SETTLEMENTS

In calculations of settlements of structures (their magnitude and time variations with account of soil creep), it is of importance to decide which of the theories of soil deformation should be applied: either the theory of creep alone, or with the simultaneous account of filtration consolidation, or with account of the compressibility of the pore water, the discrete structure of the soil, etc.

Here, we have to consider, in the first place, the significance of two main factors: *natural compaction and the degree of saturation of soils*.

For soils of liquid-plastic or soft-plastic consistency (according to the classification of BC&R), in which pore water is free or only weakly bonded with the soil skeleton, is hydraulically continuous or possesses negligible structural bonds (uncompacted loams, sand loams, very fine sands, silts, and weak clays below the ground water table), the classical theory of filtration consolidation is applicable, but *only for the first stage of loading or with a single loading*. If these kinds of soil have been preliminarily compacted by a certain load, then at subsequent stages of loading they will have structural bonds (predominantly water-colloidal) formed at the initial loading; calculations of foundation settlements then will have to take into account the discrete structure of the soil: incomplete transfer of the pressure to the pore water at the initial moment of loading ( $\beta_0 < 1$ ), structural strength ( $p_{str} > 0$ ), and the initial pressure gradient ( $i_0 > 0$ ).

What has been said above can be confirmed by the results of experiments, carried out by Z. G. Ter-Martirosyan\*, on studying the secondary consolidation (creep) of samples of Saratov clay ( $I_w = 0.98$ ;  $\gamma_s = 2.78$ ;  $W_L = 68$  per cent; and  $W_p = 32$  per cent, see Table 6.1).

As can be seen from these data, the Terzaghi — Gersevanov's assumption on complete transfer of external pressure to pore water at the initial moment of loading is strictly observed at the initial stage of loading; creep deformations constitute only an insignificant fraction of the settlement caused by filtration consolidation. But the more compacted a clayey soil, the greater fraction of the total settlement will be determined by the creep of the soil skeleton, reaching

\* Osnovaniya, fundamenty i mekhanika gruntov, No. 5, 1965.

Table 6.1

Loading stages, kgf/cm <sup>2</sup>	Effective pressure, kgf/cm <sup>2</sup>	Maximum pore water pressure, kgf/cm <sup>2</sup>	Settlement ratio $\frac{s_{\text{creep}}}{s_{\text{consol}}}$ , %	Duration of experiment, days
0-1	1	1.0	6.0	21
1-2	1	0.53	36.4	13
3-4	1	0.26	52.7	16
7-8	1	0.12	165.0	19

even 200-300 per cent (up to 165 per cent in the example considered) of the settlement through filtration consolidation.

For clayey soils of stiff-plastic, semi-hard or hard consistency, the process of their compaction cannot be described by the theory of filtration consolidation alone, since the discrete structure and deformability of all components of these soils, especially the creep of the soil skeleton, have an appreciable effect from the very beginning of loading.

The applicability of some or other solutions of the theory of consolidation and creep of soils for calculations of foundation settlements depends appreciably on the degree of water saturation of clayey soils, which is determined by the coefficient of saturation  $I_w$  (see Chap. 1).

Depending on the degree of saturation and the completeness of the process of filtration consolidation, soils can be regarded as: (1) *one-component* (or quasi-one-phase) system of particles; (2) *two-component* (soil mass) system; or, finally, (3) *three-component* system. In addition, *transient systems* may have place, for instance, when a three- or two-component system is transformed with time (for instance, owing to drying out) into a one-component system or when a quasi-one-phase system is transformed into a two- or multi-phase system through compaction and creep, etc.

Solutions for the main systems have already been obtained, but the transient ones require an additional experimental determination of the conditions for transformation of one system into another.

As has been shown by analysis, the solutions obtained for one-component (more strictly, for *quasi-one-phase*) systems are applicable in the following cases: for pure sand and coarse-skeleton dry, *non-saturated* soils (according to BC&R, *moist* soils, but undersaturated, with  $I_w < 0.80$ ); and also for almost *fully saturated* soils that contain only an insignificant amount of gases (practically below one per cent, i.e., with  $I_w \geq 0.99$ ) under conditions that the *process of filtration consolidation* has been *fully completed*. The required characteristics of deformability of soils in this case are only the creep parameters  $\delta$  and  $\delta_1$ .

The solutions obtained for two-component and *quasi-two-phase* systems (for instance, by the "theory of soil mass", "theory of spatial forces") are valid for *fully saturated* soils ( $I_w = 1$ ), but with account of the creep of the skeleton (the parameters  $\delta$  and  $\delta_1$ ) and the discrete structure of soils (the coefficients of the initial pore water pressure  $\beta_0 < 1$  and the initial pressure gradient  $i_0 > 0$ ).

The solutions for *three-phase saturated systems* are the most generalized ones and should be applied with the saturation of clayey soils of  $I_w > 0.9$  and with account of the creep of the soil skeleton (coefficients  $\delta$  and  $\delta_1$ ), compressibility of pore water (coefficient  $m_w$ ) and natural discrete structure of soils (coefficients  $\beta_0$  and  $i_0$ ). The above limit of the saturation coefficient ( $I_w \approx 0.9$ ) is to be established preliminarily on the basis of Malyshev's experiments who has shown that at a saturation degree below 0.85 pore water cannot be regarded hydraulically continuous, so that its motion cannot be described by filtration laws.

Shown in Fig. 120 are curves of consolidation and creep of Saratov clay samples (1—calculated by Terzaghi—Gersvanov's theory of purely filtration consolidation; 2—according to Florin with account of only the creep of the skeleton and the filtration consolidation of soil; 3—calculated with *simultaneous account of filtration consolidation, creep of the soil skeleton, and compressibility of pore water*, i.e., as for a three-phase system, and 4—experimentally found data\*).

These data indicate that the *simultaneous account of the creep of the soil skeleton and the compressibility of pore water* in the course of soil consolidation is of very high importance (see curves 3 and 4, Fig. 120).

It should be noted that for *transient systems* of creep and consolidation it must be additionally determined experimentally what

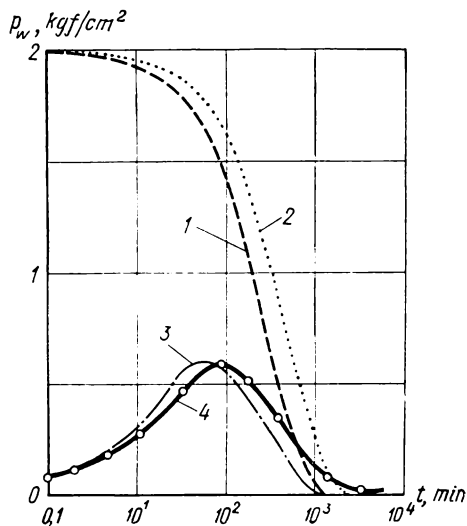


Fig. 120. Curves of consolidation and creep of a Saratov clay sample (pressure  $p = 2$  kgf/cm<sup>2</sup>; layer thickness  $h = 4$  cm, coefficient of relative compressibility  $m_v = 0.0775$  cm<sup>2</sup>/kgf, and filtration coefficient  $k_f = 2 \cdot 10^{-7}$  cm/min)

\* Osnovaniya, fundamenty i mekhanika gruntov, No. 5, 1965.

conditions of saturation and compaction and what time of the action of compaction load are required for one system to be transformed into another.

**One-dimensional problem of the theory of creep of quasi-one-phase, two-phase, and multi-phase soils.** Let us consider a one-dimensional problem, i.e., the problem of determination of settlements (vertical displacements) of a soil layer under a *continuous load*, with the compacted layer being represented as different systems of particles (from the standpoint of calculation).

1. For a *quasi-one-phase* (and also for *one-component*) system, the settlements of an individual soil layer are found under the assumption that settlement occurs only owing to the *creep* of the soil skeleton, which is characterized by a definite *creep core* in the theory of hereditary creep.

As has been shown earlier [formula (2.39)], the creep core can be described in the most convenient and practically justified form as follows:

$$\bar{K}(t - t_0) = \delta e^{-\delta_1(t - t_0)}$$

where  $\delta$  and  $\delta_1$  = creep parameters to be determined as described in the previous section

$t$  and  $t_0$  = current and initial time readings

Since the creep core is the rate of soil creep with a constant unit stress, then creep will affect only time variations of settlements, and the total stabilized settlement of the soil for the one-dimensional problem will be expressed as earlier, i.e.,

$$s = h m_{cr} p \quad (5.9^{IV})$$

where  $m_{cr}$  is coefficient of relative compressibility of the soil skeleton at creep.

As follows from the method of determining the parameters of attenuating creep discussed in the previous section, and as has been shown by the Author earlier\*, the *coefficient of relative compressibility* of the soil skeleton at creep,  $m_{cr}$ , can be expressed by the following equation

$$m_{cr} = m'_v + m''_v (1 - e^{-\delta_1 t}) \quad (6.12)$$

where  $m'_v$  and  $m''_v$  are coefficients of initial and secondary consolidation of the soil

or

$$m_{cr} = m'_v \left[ 1 + \frac{m''_v}{m'_v} (1 - e^{-\delta_1 t}) \right] \quad (6.12')$$

---

\* See the footnote on page 255.

and, since

$$\frac{\delta}{\delta_1} = \frac{m''_v}{m'_v}$$

according to formula (6.7), then, substituting (6.12) into (5.9<sup>IV</sup>), we get the expression

$$s_t = hm'_v p \left[ 1 + \frac{\delta}{\delta_1} (1 - e^{-\delta_1 t}) \right] \quad (6.13)$$

that describes time variations of creep settlements for quasi-one-phase and one-component soils.

Note that in case of the action of a local load (from foundations of structures), the value of equivalent layer  $h_{eq}$  must be substituted for  $h$  [formula (5.51).]

2. The general solution of the combined problem of creep and consolidation for a *two-phase system* has been found by Zaretsky\* on the basis of the Florin—Biot generalized theory of spatial forces with account of the interaction of soil phases, time variations of the total stressed state in any point of soil, additional pressures in pore water, and incomplete transfer of the external pressure to the pore water being compressed.

For a one-dimensional problem, this solution may be written in the following form:

$$s_t = hm'_v p \left[ 1 + \int_0^t K(t-t_0) dt_0 - \frac{8}{\pi^2} \sum_{m=1; 3; \dots}^{m=\infty} \frac{1}{m^2} \bar{\psi}(t) \right] \quad (6.14)$$

where the creep function is determined, with account of the interaction of phases and the creep core expressed by equation (2.39), by the following expression:

$$\bar{\psi}(t) = e^{-\left(\frac{\pi m}{2h}\right)^2 c_v t} + \frac{\delta}{\delta_1} \cdot \frac{e^{-\left(\frac{\pi m}{2h}\right)^2 c_v t} - e^{-\delta_1 t}}{1 - \left(\frac{\pi m}{2h}\right)^2 \frac{c_v}{\delta_1}} \quad (6.15)$$

where  $c_v = \frac{k_f}{m_v \gamma_w} =$  coefficient of consolidation of a *two-phase soil*  
 $2h =$  thickness of soil layer with two-way drainage  
 $\delta$  and  $\delta_1 =$  creep parameters

As has been proposed earlier by the Author\*\*, the formula for the settlement of a two-phase soil can be given the following simple form:

$$s_t = ph [m'_v U_0^{init} + m''_v U_0^{sec}] \quad (6.16)$$

\* Zaretsky Yu. K. Teoriya konsolidatsii gruntov (Theory of Soil Consolidation), Moscow, Nauka Publishers, 1967.

\*\* Osnovaniya, fundamenty i mekhanika gruntov, No. 5, 1965.

where  $U_0^{init}$  and  $U_0^{sec}$  are respectively the degrees of the *initial* and *secondary* consolidation of the soil.

Thus, a time variation of settlement consists of two components: the initial and the secondary settlement.

The degree of initial consolidation  $U_0^{init}$  is expressed as earlier

$$U_0^{init} = 1 - \frac{8}{\pi^2} \sum_{m=1; 3; \dots}^{m=\infty} \frac{1}{m^2} e^{-\left(\frac{\pi m}{2h}\right)^2 c_v t} \quad (5.19'')$$

and the degree of secondary consolidation  $U_0^{sec}$  and that of total consolidation (owing simultaneously to filtration consolidation and creep of the soil skeleton  $U_0^\Sigma = s_t/s_\infty$ ), by the formulae derived by Zaretsky

$$U_0^{sec} = 1 - e^{-\delta_1 t} - \frac{8}{\pi^2} \sum_{m=1; 3; \dots}^{m=\infty} \frac{1}{m^2} \cdot \left[ \frac{e^{-\left(\frac{\pi m}{2h}\right)^2 c_v t} - e^{-\delta_1 t}}{1 - \left(\frac{\pi m}{2h}\right)^2 \frac{c_v}{\delta_1}} \right] \quad (6.17)$$

$$U_0^\Sigma = \frac{U_0^{init} + \frac{\delta}{\delta_1} U_0^{sec}}{1 + \frac{\delta}{\delta_1}} \quad (6.18)$$

By way of examples, Fig. 121a shows curves of variation of the total degree of consolidation  $U_0^\Sigma$ , and Fig. 121b, curves of variation of the head function  $H_{h,t}$  for a *two-phase* soil layer of a thickness  $2h$ , characterized by the creep parameters  $\delta_1 = 0.1 \left[ \frac{1}{T} \right]$  and  $\delta = 1.0 \left[ \frac{1}{T} \right]$ , with a uniform distribution of compacting pressures in depth, where  $\left[ \frac{1}{T} \right]$  is the symbol of dimensionality of parameters in any time units. The curves are given for a number of values of  $M = \frac{\pi^2 c_v}{4h^2} \left[ \frac{1}{T} \right]$ .

Figure 121a also shows curves (dotted lines) of the degree of consolidation without account of the creep of the soil skeleton. By comparing these curves with those of the total degree of consolidation, it can be seen that discrepancies in the degree of consolidation are especially large with the factor  $M \geq 0.1 [1/T]$  (curves I and I'), i. e., at low values of the thickness of the soil layer being compressed.

The curves in Fig. 121b enable the magnitude of pore pressure to be calculated for the relationships considered by the formula

$$p_w = p H_{h,t} \quad (6.19)$$

where  $p$  = external pressure

$H_{h,t}$  = head function determined by the formula

$$H_{h,t} = \frac{4}{\pi} \sum_{m=1; 3; \dots}^{m=\infty} \frac{1}{m} \sin \frac{\pi m}{2h} \bar{\psi}(t) \quad (6.20)$$

with  $\bar{\psi}(t)$  corresponding to expression (6.15). Note that more detailed calculations of the total degree of consolidation of soil layers for

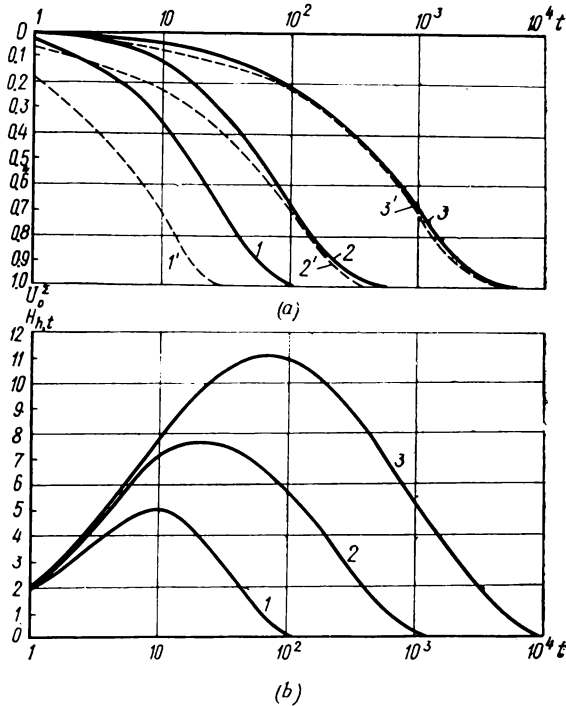


Fig. 121. Curves of the total degree of consolidation  $U_0^\Sigma$  (a) and head function  $H_{h,t}$  (b) for the one-dimensional problem of uniform compression of a soil layer between two draining surfaces with the values of the time factor as follows:

$$1 - M = 0.1 \left[ \frac{1}{T} \right]; \quad 2 - M = 0.01 \left[ \frac{1}{T} \right]; \quad 3 - M = 0.001 \left[ \frac{1}{T} \right]$$

a one-dimensional problem are made by using supplementary tables\*.

With the total degree of consolidation  $U_0^\Sigma > 0.2$ , we can limit ourselves to the first terms in expressions (5.19) and (6.17) (for the

\* Tsytoich N. A., Zaretsky Yu. K. et al. Prognoz skorosti osadok osnovanii sooruzhenii (Prediction of Settlement Rates of Structure Bases), Moscow, Stroizdat, 1967, Chapter 7.

initial and secondary degree of consolidation). Then, for a two-phase soil under conditions of the one-dimensional problem with a uniform distribution of compacting pressures over the depth (continuous load), we shall have

$$s_t = hm_v p \frac{1 - \frac{8}{\pi^2} e^{-Mt} + \frac{\delta}{\delta_1} \left\{ (1 - e^{-\delta_1 t}) - \frac{8}{\pi^2} \left[ \frac{e^{-Mt} - e^{-\delta_1 t}}{1 - M \frac{c_v}{\delta_1}} \right] \right\}}{1 + \frac{\delta}{\delta_1}} \quad (6.21)$$

where

$$M = \frac{\pi^2 c}{4h^2} \quad \text{and} \quad c_v = \frac{k_f}{\gamma_w m_v}$$

Formula (6.21) makes it possible to calculate, without special difficulties, the settlement of a two-phase soil for any instant of time with account of the interaction of phases and of the creep of the skeleton.

For *three-phase system*, the solution has been obtained for rather moist but not fully saturated soils, i.e., with the saturation coefficient varying within the limits  $1 > I_w > 0.95$ .

For determinations of settlements corresponding to any time  $t$  (i.e.,  $s_t$ ) in the one-dimensional problem of consolidation and creep of incompletely saturated soils (containing gas-laden pore water), the basic relationship is that described by expression (6.21), but with a different coefficient of consolidation  $c_v$ , equal to  $c_w$ , which is determined by expression (5.31), i.e.,

$$c_w = \frac{k_f}{m_v \gamma_w} \beta_0$$

with a multiplier  $B$ , which according to formula (5.33) is

$$B = \frac{1}{1 + \frac{m_w}{m_v} n \beta_{str}}$$

being introduced into the second and third terms in the numerator of formula (6.21). Thus, we have

$$s_t = hm_v p \frac{1 - B \frac{8}{\pi^2} e^{-Mt} + \frac{\delta}{\delta_1} B \left\{ (1 - e^{-\delta_1 t}) - \frac{8}{\pi^2} \left[ \frac{e^{-Mt} - e^{-\delta_1 t}}{1 - M \cdot \frac{c_w}{\delta_1}} \right] \right\}}{1 + \frac{\delta}{\delta_1}} \quad (6.21')$$

**Engineering method for prediction of total settlements of structural foundations due to compaction and creep.** As has been discussed in detail in Sec. 5.6, in determinations of settlements of foundations of a definite rigidity and a definite area of pressure transfer from a structure to soil, the equivalent layer method gives sufficiently accurate results by reducing the three-dimensional problem to an equivalent one-dimensional problem, but with a triangular diagram of compacting pressures, the base of the triangle being equal to the unit pressure  $p$  on soil at the level of the foundation base, and the height equal to the depth of the active compression zone,  $h_a$ .

Let it be recalled that in determinations of the depth of active compression zone [whose maximum value is  $2h_{eq}$ , where  $h_{eq}$  is the thickness of the equivalent soil layer determined by formula (5.51)], account must be taken (see Fig. 109) not only of the dimensions and area of the foundation base (in terms of  $h_{eq}$ ), but also of the consistency of soils (in terms of  $\mu_o$ ), their structural strength  $p_{str}$ , and the initial pressure gradient  $i_o$ .

Thus, the earlier expressions for total settlements through filtration consolidation and creep of the soil skeleton are also valid for settlements of soils under the action of local loads (from foundations of structures) to be determined with account of filtration consolidation, compressibility of pore water, the discrete structure and compaction of the soil (structural strength  $p_{str}$ , coefficient of initial pore-water pressure  $\beta_o$ , and initial pressure gradient  $i_o$ ). But, in doing so, we have to use the corresponding diagrams of distribution of compacting pressures over the depth, namely:

1. For cases of *two-way filtration* (i.e., when water has a drained outlet upward at the foundation base and downward at a depth equal to or less than the lower boundary of the active compression zone, i.e., equal to or less than the height of the transformed triangular diagram of compacting pressures), the problem comes to the *main case* of the action of a continuous load, but with a triangular diagram of compacting pressures. Then the settlements corresponding to any time from the beginning of loading can be calculated by the following approximate expression:

$$s_t = \frac{h_a m_v p}{2} \cdot \frac{1 - B \frac{8}{\pi^2} e^{-Mt} + \frac{\delta}{\delta_1} B \left\{ (1 - e^{-\delta_1 t}) - \frac{8}{\pi^2} \left[ \frac{e^{-Mt} - e^{-\delta_1 t}}{1 - M \frac{c_w}{\delta_1}} \right] \right\}}{1 + \frac{\delta}{\delta_1}} \quad (6.22)$$

2. For cases of *one-way filtration* only upward to the foundation base (for instance, in case of a soil which is homogeneous over the depth and has a drainage layer at the foundation base), the problem reduces to case 2 considered earlier, in which compacting pressures

are assumed to decrease linearly by a triangular diagram with the base equal to  $p$  and the height equal to the thickness  $h_a$  of the active compression zone.

Using the general solution given earlier [formulae (6.17) and (6.18)] and noting relationship (5.27) and formula (5.25), we have for the case considered

$$s_t = \frac{h_a m_v p}{2} \frac{1 - \frac{16}{\pi^2} B \left(1 - \frac{2}{\pi}\right) e^{-Mt} + \frac{\delta}{\delta_1} B \cdot D}{1 + \frac{\delta}{\delta_1}} \quad (6.23)$$

where

$$D = \left\{ (1 - e^{-\delta_1 t}) - \frac{16}{\pi^2} \left(1 - \frac{2}{\pi}\right) \left[ \frac{e^{-Mt} - e^{-\delta_1 t}}{1 - M \frac{c}{\delta_1}} \right] \right\}$$

It should be noted again that the coefficient of consolidation [according to formula (5.31)] for a three-phase undersaturated soil in formulae (6.22) and (6.23) is

$$c_w = \frac{k_f}{m_v \gamma_w} \beta_0$$

and the coefficient of the influence of pore water compressibility is

$$B = \frac{1}{1 + \frac{m_w}{m_v} n \beta_{str}}$$

For two-phase soils having no air in pore water, the compressibility of the water is very low ( $m_w \approx 0$ ) and the coefficient  $B$  becomes equal to unity ( $B = 1$ ). For undercompacted two-phase soils possessing no structural strength (i.e., those in the state of a soil mass), we have to assume that  $\beta_0 = 1$  in the formula for the coefficient of consolidation.

**Some conclusions.** The rheological processes caused by the creep of soils, which we have briefly discussed in this chapter, are of essential practical importance for all kinds of soil.

In loose soils (sands, gravels, etc.), creep has an effect only at substantial pressures, and in a dry state of these soils it is caused by the process of flow in points of contact and by development of microfissures in particles subject to appreciable local pressures.

In cohesive soils (clays and silts), creep of the soil skeleton may occur at any load, but at high pressures the process of time variations of deformations becomes critical. In stiff-plastic, semi-hard, hard and quick clays, *creep of the soil skeleton* can be responsible

---

for the major portion of their deformations and sometimes almost for the whole deformation.

In studies of the stressed and strained state of soils, account of the creep of the soil skeleton gives more reliable results than it follows from the solutions based only on the theory of purely filtration consolidation.

For that reason, without studying the rheological processes occurring in soils under the action of external forces and, in special cases, of their dead weight, it is often impossible to obtain a complete estimation of a soil as a base or a medium for various structures.

## Chapter Seven

### DYNAMICS OF DISPERSE SOILS

#### 7.1. DYNAMIC EFFECTS ON SOILS

The previous chapters of the book are devoted to the problems of stressed state and deformations of soil under the action of static effects, i.e., those invariable in time or varying very slowly. The present chapter deals with problems of studying various dynamic effects caused by dynamic loads from unbalanced machines, explosions, earthquakes, motion of transport vehicles, etc., on disperse soils.

**Dynamic loads from unbalanced machines** excite vibrations of their foundations. These, in turn, become sources of vibrations which can propagate over large distances in a soil and be transmitted to neighbouring buildings and structures. Vibrations of machine foundations may have an adverse effect on the operation of the machines proper and the technological processes carried out by means of these machines and can be harmful to the personnel. Propagation of vibrations in soils can often result in an increased development of settlements of buildings and structures and cause deformations of structural members. For that reason, dynamic loads are indispensably taken into account when designing machine foundations.

Typical curves of time variations of dynamic loads from machines are shown in Fig. 122.

*Periodic* loads (Fig. 122a) can be either harmonic (curve 1) or multi-frequency (curve 2), the first appear in operation of turbo-machines, motor-generators and other machines having rotatable parts, and the second, in operation of machines having crankshaft or other reciprocating mechanisms (for instance, piston compressors).

*Non-periodic* loads (Fig. 122b) are most often related to the class of impulse loads (curve 3), similar to those formed in operation of forging hammers, but may be of a more complicated nature. Curve 4, for instance, represents time variations of the moment of couple transmitted to the foundation by the drive motor of a rolling mill.

Methods for determining dynamic loads from unbalanced machines may be found in corresponding standards (for instance, BC&R. Foundations of Dynamically Loaded Machines, Moscow, Stroiizdat, 1970).

**Seismic effects.** As is known, the mantle of the Earth is inhomogeneous and consists of rock massifs separated by cracks and differing in their mechanical properties. Slow relative displacements of rock massifs result in accumulation of deformations which, because of their non-uniformity, attain maximum values in certain localities, or, by the adopted terminology, in seismic centres. Here the mantle becomes broken and the potential energy of deformations is liberated and transformed into the kinetic energy of elastic waves propagating all over the globe and appearing on the Earth's surface in the form of short-term intense vibrations termed earthquakes.

Seismic forces of interaction between oscillating ground and the structures erected on it cause the formation of inertial forces ("inertial seismic loads") in these structures, which can cause damage or even breakdown. In order to determine seismic forces in the general case, we have to know the displacement, speed, and acceleration of a vibrational motion. If we assume that all points of the Earth's surface within the locality being considered perform similar motions, then only one of these characteristics will be sufficient for calculations.

Calculation of structures for seismic actions in cases when vibrations of the base of a structure are given by an accelerogram of earthquakes presents certain difficulties, because of which the intensity of such vibrations is characterized, according to BC&R, by what is called the coefficient of seismicity, i.e., the ratio of the seismic acceleration to the acceleration due to gravity.

Dynamic properties of soils in the bases of structures may have an appreciable effect on the magnitude of seismic actions. These properties are taken into account when designing engineering structures for seismic regions.

It should be taken into account that seismic vibrations can cause water-saturated cohesionless soils to lose their dynamic stability and change into a *liquefied state* over large massifs; this always has a catastrophic effect on the structures erected in the locality.

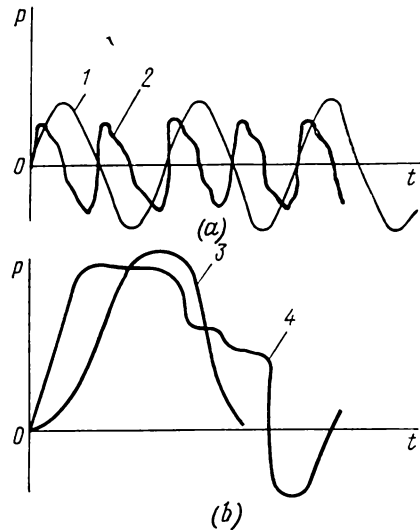


Fig. 122. Time variations of unbalanced inertia forces from operating machines (a) periodic loads (1—harmonic; 2—multi-frequency); (b) aperiodic impulse loads (3—simple; 4—complex)

**Earth vibrations caused by transport vehicles.** These vibrations are rather weak as compared with those caused by seismic forces of earthquakes, but because of prolonged action they may result in settlements of bases and vibrational flow of disperse soils.

**Explosions may cause** a whole series of rapid mechanical processes in soils: appearance of an explosion *gas chamber* within a rather short interval of time (sometimes a few thousandths of a second), which exerts an enormous pressure (of the order of a few hundred thousand atmospheres), causes the formation and propagation of *explosion waves* which change the stressed state of a soil mass and cause its particles to move with velocities varying from a few thousand metres per second to zero.

*Explosion impulses* are characterized by the maximum pressure  $p_{\max}$ , the rise time  $t_1$ , during which this pressure is formed, the fall time  $t_2$ , during which the pressure drops from the maximum to zero, and the total time of explosion action  $t_{\Sigma}$ .

As seen from experiments of Prof. G. M. Lyakhov\*, the gas chambers formed in soil through explosion of deep concentrated charges of explosives are almost spherical in shape. With time, a gas chamber (the cavity in soil) is destroyed, but the time period of its destruction may be very different, from a few minutes (in sands) to several months (in dense clays).

As has been shown by the experiments, the radius of an explosion gas chamber  $R_{ch}$ , after it has been formed completely, is determined by the following relationship:

$$R_{ch} = \kappa \sqrt[3]{C} \quad (7.1)$$

where  $C$  = weight of explosive charge, kg

$\kappa$  = proportionality factor depending on the properties of soil

According to G. M. Lyakhov, numerical values of this factor are:

for saturated sands . . . . .	$\kappa = 0.4-0.7$
for loams (according to G. I. Pokrovsky) . . . . .	$\kappa = 0.45$
for loess soils . . . . .	$\kappa = 0.35$
for clayey soils . . . . .	$\kappa = 0.6-0.7$

Explosion of a concentrated charge in a soil results in the formation of normal (radial) pressures  $p$ , lateral (tangential) pressures  $p_{\tau}$ , and the motion of particles with a velocity  $u$ .

For *non-saturated soils* and rocks, all these three parameters are determined in calculations as functions of time, i.e.,

$$p = p(t); \quad p_{\tau} = p_{\tau}(t); \quad \text{and} \quad \dot{u} = \dot{u}(t)$$

\* Lyakhov G. M. *Osnovy dinamiki vzryva v gruntakh i zhidkikh sredakh* (Fundamentals of Dynamics of Explosion in Soils and Liquid Media), Moscow, Nedra Publishers, 1964.

For *saturated soils* and liquid media, it is sufficient to investigate only two of these parameters, for instance,

$$p = p(t) \quad \text{and} \quad \dot{u} = \dot{u}(t)$$

The parameters of stress waves in soils caused by explosions and the parameters of velocities of their propagation are determined by special field tests. Using the results of such tests, empirical formulae are established for determination of the design parameters of explosion waves in soils depending on the weight of charge, the distance from explosion centre, etc.

When studying dynamic properties of soils, various methods are employed [vibrational, seismic, methods of study at intense actions (explosions, etc.)], depending on the kind of dynamic action.

The principal characteristics of dynamic properties of soils are as follows:

(a) characteristics of elastic and absorbing properties at dynamic loads of a low intensity (below the elastic limit): elastic modulus  $E$ , Poisson's ratio  $\mu$ , coefficient of attenuation of vibrations  $n$ , and also some other equivalent dynamic characteristics, for instance, the speed of propagation and the coefficient of absorption of elastic waves;

(b) generalized coefficients of rigidity of bases at uniform or non-uniform compression (respectively,  $C_z$  and  $C_\psi$ ), uniform and non-uniform shear (respectively,  $C_x$  and  $C_\psi$ ) and the corresponding coefficients of attenuation employed in calculations of vibrations of rigid massive foundations on elastic bases;

(c) characteristics of compressibility of soils at dynamic loads of appreciable intensity (above the elastic limit): stress-strain diagrams ( $p$ - $\epsilon$ ), deformation moduli at loading ( $E_l$ ) and unloading ( $E_{unl}$ );

(d) dynamic characteristics of resistance to form-changing deformations (shear) and of the ultimate state (strength) of soils, and also estimation of their structural stability when passing to a liquefied state.

Modern methods of investigation of dynamic properties of soils have been discussed in detail by N. D. Krasnikov\*.

## 7.2. WAVE PROCESSES IN SOILS UNDER DYNAMIC LOADS

Theoretical studies of wave processes occurring in soils under dynamic loads (due to operation of unbalanced machines, seismic effects, industrial explosions, etc.) are based on investigations of

\* Krasnikov N. D. Dinamicheskie svoistva gruntov i metody ikh opredeleniya (Dynamic Properties of Soils and Methods for Their Determination), Moscow, Stroiizdat, 1970.

*design models*, in which the properties of soils are generalized, with making some or other assumptions in order to describe them mathematically\*.

Models of soils are built on the basis of the generalization of quantitative results of macroscopic experiments on compression and unloading of a soil, determination of wave parameters, residual deformations, etc. Elementary microscopic relations in soil particles are then given a qualitative estimation, but their analysis makes it possible to construct more correct and substantiated models of soils. Dynamically loaded soils are regarded as solid media continuously filling the space.

At present, when investigating wave processes in soils, the following models find the most wide application: a model of an ideally elastic medium (either linear or non-linear); a model of an elastic-plastic medium (Kh. A. Rakhmatulin, S. S. Grigoryan and others); and a model of a visco-plastic medium (G. M. Lyakhov).

**The model of an ideally elastic continuous medium** is the simplest one for investigations of wave processes in soils when regarded as continuous media. This model is employed at low pressures, for instance, at seismic effects (at some distance from the seismic centre), vibrations caused by unbalanced machines, etc., and makes it possible to establish the pattern of wave propagation in soils and the interaction of waves with obstacles.

Wave propagation in an isotropic ideally *elastic medium* can be described by the following differential equations:

$$\left. \begin{aligned} \nabla^2 u - c^2 \frac{\partial^2 u}{dt^2} &= 0 \\ \nabla^2 v - c^2 \frac{\partial^2 v}{dt^2} &= 0 \\ \nabla^2 w - c^2 \frac{\partial^2 w}{dt^2} &= 0 \end{aligned} \right\} \quad (7.2)$$

where  $u$ ,  $v$ , and  $w$  = components of elastic displacements in the directions of the axes  $X$ ,  $Y$ , and  $Z$ , respectively

$$\nabla^2 = \frac{\partial^2}{\partial x^2} + \frac{\partial^2}{\partial y^2} + \frac{\partial^2}{\partial z^2} = \text{Laplacian operator}$$

$c$  = velocity of propagation of elastic waves

It can be shown that the velocity of propagation of *longitudinal elastic waves* is

$$c_1 = \sqrt{\frac{L+2M}{\rho}} \quad (7.3)$$

\* Lyakhov G. M., Polyakova N. I. *Volny v plotnykh sredakh i nagruzki na sooruzheniya* (Waves in Dense Media and Loads on Structures), Moscow, Nedra Publishers, 1967.

where  $L$  and  $M =$  Lamé's constants related to the normal elastic modulus  $E$  and coefficient of lateral elasticity  $\mu$  as follows:

$$L = \frac{\mu}{(1 + \mu)(1 - 2\mu)}$$

$$M = \frac{1}{2(1 + \mu)} \cdot E$$

$\rho = \gamma/g =$  density of medium ( $\gamma$  being the unit weight, and  $g$ , acceleration due to gravity)

The velocity of propagation of *lateral waves* (distortion waves) is determined by the expression:

$$c_2 = \frac{M}{\rho} = \frac{E}{2(1 + \mu)\rho} \quad (7.4)$$

The relationship between  $c_1$  and  $c_2$  is as follows:

$$c_1 = c_2 \sqrt{\frac{2(1 - \mu)}{1 - 2\mu}} \quad (7.3')$$

Expression (7.3') shows that always  $c_1 > c_2$ , i.e., longitudinal waves propagate in a continuous elastic medium with greater velocities than lateral ones. Applying the above relationships to soils and assuming, for instance, that for clays  $\mu = 0.4$ , we can find that longitudinal waves propagate 2.45 times faster than lateral ones, and in sands (with  $\mu = 0.2$ ), approximately 1.63 times faster. Results of direct measurements of propagation rates of vibrations show that for other kinds of soil this ratio is substantially higher (see Table 7.1).

It should be mentioned that longitudinal and lateral waves in *homogeneous elastic media* propagate independent of one another. Both these kinds of waves or only one of them may be formed in a soil, depending on the initial displacement of the medium.

Table 7.1

Velocities of Propagation of Elastic Waves in Soils

Kind of soil	Wave propagation velocity, m/s	
	$c_1$	$c_2$
Moist clay	1500	150
Naturally moist loess	800	260
Dense gravel-sand soil	480	250
Fine-grain sand	300	110
Medium-grain sand	550	160
Medium-size gravel	760	180

Besides longitudinal and lateral waves, of essential importance are the so-called *surface waves* which are formed by sources of vibrations (foundations of unbalanced machines and other exciters) located near the soil surface. With an increase of the distance from the source, surface waves become ever more important compared with longitudinal and lateral waves, since the latter attenuate rather rapidly with an increase of the distance from the source of vibrations and at a certain distance become negligible. The rate of propagation of surface waves,  $c_3$ , is slightly less than that of lateral waves. Thus, with  $\mu = 0.25$ ,  $c_3 = 0.92c_2$  approximately, and with  $\mu = 0.5$ ,  $c_3 \approx 0.95c_2$ . The amplitudes of surface waves at relatively large distances from the source of vibrations can be determined by the following formula\*:

$$A_r = A_0 \sqrt{\frac{r_0}{r}} \cdot e^{-\alpha(r-r_0)} \quad (7.5)$$

where  $A_r$  and  $A_0$  = amplitudes of soil vibration at distances  $r$  and  $r_0$  from the source

$\alpha$  = coefficient of attenuation,  $m^{-1}$  or  $cm^{-1}$

According to the results of experiments carried out by Ya. N. Smolyakov, the following values of the attenuation coefficient  $\alpha$  can be used for practical calculations of various soils:

Fine-grain sands, sand loams and loams saturated with water	$\alpha = 0.03-0.04 \text{ m}^{-1}$
Medium- and coarse-grain sands (of any moisture content); moist clays and loams	$\alpha = 0.04-0.06 \text{ m}^{-1}$
Loams and sand loams (dry or weakly moist)	$\alpha = 0.06-0.10 \text{ m}^{-1}$

Of essential importance are results of experimental studies of variations of amplitudes of surface waves with depth. Thus, it has been found that at small depths, not exceeding 0.2-0.3 of the wavelength, the amplitudes of vibrations attenuate relatively insignificantly.

The pattern of attenuation of surface waves with depth may be seen in Fig. 123 (according to D. D. Barkan), which has been plotted on the data of measurement of vertical vibrations caused by operation of a pile driver. It should be noted that in the direct vicinity of the foundation (source of waves) the pattern of variation of amplitudes with depth will be somewhat different (Fig. 123b).

As can be concluded from the figure, a foundation for a machine should not be laid deeper than neighbouring foundations of buildings; often it is more rational that the depth of foundation for machines be smaller than that for buildings (as has been shown by Smolyakov's experiments).

\* Barkan D. D. *Dinamika osnovanii i fundamentov* (Dynamics of Bases and Foundations), Moscow, Stroiizdat, 1948.

Certain problems of the dynamics of disperse soils are principally unsolvable within the frames of the model of an elastic medium.

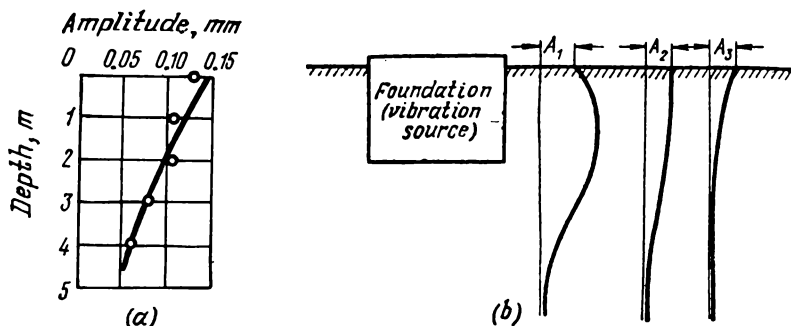


Fig. 123. Variations of amplitudes of soil oscillation (a) under foundation; (b) at various distances from foundation

Thus, for instance, it follows from the solution of the problem of propagation of a plane wave that there is no attenuation and variation of the wave profile with distance, which contradicts experimental data.

The model of non-linear elastic medium is more complicated, where the relationship between stresses and deformations is non-linear but the same both for increasing and decreasing loads. Such a model explains well the attenuation of plane waves with distance and the dependence of the reflection coefficient on stress. However, it does not follow from this model that there are residual deformations and that an impact wave is transformed into a continuous compression wave, as is observed experimentally. The model of a non-linear elastic medium can be successfully applied to water-saturated soils, since in that case it is in good conformity with experimental data.

Wave processes in unsaturated soils are described more reliably by models of elasto-plastic media, rather than by those of ideally elastic ones. With low loads, elasto-plastic media may be regarded as elastic ones, and with high loads, as plastic. With low loads, the curve for  $p(\epsilon)$  (Fig. 124) is concave, and with high loads, convex toward the

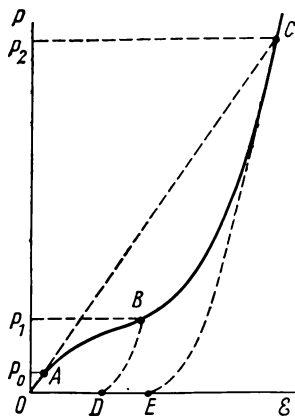


Fig. 124. Dynamic diagram of soil compression by the model of elastic-plastic medium

$OABC$ —line of loading;  $BD$ ,  $CE$ —lines of unloading

axis of deformations. The curve of unloading of the medium, i.e., the relationship  $p(\epsilon)$  corresponding to a decrease of stress, does not coincide with the curve of loading, which is responsible for the appearance of residual deformations (loading curves are shown by dotted lines  $BD$  and  $CE$  in Fig. 124). With  $p > p_2$ , a wave in a soil is an impact wave; with  $p < p_2$  it decomposes into an elastic and a plastic wave. The elastic wave propagates with a greater speed than a plastic one. The plastic wave attenuates in the course of its propagation and becomes an elastic one.

By using the model of an elasto-plastic medium, it is possible to explain a number of properties of wave processes in soils. On the other hand, some experimental data (for instance, decomposition of an impact front while moving away from the source of excitation, a greater magnitude of residual deformations than at the maximum stress, etc.) do not agree with this model. Notwithstanding these drawbacks, the model of an elasto-plastic medium is now widely used for solving wave problems in soils. Solutions by this model have been obtained by Kh. A. Rakhmatulin, S. S. Grigoryan, G. M. Lyakhov, A. Ya. Sagomonyan, and others; more complicated problems, for instance, on propagation of a spherical wave from an explosive charge, being solved by means of electronic computers, and simpler ones, analytically.

The most generalized *model of an elasto-plastic medium* is that proposed by S. S. Grigoryan, which makes it possible to describe arbitrary motions of the soil under the action of dynamic loads. It is assumed in the model that the diagram of dynamic compression is independent of the rate of deformation, and the ratio between the average normal stress and density is different for the regions of elastic and plastic deformations.

In the diagram of dynamic compression, the load branch is of double curvature: up to the point of inflection  $B$  it is convex toward the axis of pressures, and at higher pressures, toward the axis of relative deformations  $\epsilon$  (see Fig. 124). With low pressures, the compression diagram may have an initial linearly-elastic section (section  $OA$ ), while at very high pressures ( $p > p_\infty$ ) the volume compression is significant (the porosity may drop to very low values), so that all volume deformation on loading and unloading will occur reversibly.

It has been shown\* that waves of various kinds may be observed in the media considered with an instantaneous loading at various distances from the source of excitation:

- (1) *impact waves* (at pressures  $p > p_2$ , see Fig. 124);
- (2) *combined waves* (at  $p_1 < p < p_2$ );

\* Krasnikov N. A. *Dinamicheskie svoistva gruntov i metody ikh opredeleniya* (Dynamic Properties of Soils and Methods for Their Determination), Moscow, Stroizdat, 1970.

(3) *compression waves* (at substantial distances from the source of excitation);

(4) purely *elastic waves* (at  $p < p_0$ , see Fig. 124).

Experiments show, however, that the dynamic diagram of compression in many cases depends also on the rate of deformation, which is not taken into account by the model of an elasto-plastic medium.

The *model of visco-plastic medium* proposed by G. M. Lyakhov\* assumes that there exist two extreme compression curves corresponding to impact loading ( $\dot{\epsilon} \rightarrow \infty$ ) and static loading ( $\dot{\epsilon} \rightarrow 0$ ), all diagrams relating to intermediate values of the rate of deformation being located between these two curves (Fig. 125).

Impact compression involves deformations connected with compression of water films, salt films and projections of individual grains; they are partially irrecoverable. Deformations connected with displacement of grains occur in a finite time; they are fully irrecoverable. With such assumptions, the form of an unloading curve, i.e.,  $p(\epsilon)$ , at reduction of stresses depends not only on soil properties, but also on the time of action of the load that forms a wave. Thus, there exists no general diagram  $p(\epsilon)$  that would be defined only by soil properties. Different diagrams  $p(\epsilon)$  have been obtained for different loading conditions.

The model being considered also allows the possibility of deformation rise during the period of load decrease, which has been observed in experiments and cannot be obtained by the model of elasto-plastic medium.

Computer calculations have shown that a plane impact wave in a viscous medium may change into a continuous compression wave at a certain distance from the source, the maximum deformation being attained at the moment when the stress begins to decrease or a bit later.

Application of the model of visco-plastic medium entails great difficulties. Some problems may be solved satisfactorily by using simpler models, so that the use of the viscous model does not exclude application of other models.

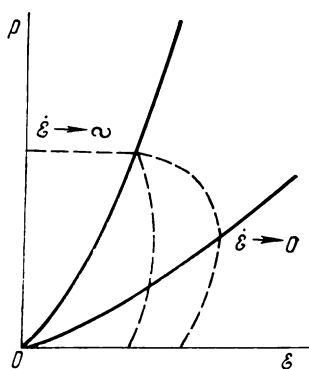


Fig. 125. Ultimate diagram of dynamic compression of soil by the model of visco-plastic medium at different rates of loading, from impact loading ( $\dot{\epsilon} \rightarrow \infty$ ) to static loading ( $\dot{\epsilon} \rightarrow 0$ )

\* Lyakhov G. M., Polyakova N. I. *Volny v plotnykh sredakh i nagruzki na sooruzheniya* (Waves in Dense Media and Loads on Structures), Moscow, Nedra Publishers, 1967.

The solution of wave problems is based on integrating the principal equations of motion of a continuous medium, which follow from the laws of conservation of mass and momentum

$$\left. \begin{aligned} \frac{\partial \rho}{\partial t} + \dot{u} \frac{\partial \rho}{\partial x} + \rho \frac{\partial \dot{u}}{\partial x} + v \frac{\dot{u} \rho}{x} &= 0 \\ \rho \left( \frac{\partial \dot{u}}{\partial t} + \dot{u} \frac{\partial \sigma}{\partial x} \right) - \frac{\partial \sigma_1}{\partial x} - v \frac{\sigma_1 - \sigma_2}{x} &= 0 \end{aligned} \right\} \quad (7.6)$$

where  $x$  and  $t$  = space and time coordinates

$\rho$  = density of soil

$\dot{u}$  = velocity of particles

$\sigma_1, \sigma_2$  = components of stress in the directions parallel and normal to that of wave propagation

For cases of plane, cylindrical and spherical motion,  $v$  is respectively equal to 0, 1, and 2.

For a plane motion, the system is closed by a single equation relating  $\sigma_1$  with  $\epsilon$ . This equation follows from the model of the medium and has different forms for viscous and elasto-plastic media. With spherical symmetry, an additional equation is used, which defines the relationship between principal stresses,  $f(\sigma_1, \sigma_2) = 0$ . In addition, boundary conditions must be specified. They are determined by the nature of the problem proper and may be a specified load in the initial section, the relationship at the impact wave front, the condition of free surface, etc.

*Wave processes in water-saturated soils*, i.e., those whose voids are filled with water and a small amount of entrapped air, may be described under an assumption that the compressibility of the skeleton exceeds that of the soil as a three-component medium (solid particles, water, and air), and further, that each of the components is compressed by the load as in a free state. According to G. M. Lyakhov, the equation of soil compressibility will then have the form

$$\frac{\rho}{\rho_0} = \alpha_1 \left( \frac{p}{p_0} \right)^{-\frac{1}{k_1}} + \alpha_2 \left[ \frac{pk_2}{\rho_2 c_2^2} + 1 \right]^{-\frac{1}{k_2}} + \alpha_3 \left[ \frac{pk_3}{\rho_3 c_3^2} + 1 \right]^{-\frac{1}{k_3}} \quad (7.7)$$

with

$$\rho = \alpha_1 \rho_1 + \alpha_2 \rho_2 + \alpha_3 \rho_3; \quad \alpha_1 + \alpha_2 + \alpha_3 = 1$$

where  $\alpha_1, \alpha_2, \alpha_3$  = volume content of gaseous, liquid and solid components respectively in unit volume of soil at the initial pressure  $p_0$

$\rho_0, \rho_1, \rho_2, \rho_3$  = densities of the medium and its components at the initial pressure

$c_1, c_2, c_3$  = sound velocities in components at the initial pressure

$k_1, k_2, k_3$  = exponents of isentropes of the components

Numerical values of the constants are:  $c_1 = 330$  m/s;  $c_2 = 1500$  m/s;  $c_3 = 4500$  m/s;  $\rho_2 = 1$  g/cm<sup>3</sup>;  $\rho_3 = 2.65$  g/cm<sup>3</sup>; and it can be approximately taken that  $k_1 = 1.4$ ,  $k_2 = 7$ , and  $k_3 = 4$ .

The rate of propagation of sound waves,  $c_0$ , in the soil at the initial pressure will then be determined by the equation

$$\frac{1}{\rho_0 c_0^2} = \frac{1}{\rho_1 c_1^2} + \frac{1}{\rho_2 c_2^2} + \frac{1}{\rho_3 c_3^2} \quad (7.8)$$

Calculations show that the sound velocity in a saturated soil appreciably depends on the content of entrapped air. With  $\alpha_1 = 0$ , it is 1550-1650 m/s, and with  $\alpha_1 = 0.01-0.03$  it falls down to approximately 100 m/s.

The solution of wave problems reduces to integrating the principal equations of motion, which are closed in the case considered by the equation of compressibility of saturated soil given above.

### 7.3. CHANGES IN THE PROPERTIES OF SOILS SUBJECT TO DYNAMIC EFFECTS

Dynamic effects, both *weak*, appearing through motions of unbalanced parts of machines (vibrations, oscillations, etc.), and *strong*—short-duration, single, and multiple (impacts, strong impulses, explosions, etc.) may have an appreciable influence on the properties of cohesionless (loose) soils, and, in a lesser extent, on those of cohesive soils (clays).

Vibrations cause a reduction of the friction between soil particles and total reduction of their shear resistance (which impairs the load-carrying capacity of soils); impulse effects of medium magnitude (at accelerations below those due to gravity) cause settlements of structures, and strong impulses, destruction of the structure of soils and loss of their stability.

**Reduction of shear resistance at vibrations in soils.** This is the main factor affecting the strength properties of soils.

Prof. G. I. Pokrovsky found as far back as the 30-s that the coefficient of internal friction of soils depends on the energy of vibrations, decreasing with an increase of the latter and tending to a definite limit. For cohesive soils, the effect of vibrations on shear resistance will be the less, the greater the soil cohesion.

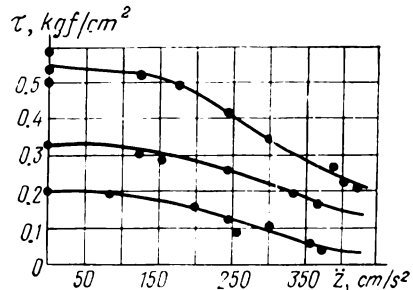


Fig. 126. Experimental curves of relation between shear resistance of differently loaded soil samples and acceleration of vibrations

According to the results of experiments carried out by V. A. Ershov and Se-Din-I (1962), the shear resistance of sandy soils gradually reduces at vibrations (Fig. 126) which can be described by the following equation:

$$\tau = \tau_0 e^{-\kappa(\ddot{z} - \ddot{z}_0)} \quad (7.9)$$

where  $\tau$  = shear resistance when  $\ddot{z} \geq \ddot{z}_0$  ( $\ddot{z}$  being the acceleration of vibrations at the given exciting force, and  $\ddot{z}_0$ , the initial acceleration, below which no variations of shear resistance occur)

$\tau_0$  = shear resistance at static loads

$\kappa$  = constant coefficient equal to 0.003 s<sup>2</sup>/cm for fine-grain sand and 0.0025 s<sup>2</sup>/cm for medium-grain sands

On the basis of experiments it has been also established that the initial acceleration  $\ddot{z}_0$  linearly depends on the external pressure on the soil until vibrations do not overcome the structural bonds at contact points of soil particles and the soil shear resistance is not reduced.

With a definite frequency of vibrations, the soil friction (especially in cohesionless soils) may decline so that the soil acquires the properties of a *viscous liquid* (vibroviscosity) with an internal friction close to zero and a negligible load-carrying capacity.

This specific effect of vibrations on soils (especially on loose soils) has been used for development of the *vibrational method* of rapid driving of sheet piles, piles, shell supports, etc. into cohesionless soils to a depth of a few tens of meters\*. The rate of driving structures into the soil by this method depends on the frequency of vibrations used, the magnitude of exciting forces, and the *vibroviscosity* of the soils.

The soil vibroviscosity may be characterized by a certain coefficient of vibroviscosity, which is different for various soils and depends on the relative acceleration of vibrations; this can be described by the following relationship:

$$vn^k = b \quad (7.10)$$

where  $v$  = coefficient of vibroviscosity, kgf·s/cm<sup>2</sup>

$n$  = ratio between the acceleration of vibrations and that due to gravity

$k, b$  = empirical coefficients

Barkan's experiments have shown that the coefficient of vibroviscosity depends on the physical state of the soil and especially on its moisture content.

\* Barkan D. D. Vibrometod v stroitelstve (Vibrational Method in Construction), Stroiizdat, 1959.

A diagram of relation between the coefficient of vibroviscosity and the moisture content for fine-grain sand is given in Fig. 127. As can be seen, the lowest coefficient of vibroviscosity is observed in dry and fully saturated sands and the maximum vibroviscosity is attained at a definite moisture content.

Similar results have been obtained for weak clayey soils, and also for loams and sandy loams.

These data show that driving of sheet piles, piles, and similar structures can be done most successfully in dry or water-saturated sands. Industrial tests indicate that the rate of driving piles into soil by means of high-frequency vibrators (especially with a spring-biased weight) can reach several metres per minute.

Figure 128 shows, by way of an example, the diagram of vibrodri-ving of a metal pile into sand soils to a depth of approximately 13 m, which required less than 6 minutes. It should be noted that the vibrational method has found wide application in construction of foundations, in drilling for taking soil samples, and in other cases when tubular structures are to be driven into the soil.

**Vibrocompaction.** Under the action of vibrations, loose soils, especially those having no cohesion, can settle substantially, which is determined by the variation of their porosity in the course of vibrating. According to D. D. Barkan, vibrations from operation of a forging hammer at one of works (with the weight of the falling hammer of 4.5 tons) caused substantial soil settlement in the base of a neighbouring brick building disposed at a distance of 6 m from the hammer foundation so that the building was gradually destroyed. Settlements of foundation bases near operating machines may sometimes attain several decimetres, which results in inadmissible deformations of buildings.

As has been found by respective studies, the soil void ratio (whose variations cause settlements of bases) and the acceleration of vibrations are linked by a relationship which is similar to compression relationship and is termed the *vibro-compressional curve* of soils (Fig. 129).

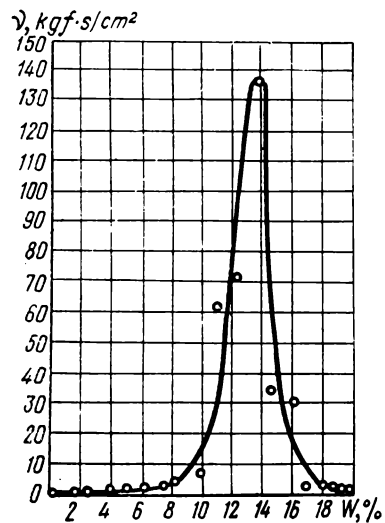


Fig. 127. Relation between the coefficient of sand vibroviscosity and moisture content

As can be seen from the figure, an increase of the relative acceleration  $n$  (the ratio of vibration acceleration to acceleration due to gravity) causes the void ratio of a sand soil to decrease by a curvilinear relationship, with the experimental points obtained at different frequencies  $N$  of vibrations coinciding well with the curve.

Some results of similar studies (O. A. Savinov et al.) of vibro-compaction of soils in samples not subject to external loads, and also in those loaded with different external pressures  $p$ ,  $\text{kgf/cm}^2$ , are shown in Fig. 130.

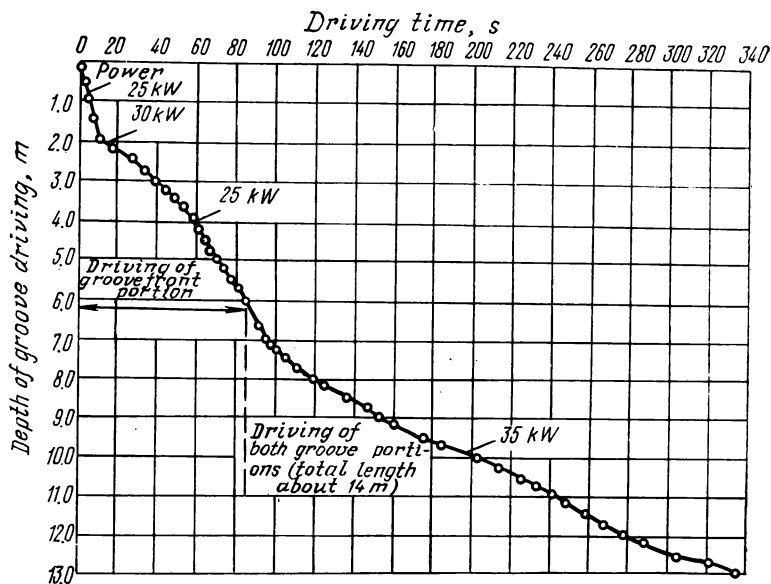


Fig. 128. Diagram of vibrodriving of a metal groove into soil

The results of the vibro-compaction tests of soils suggest the following conclusions:

1. With no external load ( $p = 0$ ), compaction of loose soils begins at any weak vibration and always results in a compaction close to complete ( $I_d \approx 1$ ), this compaction being attained at an acceleration of vibrations of from 0.2 g to 1.2 g for dry sands, from 0.5 g to 2 g for saturated sands, and at 2 g for moist sands.

2. With an external load ( $p \neq 0$ ), no compaction practically occurs up to a definite critical acceleration  $\ddot{z}_{cr}$ ; at higher accelerations (above 0.2-0.4 g for sands), vibro-compaction occurs, which with further increase of acceleration is stabilized at a definite porosity  $e_{dyn}$  or dynamic compaction  $I_{dyn}$ . The last quantity is determined

by the expression

$$I_{dyn} = \frac{e_{dyn} - e_{min}}{e_{max} - e_{min}} \tag{7.11}$$

where  $e_{dyn}$  = void ratio (dynamic) which corresponds to the vibro-compaction of the given soil at the given supercharging

$e_{max}$ ,  $e_{min}$  = maximum and minimum values of the void ratio in the densest and the loosest states of sand (see Sec. 1.4) without supercharging

Dynamic compaction of sand soils at vibrations has been found to have the following values\*:

Coarse-grain sands . . . . .	$I_{dyn}=0.55-0.80$
Medium-grain sands . . . . .	$I_{dyn}=0.58-0.60$
Fine-grain sands . . . . .	$I_{dyn}=0.80-0.82$
Slag . . . . .	$I_{dyn}=0.40-0.50$

Experiments show that if the natural density of sand soils is such that the inequality  $I_d \leq I_{dyn}$  holds true, then vibrational effects will cause settlements of foundations (see Sec. 7.4).

Impulse effects and repeated short-term loads can form stress waves that may appreciably change the soil properties.

Special tests on uniaxial and three-axial compression and shear (A. Casagrande, H. Seed et al. in the USA) have shown that the dynamic strength of clayey soils  $R_{dyn}$  (with time of loading of 0.02 s) is substantially greater than the static strength  $R_{st}$ , with  $R_{dyn} \approx 2R_{st}$  for relatively weak clays and  $R_{dyn} \approx 1.5R_{st}$  for dense clays. The shear resistance of clayey soils under conditions of a closed system also increases with an increase of the rate of loading by a factor of 1.5-2.5 compared with the shear resistance at static loads.

By comparing the strength of soils at short-term (but not destructive) impulses with that at long-term vibrations, it may be concluded that these two kinds of dynamic actions affect the mechanical pro-

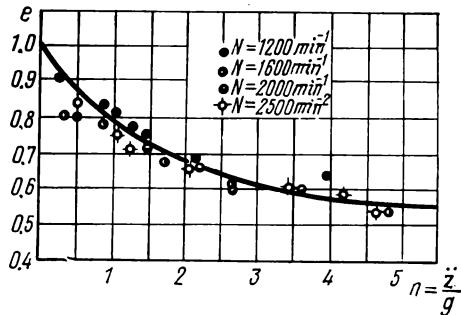


Fig. 129. Dependence of void ratio of sand,  $e$ , on the ratio of vibrations to the acceleration due to gravity,  $n$

\* Savinov O. A. *Sovremennye konstruktsii fundamentov pod mashiny i ikh raschet* (Modern Designs of Machine Foundations and Their Calculation), Moscow, Stroiizdat, 1964, Chapter 4.

properties of soils in opposite ways: the resistance of soils at imp. is substantially greater than their resistance at long-term vibrat.

197

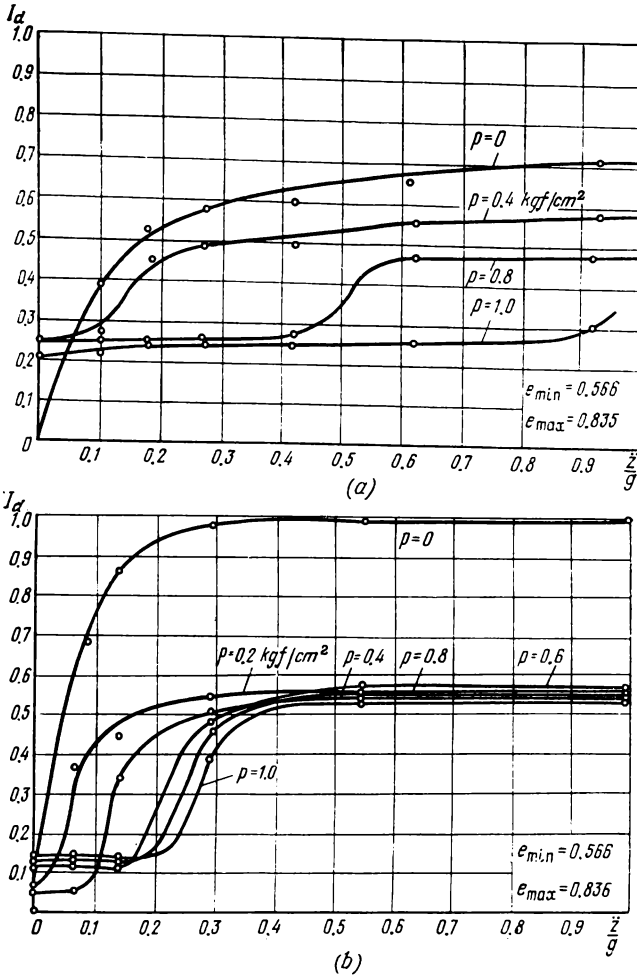


Fig. 130. Curves of dynamic compaction of sand samples with different external loads  $p$ ,  $\text{kgf/cm}^2$

(a) dry medium-grain sand; (b) saturated medium-grain sand

Experiments have also been carried out\* with soil samples subjected to repeated (up to 100 times) action of short impulses (imitating seismic effects), which show that the maximum destructive load

\* Seed H. Soil Strength during Earthquake. Proc. 2nd World Conf. Earthquake Eng., Tokyo, Vol. 1, 1960.

soils is less than the static load and, in addition, that soil deformations increase up to 11 per cent, i.e., almost to half the destructive relative deformation, which has been taken equal to 20-25 per cent.

As has been shown by S. S. Grigoryan et al., the peculiarities of *action of explosions in soils* and of propagation of explosion waves can be analyzed qualitatively by using a dynamic compression diagram (see Fig. 124).

These problems are, however, special problems in soil dynamics and are beyond the scope of this book.

#### 7.4. THE PRINCIPAL PREREQUISITES FOR TAKING THE DYNAMIC PROPERTIES OF SOILS INTO ACCOUNT IN VIBRATIONAL CALCULATIONS OF FOUNDATIONS

**The principal prerequisites for calculation.** According to the USSR standard BC&R, in dynamic calculations of machine foundations the effect of inertia of a soil may be neglected and the foundation may be regarded as a *linearly deformable ideally elastic* body.

The theory of calculation based on these assumptions has been proposed by N. P. Pavlyuk\* and further developed by D. D. Barkan, O. A. Savinov and others.

According to this theory, the resistance of a foundation to vertical displacements, shearing, and rotation can be characterized by the coefficients of rigidity of an elastic base, uniform and non-uniform compression  $C_z$ ,  $C_x$ , and shear  $C_\varphi$  and  $C_\psi$ , which are determined by the expressions

$$\left. \begin{aligned} R_z &= C_z F z \\ R_x &= C_x F x \\ M_\varphi &= C_\varphi I \varphi \\ M_\psi &= C_\psi I_z \psi \end{aligned} \right\} \quad (7.12)$$

where  $R_z$  and  $R_x$  = respectively the vertical and horizontal components of the resultant reaction force of an elastic base

$M_\varphi$  and  $M_\psi$  = moments of reaction couples acting respectively in one of the main vertical planes of the system and in the plane of the base

$z$  and  $x$  = vertical and horizontal displacements of the centre of gravity of the base area

---

\* Pavlyuk N. P. O kolebaniyakh tverdogo tela, opirayushchegosya na uprugoe osnovanie (On Oscillations of a Solid Body Supported by an Elastic Base). In a collection of papers: Vibratsii fundamentov (Vibrations of Foundations), Moscow, ONTI, 1933.

$\varphi$  and  $\psi$  = angles of rotation of the foundation in one of the main vertical planes of the foundation and in the base plane

$F$  = area of the foundation base

$I, I_z$  = moments of inertia of this area relative to the main axes of possible rotation of the foundation

The coefficients  $C_z, C_x, C_\varphi$  and  $C_\psi$  depend not only on the elastic properties of a soil, but also on a number of other factors, including the size and shape of foundation base, the structure of base, etc. Because of this, these coefficients must be regarded as certain generalized characteristics of a base.

As far back as the 30-s, an attempt was made to establish the relationships between the coefficients  $C_z, C_x, C_\varphi, C_\psi$  and the area of a foundation base by comparing the solutions obtained by the theory of total deformations and that of local elastic deformations (see Sec. 5.2).

As a result, formulae have been obtained, according to which the coefficients of rigidity  $C_z, C_x$ , and  $C_\varphi$  of a base are inversely proportional to the square root from the base area.

Comparison of the relationships obtained with the results of direct tests made by some researchers has shown, however, that these relationships are close to the actual ones only in the general nature, but, with an increase of the area of a foundation base, tend not to zero, but to a certain limit value other than zero.

More reliable relationships between the rigidity coefficients of a base and the area of foundation base have been obtained by O. A. Savinov who considered the problem of equilibrium of a massive (rigid) stamp on a local elastic (Winckler's) base with a uniformly stretched membrane being applied to the base, which ensures uniform distribution of an external load over the soil surface (according to Filonenko-Borodich's model of an elastic base).

In the final form these relationships are as follows:

$$\left. \begin{aligned} C_z &= C_0 \left[ 1 + \frac{2(l+b)}{\Delta_1 F} \right] \sqrt{\frac{p}{p_0}} \\ C_x &= 0.7 C_0 \left[ 1 + \frac{2(l+b)}{\Delta_1 F} \right] \sqrt{\frac{p}{p_0}} \\ C_\varphi &= C_0 \left[ 1 + \frac{2(l+3b)}{\Delta_1 F} \right] \sqrt{\frac{p}{p_0}} \end{aligned} \right\} \quad (7.13)$$

As regards the coefficient of elastic non-uniform shear (rotation)  $C_\psi$ , it can be taken, according to D. D. Barkan and on the basis of experimental data, to be approximately equal to

$$C_\psi \approx 1.5 C_x \quad (7.14)$$

The notation in formulae (7.13) and (7.14) is as follows:

$C_0$  = elastic constant of the base, which is independent of the size of foundation

$l$  and  $b$  = respectively the length and width of the base of a rectangular foundation

$p$  = pressure transmitted from foundation to base

$p_0$  = pressure under a test stamp for determining the coefficient  $C_0$

$\Delta_1$  = constant dimensional coefficient equal to  $1 \text{ m}^{-1}$

Numerical values of the coefficient  $C_0$  corresponding to the test stamp pressure  $p_0 = 0.2 \text{ kgf/cm}^2$  are:

For liquid-plastic clays and loams (consistency index $I_L = B > 0.75$ ) . . . . .	0.6-0.7 kgf/cm <sup>3</sup>
Same, of soft-plastic consistency ( $0.5 < I_L < 0.75$ ) . . . . .	0.8 kgf/cm <sup>3</sup>
For plastic sand loams ( $0.5 < I_L < 1$ ) . . . . .	1.0 kgf/cm <sup>3</sup>
For saturated loose sands ( $e > 0.80$ ) . . . . .	1.2 kgf/cm <sup>3</sup>
For stiff-plastic clays and loams ( $0.25 < I_L < 0.5$ ) . . . . .	2.0 kgf/cm <sup>3</sup>
For plastic sand loams ( $0 < I_L < 0.5$ ) . . . . .	1.6 kgf/cm <sup>3</sup>
For medium-dense dusty sands ( $e \leq 0.8$ ) . . . . .	1.4 kgf/cm <sup>3</sup>
For sands, irrespective of their moisture content and density . . . . .	1.8 kgf/cm <sup>3</sup>
For hard clays and loams ( $I_L = B < 0$ ) . . . . .	3.0 kgf/cm <sup>3</sup>
For hard sandy loams ( $I_L < 0$ ) . . . . .	2.2 kgf/cm <sup>3</sup>
For gravels, etc. . . . .	2.6 kgf/cm <sup>3</sup>

In some cases experimental determinations of the rigidity coefficients of an elastic base are made by testing the foundations built earlier in similar conditions or by using a special standard stamp.

Knowing the rigidity coefficients of a base, it is possible to use the formulae for vibrational calculations of massive foundations. If we neglect the effect of elasticity of the foundation material, i.e., regard it as a solid body, and consider the case when one of the principal axes of inertia of the body is vertical and passes through the centre of gravity of the base area, and two other axes are horizontal and parallel to the principal axes of this area (Fig. 134), then the differential equations of vibrations of this system can be written as follows:

$$\left. \begin{aligned} m\ddot{z} + K_z z &= P(z, t) \\ m\ddot{x} + K_x x - K_x h_0 \varphi &= P(x, t) \\ \Theta_0 \ddot{\varphi} + (K_\varphi + K_x h_0^2 - Qh_0) \varphi - K_x h_0 x &= M(\varphi, t) \\ \Theta_\psi \ddot{\psi} + K_\psi \psi &= M(\psi, t) \end{aligned} \right\} (7.15)$$

where  $m$  = mass of foundation

$z, x, \varphi,$  and  $\psi$  = corresponding displacements and angles of rotation of the centre of gravity of the foundation at the given instant of time

$\ddot{z}$ ,  $\ddot{x}$ ,  $\ddot{\varphi}$ , and  $\ddot{\psi}$  = second derivatives of the corresponding displacements and angles of rotation in time

$$K_z = C_z F; \quad K_x = C_x F; \quad K_\varphi = C_\varphi I; \quad \text{and} \quad K_\psi = C_\psi I_z^{-1}$$

$Q$  = weight of foundation and machine

$\Theta_0$ ,  $\Theta_\psi$  = moments of inertia of the foundation relative to one of the principal horizontal axes  $O_1X$  and the vertical axis  $OZ$

$h_0$  = distance from the base to the centre of gravity of foundation

$P(z, t)$ ,  $P(x, t)$  = components of the resultant of exciting forces acting on the foundation

$M(\varphi, t)$ ,  $M(\psi, t)$  = moments of these forces relative to the axes  $OY$  and  $OZ$

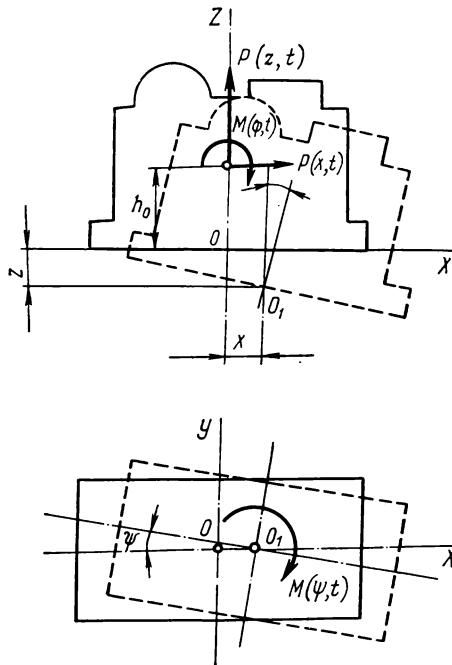


Fig. 131. Diagram of external actions for vibrational calculations of foundations

By solving equations (7.15), it is possible to determine the amplitudes of vibrations of a foundation from the action of a dynamic load of any kind.

For machine foundations being calculated by the acting standards, the following condition must be satisfied:

$$\max A < A_{al} \quad (7.16)$$

where  $A$  = maximum amplitude of vibrations of the foundation determined by calculation

$A_{al}$  = allowable amplitude of vibrations

Values of  $A_{al}$  for calculation of foundations for machines of various kinds are given in Table 7.2.

Table 7.2

Allowable Amplitudes of Vibrations of Foundations,  $A_{al}$ 

Type of machine	Rotational speed, rpm	$A_{al}$ , mm
Machines with rotating parts (motor-generators, etc.)	$> 750$	0.10
	750-500	0.15
	$< 500$	0.20
Machines with reciprocating (crankshaft) mechanisms (piston compressors, log frames, etc.)	600	0.10/0.05
	600-400	0.10-0.15/0.07
	400-200	0.15-0.25/0.10
	$< 200$	0.25 (0.3) *, 0.15
Forging hammers: (a) on saturated sands (b) on other kinds of soil	—	0.8
	—	1.2
Foundations of foundry moulding machines	—	0.5

Notes: 1. For crankshaft machines, numbers in denominators are second-harmonic amplitudes.

2. Asterisk relates to foundations higher than 5 m.

Equations (7.15) can be used for calculations of *seismic vibrations of massive structures* (for instance, gravity dams). In this case, the exciting loads  $P(z, t)$ ,  $P(x, t)$ ,  $M(\varphi, t)$ , and  $M(\psi, t)$  in the right-hand part are to be replaced with calculated inertial loads respectively  $m\ddot{z}$ ,  $m\ddot{x}$ ,  $\Theta_0\ddot{\varphi}$ ,  $\Theta_\psi\ddot{\psi}$ , where  $z_0$ ,  $x_0$ ,  $\varphi$ , and  $\psi$  are the given displacements of the structure base.

The approximate method for vibrational calculations of foundations described above is now widely employed in design practice. On the other hand, research is being made both in the USSR and other countries on a more accurate approach to the problem, which would take into account the effect of soil inertia on vibrations of

foundations; among the published works on the subject are those of O. Ya. Schechter and N. M. Borodachev and others.

In addition to direct calculations of foundations for vibrations under the action of a vibrational load according to what has been discussed above (see the previous section), it is required to determine the *settlement of the base*, and, in cases of saturated sand soils, the *conditions of their vibrational liquefaction*.

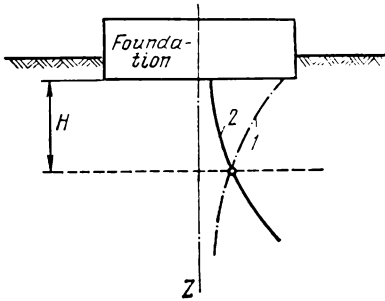


Fig. 132. Determination of the depth of vibro-compaction zone  $H$

1—curve of variation of acceleration  $\ddot{z}$  from a source of vibrations; 2—curve of critical accelerations of soil  $\ddot{z}_{cr}$

sed in the considered soil layer by an external load and the soil dead weight.

The acceleration  $\ddot{z}_{cr}$  is found from curves of vibro-compaction  $I_d = f(\ddot{z}/g)$  as the one corresponding to the beginning of an intense compaction of the soil due to vibrations.

It is further assumed that vibrational accelerations in a non-saturated soil, which are caused by vibrations of the foundations, decrease with an increase of depth by the relationship

$$\ddot{z} = \ddot{z}_0 e^{-\beta z} \quad (7.17)$$

where  $\ddot{z}_0$  = acceleration at the level of foundation base

$\beta$  = attenuation coefficient, equal to 0.07-0.10  $m^{-1}$  for sandy soils

$z$  = depth below the foundation base

By plotting a curve of variation of the effective acceleration according to the experimental data, and a curve of critical accelerations  $\ddot{z}$  [from equation (7.17)], we can find (according to O. A. Savinov) the point of intersection of these curves; the depth at which this point is located is taken as the thickness  $H$  of the layer being compacted (Fig. 132).

Assuming that the soil can be compacted by vibrations to the void ratio  $e_{dyn}$  and knowing this ratio, the settlement is found by using

formula (5.8), i.e.,

$$s_{\max} = \sum_1 h_i \frac{e_0 - e_{dyn}}{1 + e_0} \quad (7.18)$$

Here, the summation sign applies to all soil layers  $h_i$  from the base of the source of vibrations to the depth  $H$  corresponding to the thickness of the massif being compacted (Fig. 132).

**Conditions of liquefaction of saturated sand soils at vibrations** were studied in detail by N. M. Gersevanov\* and P. L. Ivanov\*\*. It has been found that water-saturated fine-grain sands and dusty sands having a loose structure are most liable to liquefaction.

The main condition for preventing liquefaction of soils is the absence of sign-variable stresses in the soil mass.

For cases of a continuous uniformly distributed load (dead weight of soil), acting both permanently ( $p$ ) and periodically or instantaneously ( $p_t$ ), the *simplest condition of no liquefaction of soil* (neglecting the compaction of the soil by a constant load) is the following inequality:

$$\gamma' h_f (2\xi\pi + 1) - (p - p_t) \geq 0 \quad (7.19)$$

where  $\gamma'$  = unit weight of soil (with account of the lifting action of water)

$h_f$  = foundation depth

$\xi$  = coefficient of lateral pressure on soil

\* Gersevanov N. M. *Osnovy dinamiki gruntovoi massy* (Fundamentals of Dynamics of Soil Mass), Moscow, ONTI, 1937.

\*\* Ivanov P. L. *Razzhizhenie peschanykh gruntov* (Liquefaction of Sandy Soils), Moscow, Gosenergoizdat, 1962.

LIST OF BOOKS RECOMMENDED FOR AN EXTENDED STUDY  
OF SOIL MECHANICS

1. Boussinesq J., Application des potentiels a l'étude de l'équilibre et du mouvement des solides élastiques. Paris, 1885.
2. Caquot A., Kerisel J., Traité de mécanique des sols. Paris, 1956.
3. Florin V. A., Osnovy mekhaniki gruntov (Fundamentals of Soil Mechanics), vols. 1 and 2. Moscow, Stroiizdat, 1959-61.
4. Gersevanov N. M., Sobranie sochinenii (Collected Works), vols. 1 and 2. Leningrad, Stroivoenmorizdat, 1948.
5. Goldstein M. N., Mekhanicheskie svoistva gruntov (Mechanical Properties of Soil). Moscow, Stroiizdat, 1971, 1973.
6. Harr M., Fundamentals of Theoretical Soil Mechanics. New York, McGraw-Hill, 1966.
7. Leonards G. et al., Foundation Engineering. Ed. by G. Leonards. New York, McGraw-Hill, 1962.
8. Lambe T. W., Whitman R. V., Soil Mechanics. New York, Wiley, 1969.
9. Maslov N. N., Osnovy mekhaniki gruntov i inzhenernoi geologii (Fundamentals of Soil Mechanics and Engineering Geology). Moscow, Vysshaya Shkola Publishers, 1968.
10. Sokolovsky V. V., Statika sypuchikh tel (Statics of Loose Bodies). 1942.
11. Suklje L., Rheological Aspects of Soil Mechanics. New York, McGraw-Hill, 1944.
12. Terzaghi K., Theoretical Soil Mechanics. New York, McGraw-Hill, 1948.
13. Terzaghi K., Peck P., Soil Mechanics in Engineering Practice. New York, 1948.
14. Tsytoovich N. A., Mekhanika gruntov (Soil Mechanics). 4th ed. Moscow, Stroiizdat, 1963.
15. Tsytoovich N. A., Zaretsky Yu. K. et al., Prognoz skorosti osadok osnovanii sooruzhenii (Prediction of Settlement Rates of Structure Bases). Moscow, Stroiizdat, 1967.
16. Tsytoovich N. A., Mekhanika merzlykh gruntov (Mechanics of Frozen Soils (general and applied)). Vysshaya Shkola Publishers, 1973. English translation published in 1975: N. A. Tsytoovich. The Mechanics of Frozen Ground. New York, McGraw-Hill Book Co.

## INDEX

- Abelev Yu. M. 10, 78, 206  
Active compression zone,  
determination of, 229  
Absorbed water 15  
Alluvial deposits 12  
Angle of internal friction 53  
Angle of maximum deviation 128  
Angle of vision 104  
Apparatus,  
dynamometric 244  
Arutyunyan N. Kh. 114, 247  
Attenuating creep 246
- Babitskaya S. S. 240  
Baranov D. S. 122  
Barkan D. D. 270, 276, 281  
Basic laws of soil mechanics 31  
Bed rock 8  
Berezantsev V. G. 10, 123, 126, 137,  
140, 142  
Biarez J. 125  
Bingham E. 238  
Borodachev N. M. 286  
Botkin A. I. 65  
Boussinesq J. 9, 86, 177  
Bulychev V. G. 10, 43  
Burger M. 122
- Cambrian clays 12  
Capillary water 15  
Caquot A. 137  
Casagrande A. 19, 202, 279  
Classification of disperse  
solids 17  
Classification indices of soils 20  
Clayey soils, 14  
consistency of, 28  
Cleavage 20  
Coagulation bonds 17  
Coefficient(s),  
of compression 38  
of elastic half-space 177  
of initial pore-water pressure 199  
of internal friction 53  
of lateral pressure 43  
of linearly deformable half-space  
89  
of relative compressibility 187  
of soil consolidation 191  
of subsidence 78  
of thawing 78  
Cohesion forces 49  
Compactibility 33  
Compaction under load 33  
Compressibility 8, 31  
Compression of soils 33  
Compression curves 35  
Concentrated force,  
effect of, 86  
Condensational bonds 17  
Conditions of ultimate equilibrium 129  
Consistency of clayey soils 28  
Consolidation,  
degree of, 192  
differential equations of, 202  
Constitution of soils 20  
Contact pressure 112  
Contact shear resistance 8, 32  
Continental deposits 12  
Continental ice 12  
Corner points 93  
Coulomb C. 9, 123  
Coulomb's law 52  
Creep of soil skeleton 32  
Creep deformations 239, 246  
Creep parameters 247  
Critical loads on soil 133  
Critical void ratio at shear 52  
Crystallization bonds 17, 18
- Dalmatov B. I. 10, 236  
Davydov S. S. 10, 118  
Deformability, 32  
of porous water 75  
Deformation,  
residual, 32  
Degree of consolidation 192

- Deluvial deposits 12  
 Denisov N. Ya. 10, 18, 78  
 Density of loose soils 26  
 Deryagin B. V. 47, 243  
 Diagenesis 18  
 Disperse soils,  
   dynamics of, 264  
 Dispersivity 8  
 Dynamic sounding 26  
 Dynamics of disperse soils 264  
 Dynamometric apparatus 244
- Earth's rock mantle 8  
 Edelman S. Ya. 122  
 Effective pressure 48  
 Egorov K. E. 10, 117, 181  
 Eluvial deposits 12  
 Eolian deposits 12  
 Equivalent layer coefficients 224  
 Ermakov V. F. 244  
 Erosion processes 148  
 Ershov V. A. 276  
 Erzhanov Zh. S. 239
- Fedorov I. S. 122  
 Feldspar 13  
 Filtration,  
   rate of, 46  
 Filtration consolidation 76  
 Flexibility of foundation 115  
 Flexible foundations 118  
 Florin V. A. 9, 122, 185, 202, 247  
 Forces of cohesion 49  
 Foundation,  
   flexibility of, 115  
 Frelich O. K. 134  
 Frozen soils 10, 81
- Gaseous inclusions in soils 15**  
 Geodynamics 8  
 Geomechanics 8  
 Gersevanov N. M. 9, 10, 40, 42, 70,  
   73, 103, 134, 185, 287  
 Glacial deposits 12  
 Global geodynamics 8  
 Goldstein M. N. 10, 156, 238, 240, 251  
 Golushkevich S. S. 10, 123  
 Gorbunov-Posadov M. I. 10, 115, 181  
 Gor'kova I. M. 239  
 Gradient,  
   hydraulic, 46  
 Grain-size distribution of soils 24  
 Gravitational water 15  
 Grigoryan S. S. 268, 272, 281
- Hooke's law 85  
 Humus soil 9  
 Hydraulic gradient 46  
 Hydrocapacity principle 42
- Index of saturation 21  
 Influence coefficients 104, 105  
 Instantaneous compression 201  
 Instantaneous strength 242  
 Irreversible shear 124  
 Ishlinsky A. Yu. 68, 138  
 Isobars 92, 106  
 Ivanov N. N. 9, 10  
 Ivanov P. L. 287
- Kaolinites 14**  
 Kerisel J. 137  
 Khakimov Kh. R. 178  
 Kirpichev V. 86  
 Klein G. K. 170  
 Korotkin V. G. 177  
 Kosterin E. V. 243, 251  
 Kötter F. 123  
 Krashenninnikova G. V. 118  
 Krasnikov N. D. 267, 272  
 Krylov A. N. 10  
 Kurdyumov V. I. 126
- Laletin N. V. 43, 62  
 Lambe T. W. 18  
 Landslides 148  
 Landslide pressure 158  
 Landslide prevention 160  
 Larionov A. K. 106, 18, 19, 240  
 Lateral pressure 106  
 Lateral waves 269  
 Law of laminar filtration 44  
 Lebedev A. F. 15  
 Leontyev N. N. 184  
 Liquefaction landslides 149  
 Liquid index 28  
 Liquid limit 25  
 Lithogenesis 18  
 Lithosphere 8  
 Loess soils 10  
 Long-term cohesion 83  
 Long-term strength 242  
 Loose soils,  
   density of, 26  
 Love A. 93  
 Lyakhov G. M. 266, 268, 272, 273  
 Lyosorbed water 15

- Maksimyak R. V.** 240  
**Malyshev M. V.** 141  
 Marine deposits 12  
**Maslov N. N.** 10, 18, 36, 57, 109, 135, 245, 238, 246, 251, 252  
**Maslov G. N.** 247  
 Matrices of influence coefficients 217  
 Mechanical compaction 33  
 Mechanical processes in soils 123  
 Mechanics of loose rocks 8  
 Mechanics of massive rocks 8  
**Medkov E. I.** 37  
**Meschyan S. P.** 75, 239, 241, 247  
 Metamorphism 18  
 Method,  
   of circular-cylindrical slip surfaces 154  
   of corner points 93  
   of direct measurement of stress relaxations 243  
   of elementary summation 101  
 Microfissures 240  
 Microstructural defects 49  
 Mineral composition of soils 13  
**Minyaev P. A.** 9  
 Modulus of settlement 36  
 Modulus of subgrade reaction 182  
**Mogilevskaya S. E.** 252  
 Mohr's theory of strength 58  
 Mohr's ultimate stress circles 58  
 Moisture content of soils 20  
 Molecular forces in soils 17  
 Montmorillonite 13  
 Movable crystal lattice 14  
**Mustafayev A. A.** 78  
  
 Natural soils,  
   age of, 12  
 Natural stresses 119  
 Neutral pressure 48  
**Nichiporovich A. A.** 10  
 Non-homogeneity of soils 20  
  
 Octahedral strength theory 65  
 One-way filtration 227  
  
 Passive resistance 130  
**Pasternak P. L.** 184  
**Patvardkhan A. Sh.** 251, 252  
**Pavlovsky N. N.** 9, 45, 190  
**Pavlyuk N. P.** 281  
 Peats 8  
**Pekarskaya N. K.** 240, 242  
 Permafrost 10, 77, 81  
  
 Phases of stressed state 125  
 Physical properties of soils 20  
 Pipe-laying,  
   methods of, 168  
 Plastic limit 25  
**Pokrovsky G. I.** 122, 275  
**Polshin D. E.** 10, 178  
**Polyakova N. I.** 268, 273  
**Ponomarev V. D.** 117  
 Porosity 20, 21  
 Porous pressure 49  
 Porous water,  
   deformability of, 75  
 Power function 78  
**Press G.** 122  
 Principle of equilibrium state of water and ice in frozen soils 82  
 Principle of linear deformability 73  
 Progressive creep 241, 246  
**Proktor G. E.** 10  
**Protodiakonov M. M.** 172  
**Puzyrevsky N. P.** 9, 10, 103, 134, 232  
  
**Quartz** 13  
 Quasi-homogeneous state of soil 238  
  
**Rakhmatulin Kh. A.** 268, 272  
 Rate of filtration 46  
 Rate of settlement 188  
 Reactive pressures 120  
**Rebinder P. A.** 17, 18, 239, 251  
 Recombination of soil structure 240  
 Regional geodynamics 8  
**Reisner M.** 238  
 Relative consistency 28  
 Relative subsidence 78  
 Relaxation 238  
**Reltov B. F.** 47, 246  
**Rendulic L.** 49  
 Residual deformation 32  
 Retaining walls 161  
 Rheological processes in soils 238  
 Rheology 238  
 Rigid foundations 118  
**Rodstein A. G.** 122  
 Rolling-out limit 25  
 Rotational landslides 149  
**Roza S. A.** 10, 47  
  
**Sagomonyan A. Ya.** 272  
 Sampling tube 27  
 Sandy soils 13  
**Savinov O. A.** 183, 278, 281  
**Schechter O. Ya.** 181, 286

- Schleicher F. 177  
 Schultz E. 122  
 Sea-glacial deposits 12  
 Secondary consolidation 200, 247  
 Seed H. 279  
 Seismic effects 265  
 Settlement rate 188  
 Settlements,  
   time variations of, 187  
 Shakhnyants G. M. 156  
 Sharov V. S. 18  
 Shear 124  
 Shear-box apparatus 51  
 Shear tests of soils 60  
 Shear zones 125  
 Shusherina E. P. 240  
 Silts 8  
 Simple compression 60  
 Simvulidi I. A. 10  
 Sinitsyn A. P. 10  
 Sitnikov S. N. 236  
 Slip landslides 149  
 Slippage 49, 124  
 Slippage surfaces 125  
 Soil(s), 8  
   classification indices of, 20  
   components of, 13  
   creep deformations in, 246  
   critical loads on, 133  
   frozen, 81  
   gaseous inclusions in, 15  
   grain-size distribution, 24  
   mechanical processes in, 123  
   mineral composition of, 13  
   moisture content, of 20  
   molecular forces in, 17  
   non-homogeneity of, 20  
   physical properties of, 12, 20  
   quasi-homogeneous state of, 232  
   rheological processes in, 238  
   specific weight of, 20  
   stability in landslides, 148  
   structural bonds in, 17  
   structural strength of, 19  
   ultimate resistance to pressing,  
     28  
   ultimate stressed state of, 123  
   undercompacted, 77  
   unit weight of, 20  
   water in, 15  
 Soil formation,  
   geological conditions  
   of, 12  
 Soil mechanics,  
   basic laws of, 31  
 Soil skeleton 24  
 Soil structure,  
   recombination of, 240  
 Sokolovsky V. V. 10, 123, 132, 138,  
   151, 167  
 Sotnikov S. N. 252  
 Sovine J. 181  
 Specific weight of soils 20  
 Spherical stamp method 66  
 Stability of soils in landslides 148  
 Stability of structural bonds 19  
 Stabilized state 76  
 Stabilometer 62  
 Stable cohesion 83  
 Stable creep 241, 246  
   at shearing 250  
 Static sounding 26  
 Stony soils 13  
 Stressed state,  
   phases of, 125  
 Stresses in soils,  
   determination of, 85  
 Stress relaxations, 239  
   method of direct measurement of,  
     243  
 Structural bonds in soils, 17  
   stability of, 19  
 Structural mechanics 8  
 Structural-phase deformability 8, 70  
 Subsidence, 77  
   relative 78  
 Subsidence soils 77  
 Sumgin M. I. 81, 238  
 Swelling,  
   coefficient of, 39  
  
 Ter-Martirosyan Z. G. 249, 253  
 Ter-Stepanyan G. I. 156, 238  
 Terzaghi K. 9, 34, 43, 137, 138, 139,  
   185, 190  
 Thawing,  
   coefficient of, 78  
 Thawing settlement 83  
 Theory of heredity creep 75  
 Theory of ultimate equilibrium 123  
 Theory of ultimate stressed state  
   of soils 123  
 Time-independent strength 242  
 Time variations of settlements  
   187  
 Triaxial compression 62  
 Tsytoich N. A. 10, 51, 67, 76, 78,  
   81, 82, 86, 109, 117, 122, 141, 155,  
   172, 184, 185, 197, 205, 216, 219,  
   235, 238, 240, 241, 242, 243, 244,  
   249, 252, 256, 259  
 Turovskaya A. Ya. 241  
 Two-way filtration 227

- Ultimate equilibrium,  
  conditions of, 59  
Ultimate resistance to pressing 28  
Ultimate shear resistance of soils 49  
Ultimate stress circles 129  
Ultimate stressed state of soils 123  
Undercompacted soils 77  
Underground pipelines,  
  soil pressure on, 167  
Uniaxial compression 61  
Unit weight of soils 20
- Van der Waals forces 17  
Vane tests 66  
Vasilyev B. D. 10  
Vibrocompaction 277  
Vlasov V. Z. 184  
Void ratio 21  
Volarovich M. P. 47, 239
- Vyalov S. S. 10, 81, 122, 239, 240,  
  242, 246
- Water-colloidal bonds 18  
Water-glacial deposits 12  
Water in soils 15  
Water permeability 8, 32  
Water perviousness 44  
Water-saturation ratio 21  
Wave processes in soils 267
- Yappu G. B. 62  
Yaroshenko V. A. 126
- Zaretsky Yu. K. 10, 114, 185, 197,  
  239, 242, 257, 259  
Zelenin A. N. 61  
Zhemochkin B. N. 10  
Zhukov N. V. 241, 251

## **TO THE READER**

*Mir Publishers welcome your comments on the content, translation, and design of the book.*

*We would also be pleased to receive any suggestions you care to make about our future publications.*

*Our address is:*

*USSR, 129820, Moscow, I-110, GSP,  
Pervy Rizhsky Pereulok, 2, Mir Publishers*

*Printed in the Union of Soviet Socialist Republics*

## **Design of Earthquake Resistant Structures**

**S. POLYAKOV, D. Sc.**

*334 pp. 16.5 × 22 cm. Cloth*

A textbook for civil engineering and building faculties of universities and schools of architecture on designing earthquake resistant structures for housing and other civil and public buildings. Discusses Soviet, American, and Japanese standards. Draws extensively on world experience of building in earthquake zones. Devotes special attention to concrete and reinforced concrete structures. Revised for translation by the author, with supplementary material.

## **Foundation Soils and Substructures**

**N. TSYTOVICH, Corr. Mem. USSR Acad. Sci., and others**

*375 pp. 14.5 × 22 cm. Cloth*

A concise textbook for civil engineers, written by a group of authors from departments of soil mechanics and foundations at leading Soviet civil engineering institutes, under the editorship of Prof. Nikolai Tsytovich, Corresponding Member of the USSR Academy of Sciences, of the Moscow Civil Engineering Institute. The exposition assumes that such general engineering subjects as engineering geology, strength of materials, and soil mechanics — the scientific basis of foundation laying — have already been studied. Formulas for analysis are therefore not as a rule included. Devotes special attention to building in permafrost and similar conditions.

## Seismic Waves

E. SAVARENSKY

292 pp. 14.5 × 21.5 cm. Cloth

A monograph on seismic waves for scientific workers, post-graduate students, and undergraduates studying problems of seismology, seismic prospecting, and related disciplines. Can serve as a manual for studying oscillations and wave propagation.

The book is concerned with the physics of seismic oscillations, including the elements of the statistical approach and of filtering. Contains data on the analysis of elastic strain and stress, on study of the relationships between them, and on the derivation of equations of the propagation of longitudinal and transverse seismic waves. Analyzes the propagation of plane and spherical waves in infinite space from the simplest sources. Considers the effect of plane boundaries on the propagation of plane waves, and pays special attention to the analysis of Love waves and waves of Rayleigh type, and also to the propagation of complex oscillations in conditions of the dispersion of wave velocity.

